



## **Carbon Capture Potential in Modified Soil**

A thesis submitted to Newcastle University in partial fulfilment of the requirement for the degree of Doctor of Philosophy in the Faculty of Science, Agriculture and Engineering

**Yala Amos Iorliam**

B.Eng. Civil Engineering

MSc Civil Engineering

School of Engineering

Newcastle University, UK

November, 2018

## Abstract

Clay soils present a range of challenges in geotechnical engineering. In addition to addressing the problematic nature of clay soils concerning ground stability, geotechnical engineering has a role in the context of climate change. As far as possible, geotechnical design should mitigate the effects of increases in carbon dioxide ( $\text{CO}_2$ ) and other greenhouse gases (such as methane, nitrous oxide, fluorinated gases), that are released to the atmosphere, thus causing the Earth to become warmer.

Lime modification of clay soils has attracted a significant amount of interest, due to its potential to improve soils for construction purposes. This tackles the issue of waste reduction, reduces the need for imported fill, and thereby reduces the  $\text{CO}_2$  emissions associated with the traffic movements. However, the production of lime itself produces additional  $\text{CO}_2$  emissions. This thesis addresses the use of lime ( $\text{Ca}(\text{OH})_2$ ) in ground stabilisation, assessing the associated formation of calcium carbonate ( $\text{CaCO}_3$ ) and the extent to which this can mitigate the  $\text{CO}_2$  emissions associated with the production of the  $\text{Ca}(\text{OH})_2$  without overly severe impacts on engineering properties.

Experimental treatment of kaolin with lime shows that average carbonate content values from 4.70-10.08% dry mass of  $\text{CaCO}_3$  for 4-8%  $\text{Ca}(\text{OH})_2$  contents in samples at 10% air voids were achieved, with a maximum recovery of 93% of  $\text{CO}_2$  lost during lime manufacture.

Based on 7 days cured specimens with a combination of 6%  $\text{Ca}(\text{OH})_2$  and 10% air voids content, a compressive strength development of 280 kPa was achieved for carbonated treated kaolin, compared to 170 kPa for non-carbonated equivalents which is a substantial increase in strength of approximately 60%. This strength is equivalent to California bearing ratio (CBR) value of 29 %, greater than the minimum CBR required for a stabilised capping layer (15%), suggesting that carbonated treated kaolin is suitable for use as a stabilised capping layer. The increases in strength and stiffness for saturated carbonated lime treated specimens are much reduced compared to what might be predicted from the literature for some non-saturated non-carbonated equivalents. However, the increases are sufficient for application to capping layers.

The freeze-thaw (FT) resistance for carbonated treated kaolin was found to be approximately 24%, and is suggested sufficient for a capping layer, when viewed in the context of the less

stringent requirements for FT durability for capping material. Treated kaolin compacted to air voids content from 3% to 15% achieves permeability values of  $1.8 \times 10^{-9}$  m/s to  $7.4 \times 10^{-9}$  m/s.

Another research focus in this thesis is to use imaging techniques to detect and quantify the amount of  $\text{CaCO}_3$  formed and the voids content of the carbonated kaolin sample. X-ray computed tomography (XRCT) analysis, using ImageJ software, showed the presence and distribution within the clay sample of  $\text{CaCO}_3$  and air voids. Furthermore, using this technique it was possible to quantify the air voids content and the amount of  $\text{CaCO}_3$  formed, with good agreement with chemical methods (calciometer, TGA). At 8%  $\text{Ca}(\text{OH})_2$ , 25% air voids, the highest amount of carbonate content of  $9.82 \pm 0.06\%$  was detected by the XRCT. The presence of  $\text{CaCO}_3$  formation in carbonated soils may be determined using the scanning electron microscope (SEM). Based on SEM results, calcium carbonate grains of about 2-3  $\mu\text{m}$  in size were found on the surface of the kaolin.

The results of this study have shown that this method of combined modification and carbonation treatment of clays has the potential to offset up to 93% of the  $\text{CO}_2$  released from lime production for stabilisation (representing 0.03% global  $\text{CO}_2$  emissions), alongside improving the compressive strength of the clays. This could be effectively used for a combined carbon capture function and engineering function such as the capping layer in road pavement. A design specification for carbon capture and ground improvement is developed, assessing the benefits in terms of carbon sequestration. If combined modification and carbonation is to be adopted in practice, then an addendum needs to be included in the specification (such as the Highways Agency, 2007; MWCH 1, 2009: Series 600) for lime-stabilisation for engineering purposes. Compaction requirements to achieve 10% air voids would give combined strength and carbon capture benefits. The combined modification and carbonation application to lime treated clay has shown the potential to mitigate climate change alongside ground stability improvement of soft clay.

## Acknowledgements

I am very grateful to God Almighty for giving me the strength to pursue this PhD to completion.

I would like to thank my supervisors Professor Stephanie Glendinning and Professor David Manning for their invaluable guidance, insight and encouragement throughout my PhD.

Many thanks to Dr. Paul Hughes for his immense contribution towards my PhD. My sincere appreciation goes to Durham XRCT service. Especially, Professor Charles Augarde and Dr. Jonathan Smith for their assistance in scanning my XRCT images.

I would like to thank all the members of Geotechnics and Structures as well as the staff of School of Engineering, Newcastle University for the friendly environment they provided for my research. I sincerely appreciate the efforts of the members of geotechnics laboratory, Newcastle University. Many thanks to Stuart Patterson, Philip Green and Bernard Bowler for their immeasurable help in my laboratory work.

I would like to thank my parents (Philip and Lydia) for their prayers and unconditional love. I also want to thank my brothers (Nguetar and Dr. Aamo) and my sisters (Nguseer and Mamfe) for their support. To my dear wife (Dr. Bridget) and children (Samuel and Sheena), I really appreciate your love, support and patience.

Special thanks to all my bosses and friends here in the UK and abroad. Professor Isaac Agbede, Professor Joel Manneseh, Dr. Matthew Aho, Dr. Delian Akpen. Dr. Terrumun Utsev, James Juluku, Ben Ikya, Pst. Samuel Ohiomokhare, Darius Ibzan, Ukya Terhide, Dr. Taiwo Alaje, Dr. Ibukun Adewale, Annock Chiwona, Eminue Oboho, Alfred Opukumo, Rose Hen-Jones and Christopher Davis all encouraged me throughout this PhD period.

I would also like to thank the Federal University of Agriculture, Makurdi for given me this opportunity to carry out my study in the UK. Lastly, I would like to thank PTDF for funding this research.

# Table of Contents

Abstract.....	i
Acknowledgements.....	iii
List of Figures.....	ix
List of Tables.....	xv
List of Abbreviations.....	xvii
Chapter 1 – Introduction.....	1
1.1 Research Context.....	1
1.2 Aim and Objectives .....	3
1.3 Thesis Overview .....	3
Chapter 2 – Literature Review.....	5
2.1 Climate Change and Greenhouse Gas Effect.....	5
2.2 Mitigation Approaches for Carbon Dioxide.....	12
2.3 Soil Stabilisation.....	17
2.4 Permeability in Lime Stabilisation .....	30
2.5 Modification of Geotechnical Properties of Clay Soils.....	33
2.6 Carbonation Process .....	36
2.7 Soil Carbonation.....	41
2.8 Freeze-Thaw Durability of Lime Treated Clay .....	44
2.9 Lime Based-Wastes for Soil Stabilisation .....	45
2.10 Techniques for Confirmation and Quantification of Carbonates .....	49
2.11 Chapter Summary .....	50

Chapter 3 – Materials and Methods .....	52
3.1 Introduction .....	52
3.2 Testing Objectives and Outline Methodology .....	52
3.3 Materials Used in the Laboratory Testing.....	53
3.4 Materials Characterisation Testing.....	54
3.4.1 Initial Consumption of Lime.....	55
3.4.2 Atterberg Limits.....	56
3.4.3 Cation Exchange Capacity Testing.....	58
3.4.4 Compaction Testing .....	58
3.4.5 Strength Testing .....	65
3.5 Modification and Carbonation Treatment .....	68
3.5.1 Soil Modification .....	68
3.5.2 Carbonation Treatment .....	69
3.5.3 Testing of Carbonated Treated Kaolin Specimen .....	71
3.5.4 Unconfined Compressive Strength Testing .....	72
3.5.5 Freeze-Thaw Durability Testing .....	72
3.5.6 Geochemical Testing .....	73
3.5.7 Mineralogical Testing .....	76
3.5.8 Calcium Carbonate Content Comparison. ....	84
3.6 Chapter Summary.....	84
 Chapter 4 – Strength Development and Calcium Carbonate Formation in Treated Kaolin Clay .....	 86

4.1 Preliminary Material Characterisation.....	86
4.1.1 Initial Consumption of Lime .....	86
4.1.2 Cation Exchange Capacity Results.....	87
4.1.3 Atterberg Limit.....	88
4.1.4 Density of Treated Kaolin Clay.....	90
4.1.5 Strength Development of Treated Kaolin Clay .....	92
4.1.6 Permeability of Treated Kaolin Clay.....	93
4.1.7 Summary of Material Characterisation .....	95
4.2 Calcium Carbonate Formation in Treated Kaolin Clay.....	95
4.2.1 Calcium Carbonate Variation with Lime Content obtained from Calcimeter Analysis .....	95
4.2.2 Calcium Carbonate Variation with Air Voids Content in Treated Kaolin .....	96
4.2.3 Calcium Carbonate Content from Thermogravimetric Analysis .....	97
4.3 Combined Modification and Carbonation Treatment.....	99
4.3.1 Strength and Stiffness Development of Carbonated Treated Kaolin. ....	99
4.3.2 Durability of Carbonated Treated Kaolin.....	103
4.4 Internal Structure Changes Using Mineralogical Analysis .....	105
4.4.1 Threshold Settings for XRCT Analysis.....	106
4.4.2 Determination of Carbonate Content in Sample Using XRCT. ....	107
4.4.3 Sample Slice Analysis Using ImageJ Software .....	110
4.4.4 Calcium Carbonate Content from XRCT versus Calcimeter Analysis.....	113
4.4.5 Determination of Voids Content Using XRCT.....	115

4.4.6 Relationship between Lime Contents and Reduction in Voids Content of Carbonated Treated Kaolin. ....	116
4.4.7 Scanning Electron Microscopy Analysis .....	117
4.5 Chapter Summary.....	120
Chapter 5 – Performance of Carbonated Modified Soil.....	123
5.1 Introduction .....	123
5.2 Initial Consumption of Lime and its Implication .....	124
5.3 The Use of Lime for Modification and Stabilisation .....	124
5.4 Permeability of Treated Kaolin .....	125
5.5 Carbonation Development.....	126
5.5.1 Background.....	126
5.5.2 Degree of Carbonation and Lime Additions .....	127
5.5.3 Degree of Carbonation and Air Voids Content .....	129
5.5.4 Carbonation and Reduction in Air Voids.....	132
5.6 Carbonation and Strength Improvement .....	133
5.6.1 Carbonated Treated Kaolin Strength Improvement Relatively to Kaolin Clay only .....	133
5.6.2 Carbonated Treated Kaolin Strength Improvement Relatively to Treated Kaolin	135
5.7 Effect of Soil pH on the Strength of Carbonated Soil.....	138
5.8 Freeze Thaw Durability.....	139
5.9 Carbonate Distribution .....	140
5.10 Conceptual Model of the Carbonation Process in Lime Treated Clay.....	141
5.11 Implication for Carbon Capture .....	143
5.12 Design Specifications.....	151

5.13 Chapter Summary .....	154
Chapter 6 – Conclusions and Recommendations.....	157
6.1 Conclusions.....	157
6.2 Recommendations for Future Work .....	159
6.2.1 Improve Carbon Capture and Modification Process .....	159
6.2.2 Investigate and Discover More Cost Effective Stabilisers .....	159
6.2.3 Investigate Carbon Capture and Modification in Lime Treatment using more Clays. .....	160
References.....	161
Appendix A: Material Properties.....	178
Appendix B: Soil Characterisation Test Results.....	181
Appendix C: Carbonate and Air Voids Content.....	183
C1: Procedure used for XRCT Data Processing.....	187
C2: XRCT Images Showing Carbonate and Air Voids Content, with corresponding Threshold Graphs.....	188
Appendix D: Determination of global <b>CO<sub>2</sub></b> emissions from lime production.....	202

## List of Figures

Figure 2.1: Greenhouse gas emissions by gas (percentages based on million metric tonnes CO <sub>2</sub> Eq.) (adapted from US Environmental Protection Agency, 2016).....	6
Figure 2.2: Measured atmospheric CO <sub>2</sub> concentrations at the Mauna Loa Observatory, Hawaii, since measurement 1958 (adapted from NOAA, 2017).....	7
Figure 2.3: An ideal carbon dioxide emission settings and response to benchmark scenario. a) CO <sub>2</sub> Emissions. (b) CO <sub>2</sub> concentration response to benchmark c) Temperature response to benchmark scenario (after Allen et al., 2009).....	8
Figure 2.4: Changes in mean surface temperature resulting from cumulative carbon emissions per annum based on the RCP8.5-extension scenarios over the period 1850 to 2300 (after Frolicher, 2016).....	9
Figure 2.5: Trend in claims for heave and subsidence damage to domestic properties (adapted from Sanders and Phillipson, 2003).....	10
Figure 2.6: Preliminary overall evaluation of the geoengineering techniques (after Shepherd, 2009). Note: CCS represents carbon capture and storage, BECS represents bioenergy with CO <sub>2</sub> capture and sequestration. ....	11
Figure 2.7: Flowchart of the proposed categorization of climate change responses (adapted from Boucher <i>et al.</i> , 2014).....	15
Figure 2.8: Unconfined compressive strength (a) montmorillonite with various additions of calcium hydroxide (b) kaolinite with various additions of calcium hydroxide (after Bell, 1996).....	18
Figure 2.9: Plasticity changes due to addition of quicklime to English china clay (kaolin) after 72 and 24 hours (after Rogers and Glendinning, 1996).....	19
Figure 2.10: Plasticity changes due to addition of quicklime to London Clay after 72 and 24 hours (after Rogers and Glendinning, 1996).....	20
Figure 2.11: Variation of undrained shear strength with curing time (a) English china clay (kaolin) (b) bentonite. Shear strength values shown as 145 kN/m <sup>2</sup> are at the measurement limit for the shear vane apparatus and the actual strength may be higher (after, Boardman et al., 2001).....	22
Figure 2.12: Variation in unconfined compressive strength (UCS) with lime (as CaO) content (a) highly expansive soil (b) residual soil (after Dash and Hussain, 2012).....	23
Figure 2.13: Influence of curing time on UCS of treated kaolin (after Muhmed and Wanatowski, 2013).....	25
Figure 2.14: Atterberg limits at 0% and 5% lime content (after Muhmed and Wanatowski, 2013).....	25
Figure 2.15: Effect of curing time on the unconfined compressive strength (UCS) development in Ca(OH) <sub>2</sub> treated tropical kaolin (after Saeed <i>et al.</i> , 2015). KUT represent untreated kaolin, KLT represents lime-treated kaolin.....	26
Figure 2.16: UCS evolution with time for specimens cured at 20°C (a) kaolinitic material (b) calcium bentonite (after (Maubec et al., 2017).....	27
Figure 2.17: (a) X-ray diffraction patterns of untreated and 5% CaO treated clay as a function of curing time (after Vitale <i>et al.</i> , 2017) (a) kaolin (b) bentonite.....	28
Figure 2.18: Increase in California bearing ratio (CBR) of Gilgai clay from Cape Preston, Western Australia, due to treatment with hydrated lime (HL), and cement based on soaked CBR vs. curing time (after Cocks <i>et al.</i> , 2010).....	29
Figure 2.19: Reduction in permeability with increasing moulding water content in lime-treated St Quentin silt. P represents Proctor compaction, K represents kneading compaction, QL represents quicklime, and HL represents hydrated lime (after Cuisinier <i>et al.</i> , 2011).....	31

Figure 2.20: Effect of curing period on the shear strength of lime-treated clay containing different humic acid contents (after Yunus <i>et al.</i> , 2016).	32
Figure 2.21: Analysis of the strength development mechanism in the cement treated sand mixture under the drying condition (after Ho <i>et al.</i> , 2017).	33
Figure 2.22: Life cycle analysis of lime (after British Lime Association, 2015). Note: A represents CO <sub>2</sub> emissions due to energy supply (combustion plus electricity) 0.341 tonnes per a tonne quicklime product. B represents process emissions (0.751 tonnes per a tonne quicklime product), C represents carbon recovery through carbonation of lime. By carbonation C could be equal to B.	35
Figure 2.23: Unconfined compressive strength (UCS) of bentonite (Impersol) with curing time for various amounts of calcium hydroxide (Ca(OH) <sub>2</sub> ) addition (after Al-Mukhtar <i>et al.</i> , 2010).	40
Figure 2.24: Changes in amount of CaCO <sub>3</sub> content in 8% cement treated Toyoura silica sand under different curing conditions (a) Natural conditions (b) Accelerated (5% CO <sub>2</sub> ) conditions (after Nakarai and Yoshida, 2015).	43
Figure 2.25: Relationship between unconfined compressive strength and CaCO <sub>3</sub> in 8% cement treated Toyoura silica sand (after Nakarai and Yoshida, 2015).	43
Figure 2.26: The effect of freeze–thaw (FT) action on unconfined compressive strength (UCS) of untreated and lime-treated expansive clay (a) untreated bentonite (Bnat) and treated bentonite (b) untreated kaolinite (Knat) and treated kaolinite (adapted from Hotineanu <i>et al.</i> , 2015).	45
Figure 2.27: Unconfined compressive strength (UCS) development of lime, and lime-based waste treated Lower Oxford Clay (LOC); (a) Lime (calcium oxide), and WSA, (b) combined WSA plus GGBS (WSA:GGBS is 50:50). L represents calcium oxide, WSA represents wastepaper sludge ash, GGBS represents ground granulated blastfurnace slag (after Rahmalt and Ismail, 2011).	48
Figure 3.1: ORION 710A pH meter used to measure pH.	55
Figure 3.2: End-over-end bottle shaker.	56
Figure 3.3: Plastic and liquid limit testing equipment.	57
Figure 3.4: Hobart mixer.	59
Figure 3.5: Compaction apparatus, 1 litre sample mould (upper), 2.5 kg compaction rammer (lower).	60
Figure 3.6: Variation of dry density with moisture content of calcium hydroxide mixed kaolin.	63
Figure 3.7a: Relationship of dry density-moisture content with air void lines in 4% Ca(OH) <sub>2</sub> treated kaolin. Red circles show the intersection of air voids lines and compaction curve. Dry density and moisture content at intersection used in compaction for formation of treated kaolin. L represents percentage Ca(OH) <sub>2</sub> content. AV represents air voids content.	63
Figure 3.7 continued: Relationship of dry density-moisture content with air void lines in treated kaolin. Red circles show the intersection of air voids lines and compaction curve (b) 6% Ca(OH) <sub>2</sub> content (c) 8% Ca(OH) <sub>2</sub> . Dry density and moisture content at intersection used in compaction for formation of treated kaolin. L represents percentage Ca(OH) <sub>2</sub> content. AV represents air voids content.	64
Figure 3.8: Split specimen mould.	67
Figure 3.9: Carbonation treatment of treated kaolin clay using triaxial cell set-up.	70
Figure 3.10: Carbonated treated kaolin sample for XRCT scanning (a) Parent sample 38 mm diameter, 76 mm height (b) Cored sample 5 mm diameter, 25 mm height. Sample axially cored from parent sample in (a).	78
Figure 3.11: ImageJ procedures on sample images: (a) sample axes (b) typical reconstructed slice xy-plane (c) cropped sample (d) post filtered image (e) enlarged section (f) post thresholding (image pixel intensities below threshold value of 44 shown black, whilst	

white spaces represents intensities above threshold value (g) selected areas (in orange) for measurement.....	80
Figure 3.12: XRCT images of carbonate sample using ImageJ software: (a) Typical carbonate sample of 8% calcium hydroxide, and 10% air voids content (b) Reflection of post-threshold image at carbonate boundary.....	82
Figure 3.13: XRCT images of non-carbonate sample using ImageJ software: (a) Typical non-carbonated sample of 8% calcium hydroxide, and 10% air voids content (b) Reflection of selected extreme image intensity value of 125 on non-carbonated Sample. ....	82
Figure 4.1: Variation of pH with calcium hydroxide [Ca(OH) <sub>2</sub> ] content (%) (average of three samples per point). Analytical error bars lie within the area of the data point. Error bars represent 1 standard deviation.....	87
Figure 4.2: Variation of Atterberg Limits with calcium hydroxide (Ca(OH) <sub>2</sub> ) addition to kaolin after 24 hours curing (average of 4 samples per point). Error bars are within the size of points and represent 1 standard deviation.....	89
Figure 4.3: Changes in maximum dry density (MDD) and optimum moisture content (OMC) in treated kaolin using calcium hydroxide (Ca(OH) <sub>2</sub> ) (average of 3 samples per point). Error bars are within the data point and represent 1 standard deviation.....	91
Figure 4.4: Variation of dry density with air voids for calcium hydroxide addition to kaolin (average of 3 samples per point). Analytical error bars represent one standard deviation. ....	91
Figure 4.5: Variation of unconfined compressive strength (UCS) of kaolin treated with calcium hydroxide (average of 3 samples per point). Analytical error bars represent one standard deviation. ....	92
Figure 4.6: Variation of unconfined compressive strength (UCS) of water saturated treated kaolin (average of 3 samples per point). Repeatability error bars represent 2 standard deviations. ....	93
Figure 4.7: Variation of permeability with air void for treated kaolin (average of 3 samples per point). Analytical error bars represent one standard deviation. ....	94
Figure 4.8: Calcium carbonate content in kaolin with varying Ca(OH) <sub>2</sub> additions obtained from calcimeter analysis (average of 3 samples per point). Analytical error bars represent 1 standard deviation.....	96
Figure 4.9: Calcium carbonate content variations with air voids content (average of 3 samples per point). Analytical error bars represent 1 standard deviation.....	97
Figure 4.10: Combine thermogravimetric curve and QMS trace, evolved gas (H <sub>2</sub> O and CO <sub>2</sub> ) for 10% air void samples (average of 3 samples per combination). Heating of samples were performed under an atmosphere of He <sub>80</sub> O <sub>20</sub> (80% helium and 20% oxygen) mixture, purge gas flow rate of 30 ml per min.....	98
Figure 4.11: Unconfined compressive strength of kaolin clay with varying calcium hydroxide additions (average of 3 samples per point). Analytical error bars represent 1 standard deviation.....	100
Figure 4.12: Unconfined compressive strength of carbonated calcium hydroxide treated kaolin clay with varying air voids (average of 3 samples per point). Analytical error bars represent 1 standard deviation.....	101
Figure 4.13: Stiffness of carbonated calcium hydroxide treated kaolin with varying air voids (average of 3 samples per point). Error bars represent 1 standard deviation. Note: untreated kaolin resulted in stiffness of 2.4 MPa.....	102
Figure 4.14: Variation of unconfined compressive strength with calcium carbonate content in carbonated treated kaolin (average of 3 samples per point). Error bars represent 1 standard deviation. ....	103
Figure 4.15: Resistance to loss in strength against three freeze-thaw cycles of carbonated treated kaolin clay (average of 3 samples per point) error bars based 1 standard deviation.....	104

Figure 4.16: XRCT images of 8% calcium hydroxide 10% air voids treated kaolin. Column (a) represents non-carbonated sample, and column (b) represents carbonated specimen. Note: white patches represents calcium carbonate particles as inferred using scanning electron microscopy (Section 4.4.7). The red circles mark areas where amorphous calcium carbonate is formed.....	108
Figure 4.16 continued: XRCT images of 8% calcium hydroxide 10% air voids treated kaolin. Column (a) represents non-carbonated sample, and column (b) represents carbonated specimen. Note: white patches represents calcium carbonate particles as inferred using scanning electron microscopy (Section 4.4.7). The red circles mark areas where amorphous calcium carbonate is formed. ....	109
Figure 4.17: XRCT image of 8% calcium hydroxide 10% air voids treated kaolin (a) carbonated sample (b) threshold showing black background (non- CaCO <sub>3</sub> ), and white foreground (CaCO <sub>3</sub> ) after application of threshold intensity of 125. Note: white patches represents calcium carbonate particles as inferred using scanning electron microscopy (Section 4.4.7).....	110
Figure 4.18: XRCT image of 8% calcium hydroxide 10% air voids treated kaolin (a) carbonated sample (b) image showing white background (solid material), and black foreground (voids) after application of threshold intensity of 88. Note: black patches represents voids, white patches represents solid material. ....	111
Figure 4.19: Calcium carbonate content relationship with sample slices of carbonated treated kaolin. Note: threshold values are given in parentheses. L represents percentage calcium hydroxide content; AV represents percentage air void content.....	112
Figure 4.20: Detected calcium carbonate in treated kaolin clay using XRCT. Note: XRCT represents X-ray computed tomography. Average of 90 slices per sample. ....	112
Figure 4.21: Relationship between calcium carbonate contents obtained from XRCT and from calcimeter analysis for samples at 3% air voids, 10% air voids and 25% air voids content. Note: XRCT represents X-ray computed tomography. ....	114
Figure 4.22: Reduction in voids content relationship with calcium hydroxide (Ca(OH) <sub>2</sub> ) content in carbonated treated kaolin using XRCT. Note: XRCT Represents X-ray Computed Tomography.....	117
Figure 4.23: Broken section of 8L10AV carbonated treated kaolin (a) Spots Point 0= CaCO <sub>3</sub> .....	118
Figure 4.24: Broken section of 8L10AV carbonated treated kaolin, spots: Point 1= CaCO <sub>3</sub> , Point 2= CaCO <sub>3</sub> . L= Percentage Ca(OH) <sub>2</sub> content, AV= Air voids content .....	119
Figure 4.25: Polished Section of 8L10AV Carbonated treated kaolin, Spot Point 3= CaCO <sub>3</sub> , L= Percentage Ca(OH) <sub>2</sub> content, AV= Air Voids Content .....	119
Figure 4.26: Elemental Analysis Points 0-3 from Figure 4.23-4.25. ....	120
Figure 5.1: Variation in degree of carbonation with calcium hydroxide content in treated kaolin (error bars are based on one standard deviation).....	128
Figure 5.2: Degree of carbonation development as a function of calcium oxide treatment in the current study and magnesium oxide treatment after Yi <i>et al.</i> (2013; 2015).....	130
Figure 5.3: Two stages of the degree of carbonation at constant calcium oxide content. ....	131
Figure 5.4: Reduction in air voids as a function of carbonation of calcium oxide treated kaolin clay in the current study and magnesium oxide treated lean clay soil produced by Yi <i>et al.</i> (2015). ....	133
Figure 5.5: Strength improvements as a function of increasing air voids for carbonated specimens.....	134
Figure 5.6: Conceptual model of a carbonation process considered to occur in calcium hydroxide treated kaolin clay (kaolin clay: grey particles; calcium hydroxide [Ca(OH) <sub>2</sub> ]: black circle; calcium silicate hydrate (CSH) plus calcium aluminate hydrate (CAH): orange particles; calcium carbonate (CaCO <sub>3</sub> ): green particles). ....	141

Figure 5.7: Typical reconstructed 2-d calcium carbonate formation as a function of air voids content detected using XRCT analysis for carbonated 8% calcium hydroxide treated kaolin (a) 3% air voids content (b) 10% air voids content. Note: white patches represents calcium carbonate grains as suggested by scanning electron microscopy (Section 4.4.7). .....	143
Figure C1: Procedure used for XRCT data processing (using ImageJ software) (Adapted from Beckett et al., 2013). .....	183
Figure C2.1: XRCT Image of 4% calcium hydroxide 3% air voids treated kaolin (a) carbonated sample (b) threshold image showing black background (non-calcium carbonate), and white Foreground (calcium carbonate) (c) threshold intensity of 31 on histogram.....	184
Figure C2.2: XRCT image of 4% calcium hydroxide 10% air voids treated kaolin (a) carbonated sample (b) threshold image showing black background (non-calcium carbonate), and white foreground (calcium carbonate) (c) threshold intensity of 80 on histogram.....	185
Figure C2.3: XRCT image of 4% calcium hydroxide 25% air voids treated kaolin (a) carbonated sample (b) threshold image showing black background (non-calcium carbonate), and white foreground (calcium carbonate) (c) threshold intensity of 41 on histogram.....	186
Figure C2.4: XRCT image of 6% calcium hydroxide 3% air voids treated kaolin (a) carbonated sample (b) threshold image showing black background (non-calcium carbonate), and white foreground (calcium carbonate) (c) threshold intensity of 49 on histogram.....	187
Figure C2.5: XRCT image of 6% calcium hydroxide 10% air voids treated kaolin (a) carbonated sample (b) threshold image showing black background (non-calcium carbonate), and white foreground (calcium carbonate) (c) threshold intensity of 50 on histogram.....	188
Figure C2.6: XRCT image of 6% calcium hydroxide 25% air voids treated kaolin (a) carbonated sample (b) threshold image showing black background (non-calcium carbonate), and white foreground (calcium carbonate) (c) threshold intensity of 48 on histogram.....	189
Figure C2.7: XRCT image of 8% calcium hydroxide 3% air voids treated kaolin (a) carbonated sample (b) threshold image showing black background (non-calcium carbonate), and white foreground (calcium carbonate) (c) threshold intensity of 46 on histogram.....	190
Figure C2.8: XRCT image of 8% calcium hydroxide 10% air voids treated kaolin (a) carbonated sample (b) threshold image showing black background (non-calcium carbonate), and white foreground (calcium carbonate) (c) threshold intensity of 125 on histogram.....	191
Figure C2.9: XRCT image of 8% calcium hydroxide 25% air voids treated kaolin (a) carbonated sample (b) threshold image showing black background (non-calcium carbonate), and white foreground (calcium carbonate) (c) threshold intensity of 61 on histogram.....	192
Figure C2.10: XRCT image of 4% calcium hydroxide 3% air voids treated kaolin (a) carbonated sample (b) threshold image showing white background (solid material), and black foreground (voids) (c) threshold intensity of 15 on histogram. Note: Black patches represents voids, white patches represents solid material.....	193
Figure C2.11: XRCT image of 4% calcium hydroxide 10% air voids treated kaolin (a) carbonated sample (b) threshold image showing white background (solid material), and black foreground (voids) (c) threshold intensity of 51 on histogram. Note: Black patches represents voids, white patches represents solid material.....	194

Figure C2.12: XRCT image of 4% calcium hydroxide 25% air voids treated kaolin (a) carbonated sample (b) threshold image showing white background (solid material), and black foreground (voids) (c) threshold intensity of 25 on histogram. Note: Black patches represents voids, white patches represents solid material. ....195

Figure C2.13: XRCT image of 6% calcium hydroxide 3% air voids treated kaolin (a) carbonated sample (b) threshold image showing white background (solid material), and black foreground (voids) (c) threshold intensity of 30 on histogram. Note: Black patches represents voids, white patches represents solid material. ....196

Figure C2.14: XRCT image of 6% calcium hydroxide 10% air voids treated kaolin (a) carbonated sample (b) threshold image showing white background (solid material), and black foreground (voids) (c) threshold intensity of 35 on histogram. Note: Black patches represents voids, white patches represents solid material. ....197

Figure C2.15: XRCT image of 6% calcium hydroxide 25% air voids treated kaolin (a) carbonated sample (b) threshold image showing white background (solid material), and black foreground (voids) (c) threshold intensity of 31 on histogram. Note: Black patches represents voids, white patches represents solid material. ....198

Figure C2.16: XRCT image of 8% calcium hydroxide 3% air voids treated kaolin (a) carbonated sample (b) threshold image showing white background (solid material), and black foreground (voids) (c) threshold intensity of 27 on histogram. Note: Black patches represents voids, white patches represents solid material. ....199

Figure C2.17: XRCT image of 8% calcium hydroxide 10% air voids treated kaolin (a) carbonated sample (b) threshold image showing white background (solid material), and black foreground (voids) (c) threshold intensity of 88 on histogram. Note: Black patches represents voids, white patches represents solid material. ....200

Figure C2.18: XRCT image of 8% calcium hydroxide 25% air voids treated kaolin (a) carbonated sample (b) threshold image showing white background (solid material), and black foreground (voids) (c) threshold intensity of 88 on histogram. Note: Black patches represents voids, white patches represents solid material. ....201

## List of Tables

Table 2.1: Carbon dioxide removal methods (adapted from Shepherd, 2009).....	12
Table 2.2: A possible categorization of responses to anthropogenic climate change along with their attributes (adapted from Boucher <i>et al.</i> , 2014).....	16
Table 2.3: Plasticity changes in lime-treated kaolin (after Vitale <i>et al.</i> , 2016). LL represents liquid limit, PL represents the plastic limit, PI represents the plasticity index.....	20
Table 2.4: Determination of lime requirements for soil stabilisation using Eades and Grim pH test and UCS test (after Cherian <i>et al.</i> , 2016). MC represents microclay, and NBT represents sodium bentonite.....	24
Table 2.5: Strength requirement for stabilised material for suitability in pavement layers in the Road Note 31 (after Sherwood, 1993). .....	29
Table 2.6: Geotechnical properties of untreated and lime-treated FoCa (high-plastic montmorillonite) clayey soil (after Al-Mukhtar <i>et al.</i> , 2012).....	30
Table 2.7: Calcium carbonate formation due to carbonation of lime in treated clays.....	38
Table 2.8: Comparison of per cent loss of strength on carbonation in the soil-cement and soil-lime mixtures (after Bagonza <i>et al.</i> , 1987). NC represent normal curing, HC represents high carbon curing.....	39
Table 2.9: Geotechnical properties of untreated and lime-treated FoCa (high-plastic montmorillonite) clayey soil (after Al-Mukhtar <i>et al.</i> , 2012).....	41
Table 2.10: Techniques for confirmation and quantification of carbonates.....	50
Table 3.1: Compaction testing data. ....	62
Table 3.2: Target sample properties. Please note that part of the data is a replication of Table 3.1 and is included here for ease of reading.....	66
Table 3.3: Calcimeter standards. ....	74
Table 3.4: List of carbonated and non-carbonated samples tested.....	77
Table 4.1: Results of cation exchange capacity of kaolin at pH of 8.1 (average of two samples). Analytical errors represent 1 standard deviation. ....	88
Table 4.2: Theoretical vs experimental calcimeter analysis values.....	96
Table 4.3: Calcium carbonate from TGA analysis vs theoretical amount for sample at 10% air voids content. ....	98
Table 4.4: Unconfined compressive strength of saturated carbonated and saturated non-carbonated kaolin specimen (average results based on three tests per mix).....	100
Table 4.5: Average unconfined compressive strength and freeze-thaw durability (average results based on three tests per mix). ....	105
Table 4.6: List of carbonated and non-carbonated samples tested.....	106
Table 4.7: Results of calcium carbonate content determined by image analysis using XRCT.....	113
Table 4.8: Comparison of calcium carbonate content from TGA, calcimeter and XRCT analysis for sample at 10% air voids content.....	115
Table 4.9: Voids contents and reduction in voids of samples after carbonation.....	116
Table 5.1: Degree of carbonation and percentage uncarbonated calcium hydroxide.....	129
Table 5.2: Strength improvement with air voids content. ....	134
Table 5.3: Compressive strength improvement due to carbonation of treated kaolin relatively to treated kaolin (average results based on three tests per mix). Part of the data is a replication of Table 4.4. ....	137
Table 5.4: Projects with stabilised capping layers (after Sherwood, 1992) (continues overleaf).....	146
Table 5.5: Carbon capture potential in treated kaolin using combined modification and carbonation technique based on the UK and Global lime production data (continues overleaf). ....	149

Table A1: Chemical properties and particle size distribution of kaolin (Polwhite E) provided by supplier, Imerys Performance Minerals (2008). .....	178
Table A2: Physical and chemical properties of lime as used in the study .....	178
Table A3: Chemical properties of sodium carbonate as used in the study .....	180
Table B1: Atterberg Limits of calcium hydroxide mixed kaolin.....	181
Table B2: Mechanical and chemical properties of kaolin (Polwhite E) as used in current study .....	182
Table D1: The determination of global CO <sub>2</sub> emissions from lime production using annual lime production, based on the global CO <sub>2</sub> emissions from cement production. ....	202

## List of Abbreviations

Abbreviation	Meaning
$\text{Al}_2\text{O}_3$	Alumina
AV	Air voids content
BECS	Bioenergy with carbon dioxide capture and sequestration.
Ca	Calcium
CaO	Calcium oxide/quicklime
$\text{CaCO}_3$	Calcium carbonate, calcite
CAH	Calcium aluminate hydrate
CASH	Calcium aluminate silicate hydrate
$\text{Ca}(\text{OH})_2$	Calcium hydroxide/slaked lime/hydrated lime
CBR	California bearing ratio
CCS	Carbon capture and storage
CCR	Carbon-climate responses
CDR	Carbon dioxide removal
CEC	Cation exchange capacity
$\text{CH}_4$	Methane
CKD	Cement kiln dust
$\text{CO}_2$	Carbon dioxide
CMIP5 – ESMs	Earth system models from coupled model intercomparison project phase 5
CSH	Calcium silica hydrate
CT	Computed tomography
$\text{C}_4\text{A}\bar{\text{C}}\text{H}$	Calcium carboaluminate hydrate
C&D	Construction and demolition
DTA	Differential thermal analysis
D – GGR	Territorial or domestic removal of atmospheric $\text{CO}_2$ and other Long-lived greenhouse gases.
DOC	Degree of carbonation
DSC	Differential scanning calorimetry
EC	Electrical conductivity
ECCP	European climate change programmes
EDX	Energy-dispersive X-ray spectroscopy

EE	Embodied energy
ESCM	Earth system climate model
ESEM	Environmental scanning electron microscope
EMIC	Earth system models of intermediate complexity
FESEM	Field emission scanning electron microscopy
F – T	Freeze-thaw.
GGBS	Ground granulated blast-furnace slag
GHG	Greenhouse Gas
$G_s$	Specific gravity
HC	High carbon
HT	High temperature
ICL	Initial consumption of lime
IPCC	Intergovernmental Panel on Climate Change
KLT	Lime-treated kaolin
KUT	Untreated kaolin
LFS	Ladle furnace basic slag
LH	Low humidity
LL	Liquid limit
LOC	Lower Oxford Clay
MC	Microclay
MCCS	Mineral carbon capture and storage
MDD	Maximum dry density
MDSAL	Method for determining stabilization ability of lime
Mg	Magagram
$MgCO_3$	Magnesium carbonate
$MgO$	Magnesium oxide or magnesia
$Mg(OH)_2$	Magnesium hydroxide
NBT	Sodium bentonite
$Na_2CO_3$	Sodium carbonate
NC	Normal curing
OLC	Optimum lime content
OMC	Optimum moisture content
PFA	Pulverised fly ash
PI	Plasticity index

PL	Plastic limit
Ppmv	Parts per million by volume
PSD	Particle size distribution
QMS	Quadrupole mass spectrometer
SEM	Scanning electron microscope
SiO <sub>2</sub>	Silica
SRM	Solar radiation management
SS	Steel slag
TEM	Transmission electron microscopy
TGA	Thermogravimetric analysis
TG	Thermo-gravimetric
TG – DSC	Thermogravimetric – differential scanning calorimetry
UCS	Unconfined compressive strength
UNFCCC	United Nations Framework Convention on Climate Change
w	Moisture/water content
WSA	Wastepaper sludge ash
XL30ESEM	FEI XL30 environmental scanning electron microscope
XRCT	X-ray computed tomography
XRD	X-ray diffraction
XRF	X-ray fluorescence
$\rho_b$	Bulk density
$\rho_d$	Dry density
$\rho_w$	Water density
$\rho_z$	Particle density of mixed calcium hydroxide and kaolin



# Chapter 1 – Introduction

## 1.1 Research Context

Climate change is one of the major challenging environmental concerns worldwide. This problematic issue is mainly caused by anthropogenic (human-induced) release of greenhouse gas to the atmosphere (IPCC, 2013). Although carbon dioxide (CO<sub>2</sub>) is not the only greenhouse gas, and others (such as methane and nitrogen oxides) have greater warming potential, it is the most abundant anthropogenic produced greenhouse gas and has the greatest concentration in the atmosphere (IPCC, 2013).

Climate change is likely to impose pressure on human infrastructure and ecosystem services. Increase in atmospheric concentrations of CO<sub>2</sub> is likely to cause increases in the intensities, duration and frequencies of heat waves and warm spells associated with increases in global temperatures due to global warming (IPCC, 2013). This would result in an increase in the frequency and magnitude of extreme events, such as drought or heavy rainfall, and rise in sea level due to accelerated ice sheet disintegration. The effect of these pressures would have impact on the environment such as increases in risk of flooding and subsequent people displacement, threat to food security (Lobell and Tebaldi, 2014), risk of increases in heat-related illness and disease, threat to wildlife and risks of increased storm damage (Butler, 2016). Climate change also potentially poses threats to the sustainability of engineering infrastructure and in particular soil based constructed infrastructure such as embankments, and pavements (Meyer *et al.*, 2014; Dawson *et al.*, 2017). Road embankments are prone to the risk of heave and subsidence if more precipitation falls as rain than snow in winter and spring due to climate change. Additionally, road embankments overlying permafrost are likely to be damaged through settlement and lateral spreading due to permafrost thawing (Meyer *et al.*, 2014; Dawson *et al.*, 2017).

Climate change due to accumulated anthropogenic CO<sub>2</sub> is traceable to the advent of the industrial revolution (IPCC, 2013). The potential threat was globally acknowledged after the unanimous reports from United Nations Framework Convention on Climate Change (UNFCCC) (1992-2009), the Intergovernmental Panel on Climate Change (1990, 1995, 2001, 2007, 2013), and the European Climate Change Programmes (ECCP) (2001-2004, 2005-2009). Atmospheric CO<sub>2</sub> concentrations since the industrial revolution up to March 2017

have increased from 278 parts per million by volume (ppmv) to 400 ppmv, representing about 40 % increase above the pre-industrial levels (NOAA, 2017).

The UNFCCC (most recent proceedings COP20: UNFCCC, 2014), aims to stabilise atmospheric greenhouse gas concentrations at a level that would avoid risky anthropogenic interference with the global climate system, and to do this has set a target of CO<sub>2</sub> concentration below 350 ppmv. The realisation of this commitment requires significant application of direct atmospheric CO<sub>2</sub> removal approaches (IPCC, 2013) in addition to those that aim to reduce emissions. Although technologies of improved energy efficiency, use of non-fossil energy sources and land management are important in mitigating greenhouse gas emissions, short to medium-term reduction of CO<sub>2</sub> in the atmosphere requires technologies that enhance its removal.

Recognising that lime, calcium oxide (CaO) or calcium hydroxide Ca(OH)<sub>2</sub>, is widely used for ground stabilisation, this thesis sets out to determine the potential use of lime treated soil to create a combination of carbon capture and strength improvement that contributes to climate change mitigation as well as improving engineering functions. The research focuses on designing the combination of carbonation and modification reactions within lime-treated soil by compacting clay at a range of air voids contents to create at the same time a carbon capture and other engineering functions. The research uses kaolin, because its mineralogical simplicity avoids interference from effects associated with other clays within a natural soil that might be poorly characterised, and allows the work to be reproduced easily.

Carbonation processes involving chemical binding of CO<sub>2</sub> with calcium (Ca) and magnesium-rich materials in soil to produce stable carbonates have been identified as a viable approach to spontaneous removal of atmospheric CO<sub>2</sub>. A number of studies (Milodwski *et al.* 2011, Lu *et al.*, 2011) have confirmed the occurrence of carbonates over geological time scale, resulting from binding of atmospheric CO<sub>2</sub> with naturally occurring Ca and magnesium minerals. Recent research (Renforth *et al.*, 2009; Renforth, 2011; Washbourne *et al.*, 2012; Washbourne, 2014; Washbourne *et al.*, 2015) has shown the formation of calcium carbonate (CaCO<sub>3</sub>, calcite) in Ca-rich artificial soils at brownfield sites containing construction and demolition (C&D) cement materials, which confirmed significant binding of atmospheric CO<sub>2</sub> with Ca-minerals in the soil. CaCO<sub>3</sub> is now well known to form in both natural and artificial soils (Milodwski *et al.* 2011; Manning *et al.*, 2013).

Earlier and recent laboratory studies have shown that carbonation could take place in lime treated clay (Goldberg and Klein, 1953; Eades and Grim, 1960; Al-Mukhtar *et al.*, 2010; Maubec *et al.*, 2017). A field study (Eades *et al.*, 1962) of lime treated clay has also confirmed the occurrence of  $\text{CaCO}_3$  due to the carbonation process. However lime treated soil is not yet intentionally designed for both engineering and carbon removal functions. This thesis therefore builds on the carbonation reactivity of stabiliser (lime) to optimise its carbonation potential in clay treatment, and not only improve its strength for engineering function but also provide a carbon capture function for climate change mitigation.

## **1.2 Aim and Objectives**

The major aim of this research is to determine whether lime treated clay can capture atmospheric carbon at the same time as improving strength and stiffness.

The above aim is achieved for a range of engineering conditions through the following specific objectives:

- a) To determine the changes in strength of lime modified kaolin clay with and without carbon capture, so defining the engineering benefits.
- b) To determine geochemical and mineralogical characteristics of clay treated with lime for carbonation, to understand the processes involved.
- c) To determine the effect of freeze-thaw (FT) cycles on strength of carbonated lime treated kaolin clay, to consider sensitive environments.
- d) To determine engineering parameters (lime content, air voids content) capable of producing best combined modification and carbonation treatment of kaolin clay, to facilitate application in practice.

## **1.3 Thesis Overview**

A brief overview of the thesis is presented below.

Chapter 2 contains a review of the relevant literature, and pays particular attention to the increase in atmospheric  $\text{CO}_2$  concentrations mainly due to human activities leading to climate change. In addition, the likely impact of climate change on human infrastructure and ecosystem services is reviewed. Also, carbonation of calcium and magnesium rich materials is critically assessed after which the reaction mechanisms of carbonation previously applied to

carbon capture, and modification mechanisms previously applied to strength development description, are reviewed.

Chapter 3 details the methods used for investigation. It contains a description of the geotechnical techniques, particularly the compressive strength techniques used in determining the effects of modification of treatments. In addition it contains an explanation of the geochemical techniques such as the calcimeter and thermogravimetric analysis (TGA), and mineralogical techniques such as scanning electron microscopy (SEM) and X-ray computed tomography (XRCT). These are the volumetric/thermal and image scanning techniques used in assessing the presence and extent of carbonation occurrence in lime treated soil.

Chapter 4 presents the results of strength improvement and  $\text{CaCO}_3$  formation in lime treated clay.

Chapter 5 discusses the design specifications of lime modified clay development based on lime and air voids content at optimal values for modification. Furthermore, it analyses the implication for climate change mitigation of modifying soil for carbon capture.

Finally, Chapter 6 provides the thesis conclusions and recommendations for further development of the presented research.

## Chapter 2 – Literature Review

The first part of this chapter explains the concept of climate change and greenhouse gas effects. Due to the fact that increasing CO<sub>2</sub> concentrations are believed to be linked to climate change, and that has negative effects on human society, mitigation strategies are further discussed in this chapter. In addition, rising populations and increasing urbanisation requires growth in construction, and more use of land that may not have ideal foundation properties. One particular challenge in geotechnical engineering is the weak strength of cohesive soils when used for an engineering function. In view of this, the use of lime-based materials for improvement of clay strength is described. Also, state-of-the-art in geotechnical techniques such as the use of compressive strength testing for clay stability, plasticity testing targeted at clay modification and site workability improvement are explained. The use of FT durability testing for frost resistance is described. Lastly, analytical techniques used for confirmation and quantification of carbonates are reviewed.

### 2.1 Climate Change and Greenhouse Gas Effect

The history of climate change can be traced as far back as the nineteenth century. Arrhenius (1896) published an early study on quantification of increased CO<sub>2</sub> concentrations and climate change. The author observed that molecular CO<sub>2</sub> can absorb long-wave Infra-Red, but not shortwave radiation. When extrapolated to the Earth's surface, Arrhenius (1896) theorised that increases in atmospheric CO<sub>2</sub> concentrations would result in more retention of heat on the global surface leading to global warming.

Even though a number of greenhouse gases have a negative impact on the climate, it is reported that CO<sub>2</sub> constitutes the greatest challenge by contributing the largest component. The proportion of greenhouse gases are namely: fluorinated gases (2.8%), nitrous oxide (6%), methane (10.3%), and carbon dioxide (81%), as shown in Figure 2.1 (US Environmental Protection Agency, 2016).

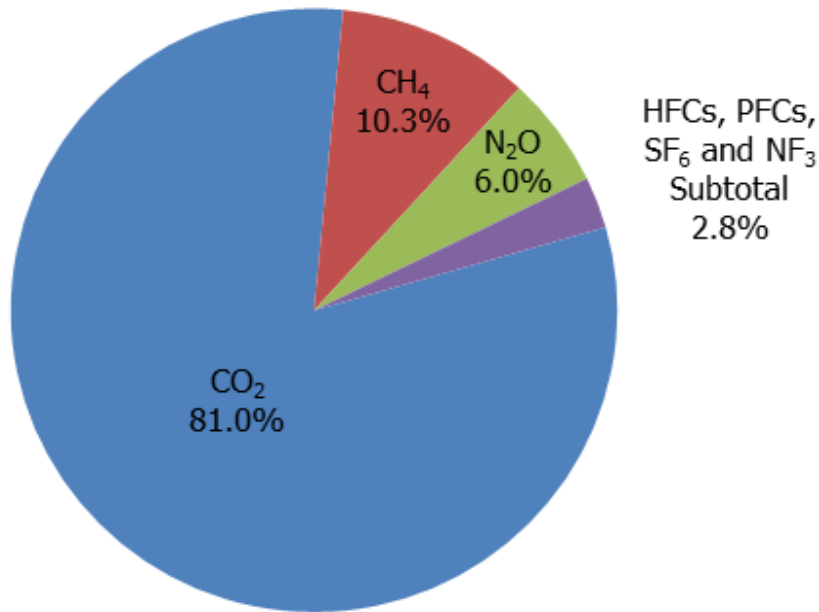


**Figure 2.1:** Greenhouse gas emissions by gas (percentages based on million metric tonnes CO<sub>2</sub> Eq.) (adapted from US Environmental Protection Agency, 2016).

Due to the high percentage of CO<sub>2</sub> emission, it is the focus of this review. CO<sub>2</sub> is emitted to the atmosphere primarily by burning fossil fuels (coal, natural gas and oil, solid waste, wood and tree products amongst others) and certain chemical reactions, including cement manufacture (US Environmental Protection Agency, 2016). The increase in the atmospheric concentrations of CO<sub>2</sub> has been attributed to the advent of industrial revolution (since 1750) (IPCC, 2013). A measurement of atmospheric concentrations of CO<sub>2</sub> since 1958 for nearly 60 years at Mauna Loa, Hawaii, has shown clearly an increase in atmospheric concentrations of CO<sub>2</sub> as presented in Figure 2.2 (NOAA, 2017).

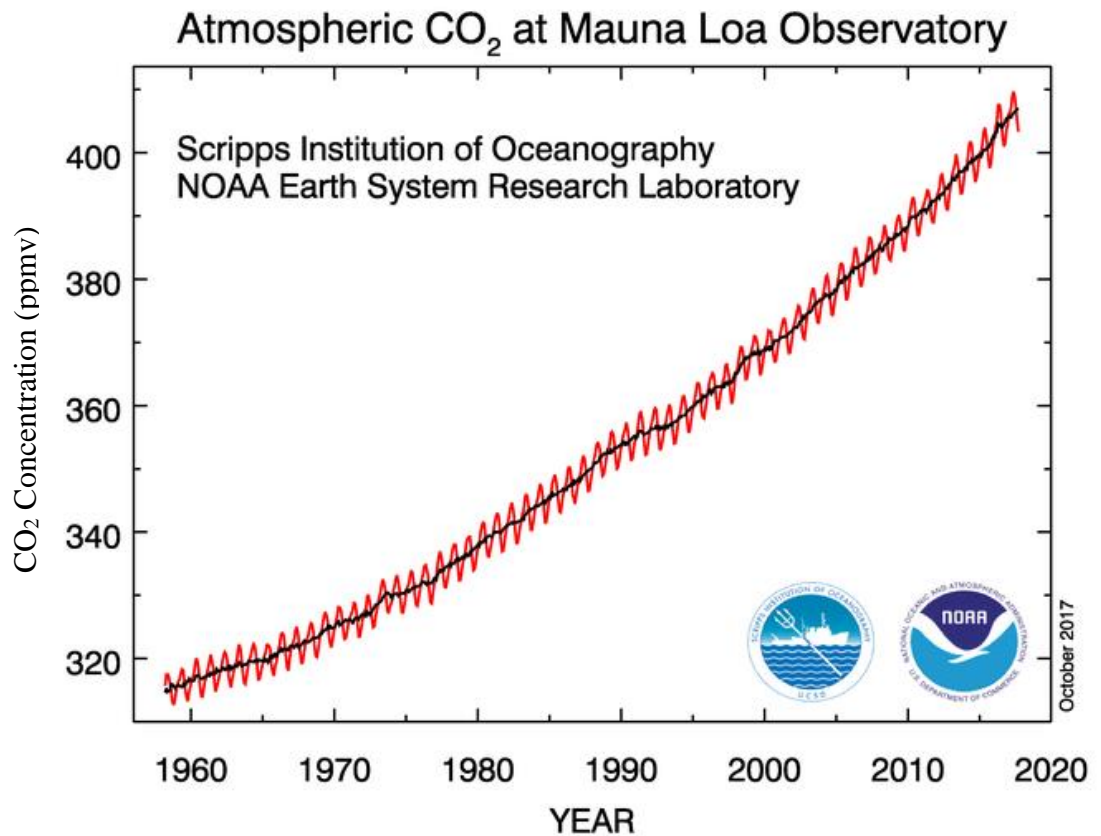


**Figure 2.2:** Measured atmospheric CO<sub>2</sub> concentrations at the Mauna Loa Observatory, Hawaii, since measurement 1958 (adapted from NOAA, 2017).

According to Shepherd (2009), reduction of CO<sub>2</sub> concentrations and other greenhouse gases would in principle mitigate the threat of climate change and the attendant global warming, and other direct damaging consequences, like ocean acidification.

It is well known that cumulative CO<sub>2</sub> is a useful metric in estimating global mean temperature change resulting from anthropogenic CO<sub>2</sub> emission (Allen *et al.* 2009; Matthew *et al.*, 2009). Fundamental research conducted by Allen *et al.* (2009) aimed to determine the relationship between cumulative CO<sub>2</sub> emissions and the peak CO<sub>2</sub>-induced warming, using ensemble simulations of simple climate cycle models (Figure 2.3). The authors found that overall anthropogenic emissions of 1 trillion tonnes carbon (3.67 trillion tonnes of CO<sub>2</sub>), of which approximately half of the carbon has been emitted since industrial era, would result in peak CO<sub>2</sub>-induced warming of approximately 2°C above pre-industrial level. The results show a 5-95% confidence interval of 1.3°C to 3.9°C. They concluded that climate change mitigation policy which focusses on limiting cumulating CO<sub>2</sub> emissions could be more robust to

scientific uncertainties than concentration or emissions rate focuses. Solid red and orange lines in Figure 2.3 show scenarios with cumulative emissions for 1750–2500.

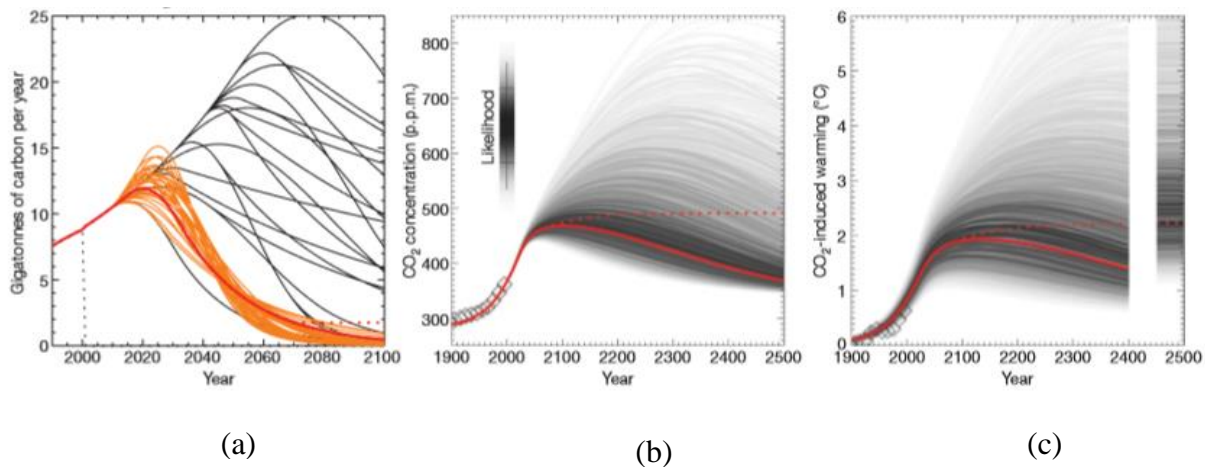


**Figure 2.3:** An ideal carbon dioxide emission settings and response to benchmark scenario. a) CO<sub>2</sub> Emissions. (b) CO<sub>2</sub> concentration response to benchmark c) Temperature response to benchmark scenario (after Allen et al., 2009).

Additionally, Matthew *et al.* (2009) looked at the relationship between carbon-climate responses (CCR), and combined atmospheric CO<sub>2</sub> plus its rate of change in decades to centuries timescale using Earth System Climate Model (ESCM). CCR is described as “the ratio of temperature change to cumulative carbon emissions”. The authors found that CCR is approximately independent of the atmospheric CO<sub>2</sub> concentration, and its rate of change on decades to centuries timescales. The values of CCR could fall from 1.0°C to 2.16°C per trillion tonnes of carbon (TtC) emitted (5th-95th percentiles) (Matthew *et al.*, 2009).

Further research by Frolicher (2016) pointed out that a constant ratio relationship exists between cumulative CO<sub>2</sub> emissions and global temperature change even at emissions greater than 2000 GtC and up to 5,000 GtC, as determined using 4 Earth system models from Coupled Model Intercomparison Project Phase 5 (CMIP5-ESMs) and from 7 Earth system models of intermediate complexity (EMIC). The authors found that a global mean warming temperature of 6.4°C - 9.5 °C could be obtained in response to simulated carbon emissions of up to 5,000 GtC, using the 4 CMIP5-ESMs model (red curve in Figure 2.4). With the use of the 7 coupled EMIC model, a warming temperature of 4.3 to 8.4 °C could be achieved (blue curve in Figure 2.4).

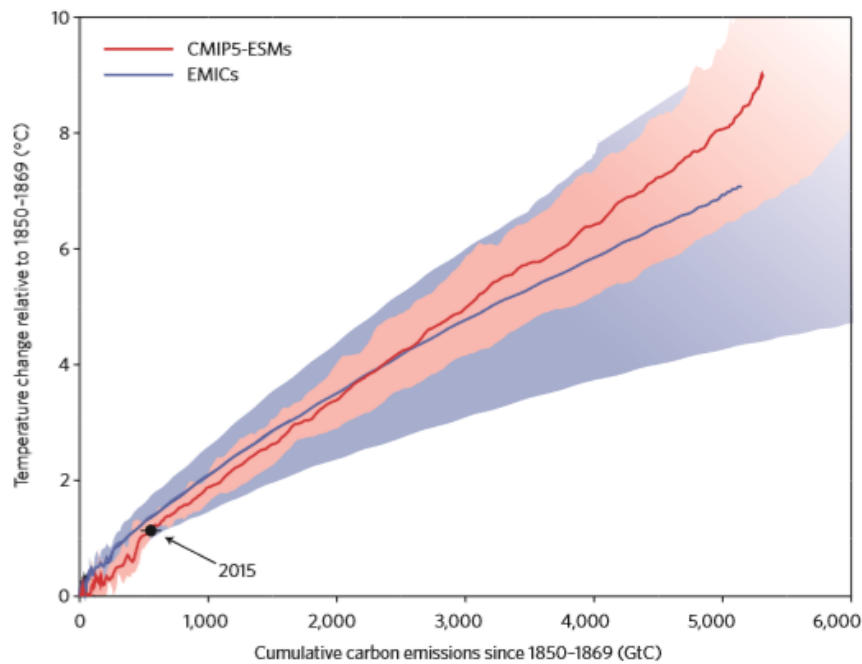


**Figure 2.4:** Changes in mean surface temperature resulting from cumulative carbon emissions per annum based on the RCP8.5-extension scenarios over the period 1850 to 2300 (after Frolicher, 2016).

Partanen *et al.* (2017) determined the extent of the linear relationship between seasonal temperature changes and cumulative CO<sub>2</sub> emissions using an ensemble 12 Earth system models from coupled model intercomparison project phase 5. The authors pointed out that cumulative CO<sub>2</sub> emissions could be used to predict regional and seasonal climate changes in terms of temperature and precipitation. The linear relationship between temperature changes and cumulative CO<sub>2</sub> emissions could be quantified robustly, whilst that between precipitation and cumulative CO<sub>2</sub> emissions could not be quantified robustly due to internal inconsistency of precipitation.

Increasing levels of atmospheric CO<sub>2</sub> concentrations have put ecosystems and humans at risk. Ecosystems such as shallow and warm water coral reefs, and the people who depend on them have been put to risk due to increasing atmospheric CO<sub>2</sub> concentration, and attendant environmental stresses (Pendleton *et al.*, 2016). Increased atmospheric CO<sub>2</sub> concentrations could cause ocean acidification, elevated sea surface temperature, followed by coral bleaching and related mortality (Pendleton *et al.*, 2016).

The negative effects of climate change cannot be overemphasised. Flooding and droughts are obvious negative effects of climate change when dealing with world's water system (Arnell and Gosling, 2016). The increase acidification of oceans and seas is attributed to the huge quantity of CO<sub>2</sub> that they have absorbed from the atmosphere (Raven *et al.*, 2005).

Climate change has caused damage to the government, individuals and engineering facilities world-wide even in the UK. Sanders and Phillipson (2003) explained these negative impacts include flooding, wind damage, driving rain impact, and effects on clay soil buildings. According to Sanders and Phillipson (2003) between 1975 to 1998, as shown in Figure 2.5, the UK has lost billions of pounds based on the number of insurance claims due to heave and subsidence damage. As point of emphasis in 1991 alone, the UK lost almost £500 million due to these claims (Sanders and Phillipson, 2003). This shows that climate change poses a real threat to the economy of the UK and other countries as well.

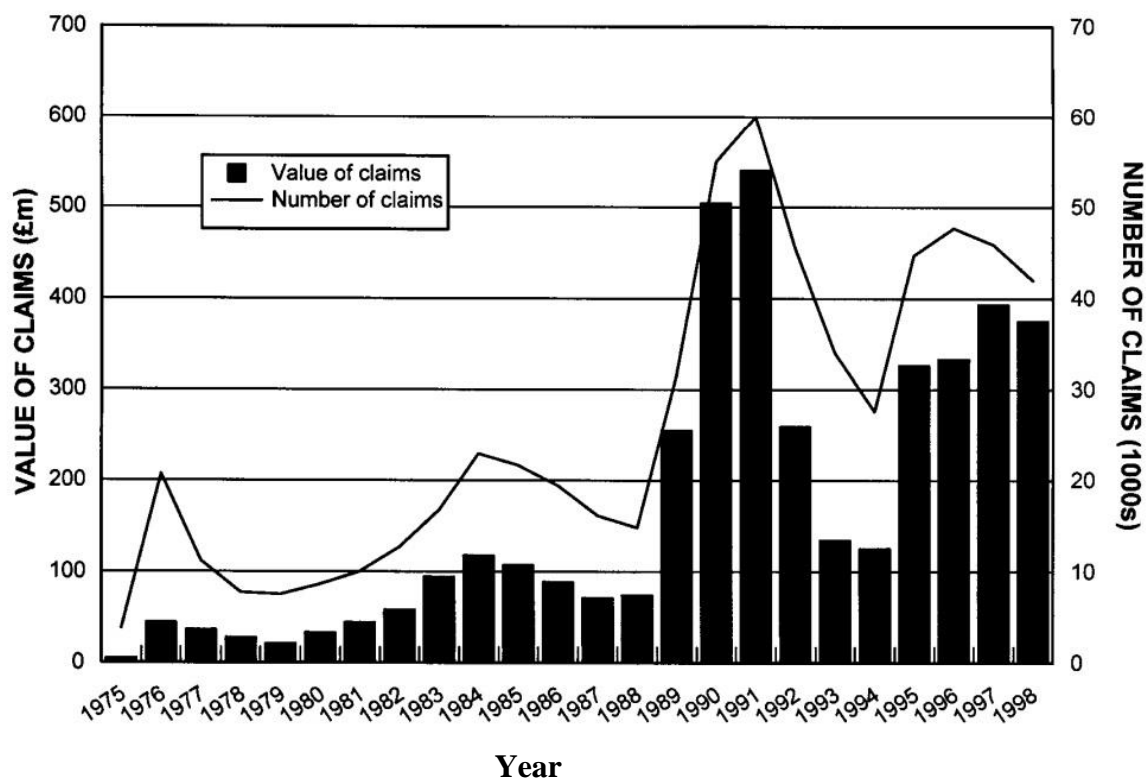


**Figure 2.5:** Trend in claims for heave and subsidence damage to domestic properties (adapted from Sanders and Phillipson, 2003).

On a global scale, the field of geoengineering is concerned with making deliberate changes to environment. These changes are targeted at reducing atmospheric CO<sub>2</sub> concentrations, in order to mitigate climate change usually caused by human activities (Keith, 2000; Dorr, 2016).

The concept of ‘geoengineering’ was originally defined in relation to a proposal for collection of CO<sub>2</sub> at the power station, injecting it into deep ocean, with sufficient storage capacity, as a mitigation strategy to address excess atmospheric CO<sub>2</sub> concentrations. However the concept has been currently defined by Shepherd (2009) to include all the techniques which focus on

large-scale modification of Earth’s climate system, for the mitigation of climate change or control of energy balance. Geoengineering is now described as “the deliberate large scale intervention in the Earth’s climate system, in order to moderate global warming” (Shepherd, 2009). His report classified geoengineering into 2 main groups: CO<sub>2</sub> removal (CDR) and solar radiation management (SRM) methods, as presented in Figure 2.6. SRM techniques aim at reducing the warming effect of climate change, by reducing the net amount of solar radiation reaching the Earth system. CDR approaches seek to remove atmospheric CO<sub>2</sub> by either increasing natural removal or engineering a new carbon sink. CDR techniques are beneficial because they seek to tackle the root cause of climate change, plus its consequences (Shepherd, 2009). The proposed method of combined modification and carbonation of lime treated clay as described in this thesis, when conducted at large (national or regional) scale, is closely related to ‘CO<sub>2</sub> air capture’ as presented in Figure 2.6. The proposed method aims to reduce atmospheric CO<sub>2</sub> for climate change mitigation similar to the CO<sub>2</sub> air capture approach. Additionally, the proposed method seeks to permanently store carbon as CaCO<sub>3</sub> in soil, whilst the ‘CO<sub>2</sub> air capture’ method seeks to recover captured atmospheric CO<sub>2</sub> for disposal or reuse (Shepherd, 2009).

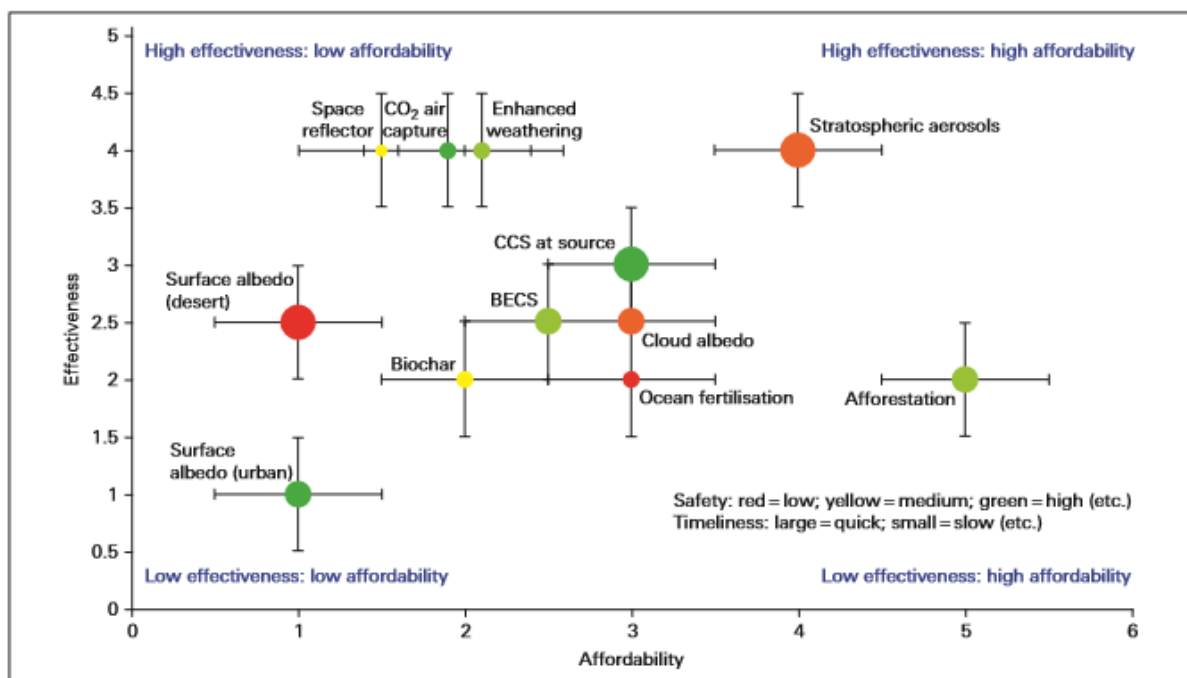


**Figure 2.6:** Preliminary overall evaluation of the geoengineering techniques (after Shepherd, 2009). Note: CCS represents carbon capture and storage, BECS represents bioenergy with CO<sub>2</sub> capture and sequestration.

In the next Section CO<sub>2</sub> mitigation strategies will be reviewed.

## 2.2 Mitigation Approaches for Carbon Dioxide

The IPCC defined mitigation as “technological change and substitution that reduce resource inputs and emission per unit output” (IPCC, 2013). The IPCC third assessment further qualifies mitigation policies to be methods targeted at reducing natural resources or enhancing natural sinks of CO<sub>2</sub> and other related greenhouse gases.

Shepherd (2009) proposed a number of methods for carbon dioxide removal (CDR) from the atmosphere. These includes biological, physical, and chemical methods as presented in Table 2.1 (Shepherd, 2009).

**Table 2.1:** Carbon dioxide removal methods (adapted from Shepherd, 2009).

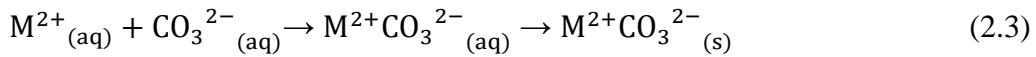
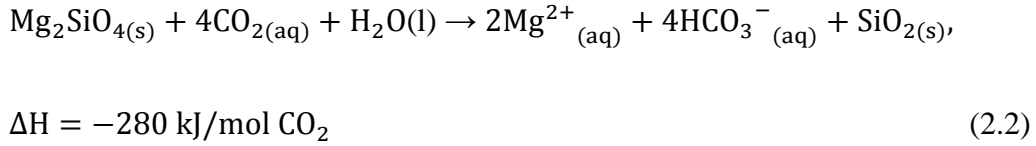
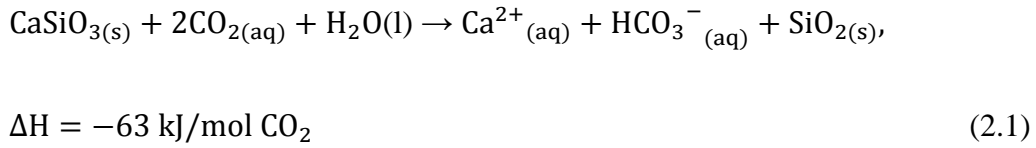
Method	Land
Biological	Afforestation and land use Biomass/fuels with carbon sequestration
Physical	Atmospheric CO <sub>2</sub> scrubbers (‘air capture’)
Chemical (‘enhanced weathering’ techniques)	In-situ carbonation of basic silicate minerals (incl. olivine) on soil

The biological method involves the removal and storage of atmospheric CO<sub>2</sub> through plant driven carbonation in a coupled plant-soil system (Zhou *et al.*, 2006; Manning and Renforth, 2012). The physical method aims at CO<sub>2</sub> capture from the atmosphere, transport and storage into underground geologic formations or ocean (Gough *et al.*, 2010; Zhang *et al.*, 2013; Zangeneh *et al.*, 2013).

The chemical method is based on in-situ reaction between CO<sub>2</sub> and basic silicate minerals such as olivine for formation of carbonates (Shepherd, 2009). It is closely related to the carbonation method which involves the reaction of carbon dioxide and cations of calcium or magnesium (Ca<sup>2+</sup> or Mg<sup>2+</sup>) for formation of stable carbonates. The chemical method includes natural, and accelerated (mineral and alkaline solid waste) carbonation

Natural carbonation which could be referred to as weathering, involves the removal of atmospheric CO<sub>2</sub> through the reaction of CO<sub>2</sub> and natural alkaline silicates to form carbonates (Milodowski *et al.*, 2011).

Natural carbonation is chemically represented by Equations 2.1, 2.2 and 2.3.



Atmospheric CO<sub>2</sub> dissolves in rain water to produce weak carbonic acid, which reacts with natural alkaline silicates to leach calcium and magnesium (Ca<sup>2+</sup> and Mg<sup>2+</sup>) cations as represented by Equations 2.1 and 2.2. Negative values for ΔH, the heat of reaction, show that the reactions are energetically favourable. The leached cations (Ca<sup>2+</sup> and Mg<sup>2+</sup>) subsequently crystallise to form carbonates as represented by Equation 2.3.

Lu *et al.* (2011) conducted a study on natural Miocene basalt samples to determine the amount of CO<sub>2</sub> trapped due to natural carbonation reactions. The authors analysed samples of Miocene basalts outcrop in the Kuanhsi-Chutung area of North eastern Taiwan using XRD and electron microprobe. They found that 94.15 kg CO<sub>2</sub> was chemically trapped per 1m<sup>3</sup> of basalt, based on semi-quantitative estimate of 32.58 g CO<sub>2</sub> per kg of basalt.

However, due to the very low concentration of atmospheric CO<sub>2</sub>, between 0.03–0.06 percent, the kinetics of natural carbonation are very slow (Lu *et al.*, 2011), and unable to sufficiently mitigate the increasing atmospheric CO<sub>2</sub> concentration.

Accelerated carbonation was proposed as an alternative to natural carbonation (Seifritz, 1990). Lim *et al.*, (2010) explained accelerated carbonation as a CO<sub>2</sub> removal method in which high-purity CO<sub>2</sub> is artificially injected into alkaline materials to enhance carbonation reaction for the production of stable carbonates in timescale of few hours. Accelerated carbonation is divided into 2 main types. These are mineral carbonation and alkaline solid waste carbonation.

Mineral carbonation involves the removal of CO<sub>2</sub> by the reaction of highly basic (i.e. they have a high content of calcium or magnesium oxide) natural minerals (olivine, wollastonite, and serpentine) and high-purity CO<sub>2</sub> in the presence of high temperature and pressure to produce stable carbonate (Huijgen *et al.*, 2006; Lu *et al.*, 2011). This method has attractive potential to remove large amounts of CO<sub>2</sub>. However, it is energy demanding due to the energy needed for grinding of the feedstock, and that for compression of CO<sub>2</sub> feed to the feedstock slurry, as well as the energy needed to achieve a high temperature (Huijgen *et al.*, 2006, 2007).

Alkaline waste carbonation is a CO<sub>2</sub> removal method which involves a single-step reaction (also referred to as direct carbonation) of high-purity CO<sub>2</sub> with solid alkaline waste for the production of carbonates. Alkaline waste carbonation does not need the extraction of reactive cations, because the cation-containing oxides, hydroxides and silicates are the main reactive phases involved in the process. Some alkaline wastes successfully used in alkaline solid waste carbonation include blast furnace slag, cement kiln dust (CKD), C&D waste, steel slag (SS), and municipal solid waste incinerated ash (Van Gerven *et al.*, 2005; Huntzinger *et al.*, 2009; Chang *et al.*, 2011; Washbourne *et al.*, 2012).

The proposed method as described in Chapter 3 of this thesis aims at enhancing carbonation in lime treated clay for atmospheric carbon capture function alongside strength improvement of engineering function, and fits into the chemical CO<sub>2</sub> removal method as described in Table 2.1.

In terms of policy, according to Boucher *et al.* (2014), response to climate change is classified into five categories as shown in Figure 2.7.

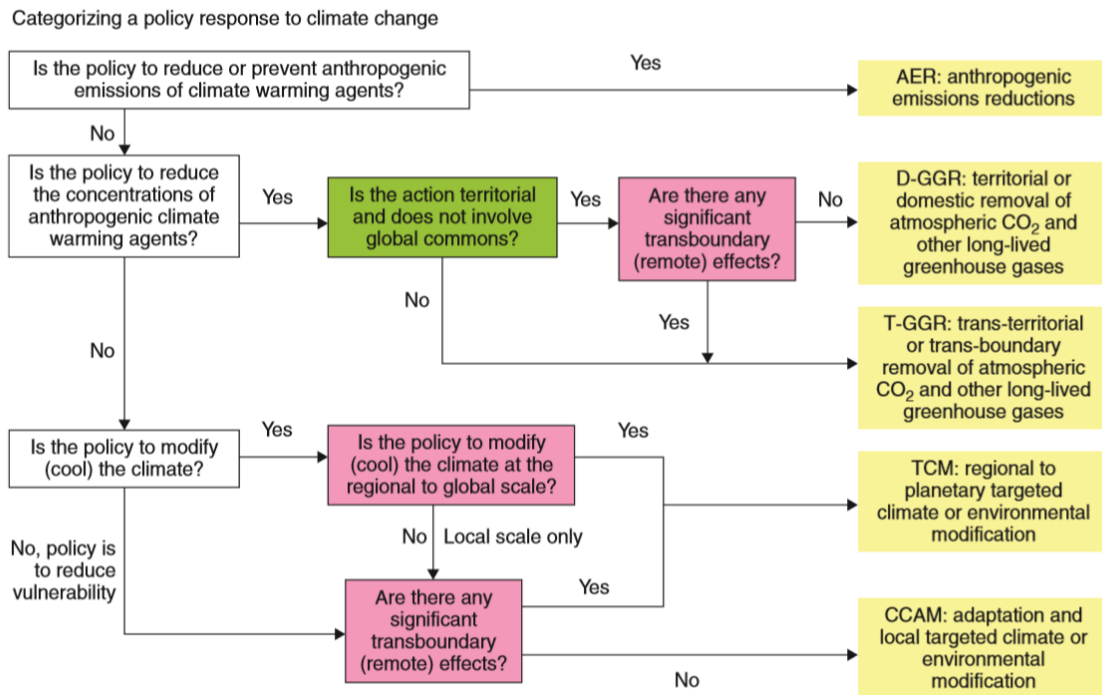


**Figure 2.7:** Flowchart of the proposed categorization of climate change responses (adapted from Boucher *et al.*, 2014).

Boucher *et al.* (2014) further explained the classification of these policies as shown in Table 2.2.

**Table 2.2:** A possible categorization of responses to anthropogenic climate change along with their attributes (adapted from Boucher *et al.*, 2014).

Proposed Name and Acronym	Short Definition	Mapping onto Previous Terminology	Examples	Scale of Action	Scale of Impacts	Impact on the Global Commons*	Trans-Boundary or Transnational Side Effects*	Permanence of the Effect
Anthropogenic emissions reductions (AER)	Initiatives and measures to reduce or prevent anthropogenic emissions of warming agents into the atmosphere	Includes most forms of mitigation but excludes human-induced CO <sub>2</sub> sink enhancement	Improved energy efficiency, reduction in production and/or consumption of goods and services, introduction of renewable energies, nuclear energy, fossil fuel energy with CCS, reducing emissions from deforestation and forest degradation, emission reductions of BC and ozone precursors	Generally a localized action or a sum of localized actions	Global through a decrease in the global-mean RF by greenhouse gases and other warming agents	None expected. Expected to slow down the depletion of fossil fuel resources (except for CCS). Expected to slow down ocean acidification for CO <sub>2</sub> measures	Generally none	Commensurate to the atmospheric lifetime of the species being mitigated, longer if emission reduction is sustained
Territorial or domestic removal of atmospheric CO <sub>2</sub> and other long-lived greenhouse gases (D-GGR)	Removal of CO <sub>2</sub> and long-lived greenhouse gases from the atmosphere operating within national jurisdictions and little consequences outside	Includes territorial CO <sub>2</sub> sink enhancement previously labeled under mitigation, with environmental side effects if any occurring within national jurisdictions	Reforestation, biochar and other means of increasing storage of C in soils, small-scale afforestation, BECCS, CO <sub>2</sub> air capture and storage in territorial (geological) reservoirs, enhanced weathering (without input of by-products into rivers or the oceans)	Generally a localized action or a sum of localized actions	Global through a decrease in the global-mean RF by greenhouse gases	None in the strict sense. May not slow down the depletion of fossil fuel resources. Expected to slow down ocean acidification for CO <sub>2</sub> measures	Possible (e.g., through changes in evaporation, runoff, river flow, changes in biodiversity) but limited	Commensurate with the permanence of the storage medium
Trans-territorial or trans-boundary removal of atmospheric CO <sub>2</sub> and other long-lived greenhouse gases (T-GGR)	Removal of atmospheric CO <sub>2</sub> and long-lived greenhouse gases from the atmosphere operating or having consequences partly or fully across or beyond national jurisdictions	Includes the more environmentally disruptive CDR techniques	Large-scale afforestation, ocean alkalinity, enhanced weathering (with input of by-products into rivers or the oceans), iron fertilization, injection of CO <sub>2</sub> into the ocean	Localized but with significant remote effects and/or diffuse with diffuse effects	Global through a decrease in the global-mean RF by greenhouse gases	Expected (e.g., through changes to the water cycle, rivers, and/or the global ocean). Expected to slow down ocean acidification in the case of CDR methods not involving iron fertilization or ocean injection	Trans-boundary or transnational side effects expected	Commensurate with the permanence of the storage medium

**Table 2.2 Continued**

Proposed Name and Acronym	Short Definition	Mapping onto Previous Terminology	Examples	Scale of Action	Scale of Impacts	Impact on the Global Commons*	Trans-Boundary or Transnational Side Effects*	Permanence of the Effect
Regional to planetary targeted climate or environmental modification (TCM)	Intentional modification of the Earth's energy fluxes in order to offset climate change at the regional to global scale	Essentially what used to be defined as SRM, but excludes small-scale SRM. Excludes removal of long-lived greenhouse gases but includes other large-scale changes to the Earth's energy budget that do not involve long-lived greenhouse gases	Injection of stratospheric aerosols, marine cloud brightening, cirrus suppression, desert brightening on a large scale, ocean heat mixing, modification to Arctic sea ice	Large-scale and/or diffuse (even though the initial action can be local)	Regional to global cooling	Yes (e.g., through the atmosphere and remote climate effects). Does not slow down ocean acidification	Measurable trans-boundary or transnational side effects	Short as this happens through rapidly-responding components of the climate system
Climate change adaptation measures including local targeted climate or environmental modification (CCAM)	Initiatives and measures to reduce the vulnerability of natural and human systems to the effects of climate change. Local risk management	Essentially what is usually considered as adaptation also includes small-scale SRM that only has small if any remote climate impacts	Relocating urban or rural settlements, building dykes, air conditioning, agricultural crop choices, reflective crops, whitening of human settlements on a small scale, irrigation	Local with no or little remote effects	Local	None expected	None, limited to the local scale, or not detectable (i.e., 'within the noise'). Some measures may however affect river flow	Commensurate to the lifetime of the adaptation measure (typically months to decades)

CCS, carbon capture and storage; BECCS, biomass energy with CCS; CDR, carbon dioxide removal; SRM, solar radiation management. RF, radiative forcing; BC, black carbon  
\*Beyond any direct effects due to decreasing concentrations of greenhouse gases and other warming agents.

The proposed method as described in Chapter 3 aims at capturing CO<sub>2</sub> with the aim of improving cohesive soils through combined modification and carbonation process. Based on this purpose, this approach fits into the territorial or domestic removal of atmospheric CO<sub>2</sub> and other long-lived greenhouse gases (D-GGR) classification approach as described in Table 2.2. In the next Section, the use of lime-based material for clay stabilisation will be discussed.

### 2.3 Soil Stabilisation

Clay soils have long been problematic for geotechnical engineering functions, often because of their instability. One way found in literature to tackle this problem is by performing a stabilisation process that involves treatment with lime, as anhydrous CaO, or as Ca(OH)<sub>2</sub>.

Fundamental research was carried out by Bell (1996) which looked at lime stabilisation of clay minerals and soils. Two clay minerals (montmorillonite and kaolinite) were treated with Ca(OH)<sub>2</sub> at a dosage of 2%, 4%, 6%, 8% and 10% by dry mass. He pointed out that clay minerals when treated with Ca(OH)<sub>2</sub> produced an increase in unconfined compressive strength (UCS) (Figure 2.8). As for kaolinite clay, UCS improvement at 28 days curing was approximately 3 times (from 350 kPa to 1050 kPa) compared with the untreated UCS of this clay mineral. A UCS improvement of 6.3 times (from 127kPa to 800 kPa) at 28 days curing was achieved in montmorillonite treatment. Bell (1996) considered that the UCS development resulted from pozzolanic reaction.

Based on UCS results, Bell (1996) noted that a nonlinear relationship exists between lime addition and strength increase after a certain lime addition in one clay (Figure 2.8).

Additionally, the peak UCS could be achieved at lime additions which he called optimum lime content (OLC). Lime additions greater than OLC could result in a decline of the strength gain (Figure 2.8). Strength gain in lime treated clay is mainly due to the reactions between lime and the available clay fraction (Sherwood, 1993). Lime additions in excess of what is needed by the available clay fraction for pozzolanic reaction tends to cause reduction in overall strength gain. This is because lime alone does not possess appreciable cohesion nor friction (Bell, 1996).

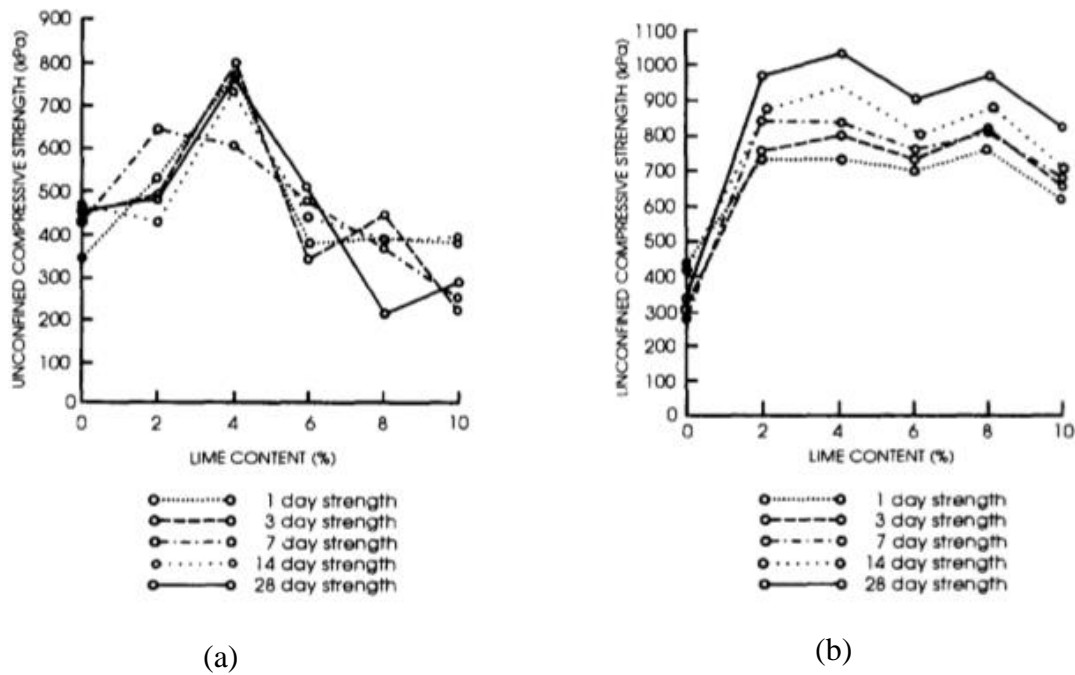


**Figure 2.8:** Unconfined compressive strength (a) montmorillonite with various additions of calcium hydroxide (b) kaolinite with various additions of calcium hydroxide (after Bell, 1996).

Bell (1996) noted that addition of lime to kaolinite and montmorillonite clays results in increases in plastic limit (PL). Changes of PL in montmorillonite are higher compared to those in kaolinite, due to their differing cation exchange capacities. Also plasticity reduces with lime addition to montmorillonite, whilst for lime additions to kaolinite it increases somewhat. He pointed out that clay deposits when treated with lime showed an increase in strength and Young's Modulus. Furthermore, the length of the curing time and temperature has a direct effect on the strength of the soil.

Rogers and Glendinning (1996) determined the lime requirement for clay modification, using a modified initial consumption of lime (ICL) test, and plasticity changes. The authors defined a modified ICL as the minimum amount of CaO at which the pH curve flattens off and a marginal change in pH results from a large change in CaO content. The modified ICL is described later in this thesis. Four British clays were mixed with quicklime (also referred to as CaO), and the graphs of pH, including full pH against lime addition were plotted. Full pH used in this thesis means the pH that corresponds to a stable pH value plotted against lime addition (Rogers and Glendinning, 2000). Based on the interpretation of full pH versus lime addition curve, the authors found the lime requirement for full clay modification to be the CaO content at which the curve approaches asymptote. This CaO content was consistent with the interpretation based on plasticity changes. The authors recommended that lime

requirement for clay modification should be determined using asymptotic interpretation of modified ICL curve or by interpretation based on plasticity changes.

Furthermore, Rogers and Glendenning (1996) determined that PL is the best indicator of lime content required to achieve the desired degree of modification, which could provide firm support in construction activities. They pointed out that the amount of lime required for clay modification is attained at the minimum lime content at which full PL is achieved. The authors' results show that modification of kaolin occurred at 1% CaO (Figure 2.9), whilst that for London Clay it occurred at 3% CaO content (Figure 2.10). The current research adopted the use of full PL for determination of the lime requirement for modification.

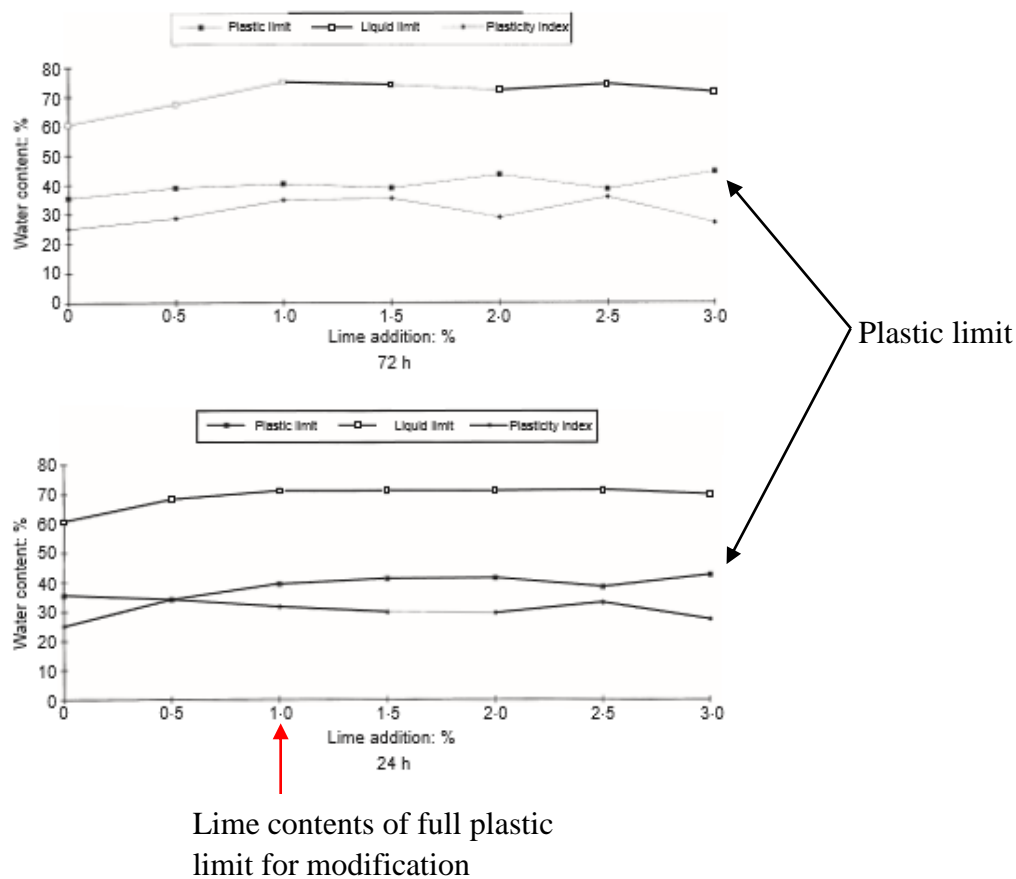


**Figure 2.9:** Plasticity changes due to addition of quicklime to English china clay (kaolin) after 72 and 24 hours (after Rogers and Glendenning, 1996).

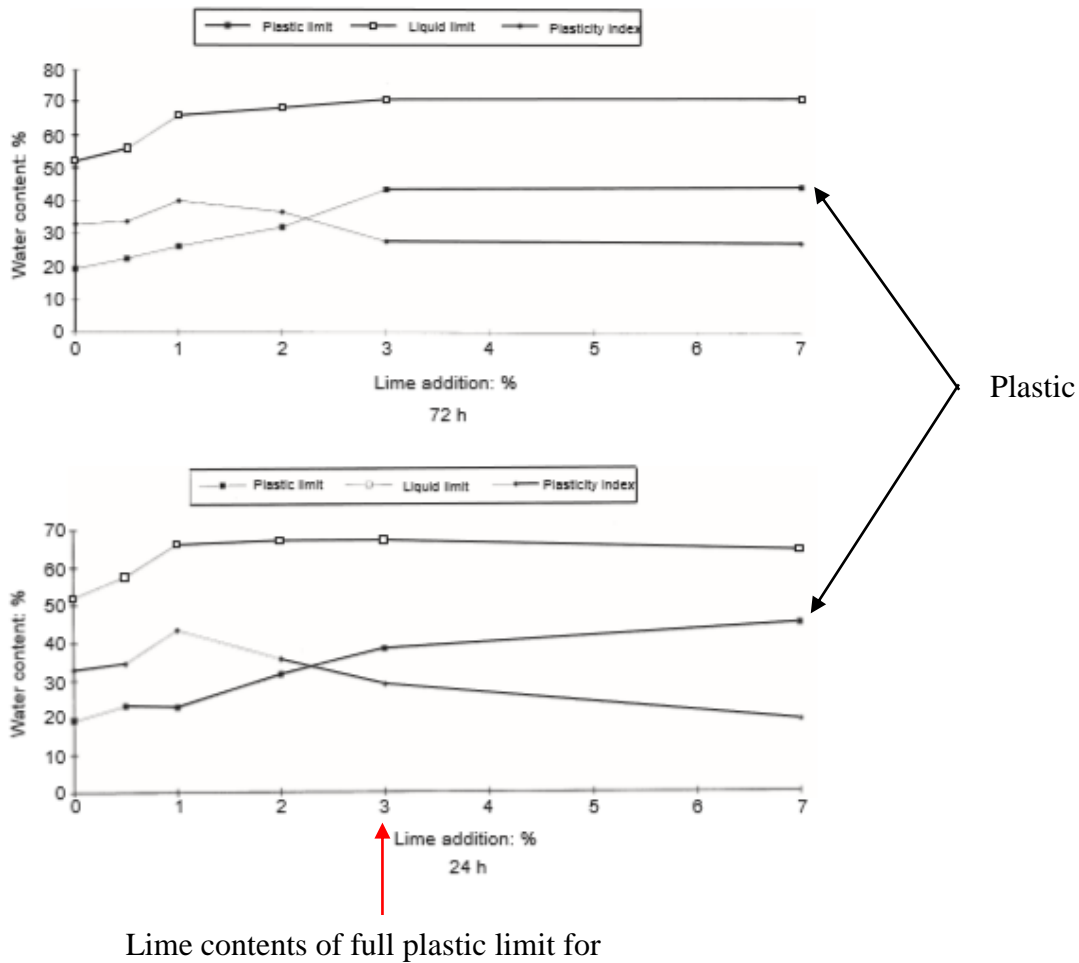


**Figure 2.10:** Plasticity changes due to addition of quicklime to London Clay after 72 and 24 hours (after Rogers and Glendinning, 1996).

Further studies on plasticity changes in 3% CaO (4% Ca(OH)<sub>2</sub> equivalent) mixed kaolin by Vitale *et al.* (2016) showed that the PL increased (from 32% to 43%) compared with untreated kaolin (Table 2.3). Additionally, the LL increased from 70% to 101%. These resulted in increases of PI from 38% to 59%.

**Table 2.3:** Plasticity changes in lime-treated kaolin (after Vitale *et al.*, 2016). LL represents liquid limit, PL represents the plastic limit, PI represents the plasticity index.

Soil sample	pH	LL (%)	PL (%)	PI (%)
Spwt kaolin	46	70	32	38
3% CaO-0 day	12.4	101	43	59
KOH	12.4	52	33	19

Rogers and Glendinning (2000) performed exhaustive research on lime requirement for stabilisation. They pointed out the fact that lime improves the strength and stiffness characteristics of clay soils when used in construction. Again, this approach has advantages of being rapid and very economical. They noticed some inconsistencies in the quantities calculated for the ASTM Standard Test Method for Determining Stabilization Ability of Lime (MDSAL) testing. They revised the interpretation of test data when dealing with lime stabilisation which provided more reliable and consistent results. As mentioned earlier in this section, based on the pH against lime addition curve, Rogers and Glendinning (1996) presented a definition of modified ICL as the minimum amount of CaO content at which the pH curve flattens off and a marginal change in pH results from a large change in CaO content. Rogers and Glendinning (2000) recommended that the lime requirement for soil stabilisation needs to be based on the interpretation of full pH versus lime addition curve, instead of the interpretation based on a specified pH value.

Again, a significant research carried out by Boardman *et al.* (2001), using English china clay (kaolin) and bentonite was targeted at determining time-dependent shear strength improvement, and chemical changes due to CaO additions (only as part of the study). Kaolin was treated with CaO content of 1.5% (the kaolin ICL) value, and 2.5% (above ICL) value. Bentonite was treated with 7.0% (the bentonite ICL) value, and 2.5% (below the bentonite ICL) value. The specimens were compacted to water content of 2% wet of OMC, into a plastic mould, and cured for 7, 175 and 301 days. The specimen were tested for chemical changes using batch leaching tests, and shear strength using shear vane apparatus. Based on determined soluble calcium, aluminium and/or silicon concentrations from element analysis, the authors concluded that “no significant pozzolanic activity (and certainly no crystallisation of reaction products) appears to take place until after 7 days' curing”. The highest corresponding undrained shear strength at 7 days curing for treated kaolin with added 2.5% CaO is approximately 80 kPa (Figure 2.11a). The authors attributed this strength gain to result primarily from cation exchange instead of pozzolanic activity. After 175 days curing, the undrained shear strength increased to 145 kPa. Pozzolanic reaction was noted to have mainly caused the strength increases. This study suggests that at 7 days curing of lime treated kaolin, no pozzolanic reactions are likely to occur.

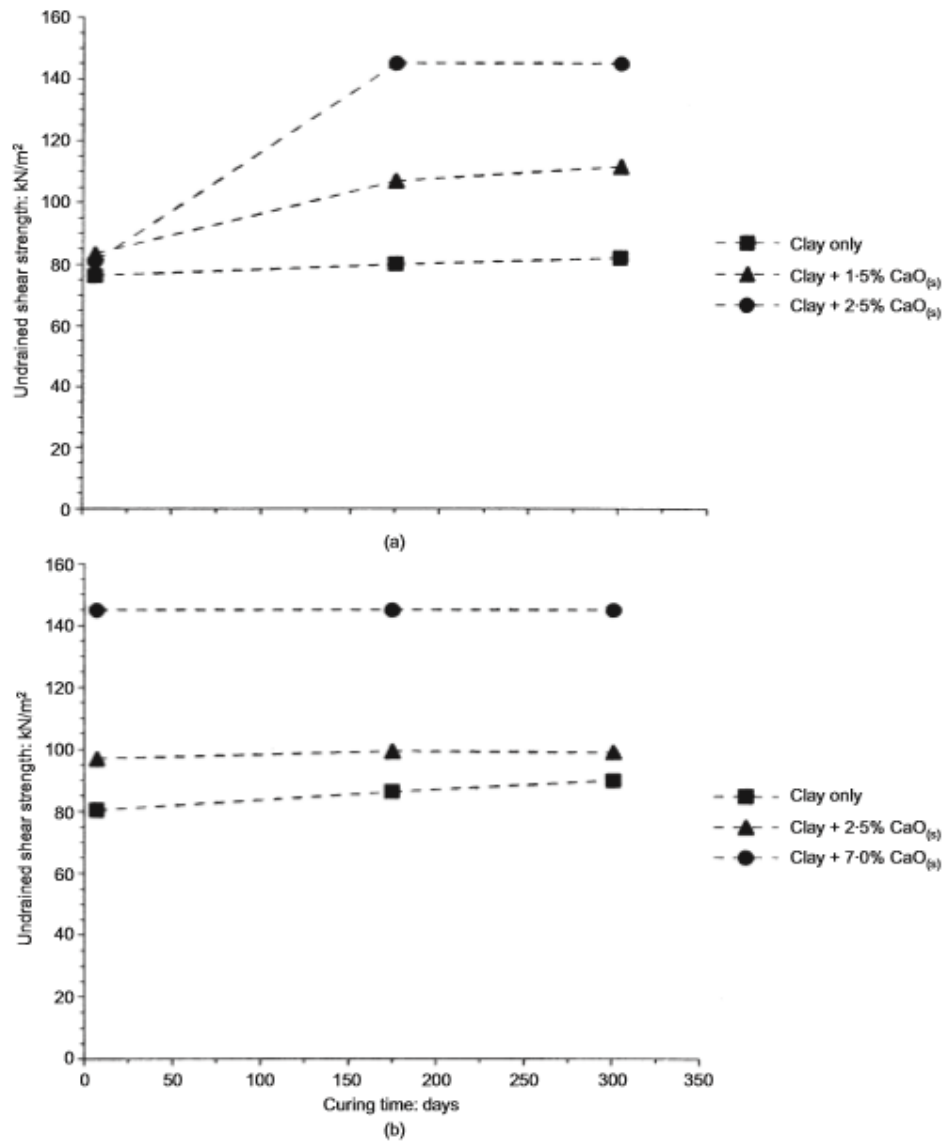


**Figure 2.11:** Variation of undrained shear strength with curing time (a) English china clay (kaolin) (b) bentonite. Shear strength values shown as 145 kN/m<sup>2</sup> are at the measurement limit for the shear vane apparatus and the actual strength may be higher (after, Boardman *et al.*, 2001).

Further significant studies on lime stabilisation were performed by Dash and Hussain (2012), which investigated the OLC requirement for dominant expansive soil, and dominant residual soil. Based on the relationship between UCS and lime additions (Figure 2.12), the authors demonstrated that the amount of clay fraction influences the OLC value. Higher clay fraction in dominant expansive soil resulted in high OLC of 9% CaO (Figure 2.11a), whilst lower clay fraction in residual soil resulted in low OLC of 5% CaO (Figure 2.11b).

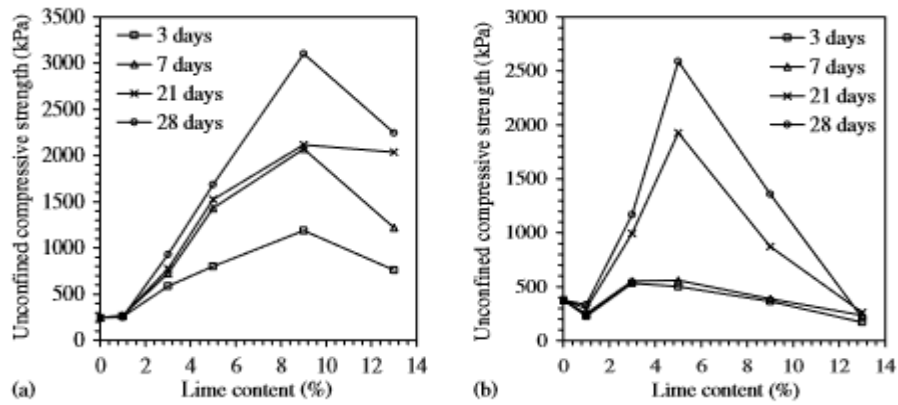


**Figure 2.12:** Variation in unconfined compressive strength (UCS) with lime (as CaO) content (a) highly expansive soil (b) residual soil (after Dash and Hussain, 2012).

Cherian and Arnepalli (2015) conducted a critical assessment of the role of clay mineralogy in lime stabilisation. The authors proposed the need to develop a precise methodology for OLC that would be based on the soil properties, such as clay mineralogy, soil pH, cation exchange capacity (CEC), specific surface area, soil acidity, buffer capacity, and base saturation capacity. Additionally they recommended the use of UCS and California bearing ratio (CBR) for determination of OLC for long term strength development (Cherian and Arnepalli, 2015).

Furthermore, Cherian *et al.* (2016) treated two commercial clays with  $\text{Ca}(\text{OH})_2$  and determined the lime requirements for soil stabilisation using the Eades and Grim pH test in accordance with D4972-13 (ASTM, 2013), and UCS test in accordance with D6276-99a (ASTM, 1999). Lime treated specimens were cured for 28 days prior to UCS testing. The two commercial clays were namely microclay (MC) and sodium bentonite (NBT). MC had activity number of 0.33, whilst NBT had activity number of 5.3 (Cherian *et al.*, 2016). Clays which have activity number  $< 0.75$  are referred to as inactive clays, whilst those having activity number  $> 2$  are referred to as highly active (Barnes, 2010). Cherian *et al.* (2016) determined from experiments conducted at  $25^\circ\text{C}$  that, for MC, the lime requirements for stabilisation using the Eades and Grim pH test and the UCS test were the same, each with the value of 2%  $\text{Ca}(\text{OH})_2$ . However, for NBT, the lime requirement using UCS test (10%  $\text{Ca}(\text{OH})_2$ ) was larger than that (2.7%  $\text{Ca}(\text{OH})_2$ ) obtained using Eades and Grim pH test (Table 2.4).

**Table 2.4:** Determination of lime requirements for soil stabilisation using Eades and Grim pH test and UCS test (after Cherian *et al.*, 2016). MC represents microclay, and NBT represents sodium bentonite.

Soil Type	Temperature (°C)	OLC (%)	
		Eades and Grim test	UCS test
MC	25	2	2
	40	1.7	4
NBT	25	2.7	10
	40	2.2	12

The lime requirement determination using Eades and Grim pH test similar to that used in Cherian *et al.* (2016) is referred to as ‘ICL’ by British Standard (BS 1924: BSI, 1990). For reading convenience, ‘Eades and Grim pH test’ from this point onward will be called ‘ICL test’. The lime requirement determination using UCS test, in which a lime treated specimen is cured for 28 days prior to UCS test, similar to that used in Cherian *et al.* (2016), is referred to as ‘OLC’ by Bell (1996). For reading convenience, the lime requirement determination using UCS test will be referred to from this point on as ‘OLC’. Cherian *et al.* (2016) attributed the same OLC (2% Ca(OH)<sub>2</sub>) value with ICL (2% Ca(OH)<sub>2</sub>) value in MC to its low reactivity (having activity number 0.33). The larger OLC value (10% Ca(OH)<sub>2</sub>) than ICL value (2.7% Ca(OH)<sub>2</sub>), was attributed to its high reactivity (having activity number 5.3). The method described in Chapter 3 of this thesis focussed on the determination of ICL and OLC of kaolin, and to determine whether OLC value is equal or greater than ICL value.

Research by Muhmed and Wanatowski (2013) on lime stabilisation has focussed on the effect of curing time on strength improvement. Kaolin was treated with 5% Ca(OH)<sub>2</sub> (also referred to as hydrated lime) and cured for a period up to 28 days (Figure 2.13). The research demonstrated increases in strength improvement (from 183 kPa to 390 kPa) with increasing curing time (from 0 day to 28 days). The increase in strength was due to formation of cementitious compounds resulting from pozzolanic reactions (Muhmed and Wanatowski, 2013).

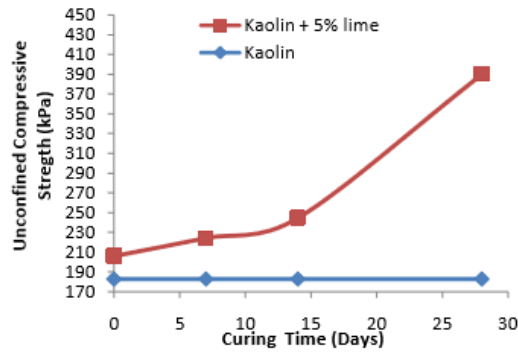


**Figure 2.13:** Influence of curing time on UCS of treated kaolin (after Muhmed and Wanatowski, 2013).

Additionally, Muhmed and Wanatowski (2013) reported that by lime addition (5%  $\text{Ca}(\text{OH})_2$ ), the PL and liquid limit (LL) increased, whilst the plasticity index (PI) decreased (Figure 2.14). The PL increased by 23.6% (from 33.3% to 56.9%), whilst LL increased by 20.6% (from 65.9% to 86.5%) resulting in reduction of PI by 3% (from 32.6% to 29.6%).

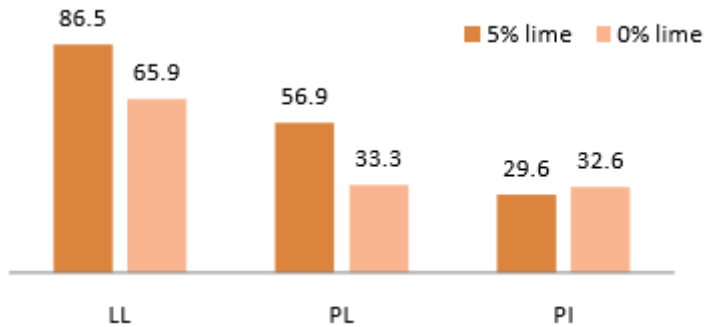


**Figure 2.14:** Atterberg limits at 0% and 5% lime content (after Muhmed and Wanatowski, 2013)

The researchers noted that PL is more important than LL in geotechnical engineering construction work. In order to achieve maximum strength in their study, compaction was performed on soil mixed at optimum moisture content (OMC), which is close to PL. The study compacted 5%  $\text{Ca}(\text{OH})_2$  mixed kaolin, at OMC of 29.9% which is closer to PL of 56.9%, compared to a LL value of 86.5%.

Saeed *et al.* (2015) looked at the effect of curing period on the strength development and minerals formation in lime treated kaolin. The kaolin was treated with 5% and 10%  $\text{Ca}(\text{OH})_2$  by dry mass, and the UCS was determined after 7 days, 14 days, 28 days, 100 days and 200 days curing respectively. Formation of minerals was determined in the 200 days cured treated kaolin using X-ray diffraction (XRD), whilst the presence of cementitious product was determined using Field Emission Scanning Electron Microscopy (FESEM) analysis. The authors showed that curing time influences the strength of lime treated kaolin.

The UCS of 10%  $\text{Ca}(\text{OH})_2$  treated kaolin cured for 200 days increased by approximately 6 times (from approximately 260 kPa to 1500 kPa) compared to that of corresponding non-cured (0 days) treated kaolin (Figure 2.15). Additionally, the authors noted that the increase in strength of 200 days cured treated kaolin was likely influenced by formation of cementitious compound called calcium aluminate silicate hydrate (CASH) due to pozzolanic reaction.

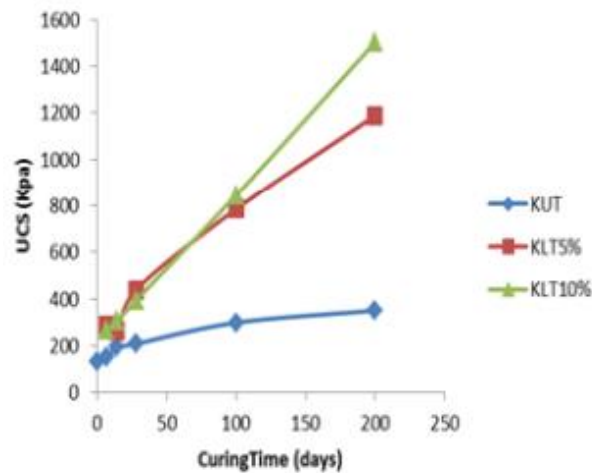


**Figure 2.15:** Effect of curing time on the unconfined compressive strength (UCS) development in  $\text{Ca}(\text{OH})_2$  treated tropical kaolin (after Saeed *et al.*, 2015). KUT represent untreated kaolin, KLT represents lime-treated kaolin.

Recently, Maubec *et al.* (2017) studied the influence of the type of clay on the strength evolution of lime treated material. This study looked at the mechanical behaviours of lime-treated clays. Two clay minerals (kaolin and calcium bentonite) were treated with 10% CaO by dry mass. The researchers noted that the nature of clay minerals influences strength improvement of lime treated clay (Figure 2.16). For CaO treated specimens cured at 20°C for 98 days, higher strength development in calcium bentonite (from 300 kPa to 1500 kPa) was achieved compared to that in kaolin (from 250 kPa to 400 kPa). The strength development was due to formation of secondary phases such as calcium carboaluminate hydrate ( $\text{C}_4\text{A}\bar{\text{C}}\text{H}$ ) in lime treated kaolin, and tetracalcium aluminate hydrate ( $\text{C}_4\text{AH}_{13}$ ) plus calcium silicate hydrate (CSH) in lime treated calcium bentonite (Maubec *et al.*, 2017).

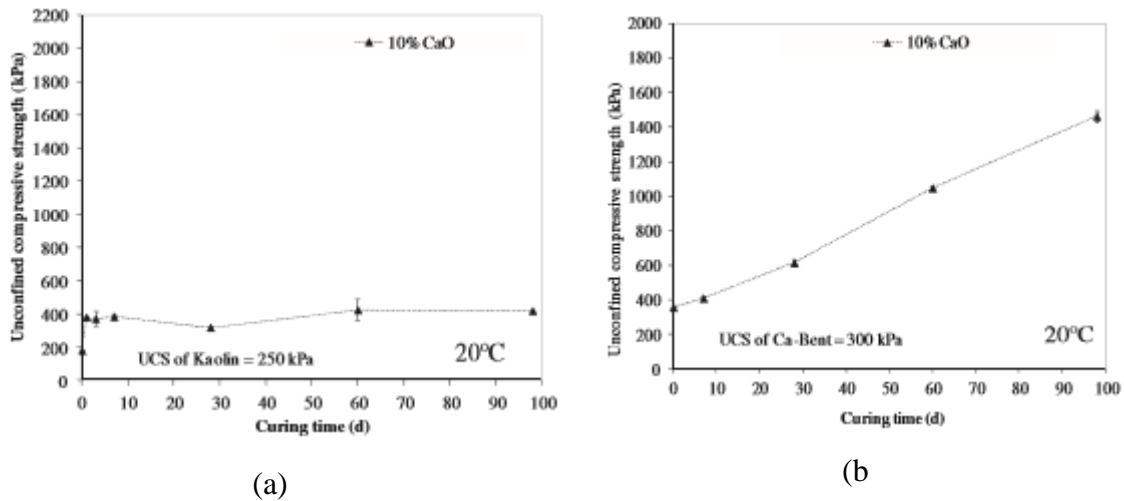
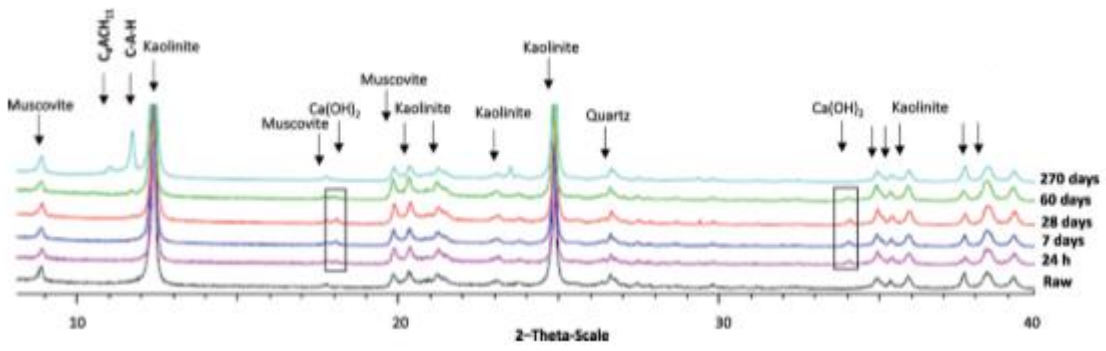


**Figure 2.16:** UCS evolution with time for specimens cured at 20°C (a) kaolinitic material (b) calcium bentonite (after (Maubec et al., 2017)).

The authors concluded that dissolution kinetics in the presence of lime influence the formation of secondary phases, and subsequent strength improvement. The slower dissolution kinetics in kaolin than in calcium bentonite accounted for lower strength gain compared to that of calcium bentonite (Maubec *et al.*, 2017).

Other research by Vitale *et al.* (2017) on lime treated clays focussed on the effects of clay minerals on pozzolanic reactivity, as a function of chemico-physical evolution over short and long term. Two clays (kaolin and bentonite) were treated with quicklime (also referred to as CaO) at the dosage of 3% and 5% by dry weight. The researchers pointed out that pozzolanic reactivity of lime treated clays is strongly controlled by the clay mineralogy. The consumption of portlandite over time (as from 28 days of curing) in lime treated kaolin is slow, which resulted in delayed formation of the cementitious compound CAH. On the other hand, consumption of portlandite in lime treated bentonite is fast and resulted in formation of the CSH compound early within 24 hours of curing. Based on XRD results of CaO treated kaolin (Figure 2.17), Vitale *et al.* (2017) stated that “a significant consumption of portlandite and the formation of new cementitious phases have been detected starting from 28 days of curing”. This result suggests that there would be no significant formation of cementitious phases (such as CSH, CAH) in lime treated kaolin cured below 28 days, due to negligible consumption of portlandite  $[Ca(OH)_2]$ . The current study focussed on 7 days curing of lime treated kaolin in order to achieve modification followed by carbonation treatment. Curing of lime treated kaolin at period below 28 days would result in a trade-off of strength produced by pozzolanic reaction.



(a)

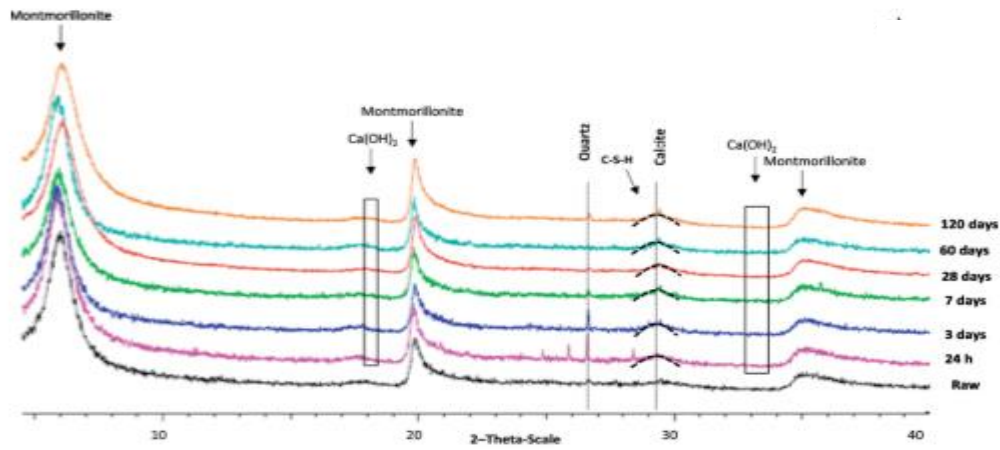


**Figure 2.17:** (a) X-ray diffraction patterns of untreated and 5% CaO treated clay as a function of curing time (after Vitale *et al.*, 2017) (a) kaolin (b) bentonite.

Sherwood (1993) showed that stabilised material using lime or cement could be used for application to pavement layer if it achieves the minimum CBR strength which is greater than 15% (Table 2.5).

**Table 2.5:** Strength requirement for stabilised material for suitability in pavement layers in the Road Note 31 (after Sherwood, 1993).

Layer	Compressive strength (MPa)	CBR
Cemented base 1 (CB1)	3.0-6.0	n/a.*
Cemented base 1 (CB1)	1.5-3.0	n/a.*
Stabilised sub-base (SSB)	0.75-1.5+	>70+
Stabilised capping (SCL)	n/a <sup>#</sup>	>15

\* the CBR test is not applicable to these materials

<sup>#</sup> the CBR test is preferred for this material

+ the strength and CBR requirements are equally acceptable alternatives

Furthermore Cocks *et al.* (2010) determined the suitability of  $\text{Ca}(\text{OH})_2$  treated Gilgai clay (described as expansive clay) for pavement layer of road construction in Western Australia. Based on CBR results, the study showed that  $\text{Ca}(\text{OH})_2$  treated Gilgai clay was suitable for use in the subgrade pavement layer. The clay treated with 4%  $\text{Ca}(\text{OH})_2$  produced an increase in CBR from 3% of untreated clay to approximately 60%, and 120% in 7 days and 28 days cured specimens prior to CBR testing respectively (Figure 2.18).

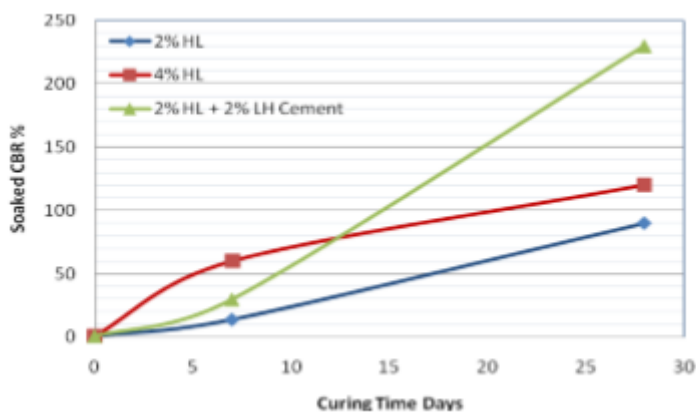


**Figure 2.18:** Increase in California bearing ratio (CBR) of Gilgai clay from Cape Preston, Western Australia, due to treatment with hydrated lime (HL), and cement based on soaked CBR vs. curing time (after Cocks *et al.*, 2010).

## 2.4 Permeability in Lime Stabilisation

Al-Mukhtar *et al.* (2012) looked at the effect of lime additions on the permeability of lime-treated high-plastic montmorillonite (FoCa) clayey soil in France. The FoCa clay was treated with 1%, 4% and 10%  $\text{Ca}(\text{OH})_2$  contents, and compacted using standard Proctor energy. The authors showed that permeability increases from  $(4 \times 10^{-8}$  to  $600 \times 10^{-8}$  m/s) for  $\text{Ca}(\text{OH})_2$  additions up to the value of 4%  $\text{Ca}(\text{OH})_2$  in 7 days cured specimen prior to permeability testing (Table 2.6). The authors noted that the 4%  $\text{Ca}(\text{OH})_2$  corresponded to the ICL for the FoCa clay treatment. However, the permeability decreases from  $(600 \times 10^{-8}$  to  $90 \times 10^{-8}$  m/s) for  $\text{Ca}(\text{OH})_2$  additions higher than the 4%  $\text{Ca}(\text{OH})_2$  (which is ICL value). The increases in permeability was due to increasing granular, and connected pores in lime additions lower than ICL value, whilst the decreases in permeability in  $\text{Ca}(\text{OH})_2$  additions higher than the ICL was due to filling of the pores by lime (Al-Mukhtar *et al.*, 2012).

**Table 2.6:** Geotechnical properties of untreated and lime-treated FoCa (high-plastic montmorillonite) clayey soil (after Al-Mukhtar *et al.*, 2012).

Properties of FoCa soil	Untreated	Lime treated		
$\text{Ca}(\text{OH})_2$ added	0%	1%	4%	10%
Plasticity index, PI (% $\pm$ 2%)	70			
After 7 days		50	10	4
After 90 days		46	6	2
Swelling Pressure (kPa $\pm$ 5kPa)	150			
After 7 days		120	20	15
After 90 days		110	10	10
Unconfined compression strength, (MPa $\pm$ 0.1 MPa)	0.3			
After 7 days		0.4	1.2	1.6
After 90 days		0.4	1.8	2.4
Permeability ( $10^{-8}$ m/s, $\pm 50 * 10^{-8}$ m/s)	4			
After 7 days		70	600	90
After 90 days		10	300	65

Furthermore, Cuisinier *et al.* (2011) conducted studies on the permeability and microstructure of compacted lime treated silt. The silt referred to as St Quentin silt (obtained in vicinity of Paris, France) was treated with 1.5%, 2% and 3% CaO content, compacted using Proctor compaction energy. The authors showed that permeability decreases with increasing moulding water content (Figure 2.19). In the current studies, treated kaolin was compacted at varying amount of water content in order to achieve a range of permeability.

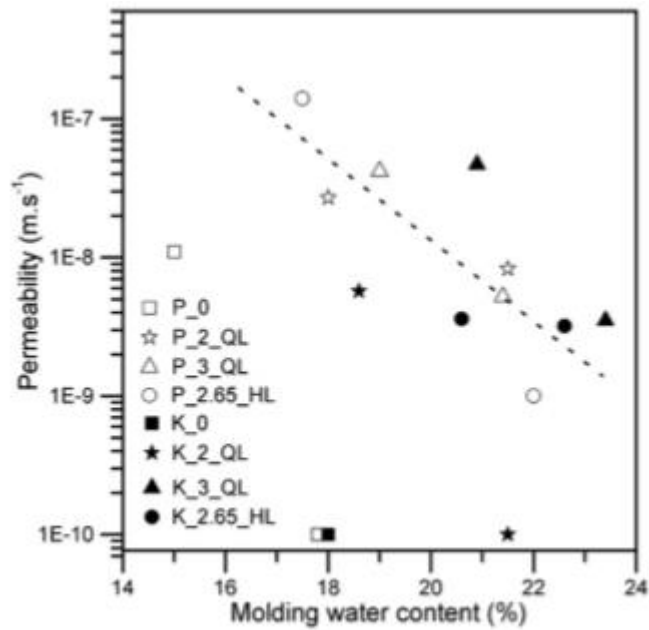


**Figure 2.19:** Reduction in permeability with increasing moulding water content in lime-treated St Quentin silt. P represents Proctor compaction, K represents kneading compaction, QL represents quicklime, and HL represents hydrated lime (after Cuisinier *et al.*, 2011).

Although lime stabilisation of soils is effective, there are some soils where it does not work. Soils containing high sulphate content (above 1%) are not suitable for lime stabilisation (Sherwood, 1993, The Highways Agency, 2007). Lime stabilisation of soils such as Lower Oxford Clay (LOC) which contains high sulphate (1.29%) could be ineffective (Wild *et al.*, 1998; Higgins *et al.*, 2002). This is because the addition of lime to sulphate rich soil could result in the formation of ettringite and thaumasite (swelling minerals), which may cause heave in soil.

Additionally lime stabilisation of soil containing high organic matter (as high as 2%) content is not suitable (Sherwood, 1993, The Highways Agency, 2007). High organic matter content in soils could reduce hydration due to its high water holding capacity (Chen and Wang, 2006). Yunus *et al.* (2016) conducted studies on changes in strength of lime treated organic clay with varying humic acid (Figure 2.20). Organic clay was prepared by the addition of humic acid (0%, 0.5%, 1.5%, and 3.0% by dry mass) to kaolin. The researchers pointed out that organic soil containing humic acid content up to 1.5% could reduce the efficiency of the lime stabilisation process. The UCS of organic soil containing up to 1.5% humic acid resulted in significant decreases of UCS after curing up to 28 days, and hence reduction in efficiency of lime stabilisation (Yunus *et al.*, 2016). The decreases in UCS are likely due to reduction in pH value at longer curing periods produced by humic acid addition (Yunus *et al.*, 2012).

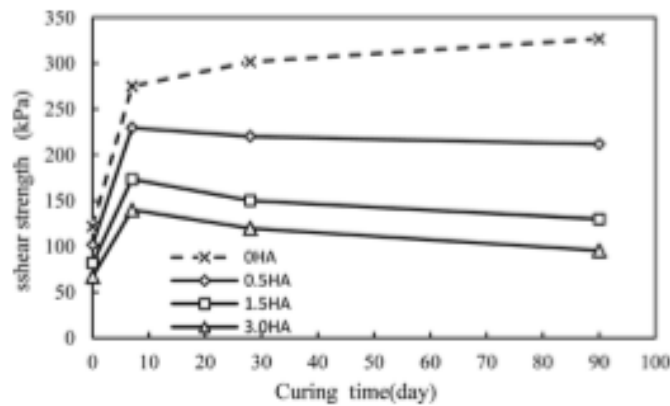
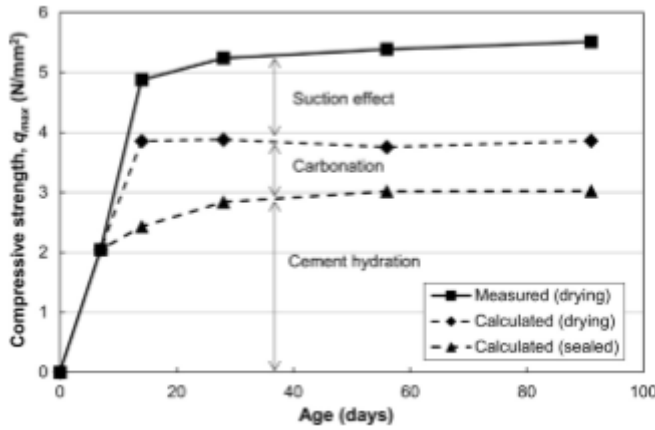


**Figure 2.20:** Effect of curing period on the shear strength of lime-treated clay containing different humic acid contents (after Yunus *et al.*, 2016).

Ho *et al.* (2017) assessed the effects of carbonation, and pozzolanic reaction on the strength development of cement treated soils. Toyoura silica sand treated with 8% cement content was initially cured under sealed conditions at 20°C for 7 days, followed by drying for 7, 14, 28, 56, and 91 days, under room temperature (20°C) and relative humidity of 60%. They reported the formation of  $\text{CaCO}_3$  and CSH based on thermogravimetric and differential thermal analyses.

Although the study was conducted on cement treated soil, the authors noted that carbonation under atmospheric drying could result in compressive strength increases by 56% of the total compressive strength at an early curing period of up to 14 days (Figure 2.21). However, contribution to strength development by carbonation decreased after longer curing periods. The researchers showed that compressive strength of the specimen at 56 days and 91 days decreased by 29% and 31% of the total strength respectively. The decrease could result from carbonation of CSH phase instead of  $\text{Ca}(\text{OH})_2$  (Ho *et al.*, 2017).



Total strength increase due to carbonation of  $\text{Ca(OH)}_2$  and CSH

**Figure 2.21:** Analysis of the strength development mechanism in the cement treated sand mixture under the drying condition (after Ho *et al.*, 2017).

The study by Ho *et al.* (2017) shows that carbonation of CSH phase due to pozzolanic reaction could result in reduction in overall strength gained. This is because part of calcium in CSH phase is consumed by carbonation reaction, thereby destroying part of the CSH phase (Cizer *et al.*, 2010). There would be a trade-off of pozzolanic reaction if carbonation of CSH phase is allowed. The current research is more focussed on modification of clay soils, followed by carbonation of  $\text{Ca(OH)}_2$  for strength improvement functions. In the next Section, soil modification of clay soil approaches is reviewed.

## 2.5 Modification of Geotechnical Properties of Clay Soils

One of the most common approaches for the modification of clay soils is by lime. One great advantage of lime modification is to dry the soil and reduce delays to construction due to very wet soil (Rogers *et al.*, 1997).

Rogers and Glendinning (1996) conducted a study on lime treated clay and showed that, when quicklime is added to clay, modification through dehydration for strength and workability improvement is achieved through the following reactions, as shown in Equation 2.4.



Additionally cation exchange takes place between calcium released by lime and the cations associated with the clay lattice, resulting in reduced susceptibility of clay to water additions. This is followed by particle flocculation which causes more attraction between clay particles due to their closeness. The clay particles agglomerate and produce increased angle of internal friction and hence shear strength.

Full stabilisation through pozzolanic reaction occurs after a curing period of at least 28 days resulting in strength and stiffness improvement (Vitale *et al.*, 2017). Such pozzolanic reaction could be substituted with carbonation reaction by reduction of curing period to 7 days. The proposed method as described in Chapter 3 of this thesis focussed on treated kaolin cured for 7 days followed by carbonation reaction. Curing for 7 days allows for short term reactions which are often considered as modification reactions (Jung and Bobet, 2008).

As noted by Rogers *et al.* (1997) the full pH against lime addition curve is recommended as the reasonable interpretation for site workability improvement. This suggestion resulted in a significant concept termed the modified ICL, which gave more consistent results and proved as a better indicator to know how much lime is required to react in order to achieve full modification.

Lime modification improves the plasticity of clay soils and makes it easier to work with in placement and compaction, which is useful to provide firm support for construction operations. Rogers *et al.* (1997) pointed out important considerations when using lime in a modification process. One such point is that in the laboratory intimate mixing of lime and clay needs to be achieved for the Atterberg limit test. In this thesis, the Atterberg limit test was also used. Furthermore, they suggested that lime used for the modification process needs to be fresh. Therefore, the experiments performed in this thesis also used fresh lime.

Lime is manufactured from natural deposits of limestone, which is mostly  $\text{CaCO}_3$ . Lime production involves the following three main stages: limestone preparation, calcination, and hydration. The preparation stage involves quarrying, transportation, and crushing of limestone. At the calcination stage, high temperatures are supplied in the kilns, which roast the limestone and trigger chemical reaction to produce  $\text{CaO}$  and  $\text{CO}_2$  as represented by Equation 2.5. Lime is produced as  $\text{CaO}$  or as  $\text{Ca(OH)}_2$  by the hydration of quick lime as described in Equation 2.6.



$\text{CO}_2$  is generated mainly during calcination stage, as shown in the life cycle analysis of lime (Figure 2.22). It is estimated that 1.092 tonnes (0.751 tonnes process emissions, 0.322 tonnes combustion emissions, and 0.019 tonnes electricity emissions) of  $\text{CO}_2$  is emitted due to the production of 1 tonne of quicklime (EuLA, 2014).

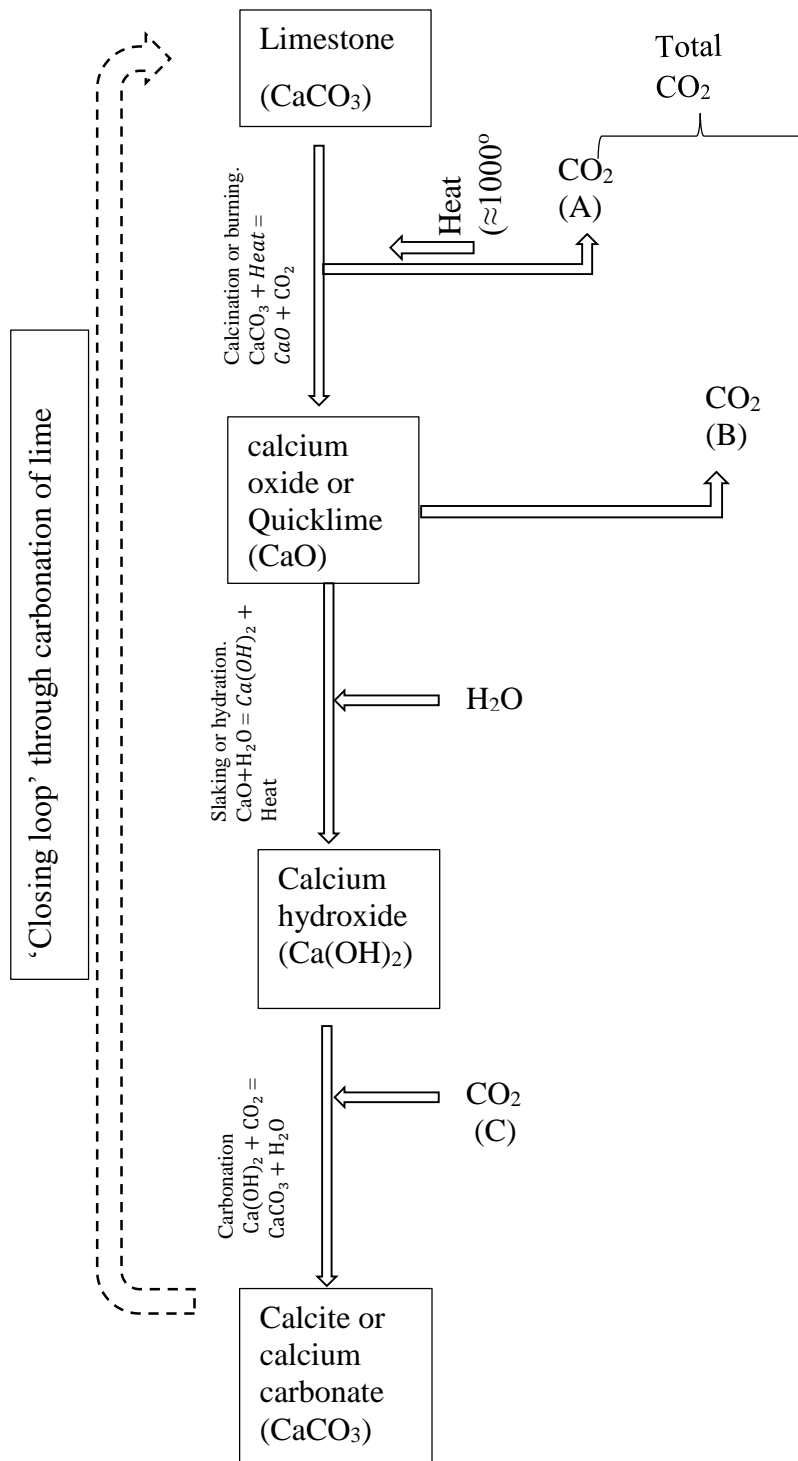


**Figure 2.22:** Life cycle analysis of lime (after British Lime Association, 2015)

Note: A represents  $\text{CO}_2$  emissions due to energy supply (combustion plus electricity) 0.341 tonnes per a tonne quicklime product. B represents process emissions (0.751 tonnes per a tonne quicklime product), C represents carbon recovery through carbonation of lime. By carbonation C could be equal to B.

The proposed method described in Chapter 3 of this thesis suggests that a recovery of CO<sub>2</sub> up to an amount corresponding to the process emission in lime production could be achieved by the combined modification and carbonation of lime treated soil (Figure 2.22).

Another material that could be used to improve soil strength is magnesia or magnesium oxide (MgO). Yi *et al.* (2013) proposed the use of magnesia-stabilised soil for carbonation process, which yields remarkable strength improvement. MgO is produced by the calcination of magnesium carbonate (MgCO<sub>3</sub>), or magnesium hydroxide Mg(OH)<sub>2</sub> (Cement, 2010). Calcination of MgCO<sub>3</sub> is chemically represented by Equation 2.7.



MgO produced from calcination is in the form of caustic calcined MgO and dead burnt MgO.

Caustic calcined MgO (also referred to as reactive MgO) production involves temperature between approximately 700°C - 1000°C. This type of MgO has large surface area and is highly chemically reactive, so it is used in soil stabilisation (Yi *et al.* 2013). Dead burnt MgO production involves a calcination at a temperature between approximately 1000°C -1500°C. This type of MgO has lower surface area, and is less chemically reactive than reactive MgO (Shand, 2006).

However, the main focus of this thesis is on the use of lime-treated soils for carbonation process and strength improvement.

For technical reasons, lime or magnesia are the preferred materials to be used for soil stabilisation. However, this is in conflict with the requirement to mitigate climate change, because their manufacture involves substantial CO<sub>2</sub> emissions. There is a need to mitigate this, whilst achieving desired engineered outcomes. Hence, in this thesis, the proposed modification approach aims at compensating for these emissions as well. In the next Section, the carbonation process will be explained and how it relates to this study.

## 2.6 Carbonation Process

Lime modification is associated with carbonation which could be based on short and long term reactions. The process of carbonation is achieved by the reaction of lime with atmospheric CO<sub>2</sub> to form CaCO<sub>3</sub>. The CaCO<sub>3</sub> formed is usually classified as a relatively weak

cementing agent. Another weakly cementing agent that could be formed due to carbonation process is  $\text{MgCO}_3$  (Davidson and Handy, 1960).

Several studies were carried out using lime-treated soils in order to confirm the presence of  $\text{CaCO}_3$  formation due to carbonation reaction (Goldberg and Klein, 1952; Eades *et al.*, 1962; Bagonza *et al.*, 1987; Al-Mukhtar *et al.*, 2010; Verbrugge *et al.*, 2011; Al-Mukhtar *et al.*, 2012).

Early research by Goldberg and Klein (1952) was conducted on some effects of lime treated clay soils. A total of 2 different clays (Porterville clay and Wyoming bentonite) were each treated with 4% and 8%  $\text{Ca(OH)}_2$  by dry mass. Distilled water was added to the mixture and thoroughly mixed to achieve a perceptible flow on slight bending. The slurry samples were then air dried for approximately 2 weeks. These samples were crushed to powder and the amount of  $\text{CaCO}_3$  determined using differential thermal analysis (DTA) and XRD patterns. The amount of  $\text{CaCO}_3$  reported by the authors is presented in Table 2.7. They concluded that  $\text{CaCO}_3$  formed was due to carbonation of  $\text{Ca(OH)}_2$  that was used in the clay treatment. They noted that the amount of  $\text{CaCO}_3$  formed increased in proportion to the lime content.

Furthermore, Eades *et al.* (1962) carried out a field study on  $\text{Ca(OH)}_2$  treated subgrade soils at three project sites in Virginia, in order to investigate the presence of  $\text{CaCO}_3$  in lime treated soil in the field. The subgrade sections were treated with 3% and 5%  $\text{Ca(OH)}_2$  contents by dry mass. Samples obtained from subgrade sections after 2 years of road construction from each of the project were tested for mineral contents using XRD. Eades *et al.* (1962) noted that  $\text{CaCO}_3$  was found in all the samples. Approximately 2.5%  $\text{CaCO}_3$  was obtained for all the sections treated with 5%  $\text{Ca(OH)}_2$  (Table 2.7). They concluded that due to the presence of  $\text{CaCO}_3$  in all the samples, not all lime for the soil treatment was used to produce calcium silicate.

**Table 2.7:** Calcium carbonate formation due to carbonation of lime in treated clays.

Author	Clay	Lime content (%)	CaCO <sub>3</sub> content (%)
Goldberg and Klein (1953)	Porterville	4% Ca(OH) <sub>2</sub>	2.83
	Wyoming bentonite	4% Ca(OH) <sub>2</sub>	3.21
	Porterville	8% Ca(OH) <sub>2</sub>	4.58
	Wyoming bentonite	8% Ca(OH) <sub>2</sub>	3.76
Eades <i>et al.</i> (1962)	A-7-5, A-7-6 class	5% Ca(OH) <sub>2</sub>	2.5
Al-Mukhtar <i>et al.</i> (2010)	Bentonite (impersol)	4% Ca(OH) <sub>2</sub>	3.21 <sup>b</sup>
Maubec <i>et al.</i> (2017)	Calcium bentonite	13.3% Ca(OH) <sub>2</sub> <sup>a</sup>	7.75 <sup>b</sup>

<sup>a</sup>lime as calcium hydroxide [Ca(OH)<sub>2</sub>] equivalence

<sup>b</sup>calculated by extrapolating calcium carbonate (CaCO<sub>3</sub>) formation in lime treated bentonite in the data of Goldberg and Klein (1953).

A study on lime treated clayey sand (described as “a poor quality calcrete”) was conducted by Bagonza *et al.* (1987), in order to confirm the occurrence of carbonation in different curing conditions (high carbon (HC), high temperature (HT) and low humidity (LH)). Furthermore, the study investigated carbonation of samples already hardened before exposure to CO<sub>2</sub> environment (only as part of the study). The samples were prepared by mixing the calcrete soil with 3% Ca(OH)<sub>2</sub> content by dry mass and moisture contents similar to a field project where lime treatment was previously applied. The mixtures were compacted using the BS 4.5 kg rammer method. Samples were cured in different environments of exclusion or contact with CO<sub>2</sub> for 3, 7, 14 and 28 days. Another set of samples was cured in air tight condition for 3 or 7 days prior to exposure to a CO<sub>2</sub> environment, in order to investigate the effect of carbonation on already hardened lime treated samples. Carbonation was identified by the use of phenolphthalein indicator based on the pH value of soil. Phenolphthalein was spread on the samples already tested for UCS, and the extent of carbonation penetration was determined as the boundary from the outside to the centre of the sample, where a colour change occurred.

Bagonza *et al.* (1987) noted that carbonation occurred in all lime treated samples that were brought in contact with CO<sub>2</sub>. The extent of carbonation (measured as carbonation penetration) was highest in HC environment with carbonation penetration of 25mm, followed by that in HT environment, which recorded 7 mm carbonation penetration. Carbonation in LH environment recorded the lowest carbonation penetration of approximately 1 mm. Also, they

reported that lime treated specimen cured in air tight condition up to 7 days prior to exposure of CO<sub>2</sub> underwent high carbonation.

Bagonza *et al.* (1987) showed that carbonation of 3% Ca(OH)<sub>2</sub> (2.25% CaO equivalent) treated calcrete with curing under HC environment for 3, 7, 14 and 28 days resulted in loss of strength (Table 2.8). The results showed a 77 % loss of strength of the specimen for 7 days carbonation curing, and 72 % loss of strength of the specimen for 28 days carbonation curing, compared with the strength of corresponding non-carbonated air tight cured specimens. Loss of strength was calculated based on the ratio of carbonated cured to ‘non-carbonated’ cured specimens (Table 2.8). ‘Non-carbonated’ in this thesis means specimen that is not subjected to carbonation treatment.

**Table 2.8:** Comparison of per cent loss of strength on carbonation in the soil-cement and soil-lime mixtures (after Bagonza *et al.*, 1987). NC represent normal curing, HC represents high carbon curing.

Age (day)	4% cement stabilized calcrete soaked strength (MN/m <sup>2</sup> )			3% lime stabilized calcrete soaked strength (MN/m <sup>2</sup> )		
	NC*	HC*	HC/NC*	NC	HC	HC/NC
3	1.76	0.74	42%	4.06	0.96	24%
7	1.85	0.65	35%	4.40	1.02	23%
14	2.67	0.81	30%	5.15	1.34	26%
28	3.10	0.71	23%	4.87	1.34	28%

\*In this series another but similar calcrete was used for the cement-stabilised samples.

The method described for carbonation treatment in Chapter 3 of this thesis used 1 molar sodium carbonate (Na<sub>2</sub>CO<sub>3</sub>) solution in order to provide HC condition. Considering that high carbonation extent can occur in a lime treated sample already cured for 7 days, specimens for carbonation described in Chapter 3 of this thesis were cured in air tight condition for 7 days prior to carbonation, in order to achieve modification prior to carbonation treatment.

Al-Mukhtar *et al.* (2010) carried out a study on the behaviour and mineral changes in Ca(OH)<sub>2</sub> treated bentonite clay expansive soil at 20°C. XRD was used in measurement of the mineral changes. Based on a strong reflection from XRD patterns, the authors reported the formation of CaCO<sub>3</sub> mineral in the Ca(OH)<sub>2</sub> treated soil. They noted that the reflections of XRD patterns for CaCO<sub>3</sub> increased with the amount of Ca(OH)<sub>2</sub> added and curing time, which was likely due to carbonation of the Ca(OH)<sub>2</sub> by CO<sub>2</sub>. The researchers showed that

UCS increased with  $\text{Ca}(\text{OH})_2$  addition and curing time (Figure 2.23).  $\text{Ca}(\text{OH})_2$  addition from 0% to 20% content produced strength increase by 8 times (from 0.21 MPa to 1.8 MPa). Curing of specimens from 28 days to 90 days resulted in strength increases from 8 times to 17 times compared with the strength of untreated specimens (Figure 2.23). Whereas calcite is detected in the specimen, strength development was due to the formation of CAH produced by pozzolanic reactions.

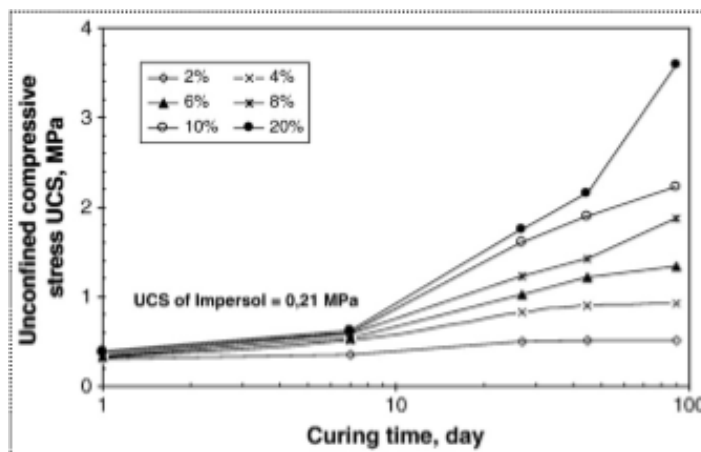


**Figure 2.23:** Unconfined compressive strength (UCS) of bentonite (Impersol) with curing time for various amounts of calcium hydroxide ( $\text{Ca}(\text{OH})_2$ ) addition (after Al-Mukhtar *et al.*, 2010).

Also, Verbrugge *et al.* (2011) noted that “the formation of calcite is attributed to the air exposure of soil during curing period and subsequent carbonation of quicklime and hydrated products”.

Additionally, Al-Mukhtar *et al.* (2012) investigated the microstructure and geotechnical properties of  $\text{Ca}(\text{OH})_2$  treated montmorillonite (also referred to as FoCa clay), using XRD, TGA, Transmission Electron Microscopy (TEM) and SEM. They reported that calcite was formed based on TGA and XRD results. A crystal of rhombohedral symmetry was found from the TEM results as additional confirmation of the formation of calcite. They reported that the formation of  $\text{CaCO}_3$  was attributed to carbonation reaction between lime and atmospheric  $\text{CO}_2$ .

The authors showed that compressive strength of lime treated specimens increased with lime addition and curing time (Table 2.9). The 7 day UCS increased by approximately 4 times (from 0.3 MPa to 1.6 MPa) for 10%  $\text{Ca}(\text{OH})_2$  treated FoCa clay compared with the strength of non-treated specimens. Additionally, the compressive strength increased with curing time. The UCS of cured specimens (from 7 days to 90 days) increased by 50% (from 1.6 MPa to

2.4 MPa). The increases in strength were due to formation of cementitious bonds such as calcium silicate aluminate hydrate (CSAH), which resulted from pozzolanic reactions (Al-Mukhtar *et al.*, 2012).

Whilst calcite is produced in lime treated FoCa clay due to lime carbonation, strength development was found to be produced by formation of cementitious compound composed of CSAH due to pozzolanic reaction (Al-Mukhtar *et al.*, 2012).

**Table 2.9:** Geotechnical properties of untreated and lime-treated FoCa (high-plastic montmorillonite) clayey soil (after Al-Mukhtar *et al.*, 2012)

Properties of FoCa soil	Untreated	Lime treated		
<b>Ca(OH)<sub>2</sub> added</b>	0%	1%	4%	10%
Plasticity index, PI (% ± 2%)	70			
After 7 days		50	10	4
After 90 days		46	6	2
Swelling Pressure (kPa ± 5kPa)	150			
After 7 days		120	20	15
After 90 days		110	10	10
Unconfined compression strength, (MPa ±0.1 MPa)	0.3			
After 7 days		0.4	1.2	1.6
After 90 days		0.4	1.8	2.4
Permeability ( $10^{-8}$ m/s, ±50 * $10^{-8}$ m/s)	4			
After 7 days		70	600	90
After 90 days		10	300	65

The current study builds on the formation of calcite in lime treated clay to determine the strength development produced by carbonation reactions.

## 2.7 Soil Carbonation

The increase in atmospheric CO<sub>2</sub> concentration by 40% since the start of the industrial revolution (since 1750) is believed to be linked to climate change and the continuing threat of the attendant global warming (IPCC, 2013). A means to mitigate the climate change is by enhancement of soil carbonation for carbon capture and storage function (Lal, 2004).

Earlier research was performed by Renforth *et al.* (2009) on carbonate precipitation in artificial soils containing Ca<sup>2+</sup> rich minerals at two sites in North East England, UK. The authors showed that carbon content of 300 ± 150.3 tonnes carbon per hectare (t C ha<sup>-1</sup>) (30 ± 15.3 kg C m<sup>-2</sup>) was stored as CaCO<sub>3</sub>. They found that an appropriately designed construction or development of a site globally could capture and store carbon up to 290 Mt carbon per annum.

Additionally, Renforth and Manning (2011) investigated a laboratory carbonation of hydrated cement gels using citric acid for enhanced leaching of calcium. They reported that the combination of silicate dissolution and carbonation provides a potential carbon capture function that can be designed into soils, which could be engineered mainly to expedite carbon capture.

Further study was carried out in urban soils (a brownfield site) at Science Central, Newcastle upon Tyne, UK by Washbourne *et al.* (2012). The soils contained calcium and magnesium minerals derived from C&D cement materials. They reported that the urban soils captured and stored 37.43 kgCO<sub>2</sub> per t in residual reactive materials, and has further potential to capture 27.3 kgCO<sub>2</sub> per t in residual reactive materials. They concluded that an engineered urban soil has a potential to capture and store large amount of CO<sub>2</sub> as carbonate.

Research to investigate carbonate precipitation in artificial soils mixed with naturally derived calcium minerals from basalt quarry fines and dolerite was performed by Manning *et al.* (2012). The authors showed that an amount of 4.8 t C ha<sup>-1</sup> to a depth of 0.3m was stored annually in the artificial soils. They concluded that the artificial soils if engineered would capture and store a substantial amount of carbon as carbonate.

Recently, Washbourne *et al.* (2015) investigated carbonate formation in urban soils which contained calcium mineral, for a period of 18 months at Newcastle Science Central, UK. The authors pointed out that 85 tonnes of CO<sub>2</sub>/ha was captured as CaCO<sub>3</sub> in the urban soils due to carbonation of calcium minerals resulting from demolished concrete. They estimated that approximately 700-1200 Mt of CO<sub>2</sub>/yr (which is equivalent to 2.0 -3.7% of total emissions from fossil fuel combustion) can be stored annually in the UK's urban soils.

Yoon *et al.* (2015) performed a study aimed at surface soil carbon storage in urban green spaces in South Korea. The authors showed that a total (organic and inorganic) carbon stock of 21.3 t C ha<sup>-1</sup> to a depth of 0.3m was stored in the urban soils.

Nakarai and Yoshida (2015) noted that the concentration of CO<sub>2</sub> influences the rate of carbonation. Cement treated Toyoura silica sand using 8% cement content were cured under sealed (0% CO<sub>2</sub>), natural atmospheric ( $\approx$  0.03% CO<sub>2</sub>), and accelerated ( $\approx$  5% CO<sub>2</sub>) conditions. For the specimens cured under accelerated CO<sub>2</sub> conditions, it took 91 days to achieve approximately 40% CaCO<sub>3</sub> content due to the carbonation of Ca(OH)<sub>2</sub> and CSH. It took 365 days to achieve approximately similar CaCO<sub>3</sub> content under natural curing (Figure 2.24). The

researchers' results suggests that the rate of carbonation of  $\text{Ca}(\text{OH})_2$  in natural to accelerated  $\text{CO}_2$  concentration could results in  $\text{CaCO}_3$  content in the ratio of 1:4.

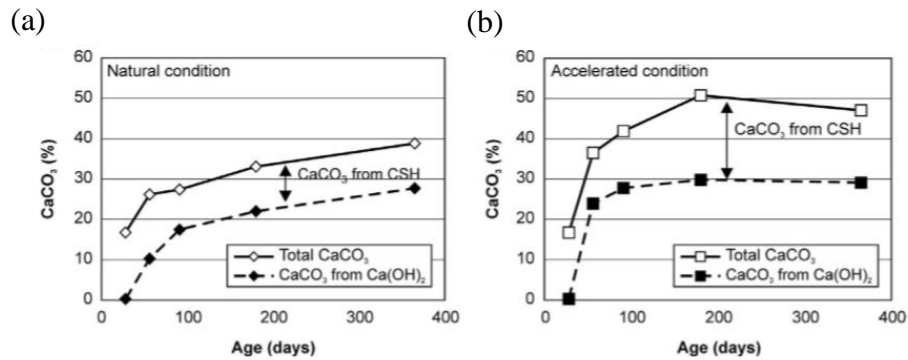


**Figure 2.24:** Changes in amount of  $\text{CaCO}_3$  content in 8% cement treated Toyoura silica sand under different curing conditions (a) Natural conditions (b) Accelerated (5%  $\text{CO}_2$ ) conditions (after Nakarai and Yoshida, 2015).

Additionally, Nakarai and Yoshida (2015) showed that carbonation of CSH phase could result in slight reduction in strength gain in treated soil. From accelerated (using 5%  $\text{CO}_2$ ) curing condition of 8% cement treated Toyoura silica sand specimens, the authors demonstrated that the compressive strength of specimens increased with  $\text{CaCO}_3$  content up to 56 days curing, but the strength slightly decreased at curing beyond 56 days (Figure 2.25). The authors attributed the reduction in strength after 56 days to result from carbonation of CSH phase. This again shows that carbonation of CSH phase could result in reduction of strength produced by pozzolanic reaction.

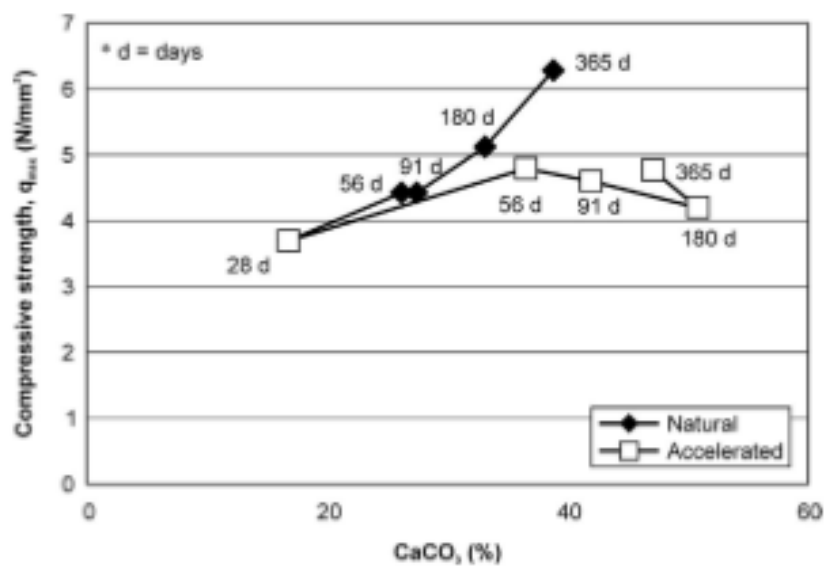


**Figure 2.25:** Relationship between unconfined compressive strength and  $\text{CaCO}_3$  in 8% cement treated Toyoura silica sand (after Nakarai and Yoshida, 2015).

It is important to note that Bagonza *et al.* (1989) used another term “HC” to denote the “high CO<sub>2</sub> concentration” used in Nakarai and Yoshida (2015). To avoid confusion, the term “HC” will be used consistently in this thesis. The current study is focussed on modification of clay soils, followed by carbonation of Ca(OH)<sub>2</sub> for strength improvement functions. In the next Section, freeze-thaw durability of lime treated clay is reviewed.

## **2.8 Freeze-Thaw Durability of Lime Treated Clay**

Lime treated soil used in engineering functions such as embankments and roads which are constructed in cold regions are exposed to periodic FT cycles. The mechanical properties of lime treated soil such as compressive strength and bearing capacity are adversely affected by ice lenses which form between soil particles during freezing, and excess water during thawing (Konrad, 1989). The compressive strength and bearing capacity of lime treated soil is substantially reduced due to repeated FT circles (Aldaood *et al.*, 2014). One way to determine frost resistance of lime treated soil is by FT testing.

Shihata and Baghdadi (2001) conducted FT durability testing of cement treated soil based on compressive strength without brushing. The authors recommended that the residual UCS could be used for determination of FT durability. The ‘residual UCS’ in this thesis means the UCS of specimens which is prior subjected to repeated FT cycles (Shihata and Baghdadi, 2001). The authors noted that this FT durability approach is essential as it produces more consistent results and eliminates the main source of variation caused by brushing. This FT durability approach is adopted in the method described in Chapter 3 of this thesis.

Using residual UCS for FT durability approach, Hotineanu *et al.* (2015) examined the effect of freezing and thawing on the mechanical properties of lime treated expansive clays (bentonite and kaolinite) (Figure 2.26 a, b). Based on short term curing of specimens for 3 days, followed by exposure to 10 FT cycles, the residual UCS for both bentonite and kaolinite specimens decreased by approximately 10% when compared with UCS of non-FT equivalents. For specimens cured for 28 days, followed by exposure to 10 FT cycles prior to UCS testing, the UCS decreased by 40% in bentonite specimens, whilst no substantial losses were achieved in kaolinite specimens. The current study focussed on short term curing of specimen for 7 days, followed by carbonation treatment, then FT cycles exposure prior to residual UCS testing.

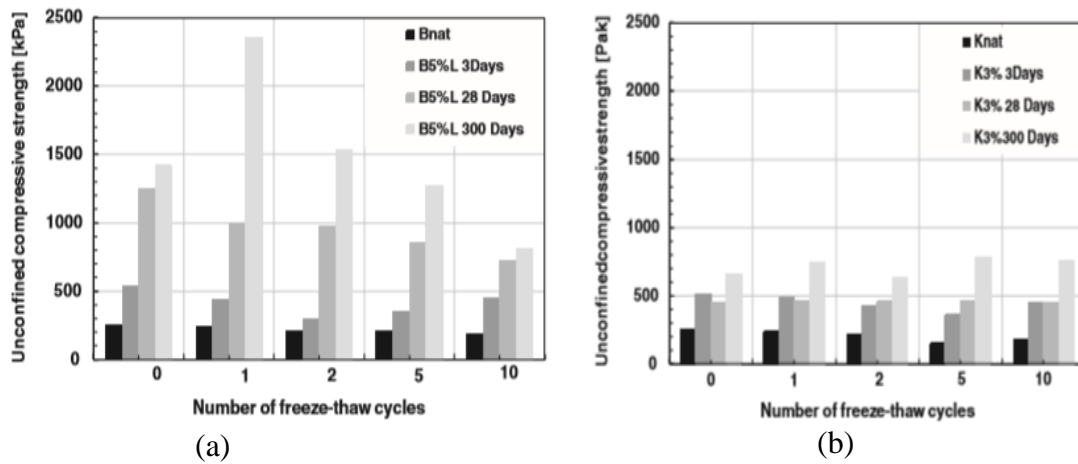


**Figure 2.26:** The effect of freeze–thaw (FT) action on unconfined compressive strength (UCS) of untreated and lime-treated expansive clay (a) untreated bentonite (Bnat) and treated bentonite (b) untreated kaolinite (Knat) and treated kaolinite (adapted from Hotineanu *et al.*, 2015).

## 2.9 Lime Based-Wastes for Soil Stabilisation

Lime has been widely used in clay treatment for improvement of its physical and mechanical properties such as plasticity, strength and stiffness (Sherwood, 1993; Bell, 1996; Rogers and Glendinning, 1996). The strength and stiffness is derived mainly from the reaction between lime and the clay fraction (Sherwood, 1993).

However, the use of lime in soil stabilisation is in conflict with climate change requirements. This is because its production produces large amounts of CO<sub>2</sub> emissions and involves a large amount of embodied energy (EE) (Hammond and Jones, 2011). Shillaber *et al.* (2016) noted that the use of waste products in ground improvement accounts to very low EE and CO<sub>2</sub> emissions. EE and CO<sub>2</sub> emission are important factors to determine the choice of a more sustainable materials in ground improvement projects. The use of waste materials in ground improvement has attracted substantial interest, due to its better environmental sustainability in terms of energy consumption and CO<sub>2</sub> emissions than lime and cement (Rahmalt and Ismail, 2011).

The potential use of waste products in soil stabilisation as an alternative to lime is influenced by their CaO content. Some waste materials contain free lime and could be used on their own to achieve the desired strength improvement. Rahmalt and Ismail (2011) pointed out that wastepaper sludge ash (WSA) contains some free lime (from 3%-5%) and could be used alone to cause strength improvement of weak clay such as LOC. Ladle furnace basic slag

(LFS) contains up to 19% free lime (Setién *et al.*, 2009) and could be used alone to bring about strength improvement of weak soil (Ortega-López *et al.*, 2014).

Some waste materials with latent CaO could be activated by combination with waste containing free-lime or with alkali for strength improvement (Rahmalt and Ismail, 2011; Sargent *et al.*, 2017). Rahmalt and Ismail (2011) activated ground granulated blastfurnace slag (GGBS) with WSA containing free lime (3% - 5%), which raised the pH, initiated pozzolanic reaction and eventually resulted in strength improvement of LOC.

Industrial wastes could be used for strength improvement of weak soils. Waste materials that are commonly used in soil improvement include GGBS, SS, pulverised fuel ash (PFA), and WSA. GGBS is a latent hydraulic cement produced during pig iron manufacture, which is rich in latent CaO content. The slag is ground in fine powder so as to make it chemically reactive (EuroSoilStab, 2002). PFA is waste ash, which is generated from coal combustion in coal-fired power plants (Mir and Sridharan, 2013). PFA is classified into two classes, namely type C and type F. Type C consists of high calcium content, and is more reactive than type F, which contains low calcium content (Mir and Sridharan, 2013). Type C PFA is preferred over type F PFA (ASTM C618-12a, 2012) due to its higher lime content and hence better reactivity and cementitious properties (McCarthy *et al.*, 1984).

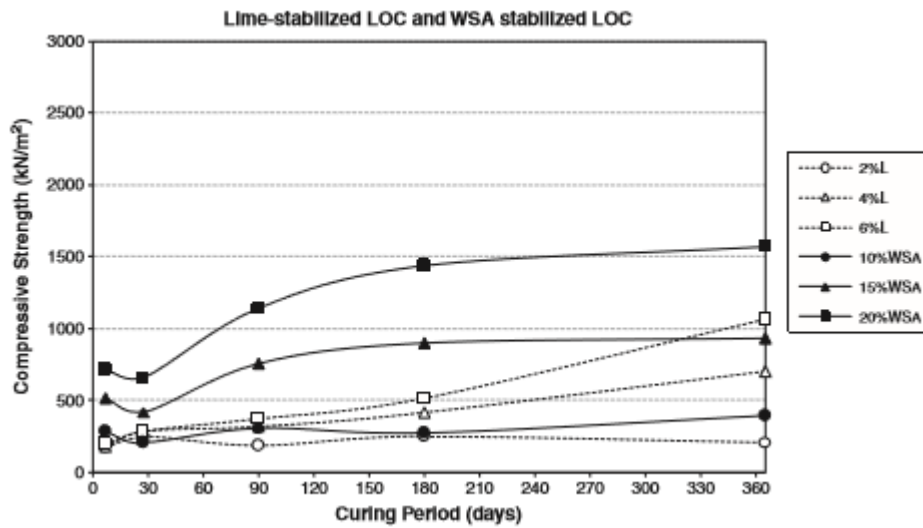
WSA is a by-product of paper industry. It has latent cementitious properties due to CaO that is confined in its glassy structure, and cementitious properties due to a small amount of free lime content. Additionally it is composed of moderate amounts of amorphous silica and alumina (Rahmat and Ismail 2011). SS is a by-product of the steelmaking industry, which consists of high CaO, some free lime, and MgO content (Poh *et al.*, 2006; Yildirim and Prezzi, 2011).

CKD is a by-product generated from cement manufacturing. CKD has a chemical composition made of CaO, free lime, silica, and alumina, which are similarly found in Portland cement (Siddique, 2007). CKD may contain free lime as high as 29% CaO. Due to the free lime content in CKD, it could be used for soil stabilization as an alternative to lime (Siddique, 2007; Peethamparan *et al.*, 2008). Sulphate present in CKD may produce ettringite and syngenite which could contribute to initial increase in strength and stiffness, but may result in expansion and long term durability issues (Peethamparan *et al.*, 2008). Ebrahimi *et al.* (2013) noted that the use of CKD in stabilisation of recycled pavement material and road surface gravel could result in detrimental expansion (from 6% to 15%) due to formation of ettringite. Wastes containing high sulphate content such as CKD are to be used in soil stabilisation with caution (Ebrahimi *et al.* 2012).

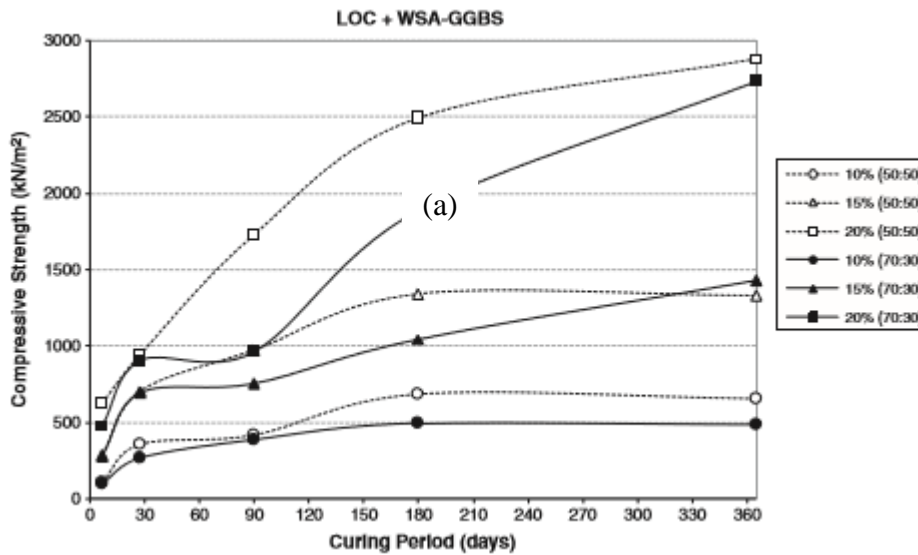
Waste materials have been used in soil improvement, and have produced high strength and stiffness mainly due to pozzolanic reaction. Rahmalt and Ismail (2011) pointed out that the addition of WSA alone containing free lime to LOC resulted in strength development, which was higher than that produced by quicklime additions. The addition of 20% WSA produced the UCS of 1600 kPa, which was higher than the strength of 1064 kPa produced by 6% quicklime additions after 365 days curing (Figure 2.27a).

Industrial by-products containing latent CaO (confined within the material structure) could be activated by blended wastes or alkali metals for soil stabilisation. Rahmalt and Ismail (2011) blended GGBS with free lime containing WSA for treatment of LOC. The addition of 20% stabiliser made up of WSA plus GGBS (WSA:GGBS, 50:50) resulted in UCS development of 2900 kPa which is higher than that of 1064 kPa produced by 6% quicklime addition after 365 days curing (Figure 2.27b).

The current thesis recommends further research on the treatment of clay with lime rich waste to achieve more cheaply and environmentally sustainable ground stability. This would achieve less expensive clay modification followed by carbonation for carbon capture function alongside strength improvement function.



(a)



(b)

**Figure 2.27:** Unconfined compressive strength (UCS) development of lime, and lime-based waste treated Lower Oxford Clay (LOC); (a) Lime (calcium oxide), and WSA, (b) combined WSA plus GGBS (WSA:GGBS is 50:50). L represents calcium oxide, WSA represents wastepaper sludge ash, GGBS represents ground granulated blastfurnace slag (after Rahmalt and Ismail, 2011).

## 2.10 Techniques for Confirmation and Quantification of Carbonates

In any geotechnical experiment to confirm the formation of carbonates and to determine their quantity, literature has shown that the calcimeter has proved to be very effective for this purpose. Basically,  $\text{CaCO}_3$  content is determined by measuring the gas volume of  $\text{CO}_2$  which results from the reaction process of hydrochloric acid with soil lime. Recently, most studies used the Eijkelkamp calcimeter (volumetric calcimeter) to determine the content of carbonate formed in soil (Washbourne *et al.*, 2015; Hu and Yang, 2016). Based on the effectiveness of this instrument, it was also used for the determination of carbonate formed in this research.

Another important instrument for the measurement of carbonates formed in clay is TGA. TGA is usually referred to as a material characterisation tool. However, this tool works in a different way to the calcimeter. The amount of carbonate formed is determined by subjecting the carbonated soil to heat and the weight loss as a function of temperature is measured. TGA is able to measure discrete quantities of carbonate and other heat-sensitive soil components (Manning *et al.*, 2005), therefore it is also used in this research.

To determine the spatial distribution of carbonate formation for strength improvement purposes, a device is needed to visualise and analyse the obtained soil sample, in order to achieve digital information usually in 3-D format. One way to achieve this is by using XRCT. Other techniques used for confirmation and quantification of minerals in soil samples includes SEM and XRD. A summary of the different techniques used for confirmation and quantification of minerals in soil samples, and what information is obtained in each case is presented in Table 2.10.

**Table 2.10:** Techniques for confirmation and quantification of carbonates.

Property	Calcimeter	TGA	XRD	SEM	XRCT
CaCO <sub>3</sub> content	✓	✓			
Mineralogical composition		✓	✓		
Chemical composition				✓	
Surface appearance				✓	
Internal structure					✓

## 2.11 Chapter Summary

This chapter presents a detailed review of climate change due to anthropogenic CO<sub>2</sub> emissions and other greenhouse gases. Additionally, the process of lime modification, and carbonation in soils are described. The potential for development of combined modification and carbonation technique for carbon capture alongside strength improvement is reviewed. The following are the key summary points.

- Factors responsible for climate change such as anthropogenic CO<sub>2</sub> emissions and instability of clay for engineering function due to strength weakness, make combined modification plus carbonation technique ideal for carbon capture alongside strength improvement.
- Lime and cement are the preferred materials to be used in soil stabilisation. However, their manufacture involves substantial CO<sub>2</sub> emissions. This is in conflict with climate mitigation requirements. Therefore, there is need to recover this CO<sub>2</sub> emissions by developing a carbon capture function, whilst achieving desired soil strength improvements.
- To ensure soil, lime and CO<sub>2</sub> react so that combined carbon capture and strength improvement functions are achieved, a clear understanding of modification and carbonation mechanisms for combined modification plus carbonation treatment is important. Additionally thorough soil assessment must be done to include mineralogy and chemical characteristics. Soils suitable for lime stabilisation are to contain PI

value of greater than 10%, total sulphate content of at most 1%, and organic content of less than 2%.

- It is well known that lime is used for strength and stiffness improvement of clay. Clay modification is mainly achieved by dehydration, cation exchange, particle flocculation and agglomeration, whilst strength by pozzolanic reaction. Such pozzolanic reaction could be substituted with carbonation reaction by reduction of curing period to 7 days.
- Addition of lime to clay has great potential for modification followed by carbonation. This is because sufficient lime addition produces calcium ions for cation exchange and the amount required for carbonation reactions. Carbonation is known to remove significant amounts of atmospheric CO<sub>2</sub> as well as producing weak cementation.
- For suitability of lime or cement treated material for use in engineering function such as capping in road pavement, the material needs to meet some requirements of strength (UCS or CBR), stiffness, and durability such as freeze-thaw resistance.
- Lime-based waste material has the potential for use as an alternative to lime for strength, stiffness and durability improvement of weak soil. This could be followed by carbonation to achieve carbon capture alongside strength improvement. This is important for climate change mitigation alongside improvement of soil stability at a less expensive cost.
- To detect the presence and quantity of calcite formed, the calcimeter and TGA have been used successfully. XRCT technique has shown the potential for confirmation and quantification of carbonates. This is due to its ability of visualising image along the planes that cut the sample so that the volume elements (voxels) could be analysed.



## Chapter 3 – Materials and Methods

### 3.1 Introduction

This chapter presents the details of materials and testing methods used in the laboratory for this study. It includes a description of the preparation method for the compacted  $\text{Ca}(\text{OH})_2$  treated kaolin specimens. Compacted  $\text{Ca}(\text{OH})_2$  treated kaolin in this thesis is henceforth referred to as ‘treated kaolin’. Additionally, a description of the method and apparatus used for the formation of carbonated specimens by permeating  $\text{Na}_2\text{CO}_3$  (HC) solution through the treated kaolin is included, and the methods used to test the performance of the resulting specimens against a set of key performance indicators.

### 3.2 Testing Objectives and Outline Methodology

The following were the objectives of the laboratory testing

- 1) Determine the minimum percentage of  $\text{Ca}(\text{OH})_2$  content by dry mass, for significant strength gain of kaolin, based on the modified ICL test recommended by Rogers *et al.* (1997).
- 2) Produce treated kaolin specimens with a range of set densities (or air voids) and water contents using normal Proctor (light) compaction in accordance with BS 1924, part 2 (BSI 1990a) to determine the effect of air voids on carbonation.
- 3) Determine the effect of  $\text{Ca}(\text{OH})_2$  addition on strength property of kaolin, using the UCS testing after 7, 14 and 28 days curing period in accordance with BS 1924, part 2 (BSI, 1990a).
- 4) Determine the effect of permeating  $\text{Na}_2\text{CO}_3$  solution through treated kaolin specimen on the strength, stiffness and durability of the specimen, and examine the effect on geochemical and mineralogical changes of the specimen.

The outline methodology for achieving the objectives was

- 1) Dry mix  $\text{Ca}(\text{OH})_2$  (percentage by dry mass) and kaolin clay, and determine the minimum amount of lime for significant strength gain of kaolin based on the modified ICL recommended by Rogers *et al.* (1997).
- 2) Develop a method of carbonation treatment of treated kaolin based on the permeability in a triaxial cell test in accordance with BS 1377, part 6 (BSI, 1990b).

- 3) Use carbonation treatment method to permeate  $\text{Na}_2\text{CO}_3$  solution through the treated kaolin specimens for carbonation treatment, and test the performance of the resulting specimen in terms of strength, stiffness and FT durability.
- 4) Conduct geochemical and mineralogical analysis on selected carbonated treated kaolin samples to confirm the presence of  $\text{CaCO}_3$ , and quantify the  $\text{CaCO}_3$  content in the samples. 'Carbonated treated kaolin' in this thesis means the treated kaolin specimen that underwent carbonation treatment.

These steps will be discussed in more detail in the following sections:

### **3.3 Materials Used in the Laboratory Testing**

The list of the materials used in the laboratory testing in this study with the names and addresses of the suppliers are as follows:

The clay used is Imerys Polwhite Grade E kaolin. This clay was supplied by IMERYS Minerals Ltd, Par Moor Centre, Par Moor Road, Par, Cornwall, PL24 2SQ, UK. The chemical composition of the kaolin clay as provided by the supplier is contained in Appendix A, Table A1. The kaolin has a high silica content ( $\text{SiO}_2$ : 50 %) closely followed by alumina ( $\text{Al}_2\text{O}_3$ : 35 %), low surface area ( $8 \text{ m}^2/\text{g}$ ) and low soil pH (5.5). The rationale behind the use of kaolin clay in the current study was because it is chemically inert (Manning, 1995). Its mineralogical simplicity avoids interference from effects associated with other clays within a natural soil that might be poorly characterised. This allows experimental work to be done in a way that is easily reproducible.

The lime used is  $\text{Ca}(\text{OH})_2$  supplied by Lafarge Tarmac Cement & Lime, Tunstead House, Buxton, Derbyshire SK17 8TG, UK. The chemical composition of the lime as provided by the manufacturer is attached as Appendix A, Table A2. The lime is composed of a high quantity of  $\text{Ca}(\text{OH})_2$  (96.9 %) and a small quantity of  $\text{CaCO}_3$  (1.4 %). The rationale behind the choice of  $\text{Ca}(\text{OH})_2$  as the stabiliser used in the current study was as a result of cost and its availability. As of 2016 the prices of  $\text{Ca}(\text{OH})_2$  ranged from \$10-15 per 22.5 kg bag. It is also reported that it is readily available. However, the cost of MgO (alternative stabiliser) for the same quantity are higher and its availability as compared to  $\text{Ca}(\text{OH})_2$  is limited (Magwood, 2016). Additionally, the use of  $\text{Ca}(\text{OH})_2$  in soil treatment requires less water to achieve modification reaction, and this allows the treatment also to be applied at dry sites (Sherwood, 1993).

Na<sub>2</sub>CO<sub>3</sub> used in this study was supplied by VWR International Hunter Boulevard, Magna Park, Lutterworth, Leicestershire, LE17 4XN, UK. The chemical composition of the Na<sub>2</sub>CO<sub>3</sub> as provided by the supplier is attached as Appendix A, Table A3. The chemical composition shows predominant composition of Na<sub>2</sub>CO<sub>3</sub> (99.5 % min).

1 molar Na<sub>2</sub>CO<sub>3</sub> solution was used in the current study to produce the environment for carbonation treatment. The rationale behind the use of Na<sub>2</sub>CO<sub>3</sub> solution was that it produces high CO<sub>2</sub> concentration (Blencoe, 2003), which promotes fast carbonation kinetics (Nakarai and Yoshida, 2015). This was used instead of atmospheric CO<sub>2</sub> to overcome the low concentration that atmospheric CO<sub>2</sub> provides, which produces very slow carbonation kinetics (Nakarai and Yoshida 2015). Additionally, Na<sub>2</sub>CO<sub>3</sub> solution was used instead of CO<sub>2</sub> gas in order to avoid the experimental problem associated with CO<sub>2</sub> gas partitioning into solutions and then ionising. Furthermore, Na<sub>2</sub>CO<sub>3</sub> solution was used as a way of producing a controlled amount of carbonate in solution. This provides a simple and reproducible experimental method. Na<sub>2</sub>CO<sub>3</sub> solution from this point on is referred to as “HC solution” for convenience.

Deionised water was used throughout the experiment including mixing with untreated kaolin clay, Ca(OH)<sub>2</sub> mixed kaolin, and treated kaolin. Additionally, it was used in preparation of HC solution. The rationale for the use of deionised water was to avoid introducing competition reactions, which could be produced by addition of water containing dissolved ions. Since deionised water was used throughout the experiment, it may have dissolved some calcite, but in quantities that are negligible given the low water-solid ratios.

### **3.4 Materials Characterisation Testing**

To design a programme for this study, several experiments were conducted on untreated kaolin, Ca(OH)<sub>2</sub> mixed kaolin and treated kaolin to determine the resulting characteristic properties. ‘Untreated kaolin’ in this thesis means kaolin with no added Ca(OH)<sub>2</sub>.

The details of the experiments will be described in the following section:

- Initial consumption of lime
- Atterberg Limits
- Cation Exchange Capacity
- Compaction Testing
- Compressive Strength Testing

### 3.4.1 Initial Consumption of Lime

To determine the minimum lime required to achieve a significant strength gain of the kaolin, the ICL test was conducted on untreated and  $\text{Ca}(\text{OH})_2$  mixed kaolin. The ICL is defined as the minimum lime content required to be added to a soil to bring about a significant change in its properties, such as strength (BS 1924-2, BSI 1990a). The ICL used for this study, was determined based on a modified ICL test recommended by Rogers *et al.* (1997). Modified ICL test was established on the basis of full pH versus lime addition curve. The percentage amount of CaO by dry mass at which the pH curve flattens off (rises to asymptote) was used as the point of ICL value. This was used as an indicator of the amount of lime required for significant change in soil properties. The modified ICL method is described in detail by Rogers *et al.* (1997). The pH of the  $\text{Ca}(\text{OH})_2$ , and  $\text{Ca}(\text{OH})_2$  mixed kaolin used in the current study was determined using an Orion 710A pH/ISE meter in accordance with BS 1924 Part 2 (BSI, 1990a) (Figure 3.1)

Prior to the test, the pH meter was calibrated using the manufacturer standardisation solutions at pH 4, 7 and 9.2. The pH of  $\text{Ca}(\text{OH})_2$  was determined to check the suitability of the lime for stabilisation purpose. The pH of lime at 25 °C is required to be in the range of 12.35 to 12.45 for its suitability for lime stabilisation in accordance with BS 1924 Part 2 (BSI, 1990a).

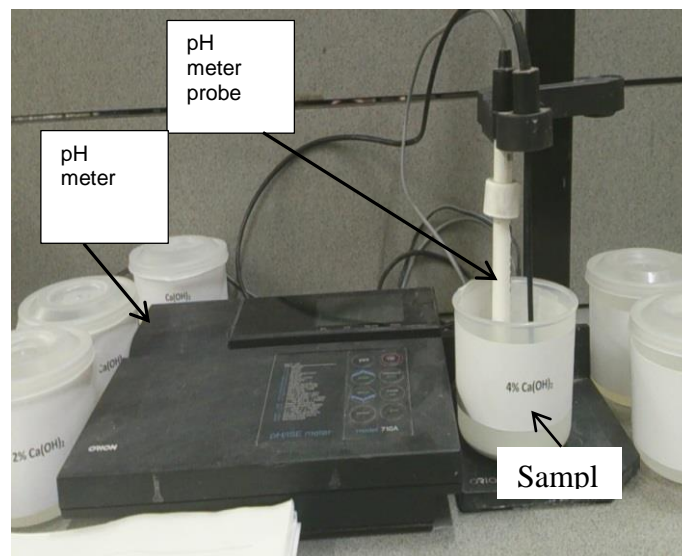


**Figure 3.1:** ORION 710A pH meter used to measure pH.

The pH test was performed on six specimens of  $\text{Ca}(\text{OH})_2$  mixed kaolin. 20.0g of kaolin was mechanically mixed each with 2.0%, 3.0%, 4.0%, 5.0%, 6.0%, 7%  $\text{Ca}(\text{OH})_2$  by dry mass and 100ml of deionised water in watertight plastic bottles. This was mixed for 15 minutes using an ‘end-over-end bottle shaker’ to achieve proper mixing (Figure 3.2). The suspension in air

tight covered bottles was kept for 24 hours, for sufficient initial reaction. Then the pH of samples was determined. A curve of full pH against lime addition was drawn, and the value of ICL was determined from the curve as the amount of lime at which the pH curve flattened off (asymptote was approached) as recommended by Rogers *et al.* (1997). The ICL value was measured with precision to 0.1% in accordance with BS 1924, Part 2 (BSI, 1990a).



**Figure 3.2:** End-over-end bottle shaker.

### 3.4.2 Atterberg Limits

Plastic and Liquid (Atterberg) Limit tests were performed on the untreated and  $\text{Ca}(\text{OH})_2$  mixed kaolin clay sample, to determine the PL and LL for the samples, and subsequently the plasticity properties of the untreated and  $\text{Ca}(\text{OH})_2$  mixed kaolin clay. Atterberg Limit (particularly PL) test was used to determine the  $\text{Ca}(\text{OH})_2$  content required for kaolin modification. The use of PL in determination of lime requirement for modification is a common approach. Rogers and Glendinning (1996) studied the modification of four British Clays (English China Clay also known as kaolin, Weathered Mercia Mudstone, Lower Lias Clay, and London Clay) using  $\text{CaO}$ . The authors concluded that “PL is the best indicator of the lime content necessary to achieve the degree of modification sought in general since the pattern of PL change is consistent for any one clay”. In the current study, Atterberg Limit tests were performed on the untreated and  $\text{Ca}(\text{OH})_2$  mixed kaolin clay using the Atterberg Limit testing equipment (Figure 3.3) in accordance with BS 1924, Part 2 (BSI, 1990a).

LL of the untreated and  $\text{Ca}(\text{OH})_2$  mixed kaolin clay was determined using cone penetrometer equipment in accordance with BS 1924, Part 2 (BSI, 1990a). The choice to use cone penetrometer equipment instead of Casagrande apparatus was because results obtained from cone penetrometer equipment are more reproducible and less dependent on the operator’s judgement, unlike the results from the Casagrande equipment. The equipment used in performing LL test is presented in Figure 3.3. The penetration of cone shaft into the test

sample was measured using the corresponding dial gauge with a precision to 0.1 mm, whilst the LL was determined using a balance with mass measurement precision to 0.01g in accordance with BS 1924, Part 2 (BSI, 1990a).

PL test was performed on the untreated and  $\text{Ca}(\text{OH})_2$  mixed kaolin clay to determine their PL, using the PL equipment in accordance with BS 1924, Part 2 (BSI, 1990a).

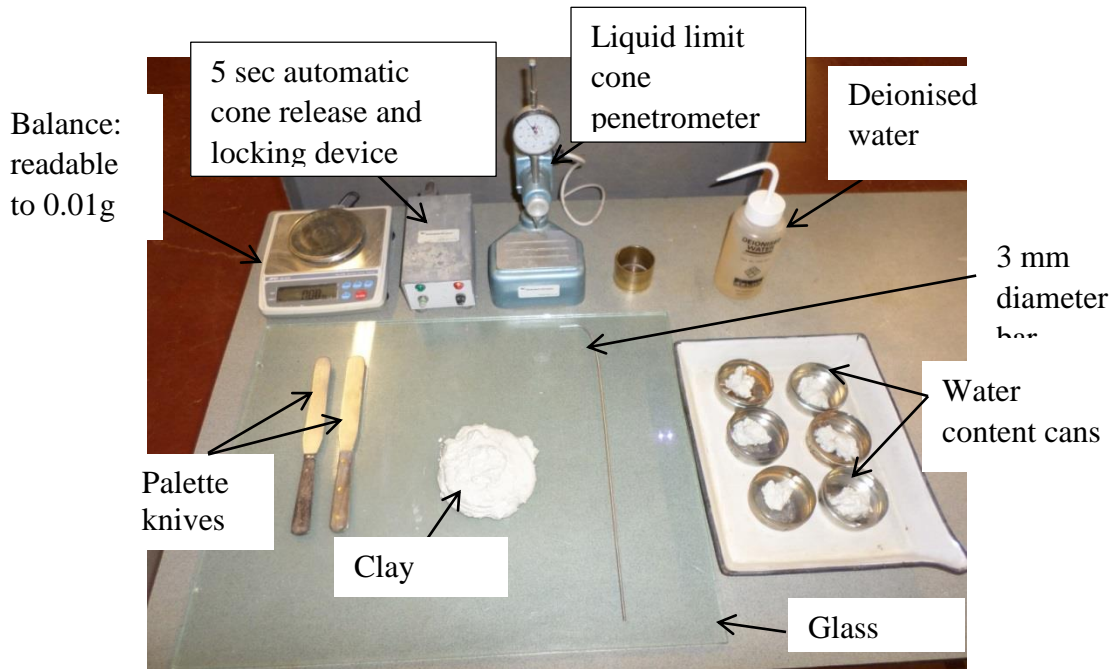


**Figure 3.3:** Plastic and liquid limit testing equipment.

To produce a homogenous paste for PL testing, seven portions each of 25 g of kaolin paste was prepared. 75 ml of water was added to 175 g of kaolin and mechanically mixed for 10 minutes to achieve thick kaolin paste, using a mixing composition of 70% kaolin to 30% deionised water by weight. The choice of the mixture ratio was based on the study by Murray (1980): which noted that a mixing composition of 70% kaolin to 30% water by weight could produce thick slurry kaolin.

Test was performed on the seven kaolin clay pastes, one untreated kaolin (this sample being the experimental control), and six  $\text{Ca}(\text{OH})_2$  mixed kaolin samples. To prepare  $\text{Ca}(\text{OH})_2$  mixed kaolin pastes, each of 25 g of the kaolin clay pastes was thoroughly mixed with  $\text{Ca}(\text{OH})_2$  at 1%, 2% and 3%, 4%, 6% and 8% (by dry mass) respectively using palette knives on a glass plate. The untreated and  $\text{Ca}(\text{OH})_2$  mixed kaolin paste samples were cured in airtight heavy duty polyethylene bags for 24 hours to allow for initial reaction between the clay and  $\text{Ca}(\text{OH})_2$ , and/or water. The mixes were then tested for PL using a mass balance with measurement precision to 0.01g in accordance with BS 1924, Part 2 (BSI, 1990a).

### ***3.4.3 Cation Exchange Capacity Testing***

To determine the capacity of kaolin to hold exchangeable positively charged ions, CEC testing was performed on untreated and  $\text{Ca}(\text{OH})_2$  mixed kaolin clay, using barium chloride solution buffered at pH of 8.1 (using triethanolamine) in accordance with BS 7755 part 3 (BSI, 1996). The CEC test was based on the clay capacity to exchange metal ions within the clay lattice with cations from the solution (BS 7755, part 3 BSI, 1996). The CEC of kaolin clay was used to determine the capacity of the kaolin clay to change in index properties (such as plasticity) on treatment with  $\text{Ca}(\text{OH})_2$ .

CEC testing was performed on 2.5 g of dry mass per sample. Seven specimens of untreated and  $\text{Ca}(\text{OH})_2$  mixed kaolin clay were tested for CEC. One untreated kaolin sample was used as experimental control, while the rest six kaolin clay samples were each mixed with  $\text{Ca}(\text{OH})_2$  content at 1%, 2%, 3%, 4%, 6% and 8% by dry mass respectively. The samples were saturated with barium chloride by treating it three times with buffered barium chloride solution. Subsequently, a known excess amount of 0.02 mol/l of magnesium sulphate solution was added to the samples. All the barium present as adsorbed (with the clay lattice) and present in solution was precipitated in form of insoluble barium sulphate ( $\text{BaSO}_4$ ). The clay sites with exchangeable ions were then filled up by magnesium. The concentration of excess magnesium in solution was determined using flame atomic absorption spectrometry (FAAS). In addition the concentration of the blank solution (as the control solution with concentration of magnesium solution without specimen) was determined using FAAS. Cation concentration was measured with precision to 0.01 cmol/kg. The CEC of the untreated and  $\text{Ca}(\text{OH})_2$  mixed kaolin clay samples were determined by the net ion concentration between the blank and that of excess magnesium solution, in accordance with BS 7755, part 3 (BSI, 1996).

### ***3.4.4 Compaction Testing***

Previous work (De Silva *et al.*, 2006) has shown that when density of compacted lime is increased, carbonation of the lime is decreased; indicating that density of compacted lime has an effect on carbonation. Therefore, one of the objectives of the experiment was to form specimens with a range of set densities as well as air voids contents, in accordance with BS1924 part 2 (BSI 1990a) to determine the effect of air voids on carbonation. To achieve the set range of densities and air voids contents, compaction testing was performed with seven test portions. This was to achieve a wide range of dry densities and water contents from the compaction curve of the test samples (this is described further in this section). Each of the

seven test portions comprised of 2.5 kg mass of kaolin clay and the set amount of percentage  $\text{Ca}(\text{OH})_2$  by dry mass. The compaction testing programme comprised of mixing phase and compaction phase.

### ***Soil Mixing***

The kaolin clay used for all trial mixes was first oven-dried at  $105 \pm 5 \text{ }^\circ\text{C}$  to constant weight for 24 hours. The rationale for soil drying was to remove water content in the soil. This allows for quantification of additives (such as  $\text{Ca}(\text{OH})_2$ , and water) with reference to the dry soil by mass.

Untreated kaolin clay, and  $\text{Ca}(\text{OH})_2$  mixed kaolin were each mechanically mixed with deionised water at minimum water content of 13 % below the PL, and further at increments of 3 %. Mechanical mixing of all the combinations were carried out using a Hobart rotary mixing machine (Figure 3.4).



**Figure 3.4:** Hobart mixer.

The untreated kaolin clay was mechanically mixed with the pre-calculated amount of water for 8 minutes in accordance with BS 1377, part 4 (1990b). The amount of water was determined based on moisture content (this is described further in this section).

Once mixed, the sample was placed in an airtight polythene bag and stored for 24 hours in a temperature controlled room ( $20 \text{ }^\circ\text{C}$ , and 55% relative humidity). The rationale for airtight storage was to avoid water loss by evaporation. The sample was then ready for compaction testing.

For the  $\text{Ca}(\text{OH})_2$  mixed kaolin, kaolin only was firstly mechanically mixed with the pre-calculated amount of water, which was reduced by amount equal to 3% of the mass of dry kaolin clay. The mixing was carried out for 8 minutes to achieve uniform moisture distribution, then immediately placed in an airtight polythene bags, and stored in a temperature controlled room (20 °C, 55% relative humidity) for 24 hours.  $\text{Ca}(\text{OH})_2$  amounts at 1%, 2%, 3%, 4%, 6%, and 8% by dry mass were further added to the moistened kaolin and mechanically mixed for 2 minutes, and then the remaining water (amount of 3% mass of dry kaolin clay) was added. This was mechanically mixed for further 8 minutes. The mixture was cured for additional 24 hours in airtight polythene bags to allow for initial reactions between the clay, lime and/or water. Thereafter, the sample was mixed for an additional 5 minutes before compaction testing.

### Compaction

Compaction tests were performed on untreated kaolin, and  $\text{Ca}(\text{OH})_2$  mixed kaolin using the normal Proctor (Light) compaction method according to BS 1377 (1990b). This method consists of 1L mould and a 50mm diameter circular faced 2.5 kg rammer, which is released to fall free from 300 mm height. It also involve the application of 27 blows for each of layer for three compaction layers (Figure 3.5). The untreated kaolin, and  $\text{Ca}(\text{OH})_2$  mixed kaolin prepared as stated previously in this Section, were each compacted using normal Proctor (Light) compaction method.

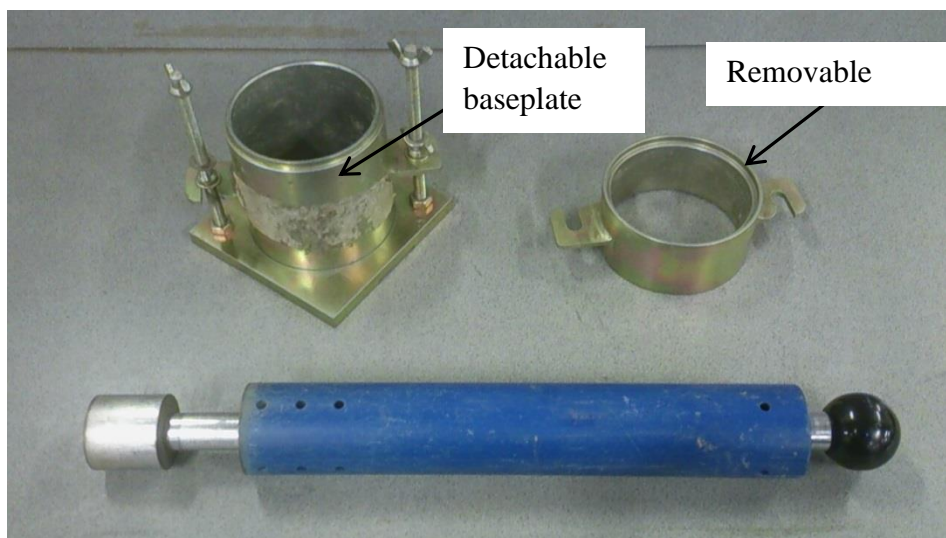


**Figure 3.5:** Compaction apparatus, 1 litre sample mould (upper), 2.5 kg compaction rammer (lower).

The resulting dry density and the corresponding moisture content per test specimen were determined. For the  $\text{Ca}(\text{OH})_2$  mixed kaolin, seven results of dry densities and the

corresponding moisture content were determined. The dry densities were plotted against the corresponding moisture contents and a smooth curve that joined the points was drawn. Maximum dry density (MDD) and the corresponding OMC were determined from the curve in accordance with BS 1924-2 (1990a). On the same graph plots of curves corresponding to 0%, 10%, 15%, 20% and 25% air voids lines were drawn in accordance with BS 1924 (1990a). The dry density ( $\rho_d$ ) values for the air void lines were determined using Equation 3.1. Specimen densities were determined by mass measurement using a balance with precision to 0.01g. Moisture contents were determined by mass measurement using a balance with precision to 1g in accordance with BS 1924 part 2 (BSI 1990a).

$$\rho_d = \rho_w \left[ \frac{1 - \frac{AV}{100}}{\frac{1}{\rho_z} + \frac{w}{100}} \right] \quad (3.1)$$

where, AV is the air voids content in the treated kaolin expressed as a percentage.

w is the moisture content of the treated kaolin (in %).

$\rho_w$  is the density of water taken as 1.00 Mg/m<sup>3</sup>

$\rho_z$  is the combined particle density (in Mg/m<sup>3</sup>) of Ca(OH)<sub>2</sub> and kaolin determined from Equation 3.2:

$$\rho_z = \frac{1 + \frac{c}{100}}{\frac{1}{\rho_m} + \frac{c}{\rho_c}} \quad (3.2)$$

where, c is the Ca(OH)<sub>2</sub> content expressed as a percentage of the dry kaolin (in Mg/m<sup>3</sup>).

$\rho_m$  is the particle density of kaolin, taken as 2.60 Mg/m<sup>3</sup> (as provided by the supplier).

$\rho_c$  is the particle density of the Ca(OH)<sub>2</sub>, assumed to be 2.13 Mg/m<sup>3</sup> at 20°C in accordance with BS 1924 part 2 (BSI 1990a).

Dry densities and corresponding moisture contents at the intersection of air voids curves and compaction curve were read as presented in Table 3.1. The detailed compaction curves are presented in Figures 3.6 and 3.7. These dry densities and moisture contents were used in the compaction programme for formation of treated kaolin specimen.

**Table 3.1: Compaction testing data.**

Calcium hydroxide content (%)	Air void (AV) (%)	W (%)	<sup>c</sup> Dry density (Mg/m <sup>3</sup> )	Bulk density (Mg/m <sup>3</sup> )	Bulk mass (g)
0	3 <sup>a</sup>	27 <sup>b</sup>	1.44	1.82	157
4	3 <sup>a</sup>	30 <sup>b</sup>	1.43	1.85	160
	10	26	1.41	1.77	152
	15	23	1.38	1.70	147
	20	21	1.35	1.64	141
	25	18	1.34	1.58	136
6	3 <sup>a</sup>	30 <sup>b</sup>	1.42	1.85	159
	10	26	1.40	1.76	152
	15	24	1.37	1.70	146
	20	21	1.34	1.62	140
	25	18	1.32	1.56	135
8	3 <sup>a</sup>	30 <sup>b</sup>	1.42	1.84	159
	10	26	1.39	1.75	151
	15	24	1.36	1.69	145
	20	22	1.33	1.62	139
	25	19	1.31	1.55	134

<sup>a</sup>Air void (AV) at maximum dry density (MDD).  
AV was determined using Equation 3.3,

$$AV=100 - 100\rho_d \left[ \frac{1}{\rho_z\rho_w} + \frac{w}{100} \right] \quad (\text{Equation 3.3})$$

<sup>b</sup>Moisture content at OMC.

<sup>c</sup>Dry density ( $\rho_d$ ) determined using  $= \frac{\rho_b}{1+w}$ , where  $\rho_b$  is the bulk density  $= \frac{\text{bulk mass}}{\text{Specimen Volume}}$

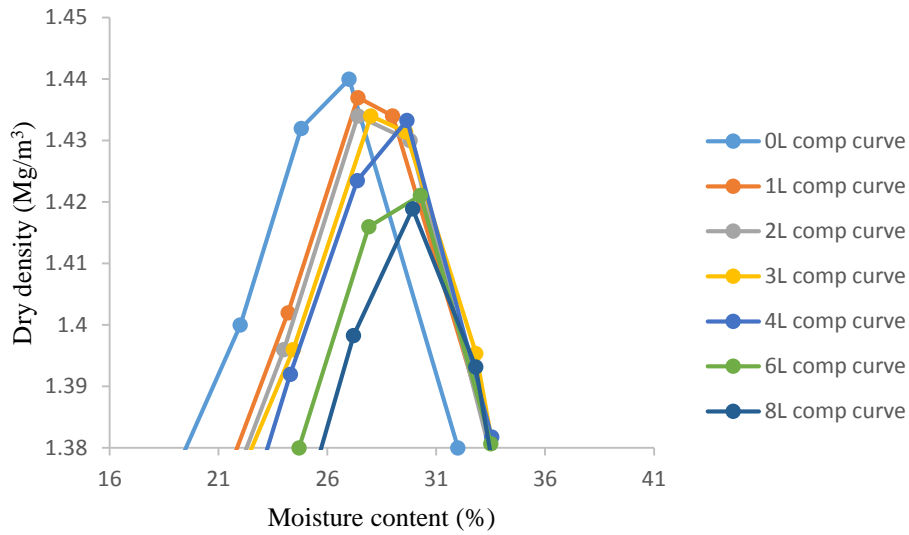


**Figure 3.6:** Variation of dry density with moisture content of calcium hydroxide mixed kaolin. L represents percentage  $\text{Ca}(\text{OH})_2$  content.

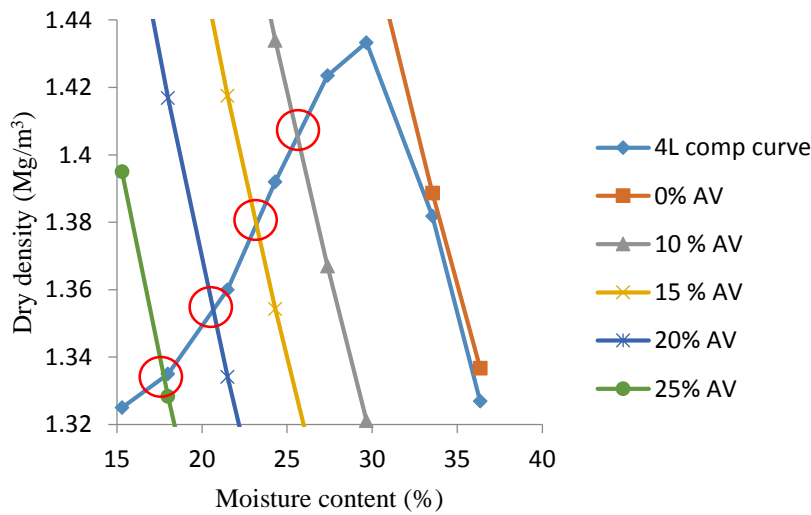
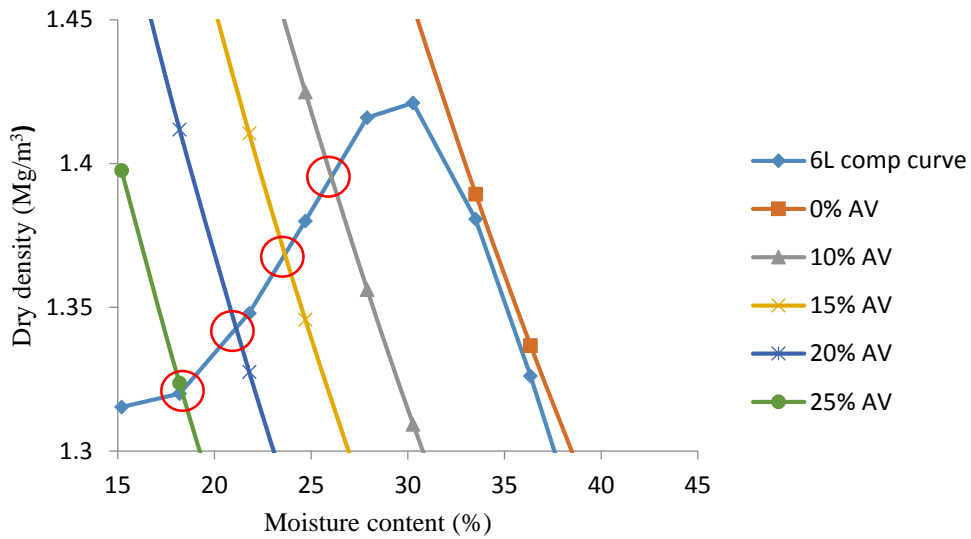
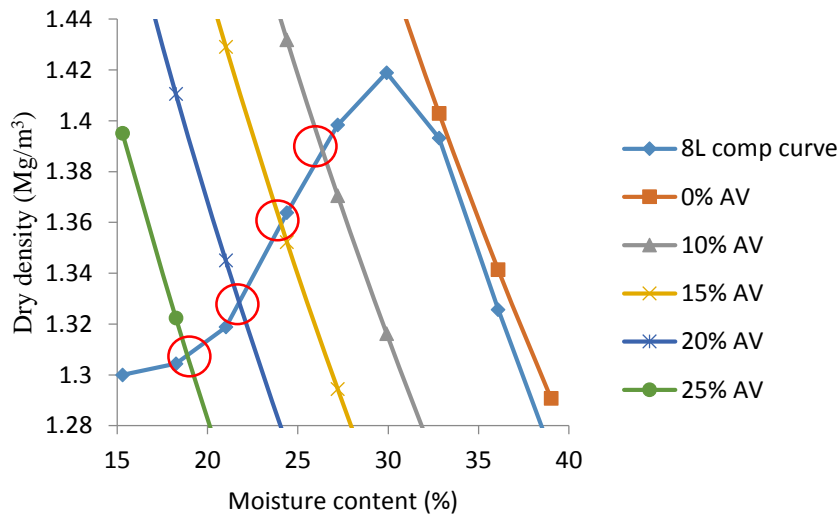


**Figure 3.7a:** Relationship of dry density-moisture content with air void lines in 4%  $\text{Ca}(\text{OH})_2$  treated kaolin. Red circles show the intersection of air voids lines and compaction curve. Dry density and moisture content at intersection used in compaction for formation of treated kaolin. L represents percentage  $\text{Ca}(\text{OH})_2$  content. AV represents air voids content.



(b)



(c)

**Figure 3.7 continued:** Relationship of dry density-moisture content with air void lines in treated kaolin. Red circles show the intersection of air voids lines and compaction curve (b) 6% Ca(OH)<sub>2</sub> content (c) 8% Ca(OH)<sub>2</sub>. Dry density and moisture content at intersection used in compaction for formation of treated kaolin. L represents percentage Ca(OH)<sub>2</sub> content. AV represents air voids content.

### ***3.4.5 Strength Testing***

The strengths of untreated, treated, and carbonated treated kaolin clay were determined using UCS in accordance with BS 1377, Part 7 (BSI, 1990b). Specimens used for UCS testing were initially compacted and cured to enable determination of strength gain due to desired treatments (combined modification and carbonation treatments in the current study). The strength testing programme consisted of specimen preparation phase, curing phase and compressive strength testing. The details of these will be described below:

#### **Specimen preparation**

To achieve the set densities as well as air voids content of untreated and treated kaolin specimens, the specimens were prepared based on pre-calculated data in Table 3.2. Pre-calculated masses of  $\text{Ca}(\text{OH})_2$ , kaolin clay and water were mechanically mixed as described in Section 3.4.4. The mixture of  $\text{Ca}(\text{OH})_2$ , kaolin and water were then tamped into a split mould of dimensions 38 mm diameter and 76 mm length (Figure 3.8) in three layers. After the lower plug was inserted, the samples were uniformly tamped into a split mould and the upper plug inserted. The mould assembly was placed in a hydraulic press and compressive force applied to the plugs until the flanges made contact with the barrel of the specimen mould. The plugs were removed and specimen extruded using hydraulic plunger. Specimens were immediately placed in 38 mm PVC plastic specimen tubes and the ends sealed with wax for curing. Samples were prepared in batches of nine for each combination. This technique allowed the formation of specimens of consistent dimensions (38 mm diameter and 76 mm length) and the target densities.

**Table 3.2:** Target sample properties. Please note that part of the data is a replication of Table 3.1 and is included here for ease of reading.

Calcium hydroxide content (%)	W (%)	<sup>c</sup> Dry density (Mg/m <sup>3</sup> )	Bulk density (Mg/m <sup>3</sup> )	Bulk mass (g)
0	27 <sup>a</sup>	1.44 <sup>b</sup>	1.82	157
1	27 <sup>a</sup>	1.44 <sup>b</sup>	1.84	159
2	27 <sup>a</sup>	1.43 <sup>b</sup>	1.84	158
3	28 <sup>a</sup>	1.43 <sup>b</sup>	1.84	158
4	30 <sup>a</sup>	1.43 <sup>b</sup>	1.85	160
	26	1.41	1.77	152
	23	1.38	1.70	147
	21	1.35	1.64	141
	18	1.34	1.58	136
6	30 <sup>a</sup>	1.42 <sup>b</sup>	1.85	159
	26	1.40	1.76	152
	24	1.37	1.70	146
	21	1.34	1.62	140
	18	1.32	1.56	135
8	30 <sup>a</sup>	1.42 <sup>b</sup>	1.84	159
	26	1.39	1.75	151
	24	1.36	1.69	145
	22	1.33	1.62	139
	19	1.31	1.55	134

<sup>a</sup> Optimum moisture content (OMC). <sup>b</sup> maximum dry density (MDD)

<sup>c</sup> Dry density ( $\rho_d$ ) determined using  $\rho_d = \frac{\rho_b}{1+w}$ , where  $\rho_b$  is the bulk density =  $\frac{\text{bulk mass}}{\text{Specimen Volume}}$ ,



**Figure 3.8:** Split specimen mould.

### **Curing**

Treated kaolin clay specimens placed in 38 mm PVC plastic tubes, with ends sealed with wax, were cured in a temperature controlled room (20 °C, and 55 % relative humidity) for 7, 14 and 28 days period for stabilisation treatment, in accordance with BS 1924, part 2 (BSI, 1990a). The curing of treated kaolin as from 28 days allows for pozzolanic reaction resulting in formation of cementitious compound such as calcium aluminate hydrate (CAH), and subsequent strength development (Vitale *et al.*, 2017). Once the curing period was completed, specimens were extruded using a hydraulic plunger and tested for UCS immediately.

The set of specimens used for carbonation treatment were cured for 7 days prior to carbonation treatment (described in Section 3.5.2). The 7 days curing was to allow for short term reactions which are often considered as modification reactions (Jung and Bobet, 2008). Curing of lime treated clay for 7 days is lower than a single fixed curing period of 28 days for strength development in lime stabilisation treatment according to BS 1924, part 2 (BSI, 1990a).

In order to simulate a critical moisture state for lime treated soil under reasonable pavement condition, post 7 days cured specimens were soaked in water for 24 hours as required for low to moderate plasticity soils, according to the method by Little (2000). The soaking was carried out by allowing water to permeate through the specimen for 24 hours, using a triaxial cell set-up (this is further described in Section 3.5.2). The soaking using triaxial cell set-up was selected in order to compare UCS results of water soaked specimen with that of HC solution soaked carbonated specimen.

## **Unconfined compressive strength**

Treated kaolin specimens were tested for their UCS, using an INSTRON 5585H loading frame, at a strain rate of 1 mm/min (1.3%/mm), in accordance with BS 1377, Part 7 (BSI, 1990b). The INSTRON 5585H loading frame has load measurement precision to  $\pm 0.4\%$ , and strain measurement precision to 0.5%/mm. Three samples were tested for each mix combination after a curing period of 7, 14 and 28 days.

### **3.5 Modification and Carbonation Treatment**

A combination of modification and carbonation treatment was performed on kaolin clay to determine the resulting effect on the kaolin clay in terms of strength, geochemical and mineralogical composition. The combination of modification and carbonation treatment techniques consisted of three parts:

- Soil modification
- Carbonation treatment
- Strength and durability, geochemical and mineralogical testing

#### **3.5.1 Soil Modification**

To achieve modification treatment, treated kaolin specimens were cured for 7 days. This curing allows for short term reaction which could achieve modification treatment (Jung and Bobet, 2008). Modification of kaolin clay is important because it improves the workability of the clay, and provides firm support for construction activities, due to increases in PL (Sherwood, 1993; Rogers *et al.*, 1997).

In order to achieve significant strength gain, the amount of  $\text{Ca(OH)}_2$  addition for formation of treated kaolin specimens was based on the result of the modified ICL test recommended by Rogers *et al.* (1997). In this study the ICL value obtained was 4 %  $\text{Ca(OH)}_2$  (3% CaO equivalent) by dry mass. The ICL value was used as the baseline lime addition for significant strength gain of the kaolin clay. Therefore lime added to the kaolin clay was from equivalence of ICL value,  $\text{ICL}+1\frac{1}{2}\%$  CaO, and  $\text{ICL}+3\%$  CaO contents by dry mass. This resulted in addition of  $\text{Ca(OH)}_2$  at 4%, 6% and 8% by dry mass to kaolin clay. These amounts of  $\text{Ca(OH)}_2$  (% by dry mass) were added to kaolin clay and mechanically mixed (as described in Section 3.4.4) for formation of treated kaolin specimens.

Treated kaolin specimens were prepared by compacting a mixture of pre-calculated amounts of  $\text{Ca}(\text{OH})_2$  and kaolin clay (as earlier described in Section 3.4.5) to achieve consistent set density. After insertion of the lower plug of a split mould, the mixtures of  $\text{Ca}(\text{OH})_2$  and kaolin clay were uniformly tamped into the split mould in three layers, and the upper plug inserted. The mould assembly was placed in a hydraulic press and compressive force applied to the plugs until the flanges were in contact with the barrel of the specimen mould. The plugs were removed and specimen extruded using a hydraulic plunger.

The treated kaolin samples were immediately placed in 38 mm PVC plastic specimen tubes and the ends sealed with wax. Specimens were prepared in batches of three. These specimens were cured in a temperature-controlled room (20 °C, and 55 % relative humidity) for 7 days in accordance with BS 1924, part 2 (1990a). Once the curing period was completed, specimens were extruded using a hydraulic plunger and immediately transferred for carbonation treatment.

### ***3.5.2 Carbonation Treatment***

To form carbonated treated kaolin specimens, a carbonation treatment experiment was conducted on treated kaolin specimens based on the permeability in a triaxial cell test in accordance with BS 1377-6 (BSI, 1990b). The triaxial cell used in this study was fitted with a measurement and control system (Geotechnical Digital Systems: GDS) having automatic pressure and volume control units (Figure 3.9).

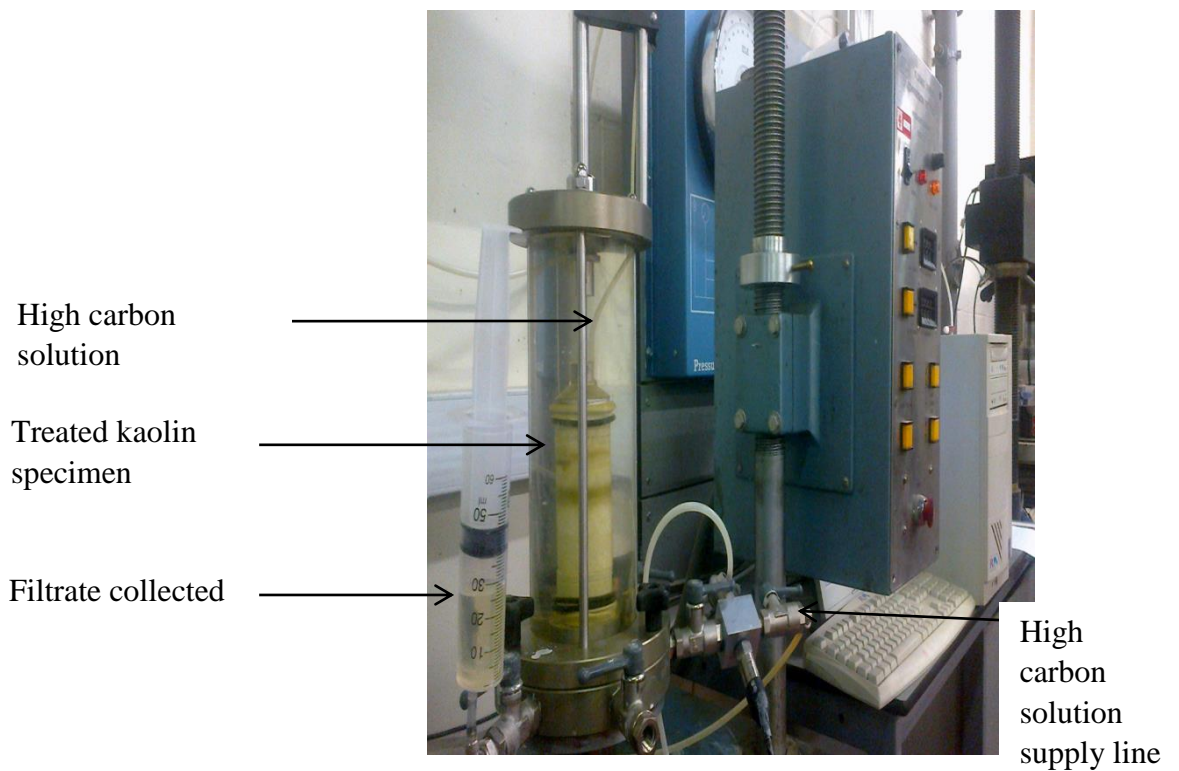


**Figure 3.9:** Carbonation treatment of treated kaolin clay using triaxial cell set-up.

In order to perform carbonation treatment, some adjustments to the triaxial cell test were carried out. This was because HC solution was required to permeate through the treated kaolin specimen to achieve accelerated carbonation. Therefore, a carbonate solution tank was required to be added to the triaxial cell arrangement for storage of the HC solution. In addition, the dimensions of the treated kaolin specimens for carbonation treatment were to be consistent with those required for UCS testing. This was to allow for strength testing of the specimens after carbonation treatment. To avoid corrosion that could result from contact between steel and HC solution (Cui *et al.*, 2006), the triaxial base pedestal and top cap (flow line components of HC solution) were made of perspex instead of steel.

The carbonation treatment method was varied from the permeability in triaxial test according to BS 1377-6 (BSI, 1990b) in the following ways:

- A carbonate solution tank was added to the system, to accommodate the HC solution. The tank was connected to the volume change gauge, and then to pore-pressure line onto the top cap of the cell.
- HC solution (under constant pressure) was supplied to the treated kaolin specimen via the pore-pressure line onto the top of specimen.

- An air-tight syringe was connected to the drainage line to collect filtrate from the treated kaolin specimen. The syringe consisted of a movable piston which allowed the collection of filtrate from the specimen.
- The treated kaolin specimens were produced with cylindrical dimensions of 38mm diameter and 76 mm length, based on diameter to length ratio of 1:2. This is different from the dimension of diameter to length ratio of 1:1 for specimens of permeability test only (BS 1377, part 6: BSI, 1990b). Considering that UCS testing for post carbonated treated kaolin specimens was required, the dimensions ratio (diameter to length ratio of 1:2) of specimen specified for UCS testing was chosen.

Due to these adjustments, the triaxial cell allowed for both permeability and carbonation treatment.

The treated kaolin specimen, which was cured for 7 days was placed in the triaxial cell. Specimens were saturated using HC solution at Skempton's pore pressure parameter B, of at least 0.95. Fluid pressure was applied to the specimen, concurrently with increased cell pressure to achieve saturation in accordance with BS 1377, part 6 (BSI, 1990b).

HC solution was permeated downward through the treated kaolin specimen at gauge pressure of 100 kPa, and cell confining pressure of 150 kPa. The filtrate was collected through the syringe at intervals of 1 hour period until the carbonation treatment was completed. The carbonation treatment was considered completed when the electrical conductivity (EC) of the filtrate was the same as the EC of the supplied HC solution.

The EC of the filtrate from the specimen was determined in accordance with BS 7755-3.4 (BSI, 1995b) using a microprocessor controlled electrical conductivity/TDS meter (HANA HI 9835 model).

### ***3.5.3 Testing of Carbonated Treated Kaolin Specimen***

The testing programme for the carbonated treated kaolin consisted of 4 separate parts

- UCS Testing
- Freeze Thaw Durability Testing
- Geochemical Testing
- Mineralogical Testing

### ***3.5.4 Unconfined Compressive Strength Testing***

In order to determine the strength of carbonated treated kaolin, specimens were tested for their UCS using an INSTRON 5585H loading frame, at a strain rate of 1 mm/min (1.3 %/mm), in accordance with BS 1377, Part 7 (BSI, 1990b). Three specimens were tested for each mix combination, and the average value of UCS was taken to represent the strength of the specimen. The tested specimens were retained for geochemical and mineralogical analysis.

### ***3.5.5 Freeze-Thaw Durability Testing***

FT test was performed on carbonated treated kaolin specimen to determine the resistance of the specimen to the effect of freezing and thawing cycles (3 FT cycles in each case).

The FT test performed in this study was partly based on ASTM procedure D560-03 (ASTM, 1989), and a design procedure of the National Lime Association (NLA, 2006). Carbonated treated kaolin specimens with dimension of 38 mm diameter, 76 mm length, were used instead of the specified dimensions ( $101.6 \pm 0.41$  mm diameter, and 116.43 mm length). The choice of this specimen dimension was because specimens were to undergo permeability/carbonation testing in a triaxial cell prior to FT testing. Also, the same specimens after FT exposure were to be tested for UCS. Therefore, specimen dimensions (38 mm diameter, 76 mm length) were used to suit the experimental set up in triaxial cell, as well specified dimension for UCS testing. This modified dimension has been successfully used in FT testing of stabilised soil by Hughes and Glendinning (2004).

In accordance with D560-03 (ASTM, 1989), the specimens were placed on water saturated felt pads and placed in a freezing chamber, at  $-10^{\circ}\text{C}$  for 24 hours after which specimens were removed and placed in a moisture-controlled room at  $20^{\circ}\text{C}$  for thawing. During the thawing phase, free water was made available under the felt pads.

A complete FT cycle was made up of 24 hours freezing and 23 hours thawing session. The specimens were subjected to three FT cycles. This study adopted a minimum of three FT cycles for testing as recommended by the National Lime Association, (2006). On completion of the three FT cycles, the specimens were tested for UCS and compared with the UCS of the control specimens (corresponding samples not subjected to FT cycles). The specimens in all cases were not brushed, so as to achieve a consistent result as recommended by Shihata and Baghdadi (2001), and to prevent further reduction in size of the specimens for UCS testing. According to Hughes and Glendinning (2004) brushing this type of specimen would render

them more susceptible to destruction in freezing and thawing effect than the samples specified in the standard (D560-03: ASTM, 1989).

Due to the time involved, 6 batches with 3 samples in each batch of carbonated treated kaolin were selected for the FT testing. The selection was based on the specimens at air voids of OMC (specimens at 3% air voids content in this study). Also specimens at air voids with highest strength in carbonated treated kaolin specimens (in this study 10% air voids content) were selected for the FT testing. These samples were selected for each of the  $\text{Ca(OH)}_2$  combinations of 4%, 6% and 8%  $\text{Ca(OH)}_2$  content.

### ***3.5.6 Geochemical Testing***

Geochemical analysis was performed on carbonated treated kaolin samples to confirm the presence and quantify  $\text{CaCO}_3$  content. The geochemical analysis consisted of two distinct parts, these are:

- Calcimeter Analysis, and
- TGA

## Calcimeter Analysis

Calcimeter analysis was performed on carbonated treated kaolin samples to confirm the presence and quantify  $\text{CaCO}_3$  content. The calcimeter is an instrument used to determine quantity of carbonate in soil. In this study calcimeter analysis was used to determine the quantity of inorganic carbonate present in the carbonated treated kaolin and was compared to the result of non-carbonated treated kaolin. The testing was carried out using an Eijkelkamp calcimeter in adherence with BS 7755-3.10 (BSI, 1995a). The technique determines carbonates in a sample based on a volumetric approach. Mass measurement precision to  $\pm 0.0001$  g was carried out using Mettler AE 163 calibrated balance.

About 2 g of sample was mixed with 20 ml of deionised water in a 200 ml conical flask. 7 ml of 4 mol /l hydrochloric acid was measured into a 10 ml reaction vessel and placed upright in the conical flask using tweezers. With the atmospheric switch open, the bungs connecting the inlet tubes of calcimeter were fitted securely to the flask necks. The water levels in the burette were set to a value of 3 ml, and the atmospheric switch closed. The conical flask was agitated and hydrochloric (HCl) acid in the reacting vessel mixed with the sample. The sample reacted with the HCl acid and carbonates present were converted to  $\text{CO}_2$ . The converted  $\text{CO}_2$  gas released during this reaction was collected in the burette and measured against a standard calibration to determine the percentage of  $\text{CaCO}_3$  contained in the original sample (Calcimeter, 2012).

The calcimeter technique was calibrated with analytical grade  $\text{CaCO}_3$ , and checked with WEPAL standard reference material ISE 930 2004:1 carbonate standard. Results of analysis of the reference material is presented in Table 3.3.

**Table 3.3:** Calcimeter standards.

	ISE 930 2004: 1/2 Clay soil, Ivory Coast	Pure $\text{CaCO}_3$
Actual value	7.63	> 98 %
Mean determined	7.46	99.15
Standard deviation	0.12	1.50

## **Thermogravimetric – Differential Scanning Calometry – Quadrupole Mass Spectrometry**

TGA was performed on carbonated treated kaolin samples to confirm the presence and quantify  $\text{CaCO}_3$  content. TGA is a technique that measures the mass change of a sample as a function of temperature or time in a controlled atmosphere. Due to cost involved TGA was performed on selected samples with remarkable compressive strength. The selected samples represented the three  $\text{Ca}(\text{OH})_2$  contents used in this study. The samples were carbonated treated kaolin at same target air voids value of 10%, with various  $\text{Ca}(\text{OH})_2$  contents of 4%, 6% and 8%. The amount of  $\text{CaCO}_3$  decomposed during heating in the carbonated samples was determined. Also, the mass loss of carbonate formed in carbonated treated kaolin samples with varying  $\text{Ca}(\text{OH})_2$  content was determined.

This analysis was performed by staff in Newcastle University. The thermogravimetric (TG) system (Netzsch TG209) in Newcastle University utilises between 30 and 60 mg of powdered sample, with mass measurement precision to  $\pm 0.1$  mg. This mass of sample was weighed into a platinum crucible and placed on a balance ( $10^{-3}$  mg sensitivity) inside a heating chamber. The atmosphere inside the furnace was continually flushed with  $\text{He}_{80}\text{O}_{20}$  mixture while the sample was heated to a temperature between 900-1000°C with a linear heating rate of 10°C per min. The Newcastle University's Thermogravimetric – Differential Scanning Calometry (Netzsch STA449C Jupiter) machine records the weight loss as a function of time. It also simultaneously measures energy flux inside the heating chamber by differential scanning calorimetry (DSC). The system is attached to a quadrupole mass spectrometer (Netzsch QMS403C Aëolos), which speciates the evolved gas during thermal decomposition, and provides a qualitative indicator of sample chemistry. With the recorded data, the TG curve was plotted from sample mass against temperature.

### **3.5.7 Mineralogical Testing**

Mineralogical analysis was performed on carbonated treated kaolin specimens to confirm the presence and quantify  $\text{CaCO}_3$  content. The mineralogical analysis consisted of two separate parts:

- X-ray computed tomography
- Scanning Electron Microscopy

#### **X-ray Computed Tomography Analysis**

XRCT analysis was performed on carbonated treated kaolin samples to confirm the presence and quantify  $\text{CaCO}_3$  content. XRCT is a non-destructive technique with high resolution used to obtain tomographic images of internal structures of the sample in 3-D geometry. The samples were scanned in XRCT, by directing a beam of X-rays to the sample from multiple orientations. Computed tomography (CT) slice images were measured from decreased intensity along a series of linear paths. A typical CT slice image is made up of voxels (volume elements); instead of the pixels (picture element) such as produced in digital image (Ketcham *et al.*, 2001; ASTM, 1992).

In this study, XRCT scanning was performed on two groups of samples (treated kaolin and carbonated treated kaolin), and images obtained. Minerals formed, and changes in voids after carbonation treatment were determined by processing the XRCT images. Details of the process performed in this study are presented in this section.

#### **Sample Selection**

It was decided to conduct XRCT testing on selected carbonated treated kaolin, and treated kaolin (which is non-carbonated) samples. Details of the sample preparation are contained in previous sections (Section 3.4.4). Samples were selected based on samples with the highest compressive strength and compressive strengths at extreme cases. Samples were selected also based on extreme and limiting air voids for  $\text{CaCO}_3$  content (results contained in Chapter 4: Sections 4.2 and 4.3). A total of ten samples were selected; nine carbonated treated kaolin, and one treated kaolin samples. The selection was for all  $\text{Ca}(\text{OH})_2$  (4%, 6% and 8%) contents used in this study. Samples at 10% air voids content had highest strength and remarkable  $\text{CaCO}_3$  content, whilst samples at 3% and 25% air voids contents represent those at extreme compressive strength and  $\text{CaCO}_3$  contents (Table 3.4).

**Table 3.4:** List of carbonated and non-carbonated samples tested.

Sample name	Sample description	
	Carbonated sample	Non-carbonated sample
4L3AV	4% Ca(OH) <sub>2</sub> content, at 3 % air voids content	–
6L3AV	6% Ca(OH) <sub>2</sub> content, at 3 % air voids content	–
8L3AV	8% Ca(OH) <sub>2</sub> content, at 3 % air voids content	–
4L10AV	4% Ca(OH) <sub>2</sub> content, at 10 % air voids content	–
6L10AV	6% Ca(OH) <sub>2</sub> content, at 10 % air voids content	–
8L10AV	8% Ca(OH) <sub>2</sub> content, at 10 % air voids content	8% lime content, at 10 % air voids content
4L25AV	4% Ca(OH) <sub>2</sub> content, at 25 % air voids content	–
6L25AV	6% Ca(OH) <sub>2</sub> content, at 25 % air voids content	–
8L25AV	8% Ca(OH) <sub>2</sub> content, at 25 % air voids content	–

### XRCT Sample Preparation

To assess the changes in internal structure (such as voids, particle arrangement) of carbonated treated kaolin clay, the sample was scanned using an Zeiss VersaXRM410 XRCT scanner (Durham University School of Engineering and Computing Sciences, UK). The XRCT scanner has a measurement precision to 0.9  $\mu\text{m}/\text{pixel}$ . High resolution scanning was required to distinguish voids spaces, CaCO<sub>3</sub> and kaolin clay particles in the sample. CaCO<sub>3</sub> grains from lime carbonation can be from 2-4 microns (De Silva *et al.*, 2006), whilst particle size of kaolin clay can be up to 30  $\mu\text{m}$ . Therefore it was decided to select scanning resolution of 1 pixel to 2.5  $\mu\text{m}$  for the sample scans. This scan was intended to distinguish the particles of CaCO<sub>3</sub>, kaolin clay and voids spaces in the sample.

It is recommended that the specimen be of the order of 1,000 times larger than the desired resolution for XRCT scanning (Ketcham and Carlson, 2001). To prepare samples for high resolution scanning, a core sample of 5 mm diameter and 25 mm height was obtained from parent carbonated treated kaolin sample (38 mm diameter, 76 mm height) (Figure 3.10 (a)). Plastic tube (5 mm diameter, 25 mm height) was axially driven through the central carbonated treated kaolin sample, and the core sample recovered in the plastic tube Figure 3.10 (b). The sample was then used for scanning, and resulting images obtained for analysis.

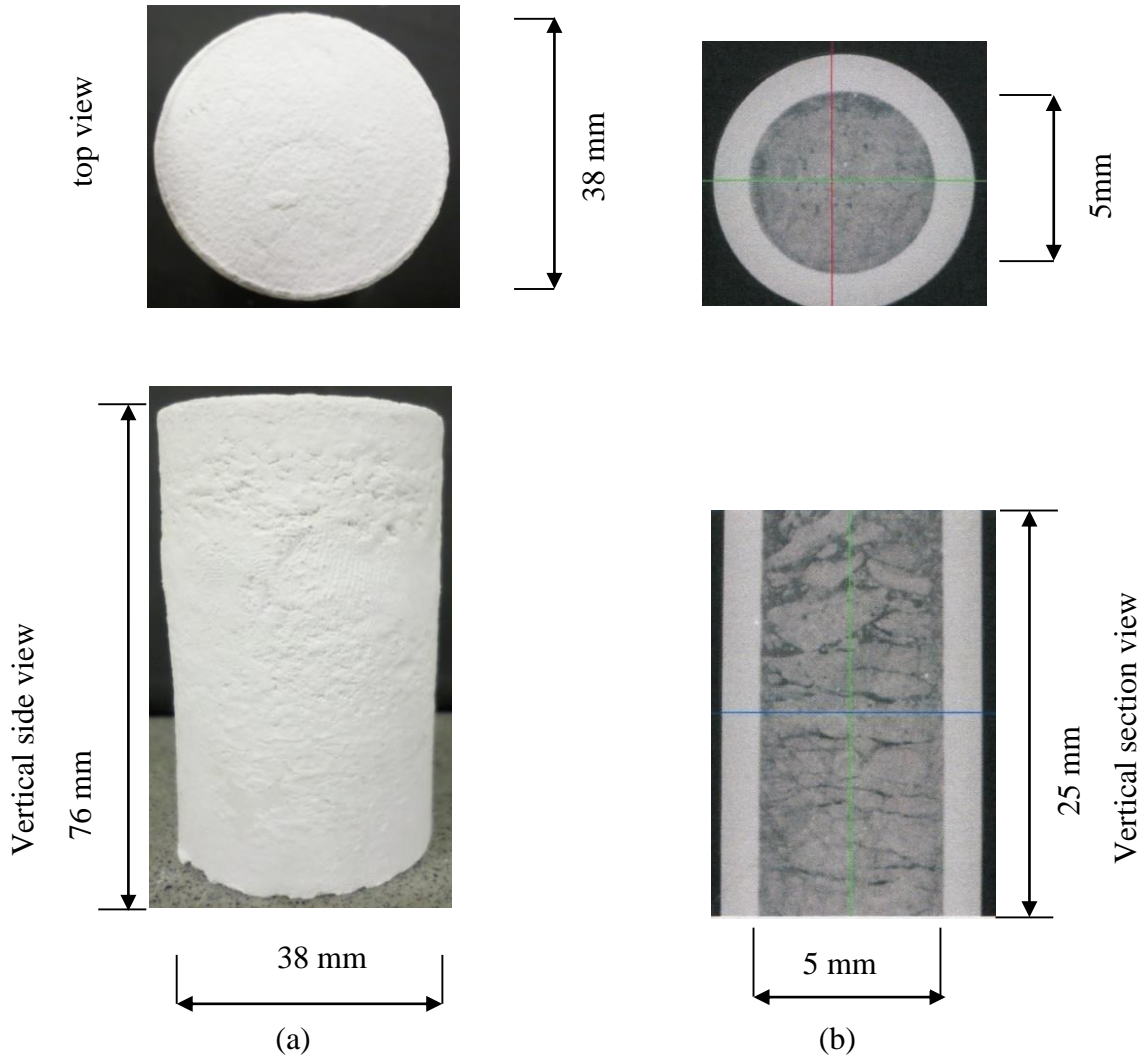


**Figure 3.10:** Carbonated treated kaolin sample for XRCT scanning (a) Parent sample 38 mm diameter, 76 mm height (b) Cored sample 5 mm diameter, 25 mm height. Sample axially cored from parent sample in (a).

## XRCT Analytical Procedure

To examine the changes in internal structure (such as voids, particle arrangement) of carbonated treated kaolin clay, nine carbonated treated kaolin clay and one non-carbonated kaolin clay (as a control) samples were examined (as earlier described in this section). Images of the scanned samples were reconstructed using ImageJ (v.1.43u) software (Rasband, 2002), such as the reconstruction performed by Beckett *et al.* (2013). An overview of the images for analysis is presented in Figure 3.11, whilst the flowchart of the XRCT data processing using ImageJ is included in Appendix C.

Firstly, the first and last 100 image slices were deleted from the data sequence. Removal of first and last 100 slices from the sequence was required in order to prevent shadowing, as carried out by Beckett *et al.* (2013), and Smith and Augarde (2014). The removal of these extreme slices also reduces the chance of damaged materials, likely to be found at ends of sample, from affecting the analysis. In this study 900 slices were available after removal of extreme slices. This was required so that measurement of result can be presented in calibrated real value ( $\mu\text{m}$  in this case).

The images were converted from 32 bit to 8 bit. Converting the image to 8 bit greyscale meant that there are 256 intensity values which can be assigned to a pixel. This was required for two reasons: firstly to fit into thresholding window (ImageJ) which requires 256 grey shades. Secondly converting from original 32 bit data to 8 bit data has an advantage of reducing the data size. For example 15.4 MB/slice in 32 bit data was reduced to 3.9 MB/slice in 8 bit data format. This assists in speeding up later ImageJ software analysis and improves data handling.

Cropping of image slice was performed on a typical carbonated treated kaolin image. This was required to avoid shadowing at the sample edges. It further reduced data size. For example cropping a 5 mm diameter slice to square (3.3 mm  $\times$  3.3 mm) image, reduced the size from 1004 kb to 413 kb (Figure 3.11c).

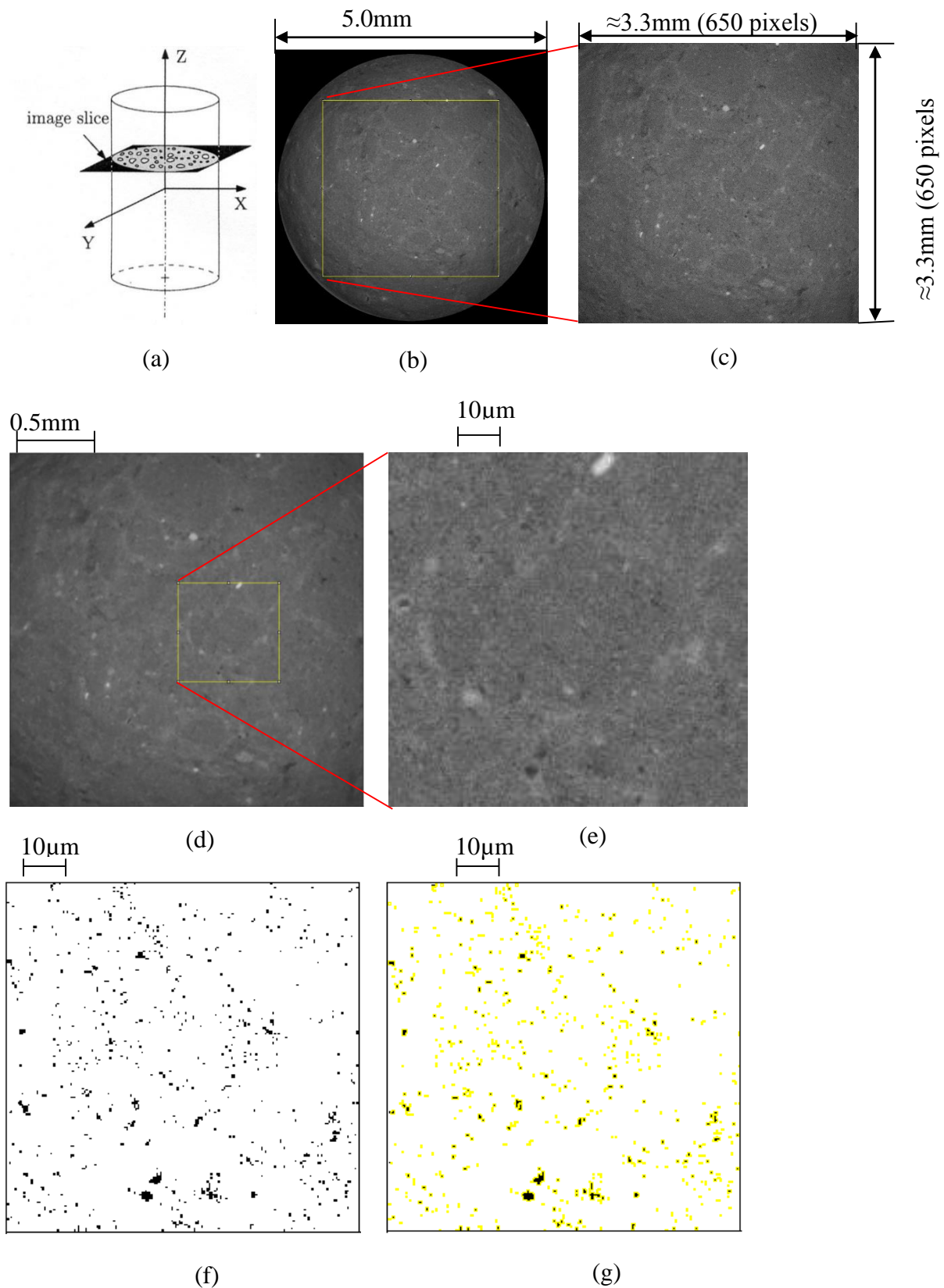


**Figure 3.11:** ImageJ procedures on sample images: (a) sample axes (b) typical reconstructed slice xy-plane (c) cropped sample (d) post filtered image (e) enlarged section (f) post thresholding (image pixel intensities below threshold value of 44 shown black, whilst white spaces represents intensities above threshold value (g) selected areas (in orange) for measurement.

Additionally, filtering the image was carried out in order to reduce noise and enhance sample features. The “adaptive median” filter was applied to the sample image to remove the outlying intensity regions as also performed by Beckett *et al.* (2013). This filter method removes the extreme outliers from the image, whilst preserving the original details in the image. It replaces a pixel being considered with a pre-selected median pixel value. A pixel is square shaped, to keep the pixel entries intuitively similar to the neighbouring pixels, at the same time keep the edges not eroded, adaptive median filter was required. This median filter radius defines the size of a square pixel and preserve the small details of original image (Khryashchev *et al.*, 2005). In this study 2.0 pixels radius was applied as in the study of Beckett *et al.* (2013). A typical filtered image is presented in Figure 3.11 d.

Furthermore, setting a threshold value was applied to the images. This was essential to separate pixels which fall within a desired range of intensity values from those which do not. The converted image to 8-bits grey scale turns pixel with the lowest value of 0 (zero) to black and pixel with highest intensity of 255 to white, whilst every pixel intensity between 0 and 255 is a shade of grey.

Ten different randomly located small regions for each sample were taken and an operator selected threshold value was obtained as performed by Smith and Augarde (2014). The threshold value was then applied to the entire slices in the sequence, resulting in two phase separation.

For measurement of air voids content for example, threshold values were applied for all the samples which separated voids from solid material areas. Voids areas showed black, whilst areas of solid materials (kaolin plus carbonate) showed white.

For determination of carbonate content, a threshold intensity value was applied to distinguish carbonate and non-carbonate phases. A preliminary threshold intensity value was selected from histogram of the corresponding carbonated sample image. It was compared with the highest intensity value for an image of a corresponding non-carbonated sample. Typical XRCT scan images of carbonated and non-carbonated sample are shown in Figure 3.12 and Figure 3.13 respectively. Full images and corresponding threshold graphs are included in Appendix C. The threshold intensity value separating carbonated and non-carbonated phase was similar to the extreme intensity of the corresponding non-carbonated sample. In this case the intensity value of 125 was same for both image cases.

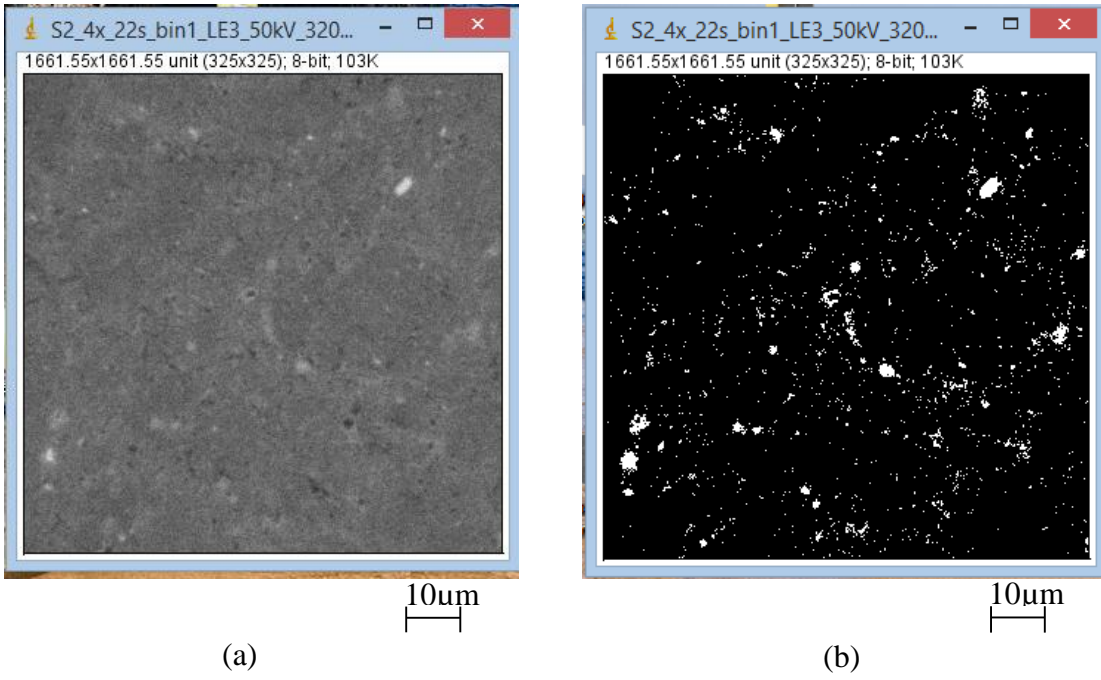


**Figure 3.12:** XRCT images of carbonate sample using ImageJ software: (a) Typical carbonate sample of 8% calcium hydroxide, and 10% air voids content (b) Reflection of post-threshold image at carbonate boundary

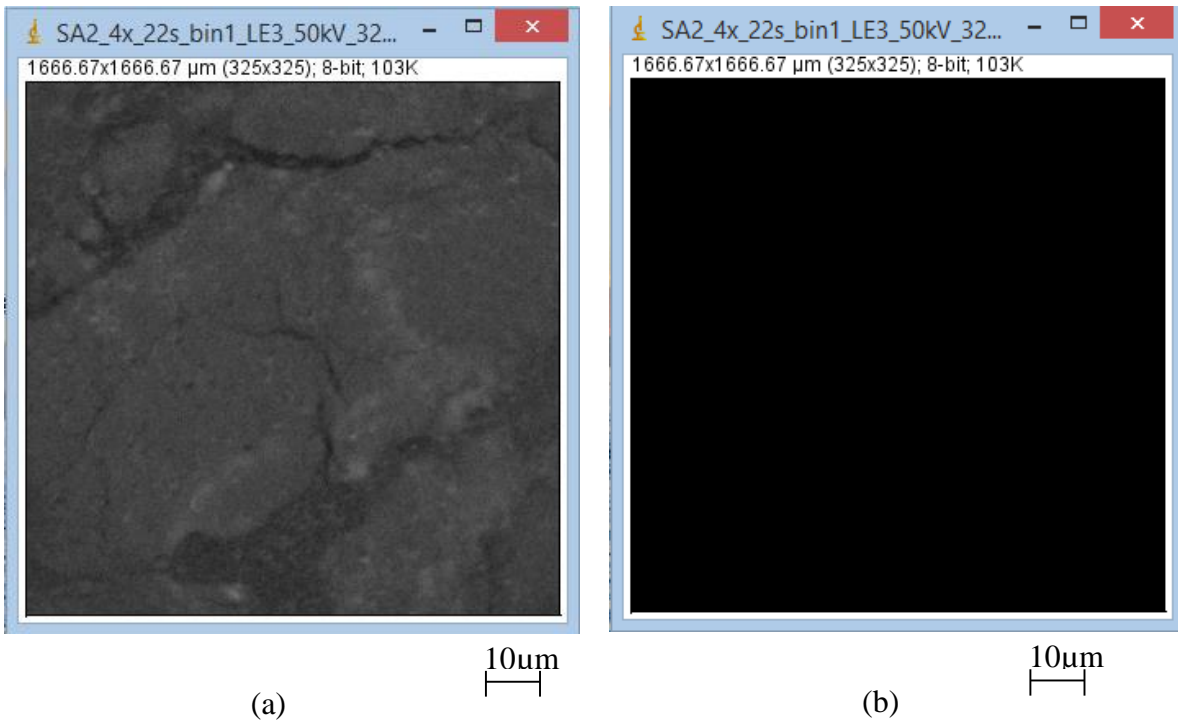


**Figure 3.13:** XRCT images of non-carbonate sample using ImageJ software: (a) Typical non-carbonated sample of 8% calcium hydroxide, and 10% air voids content (b) Reflection of selected extreme image intensity value of 125 on non-carbonated sample.

For measurement of the desired feature in an image, it was required to select the perimeter around the feature for measurement. The selection was required to isolate the features for measurement and the desired information (such as area, minimum and maximum grey value) recorded. A typical selection of property (voids spaces) is shown in Figure 3.11(g).

For measurement of image parameters (such as void and carbonate areas), only one per every ten images was processed due to large number of sample images, as performed by Beckett *et al.* (2013). For example 90 images were analysed out of 900 images available in this study.

Voids content (% by volume) was determined using Equation 3.4.

$$\text{Voids contents (\% by volume)} = \frac{\text{detected area of voids} \times \text{sample thickness}}{\text{Total area of sample} \times \text{sample thickness}} \quad (3.4)$$

Carbonate contents (% by mass) was determined using Equation 3.5

$$\text{Carbonate contents (\% by mass)} = \frac{\text{detected area of calcite} \times \text{sample thickness} \times \text{density of calcite}}{\text{Total area of non-calcite} \times \text{sample thickness} \times \text{density of clay}} \quad (3.5)$$

### Scanning Electron Microscope

SEM analysis was performed on carbonated treated kaolin samples to confirm the presence of CaCO<sub>3</sub>. SEM analysis is a technique which scans a focused electron beam over a sample surface to create an image. The high energy electron interacts with the sample and dissipates energy as a variety of signals. The signals includes backscattered electrons, secondary electrons (that produce SEM images), characteristic X-ray photons (that are used for elemental analysis) from which information about the surface composition and topography is obtained (Egerton, 2006). In this study, an FEI XL30 environmental scanning electron microscope (XL30 ESEM) was used. It is fitted with a field emission gun, and a Centaurus backscattered electron detector to collect the images reproduced. A point elemental analysis was performed on the crystal grains within the sample to determine mineral elements using a Rontec Quantax Energy Dispersion X-ray analyser (EDX) attached to the environmental scanning electron microscope (ESEM). Due to cost and time involved two samples (broken and polished thin sections) were analysed. The samples were selected to represent the highest lime content (8% Ca(OH)<sub>2</sub>), and expected to undergo highest mineral changes due to carbonation.

### 3.5.8 Calcium Carbonate Content Comparison.

To test the similarity of CaCO<sub>3</sub> content obtained from two techniques such as XRCT and calcimeter, and XRCT and TGA, the t- test was used (FAO, 1998; Morad, 2009). The CaCO<sub>3</sub> results obtained from XRCT, calcimeter and TGA were expressed as the mean ±SEM (standard error of the mean). Statistical significance of the difference in CaCO<sub>3</sub> contents obtained from each pair of techniques were determined by a paired t-test. P≤0.05 was considered to be significant.

The t-test is expressed as in Equation 3.6.

$$t = \frac{\bar{X}_1 - \bar{X}_2}{\sqrt{\frac{s_1^2}{n_1} + \frac{s_2^2}{n_2}}} \quad (3.6)$$

Where,  $\bar{X}_1$  is the mean of CaCO<sub>3</sub> values obtained from calcimeter or TGA,  $\bar{X}_2$  is the mean of CaCO<sub>3</sub> values from XRCT. S<sub>1</sub> is the standard deviation of CaCO<sub>3</sub> values from calcimeter or TGA, S<sub>2</sub> is the standard deviation of CaCO<sub>3</sub> values from XRCT. n<sub>1</sub> is the total number of CaCO<sub>3</sub> values from calcimeter or TGA, and n<sub>2</sub> is the total number of CaCO<sub>3</sub> values from XRCT.

The standard deviation was calculated using Equation 3.7

$$S = \sqrt{\frac{\sum(X - \bar{X})^2}{n-1}} \quad (3.7)$$

Where,

x = CaCO<sub>3</sub> values determined

$\bar{X}$  = Mean calcite

n = Total number of values

## 3.6 Chapter Summary

The methods used for preparation of treated kaolin specimens were described. Additionally, method used in formation of carbonated treated kaolin was described. Furthermore, the methods for determination of the content, presence, and internal structure of CaCO<sub>3</sub> were presented.

The following is the summary of the methods:

- $\text{Ca}(\text{OH})_2$  addition for the preparation of treated kaolin specimens was carried out using modified ICL test according to the definition presented by Rogers *et al.* (1997). The compaction was performed using normal Proctor (Light) compaction method according to BS 1377 (1990b).
- Previous work by Nakarai and Yoshida (2015) noted that carbonation reaction increases with increasing  $\text{CO}_2$  concentration. Additionally, higher rate of carbonation could be achieved in HC environment, compared to low  $\text{CO}_2$  concentration typical of the natural atmosphere environment. Therefore 1 molar  $\text{Na}_2\text{CO}_3$  solution, referred to as HC solution, was used to produce HC environment.
- Methods for testing the performance of carbonated and non-carbonated treated kaolin against sets of key performance indicators were described.
- Strength and stiffness testing of carbonated and non-carbonated treated kaolin specimens were carried out using UCS testing in accordance with BS 1377, Part 7 (BSI, 1990b).
- Permeability of treated kaolin was performed using a modified permeability in a triaxial cell test in accordance with BS 1377, part 6 (BSI, 1990b). HC solution was permeated through the treated kaolin specimen to achieve accelerated carbonation
- FT durability testing was applied to carbonated and non-carbonated treated kaolin specimens to determine the specimens' resistance against detrimental weather conditions.
- For determination of  $\text{CaCO}_3$  content, calcimeter and TGA technique in adherence with BS 7755-3.10 (BSI, 1995a) were applied to carbonated and non-carbonated treated kaolin specimens. Additionally, TGA technique was used in determining the presence of  $\text{CaCO}_3$ .
- XRCT technique was used for the determination of internal structure of carbonated and non-carbonated treated kaolin specimens.



## Chapter 4 – Strength Development and Calcium Carbonate

### Formation in Treated Kaolin Clay

Chapter 3, Materials and Methods, set out the methods used to investigate the effect of carbonation on strength and carbon capture properties of treated kaolin clay. It described how kaolin clay was treated with  $\text{Ca}(\text{OH})_2$  and exposed to  $\text{Na}_2\text{CO}_3$  solutions for carbonation treatment. The carbonated treated kaolin specimens were tested for strength development and  $\text{CaCO}_3$  content, and the resulting changes are presented in this section.

The following are presented in this chapter:

- Material Characterisation;
- Strength development and  $\text{CaCO}_3$  formation due to combined modification and carbonation treatment; and
- FT durability of carbonated treated kaolin
- Use of XRCT in determination of internal structure of carbonated treated kaolin.

#### 4.1 Preliminary Material Characterisation

This section presents the preliminary characterisation results of treated and untreated kaolin clay. Also presented is the lime required to stabilise kaolin clay and the permeability of treated kaolin clay.

##### 4.1.1 Initial Consumption of Lime

Figure 4.1 shows the variation in pH of kaolin for increasing  $\text{Ca}(\text{OH})_2$  additions. As can be seen, the pH increased with lower  $\text{Ca}(\text{OH})_2$  additions up to 4 % value. The sample however, did not show changes in pH with  $\text{Ca}(\text{OH})_2$  additions above 4 %. Based on BS 1924-2 (BSI, 1990a) the equivalent amount of CaO content is given as 75% of  $\text{Ca}(\text{OH})_2$  content. The ICL was determined according to the definition presented by Rogers *et al.* (1997). Rogers *et al.* (1997) presented a modified definition of ICL value as the minimum amount of CaO at which the pH curve flattens off and a marginal change in pH results from a large change in CaO content. The ICL can be seen to occur at 4%  $\text{Ca}(\text{OH})_2$  (3% CaO equivalent) addition, as shown in Figure 4.1. This implies that the ICL value for the kaolin used in this study is 3% CaO by dry mass according to the definition presented by Rogers *et al.* (1997).

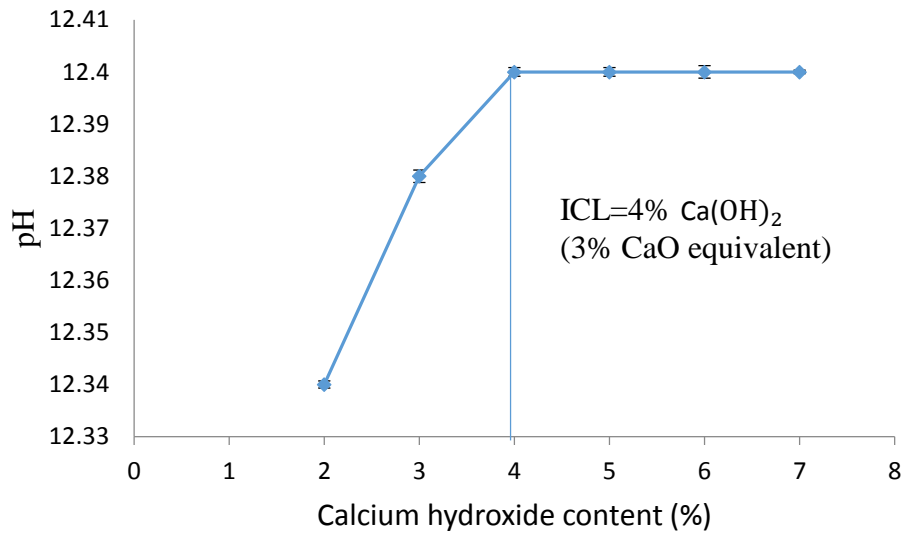


**Figure 4.1:** Variation of pH with calcium hydroxide [ $\text{Ca}(\text{OH})_2$ ] content (%) (average of three samples per point). Analytical error bars lie within the area of the data point. Error bars represent 1 standard deviation.

#### 4.1.2 Cation Exchange Capacity Results

Table 4.1 shows results for CEC of kaolin with added  $\text{Ca}(\text{OH})_2$ . The CEC values decreased with  $\text{Ca}(\text{OH})_2$  additions up to 2 % (having CEC value of  $3.21 \pm 0.40$  cmol/kg), then slightly rose with further  $\text{Ca}(\text{OH})_2$  additions and remain about the same at  $\text{Ca}(\text{OH})_2$  additions above 6 % (with CEC value of  $3.10 \pm 0.06$  cmol/kg).

Generally, CEC of the clay decreased with  $\text{Ca}(\text{OH})_2$  additions when compared with the untreated clay sample as shown in Table 4.1. For example, the least CEC showed a value 1.1 cmol/kg less than the CEC value of untreated sample.

CEC of clay provides an estimate of the ability of the clay to exchange metal ions located on and between the mineral's layers. The smaller value of CEC on lime addition indicates a reduced ability to exchange metal ions. Based on the interpretation of Bell (1996), lime fixation would occur around the least values of CEC. At this lime value, the amount of lime fixed in the soil on lime addition satisfies the affinity of the soil for lime (Hilt and Davidson, 1960).

Rogers and Glendinning (1996) reported that lower percentages of lime are needed to achieve the lime requirement of CEC, whilst a greater percentage of lime is needed to satisfy the lime requirement of ICL. In the current study CEC of kaolin ( $4.17 \pm 0.54$ ) at pH of 8.1 is negligible

compared with bentonite, which is typically 80-100 cmol/kg (Kaufhold and Dohrmann, 2013; Reeves *et al.*, 2006) and has no effect on ICL.

**Table 4.1:** Results of cation exchange capacity of kaolin at pH of 8.1 (average of two samples). Analytical errors represent 1 standard deviation.

Calcium hydroxide content (%)	Average CEC (cmol/kg)
0	4.17 ± 0.54
1	3.32 ± 0.03
2	3.21 ± 0.40
3	3.26 ± 0.35
4	3.64 ± 0.21
6	3.10 ± 0.06
8	3.07 ± 0.91

#### 4.1.3 Atterberg Limit

Figure 4.2 shows the plasticity changes of kaolin with increasing Ca(OH)<sub>2</sub> addition. Detailed data are included in Appendix B. As would be expected the plasticity changes were small due to the low CEC of kaolin (Table 4.1). The CEC of a clay directly influences how its plasticity changes on lime addition (Rogers and Glendinning, 1996).

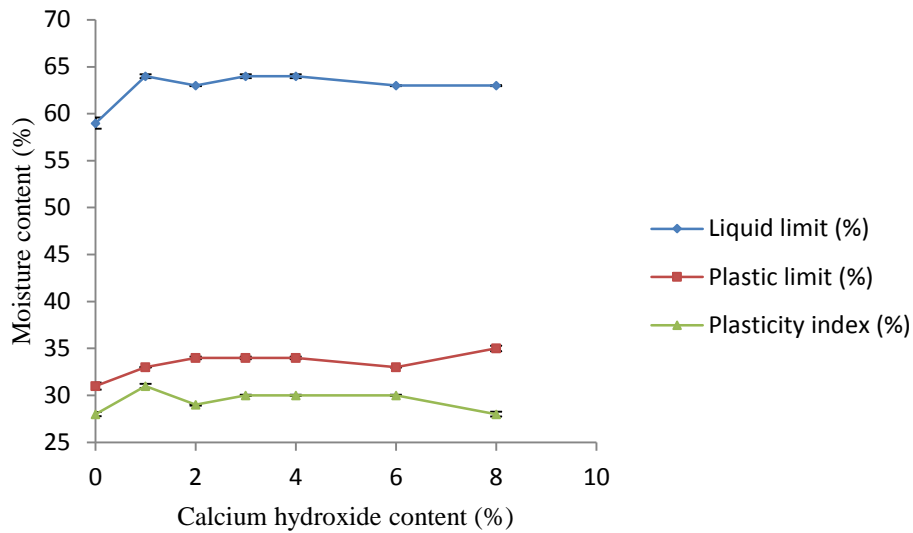


**Figure 4.2:** Variation of Atterberg Limits with calcium hydroxide  $[\text{Ca}(\text{OH})_2]$  addition to kaolin after 24 hours curing (average of 4 samples per point). Error bars are within the size of points and represent 1 standard deviation.

The PL results were used to determine the amount of  $\text{Ca}(\text{OH})_2$  content required for modification of kaolin. The lime content in lime mixed clay at which PL rises to asymptote is taken as the lime content for modification of the clay (Rogers and Glendinning, 1996). Figure 4.2 shows that as would be expected, PL slightly increased by 3% (from 31% to 34%) with  $\text{Ca}(\text{OH})_2$  addition up to 2%, and did not exhibit remarkable change with  $\text{Ca}(\text{OH})_2$  additions above 2%. It can be seen in Figure 4.2 that the PL rose to asymptote at 2%  $\text{Ca}(\text{OH})_2$  therefore 2%  $\text{Ca}(\text{OH})_2$  is the lime content at which modification occurred in the kaolin. The overall PL was observed to increase by 4% at 8%  $\text{Ca}(\text{OH})_2$  addition. An increase in PL with  $\text{Ca}(\text{OH})_2$  additions is consistent with other studies on lime mixed kaolin (Rogers and Glendinning, 1996; Kassim *et al.*, 2005; Muhmed and Wanatowski, 2013; Vitale *et al.*, 2016).

It can be seen in Figure 4.2 that the LL increased initially with 1%  $\text{Ca}(\text{OH})_2$  addition, then declined and did not show remarkable change with  $\text{Ca}(\text{OH})_2$  additions above 2%. The overall LL shows 4% increase at 8%  $\text{Ca}(\text{OH})_2$  addition.

Similarly, PI rose initially with addition of 1%  $\text{Ca}(\text{OH})_2$ , then declined and did not show remarkable change with further  $\text{Ca}(\text{OH})_2$  additions above 2%. There is an overall increase in PI with  $\text{Ca}(\text{OH})_2$  addition, with the exception of PI at 8%  $\text{Ca}(\text{OH})_2$  addition, which resulted in the same PI when compared to that of untreated kaolin. The results of increase in PI with  $\text{Ca}(\text{OH})_2$  additions in the current study is consistent with the results of other studies (Rogers and Glendinning, 1996; Kassim *et al.*, 2005; Vitale *et al.*, 2016) on lime mixed kaolin.

However, this pattern does not agree with the results of PI in some literature. The studies by Muhmed and Wanatowski (2013) on  $\text{Ca}(\text{OH})_2$  mixed kaolin showed decreases in PI with 5%  $\text{Ca}(\text{OH})_2$  addition. The reason for this could be due to the variable pattern of changes in LL, and hence PI for a particular one clay (Rogers and Glendinning, 1996). This is discussed further in Section 5.3 of this thesis.

It is well known for lime mixed clay that the point of full PL increase corresponds to lime fixation capacity (Hilt and Davidson, 1960; Kassim *et al.*, 2005), whilst the value of ICL gives the minimum lime content for soil stabilisation (Grim and Eades, 1966; Rogers and Glendinning, 2000). In the current study the full PL is achieved at 2%  $\text{Ca}(\text{OH})_2$  content, which is equivalent to 1.5% CaO (Figure 4.2). The  $\text{Ca}(\text{OH})_2$  content at full PL is lower than the ICL value of 4%  $\text{Ca}(\text{OH})_2$  (3% CaO equivalent) (Figure 4.1). A similar observation is reported by Rogers and Glendinning (1996) that a full PL of kaolin was achieved at 1% CaO content, whilst the ICL was attained at 1.5% CaO content. Also, Kassim *et al.* (2005) reported that the PL of Topah kaolin was attained at 1.5%  $\text{Ca}(\text{OH})_2$  (approximately 1.1% CaO) content, whilst ICL for the kaolin was achieved at 2%  $\text{Ca}(\text{OH})_2$  (1.5% CaO) content.

It was observed in Figure 4.2 that the errors of individual curves (Atterberg limit) are between 0.02 and 0.6. Rogers *et al.* (1997) stated that these errors are usually between the range of  $\pm 2$  percentage. This shows that the errors achieved during these experiments are within the recommended errors. Interestingly, the errors are minimal and it could be inferred that human errors during the experiments were properly controlled.

#### **4.1.4 Density of Treated Kaolin Clay**

The results of the experiment assessing the MDD, and OMC in treated kaolin are presented in Figure 4.3. Full curves showing relationship between MDD and OMC for the treated kaolin are previously presented in Chapter 3 (Section 3.4.4) of this thesis. As can be seen from Figure 4.3, MDD of the samples decreased with  $\text{Ca}(\text{OH})_2$  addition. In contrast, OMC increased with  $\text{Ca}(\text{OH})_2$  addition. For example, the MDD of untreated kaolin decreased by 2 % at 8 %  $\text{Ca}(\text{OH})_2$  addition. On the other hand, OMC of untreated kaolin increased by 10 % at 8 %  $\text{Ca}(\text{OH})_2$  addition.

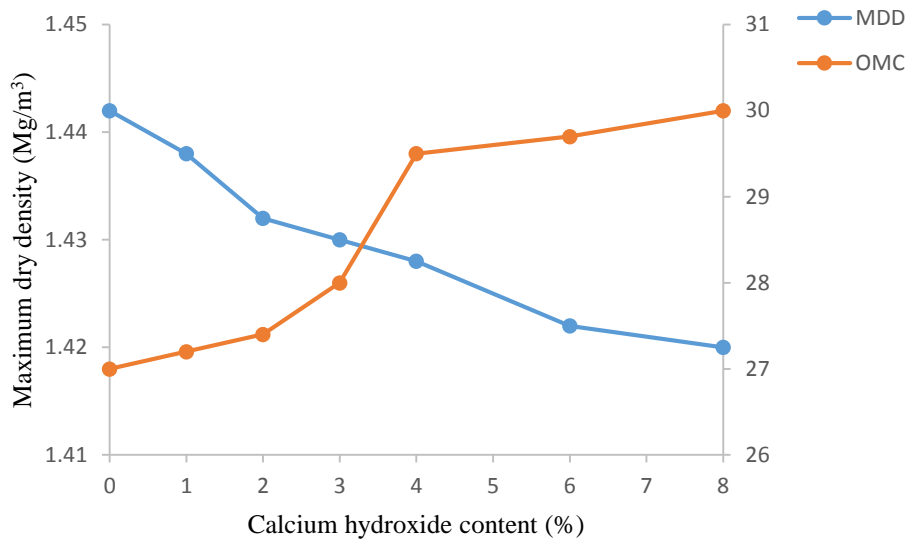


**Figure 4.3:** Changes in maximum dry density (MDD) and optimum moisture content (OMC) in treated kaolin using calcium hydroxide [Ca(OH)<sub>2</sub>] (average of 3 samples per point). Error bars are within the data point and represent 1 standard deviation.

Figure 4.4 shows the variation of dry densities with air voids in treated kaolin. Full curves for the relationship between dry density and air voids are included previously in Chapter 3 (Section 3.4.4) of this thesis. As can be seen in Figure 4.4, dry densities of the Ca(OH)<sub>2</sub> treated kaolin reduced with increasing air voids, and sample dry densities reduced with increasing Ca(OH)<sub>2</sub> addition. For example, samples at 8 % Ca(OH)<sub>2</sub> additions showed lower dry densities than those at 4 % Ca(OH)<sub>2</sub> additions.

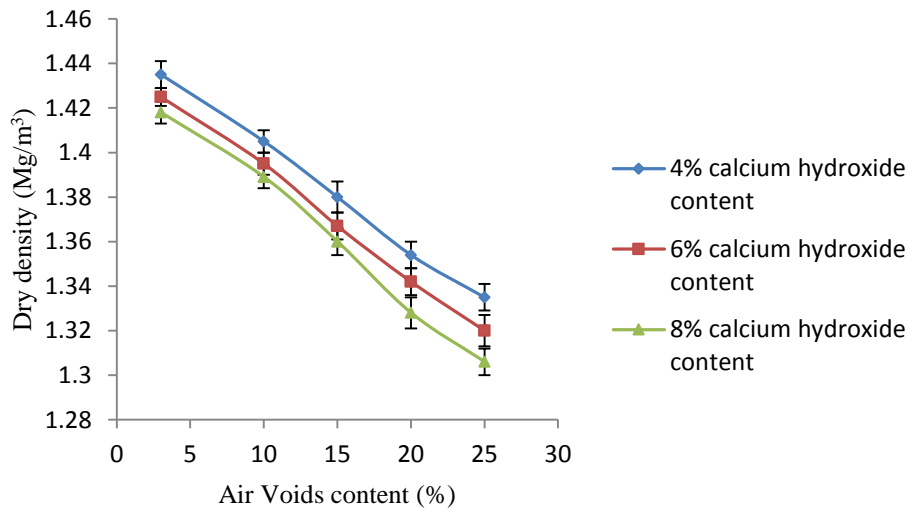


**Figure 4.4:** Variation of dry density with air voids for calcium hydroxide addition to kaolin (average of 3 samples per point). Analytical error bars represent one standard deviation.

#### 4.1.5 Strength Development of Treated Kaolin Clay

The experimental result investigating the peak strength and the corresponding OLC of treated kaolin is shown in Figure 4.5. Full curves of UCS showing the specimens' stress versus strain relationship are included in the CD-ROM (Appendix E) which accompanies this thesis. OLC is the lime content in treated soil at which peak strength is achieved (Grim and Eades, 1966; Bell, 1996). As can be seen, the UCS increased with  $\text{Ca}(\text{OH})_2$  additions up to 4 %, and then decreased with  $\text{Ca}(\text{OH})_2$  additions above 4 %. It can be seen that the peak strength is achieved at 4%  $\text{Ca}(\text{OH})_2$  therefore 4%  $\text{Ca}(\text{OH})_2$  is the OLC. These data support the argument that 4%  $\text{Ca}(\text{OH})_2$  which is 3%  $\text{CaO}$ , is equivalent to the ICL value.

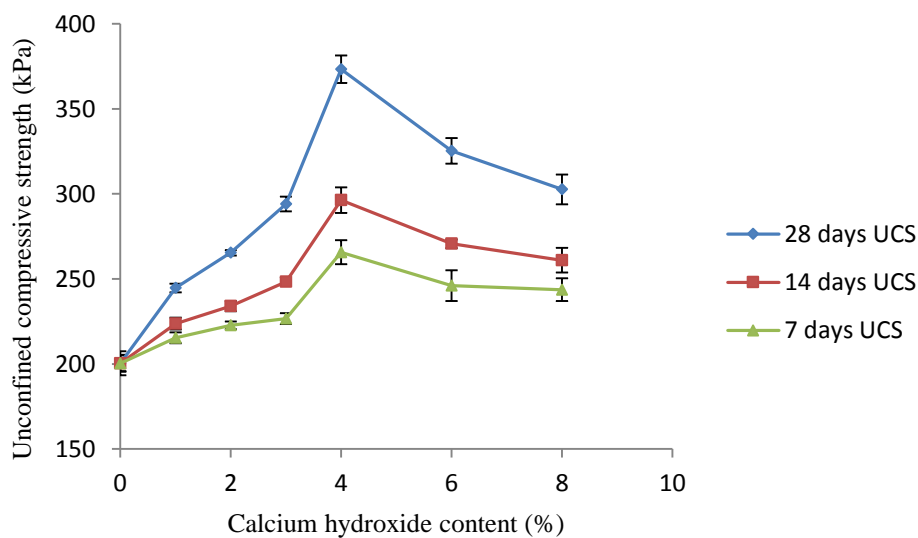


**Figure 4.5:** Variation of unconfined compressive strength (UCS) of kaolin treated with calcium hydroxide (average of 3 samples per point). Analytical error bars represent one standard deviation.

For a particular clay, the OLC value could be equal or greater than the ICL value (Cherian *et al.*, 2016). In the current study the OLC value is equal to the ICL value of kaolin, which is 4%  $\text{Ca}(\text{OH})_2$ . This could be due to low change in properties associated with kaolin which is influenced by small CEC (4 cmol/kg) (Rogers and Glendinning, 1996). Additionally, Cherian *et al.* (2016) showed that for clays with low activity number such as MC (0.33), the OLC value (2%  $\text{Ca}(\text{OH})_2$ ) could be equal to the ICL value (2%  $\text{Ca}(\text{OH})_2$ ) due to low reactivity of the clay. For clays with high activity number such as NBT (5.3), the OLC (10%  $\text{Ca}(\text{OH})_2$ ) could be higher than the ICL (2.7%  $\text{Ca}(\text{OH})_2$ ) due to its high reactivity. Since kaolin clay has low activity number (typically 0.4; Barnes, 2010), it suggests that the OLC value would be equal to ICL value due to low reactivity of kaolin. The UCS also increased with increasing curing time. For example, for 4%  $\text{Ca}(\text{OH})_2$  treatment, specimens when compared to the

control (the corresponding untreated kaolin) exhibited up to 54 % strength gain between 7 and 28 days curing times.

The experimental results investigating the strength of water saturated treated kaolin are shown in Figure 4.6. A common means to simulate a critical field moisture condition of lime treated clay, having low to moderate plasticity, is to soak the specimen with water for 24 hours prior to UCS testing (Little, 2000). Therefore 7 days cured treated kaolin (compacted to target air voids of 3%) was soaked in deionised water for 24 hours in the triaxial cell, as described in Chapter 3 (Section 3.2.5), prior to UCS testing.

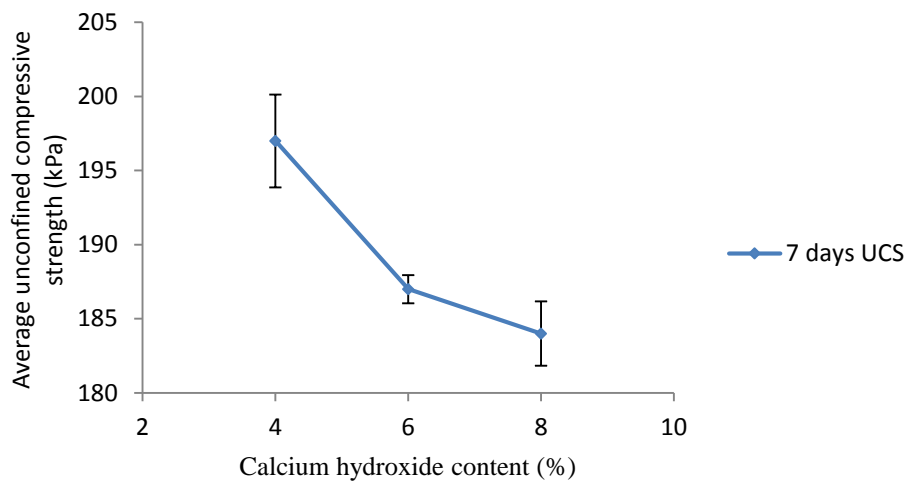


**Figure 4.6:** Variation of unconfined compressive strength (UCS) of water saturated treated kaolin (average of 3 samples per point). Repeatability error bars represent 2 standard deviations.

#### ***4.1.6 Permeability of Treated Kaolin Clay***

The result of the experiment investigating the effect of specimen air voids on permeability of treated kaolin is shown in Figure 4.7. As stated in the previous chapter (Chapter 3 Materials and Methods) HC solution was passed through treated kaolin to promote the reaction of  $\text{CO}_2$  with  $\text{Ca}(\text{OH})_2$ . As shown, the clay permeability increased with increasing air voids for all  $\text{Ca}(\text{OH})_2$  treatments. For example, for 6 %  $\text{Ca}(\text{OH})_2$  treatment, the permeability of samples at 25 % air voids is approximately 6 times more than that at 3 % air voids. The increase in permeability with increasing target air voids could be due to increase in interconnectivity of air void spaces. Interconnected air void spaces are the channel through which water can flow through a compacted soil (Gogula *et al.*, 2004).

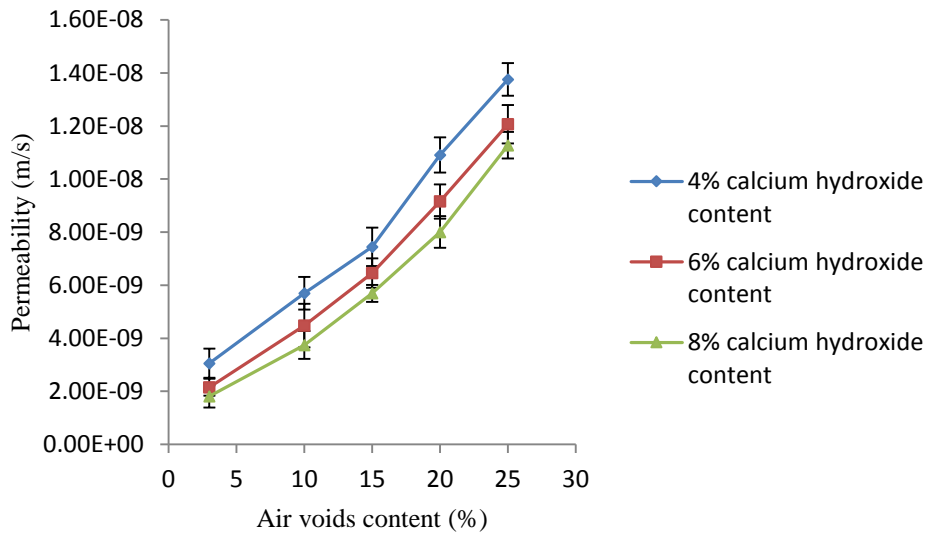


**Figure 4.7:** Variation of permeability with air void for treated kaolin (average of 3 samples per point). Analytical error bars represent one standard deviation.

It is observed from Figure 4.7 that there is a linear relationship between air voids and permeability as represented by Equations 4.1 to 4.3. Equation 4.1 represents the permeability relationship with air voids content of specimen at 4%  $\text{Ca}(\text{OH})_2$ , whilst Equation 4.2 for that at 6%  $\text{Ca}(\text{OH})_2$  content and Equation 4.3 for specimen at 8%  $\text{Ca}(\text{OH})_2$  content.

$$k = AV \times (3.66 \times 10^{-10}) \quad (4.1)$$

$$k = AV \times (3.59 \times 10^{-10}) \quad (4.2)$$

$$k = AV \times (3.24 \times 10^{-10}) \quad (4.3)$$

where  $k$  represents permeability (m/s), and  $AV$  represents air voids content (%).

Al-Tabbaa and Wood (1987) reported that variation in the permeability of kaolin clay is linear with void ratio in the range of permeability values from approximately  $0.6 \times 10^{-9}$  m/s to  $7.0 \times 10^{-9}$  m/s. The results of the current study (Figure 4.7) may be valid for air void contents of 3% to 15%, which correspond to the measured permeability values of  $1.8 \times 10^{-9}$  m/s to  $7.4 \times 10^{-9}$  m/s.

#### ***4.1.7 Summary of Material Characterisation***

Based on the modified ICL test according to the definition presented by Rogers *et al.* (1997), the ICL value was derived as 3 % CaO content by dry mass. The UCS data supports the argument that 3% CaO is the ICL value. The minimum lime content applied for treatment of the kaolin clay in the current study was based on the ICL value.

#### **4.2 Calcium Carbonate Formation in Treated Kaolin Clay**

This section presents the results of CaCO<sub>3</sub> formation in treated kaolin clay based on Eijkelkamp calcimeter results. Also, the CaCO<sub>3</sub> content in the samples was confirmed with TGA results, for selected samples. The results presented below are:

- CaCO<sub>3</sub> content variation with lime content based on calcimeter results
- CaCO<sub>3</sub> content variation with lime content based on TGA results
- CaCO<sub>3</sub> content variation as a function of air voids

##### ***4.2.1 Calcium Carbonate Variation with Lime Content obtained from Calcimeter Analysis***

CaCO<sub>3</sub> contents as a function of increasing Ca(OH)<sub>2</sub> additions to kaolin clay, derived from Eijkelkamp calcimeter analysis, are shown in Figure 4.8 and Table 4.2. CaCO<sub>3</sub> content increased with increasing Ca(OH)<sub>2</sub> additions. For example, for samples at 10% air voids, 4 % Ca(OH)<sub>2</sub> addition resulted in a CaCO<sub>3</sub> content of  $4.70 \pm 0.24$  % wt (min. 3.72 % max. 5.01 %). This was in reasonable agreement with the theoretical CaCO<sub>3</sub> content of 5.40 % wt (Table 4.2). 6 % Ca(OH)<sub>2</sub> addition produced higher CaCO<sub>3</sub> contents of  $7.46 \pm 0.16$  % wt (min. 6.87 % max. 7.52 % ) corresponding to the theoretical CaCO<sub>3</sub> value of 8.11 %. Again, 8 % Ca(OH)<sub>2</sub> addition produced the highest CaCO<sub>3</sub> content of  $10.08 \pm 0.15$  % wt. (min. 9.14 % max. 10.20 %) corresponding to the theoretical CaCO<sub>3</sub> value of 10.81 %.

The amount of CaCO<sub>3</sub> formed increased proportionally with Ca(OH)<sub>2</sub> content in the treated kaolin as shown in Figure 4.8.

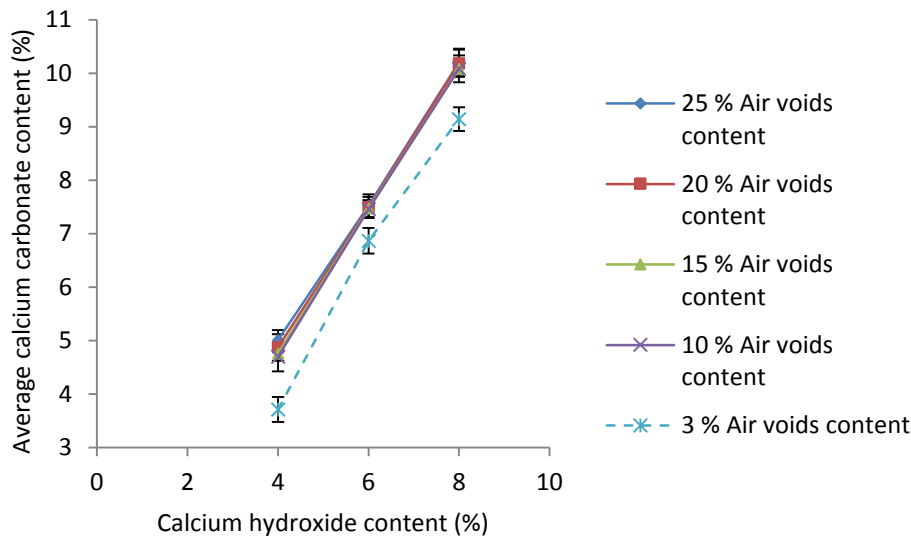
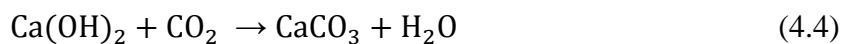


**Figure 4.8:** Calcium carbonate content in kaolin with varying Ca(OH)<sub>2</sub> additions obtained from calcimeter analysis (average of 3 samples per point). Analytical error bars represent 1 standard deviation.

**Table 4.2:** Theoretical vs experimental calcimeter analysis values.

Calcium hydroxide content (%)	<sup>a</sup> Theoretical percentage carbonate	<sup>b</sup> Calcium carbonate content derived from calcimeter analysis (%)				
		3% AV	10% AV	15% AV	20% AV	25% AV
4	5.40	3.72±0.33	4.70±0.24	4.76±0.36	4.87±0.35	5.01±0.26
6	8.11	6.87±0.17	7.46±0.16	7.47±0.14	7.50±0.12	7.52±0.15
8	10.81	9.14±0.30	10.08±0.15	10.08±0.14	10.19±0.16	10.20±0.16

<sup>a</sup>Determined using Equation 4.4: <sup>b</sup>Analytical error from calcimeter represent 1 standard deviation (average of 3 samples per combination) ranged from ±0.12 to ± 0.36 % wt CaCO<sub>3</sub>.



#### 4.2.2 Calcium Carbonate Variation with Air Voids Content in Treated Kaolin

The CaCO<sub>3</sub> content relationships with air voids content in carbonated treated kaolin as determined using the calcimeter are presented in Figure 4.9. As shown CaCO<sub>3</sub> contents increased with increasing air voids up to 10 %. There was, however, no remarkable change in CaCO<sub>3</sub> content for air voids above 10 %.

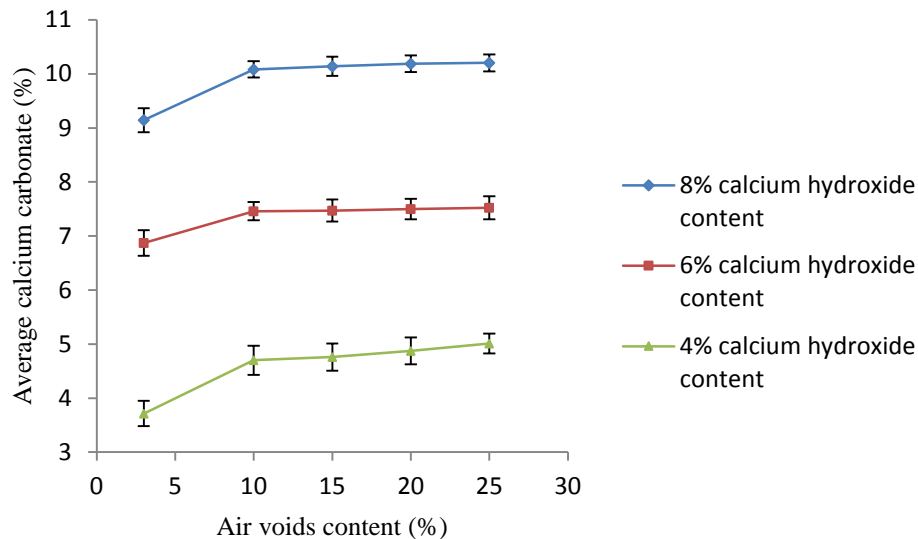


**Figure 4.9:** Calcium carbonate content variations with air voids content (average of 3 samples per point). Analytical error bars represent 1 standard deviation.

#### 4.2.3 Calcium Carbonate Content from Thermogravimetric Analysis

To quantify precisely the amount of  $\text{CaCO}_3$  in treated kaolin, experiments were conducted on the samples using thermogravimetry-differential scanning calorimetry coupled with quadrupole mass spectrometry analysis. TGA measures the mass loss as a function of temperature, and allows for a discrete quantification of  $\text{CaCO}_3$  and other heat-sensitive soil components. The experimental results investigating the amount of  $\text{CaCO}_3$  from TGA for treated kaolin, compacted to 10% air voids, are shown in Figure 4.10.

It is observed in Figure 4.10 that the peaks characteristically occurred in ranges from 80-100 °C, 450-600 °C and 660 to 740 °C. The peak between 80-100 °C shows mass loss from water absorbed by the soil. The peak between 450 and 600 °C shows loss of hydroxyl water from kaolinite and the peak characteristic between 660 and 740 °C shows mass loss from decarbonation reactions ( $\text{CO}_2$  derived from calcite,  $\text{CaCO}_3$ ). Quadrupole mass spectrometry (QMS) data confirm the loss of water and  $\text{CO}_2$  at these temperatures (Figure 4.10).

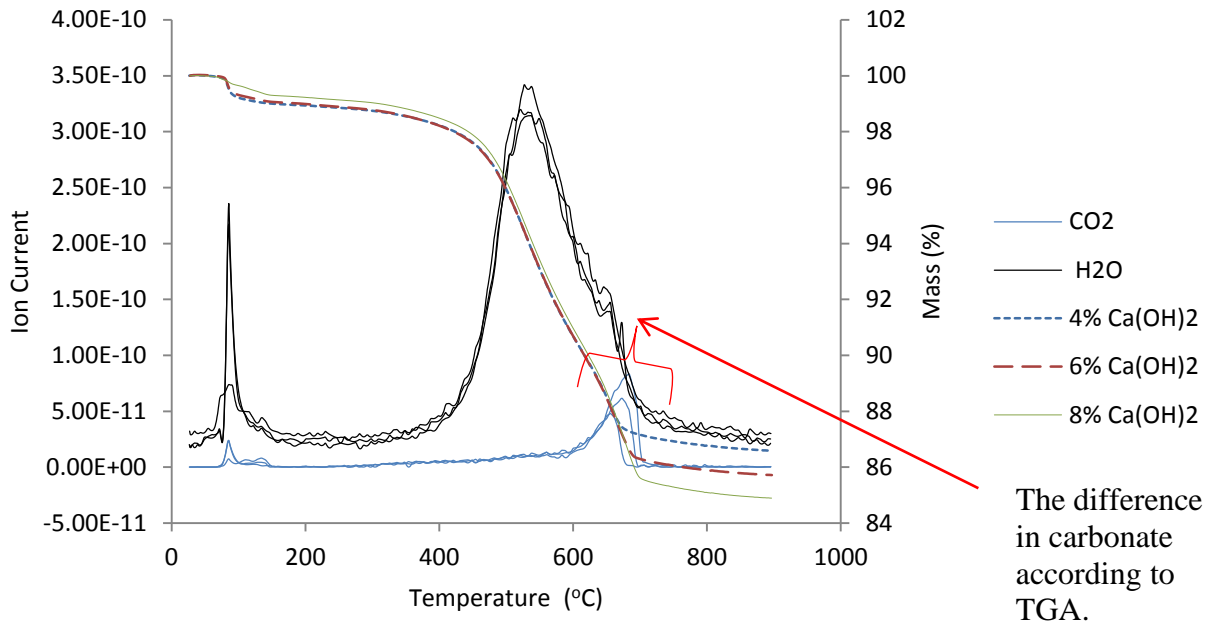


**Figure 4.10:** Combine thermogravimetric curve and QMS trace, evolved gas ( $\text{H}_2\text{O}$  and  $\text{CO}_2$ ) for 10% air void samples (average of 3 samples per combination). Heating of samples were performed under an atmosphere of  $\text{He}_{80}\text{O}_{20}$  (80% helium and 20% oxygen) mixture, purge gas flow rate of 30 ml per min.

$\text{CaCO}_3$  contents derived from TGA results for samples at 10% air voids are presented in Table 4.3. Again the  $\text{CaCO}_3$  content increased with increasing  $\text{Ca}(\text{OH})_2$  content.  $\text{CaCO}_3$  derived from TGA confirms that from calcimeter analysis (Section 4.2.1).

**Table 4.3:** Calcium carbonate from TGA analysis vs theoretical amount for sample at 10% air voids content.

Calcium hydroxide content (%)	<sup>a</sup> Theoretical percentage carbonate	<sup>b</sup> Calcium carbonate content (%) (from TGA)	Calcium carbonate content (calcimeter)
4	5.40	4.54±0.21	4.70±0.24
6	8.11	6.97±0.13	7.46±0.16
8	10.81	9.40±0.23	10.08±0.15

<sup>a</sup>determined from the Equation 4.4:  $\text{Ca}(\text{OH})_2 + \text{CO}_2 \rightarrow \text{CaCO}_3 + \text{H}_2\text{O}$

<sup>a</sup>analytical error from TGA based on standard deviation ranged from ±0.13% to ± 0.23 % wt  $\text{CaCO}_3$ .

It is important to note that the amount of  $\text{CaCO}_3$  formed in real world situations over time may not be as much as that obtained in the laboratory over the same time. Earlier field study by Eades *et al.* (1962) determined  $\text{CaCO}_3$  content in 5%  $\text{Ca}(\text{OH})_2$  treated subgrade in road construction at Virginia, after 2 years. The authors noted that 2.5%  $\text{CaCO}_3$  content was achieved due to carbonation of 5%  $\text{Ca}(\text{OH})_2$  in the treated subgrade soil. This represents 50% degree of carbonation in 2 years. Based on the field degree of carbonation in Eades *et al.* (1962), it could be estimated that, in 2 years duration, approximately 4% of  $\text{CaCO}_3$  would be produced in 8%  $\text{Ca}(\text{OH})_2$  treated clay such as kaolin in the field, due to carbonation.

### **4.3 Combined Modification and Carbonation Treatment**

This section presents the results of kaolin improvements due to the combined effects of modification and carbonation treatment. Presented in this section are:

- Strength and stiffness development of carbonated treated kaolin
  - Variation of strength with lime content
  - Variation of strength with air voids content
  - Variation of stiffness with air voids content
  - UCS variation with  $\text{CaCO}_3$  content
- Durability (particularly FT) of carbonated treated kaolin.

#### ***4.3.1 Strength and Stiffness Development of Carbonated Treated Kaolin.***

##### **Variation of Strength with Lime Content**

The experimental results investigating the UCS of carbonated treated kaolin for increasing  $\text{Ca}(\text{OH})_2$  additions are shown in Figure 4.11. For comparison purposes, the UCS values of saturated carbonated treated kaolin using HC solution, and water saturated 7 days cured non-carbonated treated kaolin, are presented in Table 4.4. Full curves showing the samples' stress-strain behaviour are included in the CD-ROM (Appendix E) which accompanies this thesis. UCS was performed on 7 days cured treated kaolin, which underwent carbonation treatment and saturation through permeation of HC solution. As earlier mentioned (Section 3.4.5), 24 hours saturation of the specimen prior to UCS testing is important to simulate a critical field moisture condition typical of lime treated clay, having low to moderate plasticity (Little, 2000). As shown in Figure 4.11, the UCS increased with  $\text{Ca}(\text{OH})_2$  additions up to 6 %, then

decreased with  $\text{Ca}(\text{OH})_2$  additions above 6 %. In general, the current study shows that samples with 6 %  $\text{Ca}(\text{OH})_2$  content (for all air void contents) resulted in the highest strength.

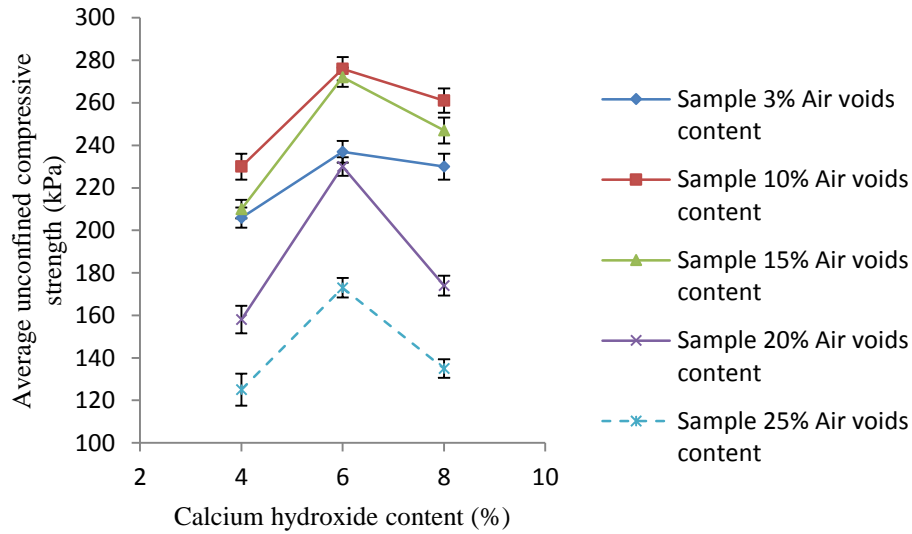


**Figure 4.11:** Unconfined compressive strength of kaolin clay with varying calcium hydroxide additions (average of 3 samples per point). Analytical error bars represent 1 standard deviation.

**Table 4.4:** Unconfined compressive strength of saturated carbonated and saturated non-carbonated kaolin specimen (average results based on three tests per mix)

Sample Description	<sup>a</sup> UCS of water saturated non-carbonate treated kaolin specimen (kPa)	<sup>b</sup> UCS of HC solution saturated carbonated treated kaolin specimen (kPa)
4L 3AV	200±3.1	210±4.2
4L 10AV	180 ±1.6	230±2.1
6L 3AV	190±1.0	240±3.1
6L 10AV	170±1.2	280±3.5
8L 3AV	180±3.0	230± 4.0
8L 10AV	170±2.1	270± 3.7

<sup>a</sup>Prior to UCS testing, 7 days cured specimens were saturated for 24 hours using deionised water. <sup>b</sup>Prior to UCS testing, carbonated specimens were saturated with HC solution in triaxial cell set-up. Note: UCS represents unconfined compressive strength, HC represents high carbon

As noted by Bell (1996), peak strength for lime treated soils is obtained when OLC is attained. Considering Figure 4.11, an OLC of 6%  $\text{Ca}(\text{OH})_2$  achieves peak strength of 280 kPa for carbonated treated kaolin, which was compacted to air voids of 10%. Based on 7 days cured specimen comparison was made between the UCS at the OLC of carbonated treated

kaolin (that is at peak strength) and non-carbonated treated kaolin at 6%  $\text{Ca}(\text{OH})_2$ , 10% air voids combination (Table 4.4). It is observed that the carbonated treated kaolin has higher UCS of 280 kPa as compared to a UCS of 170 kPa for non-carbonated treated kaolin. Higher UCS would be expected in carbonated 7 day cured treated kaolin compared with non-carbonated 7 day cured treated kaolin. This is because usually significant strength in treated kaolin is achieved as from 28 days curing, due to slow pozzolanic reaction which starts as from 28 days curing (Vitale *et al.*, 2017). However, the observed higher strength development in carbonated treated kaolin indicates the strength development produced due to carbonation.

### Variation of Strength with Air Voids Content

The experimental results investigating the effect of specimen air voids on the UCS of carbonated treated kaolin are shown in Figure 4.12. As can be seen, the UCS of the carbonated specimens increased with increasing air voids up to 10 %, and then decreased with further increases in air voids above 10 %. The specimens at 10% air voids content showed the highest strength.

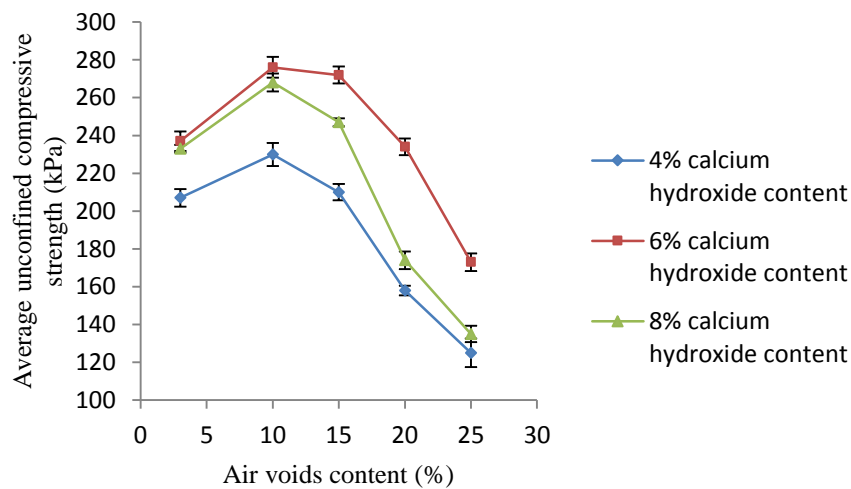


**Figure 4.12:** Unconfined compressive strength of carbonated calcium hydroxide treated kaolin clay with varying air voids (average of 3 samples per point). Analytical error bars represent 1 standard deviation.

The peak UCS was observed at 6 %  $\text{Ca}(\text{OH})_2$  content for all air voids contents (Figure 4.12). The results in Figures 4.11 and 4.12 show that there is non-linear relationship between UCS increases and  $\text{Ca}(\text{OH})_2$  additions in carbonated treated kaolin.

### Variation of Stiffness with Air Voids/Lime Content for Carbonated Treated Kaolin.

Figure 4.13 shows the stiffness variation with varying air voids for carbonated treated kaolin clay. As shown, the stiffnesses increased with increasing air voids up to 10 %, and then decreased with air voids above 10 %. Samples treated at 6 %  $\text{Ca(OH)}_2$  exhibited the highest stiffnesses for all air voids. As would be expected the development of peak stiffness occurred at 10% air voids and 6%  $\text{Ca(OH)}_2$  combination (Figure 4.13). The pattern of peak stiffness at this combination is similar to the combination in development of peak UCS of corresponding specimens (Figure 4.12).

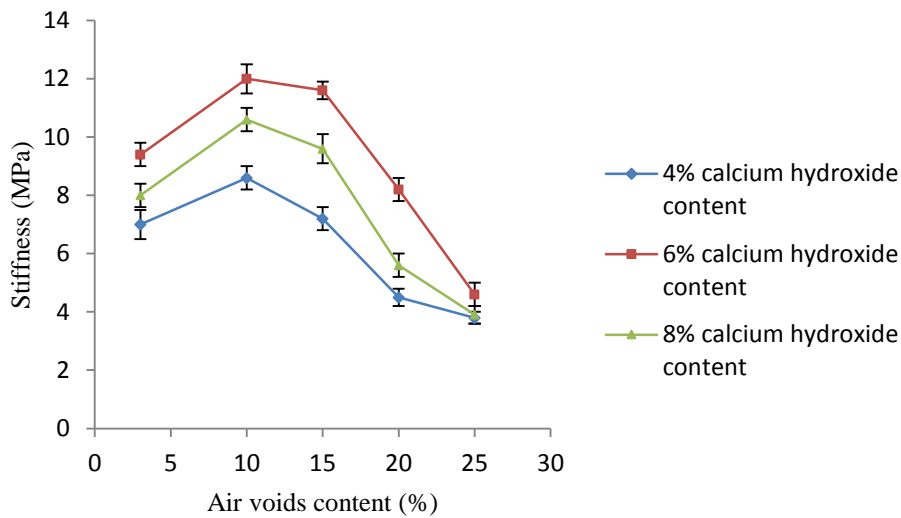


**Figure 4.13:** Stiffness of carbonated calcium hydroxide treated kaolin with varying air voids (average of 3 samples per point). Error bars represent 1 standard deviation. Note: untreated kaolin resulted in stiffness of 2.4 MPa

The highest stiffnesses developed for 4 %, 6 % and 8 %  $\text{Ca(OH)}_2$  treated kaolin, when compared with stiffness of untreated kaolin (2.4 MPa), were approximately 4, 5 and 4 times greater respectively.

## Unconfined Compressive Strength Variation with Calcium Carbonate Content

Figure 4.14 shows the UCS variations with  $\text{CaCO}_3$  content in carbonated treated kaolin. As shown, samples (for all air voids) exhibited UCS increase with increasing  $\text{CaCO}_3$  content. The highest strength was achieved at 10% air voids, as also shown in Figure 4.11. This shows that there is non-linear relationship between UCS development and increase in air void contents in carbonated treated kaolin. Additionally, a non-linear relationship between increases in UCS and increases in  $\text{CaCO}_3$  formation was observed in the carbonated treated kaolin (Figure 4.14).

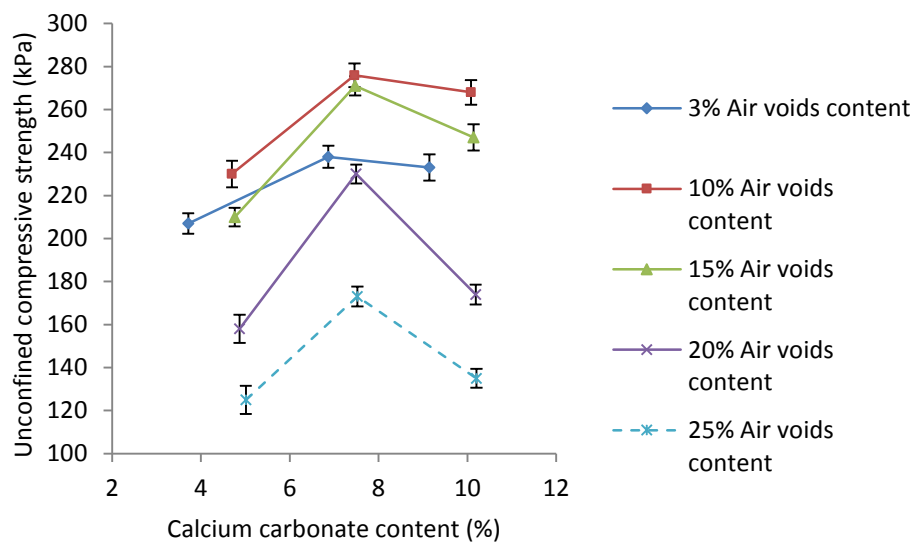


**Figure 4.14:** Variation of unconfined compressive strength with calcium carbonate content in carbonated treated kaolin (average of 3 samples per point). Error bars represent 1 standard deviation.

### 4.3.2 Durability of Carbonated Treated Kaolin.

The experimental results investigating the effect of freezing and thawing on the strength of carbonated treated kaolin are shown in Figure 4.15 and Table 4.5. Full curves for FT durability results of the specimens are included in the CD-ROM (Appendix E) accompanying this thesis. The FT experiment allows for determination of the ability of soil to sustain the detrimental effect of freezing and thawing cycles. As mentioned in Chapter 3, specimens were selected for FT testing based on specimens at air voids of OMC from density/moisture relationship (in this case samples at 3% air voids content). Also specimens at air voids with highest strength in carbonated specimens (in this case 10% air voids content) were selected for the FT assessment. FT durability of specimens was assessed by the results of resistance to three freezing and thawing cycles. The resistance to FT was achieved by comparing the

strength of carbonated treated kaolin specimen subjected to FT with that of equivalent specimen not subjected to FT (control).

As presented in Table 4.5, the untreated sample failed before the end of FT testing, thus had no post FT UCS value. The resistance to FT for carbonated samples increased with  $\text{Ca(OH)}_2$  contents (whilst maintaining constant air voids content; Figure 4.15). For example, the resistance to FT increased by 8% (12-20%) for 4-8%  $\text{Ca(OH)}_2$  increase in samples of 3 % air voids content. Also, the resistance to FT increased by approximately 5% (from 20 - 25%) for 4-8%  $\text{Ca(OH)}_2$  increase in samples of 10 % air voids content (Table 4.5).

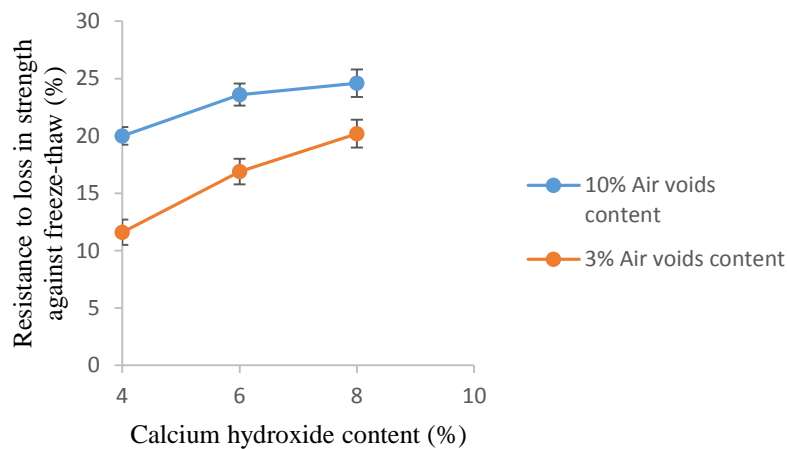


**Figure 4.15:** Resistance to loss in strength against three freeze-thaw cycles of carbonated treated kaolin clay (average of 3 samples per point) error bars based 1 standard deviation.

Considering Figure 4.11, 4.13 and 4.15, it is observed that at 6%  $\text{Ca(OH)}_2$  with 10% air voids content, enhanced strength and stiffness was achieved. Furthermore, peak strength for the carbonated treated kaolin and the maximum resistance to the FT cycles were achieved at this  $\text{Ca(OH)}_2$  and air voids content combination.

**Table 4.5:** Average unconfined compressive strength and freeze-thaw durability (average results based on three tests per mix).

Sample Description	UCS (kPa)		UCS after FT durability (kPa)	
	Water saturated non-carbonate treated kaolin specimen (kPa)	<sup>a</sup> HC saturated carbonated treated kaolin (kPa)	Specimens' UCS after 3 FT cycles	Resistance to FT (%)
Untreated kaolin	108	-	<sup>b</sup> FBT	<sup>c</sup> ND
4L 3AV	200±3.1	210±4.2	24	12
4L 10AV	180 ±1.6	230±2.1	46	20
6L 3AV	190±1.0	240±3.1	40	17
6L 10AV	170±1.2	280±3.5	65	24
8L 3AV	180±3.0	230± 4.0	47	20
8L 10AV	170±2.1	270± 3.7	66	25

<sup>a</sup> Saturation was achieved using high carbon solution.

- No test conducted, <sup>b</sup>FBT represents failed before test, <sup>c</sup>Not determined. FT=freeze-thaw, UCS=unconfined compressive strength, HC=high carbon

#### 4.4 Internal Structure Changes Using Mineralogical Analysis

This section presents results of internal structure of carbonated treated kaolin samples obtained from mineralogical testing. XRCT and SEM techniques were used for examination of internal structure (such as air voids and particle arrangement) of the samples. Details of the testing techniques are contained in Chapter 3 Materials and Methods. Samples listed in Table 4.6 below were tested using XRCT technique. Additionally, three samples from the specimen with highest carbonate were analysed using the SEM. These samples were selected so that comparison could be made between changes in internal structure of carbonated samples at highest strength with those at extreme (lowest and highest air voids contents) conditions.

**Table 4.6:** List of carbonated and non-carbonated samples tested

Sample name	Sample description		Notes
	carbonated sample	Non-carbonate sample	
4L3AV	4% Ca(OH) <sub>2</sub> content, at 3 % air voids content	–	sample at lowest air voids
6L3AV	6% Ca(OH) <sub>2</sub> content, at 3 % air voids content	–	sample at lowest air voids
8L3AV	8% Ca(OH) <sub>2</sub> content, at 3 % air voids content	–	sample at lowest air voids
4L10AV	4% Ca(OH) <sub>2</sub> content, at 10 % air voids content	–	sample at air voids with highest strength
6L10AV	6% Ca(OH) <sub>2</sub> content, at 10 % air voids content	–	sample at air voids with highest strength
8L10AV	8% Ca(OH) <sub>2</sub> content, at 10 % air voids content	8% Ca(OH) <sub>2</sub> content, at 10 % air voids content	sample at air voids with highest strength
4L25AV	4% Ca(OH) <sub>2</sub> content, at 25 % air voids content	–	sample at highest air voids
6L25AV	6% Ca(OH) <sub>2</sub> content, at 25 % air voids content	–	sample at highest air voids
8L25AV	8% Ca(OH) <sub>2</sub> content, at 25 % air voids content	–	sample at highest air voids

#### 4.4.1 Threshold Settings for XRCT Analysis.

Analysis of XRCT was performed using imageJ. One of the acceptable techniques to analyse the presence of carbonate in soil is by using the threshold technique (Gomez *et al.*, 2008). Even though this technique is very effective in the detection and quantification of carbonate formed, it has a shortcoming. The manufacturers of ImageJ clearly stated “if other parameters than the intensity define the structure outline or area a simple threshold does not lead to satisfying results or even fails completely doing the job” (ImageJ 2016). Furthermore, Smith (2014) clearly pointed out that “unfortunately however the use of a single threshold still produced some uncertainties in the final conclusions...”. Based on the fact that a single threshold cannot work on all the samples to determine the presence of CaCO<sub>3</sub>, different thresholds were used for the analysis.

#### ***4.4.2 Determination of Carbonate Content in Sample Using XRCT.***

The presence of  $\text{CaCO}_3$  in carbonated treated kaolin clay has been determined using the calcimeter, and TGA. To understand the distribution of carbonate in the treated kaolin clay, XRCT was used to examine images of carbonated and non-carbonated treated kaolin. The images used for this purpose are presented in Figure 4.16. Figure 4.16a shows images of non-carbonated treated kaolin (this sample being the experimental control). Figure 4.16b shows images of carbonated treated kaolin samples. Samples were scanned at a resolution of 1 pixel to  $2.5 \mu\text{m}$ .

It is observed that the original  $\text{Ca(OH)}_2$  used in treated kaolin clay is composed of 1.4%  $\text{CaCO}_3$  content (previously mentioned in Section 3.3). In the current study, the highest amount of 8%  $\text{Ca(OH)}_2$  content was used, which produced approximately 10%  $\text{CaCO}_3$  due to carbonation (previously presented in Table 4.2). This would be so finely dispersed grain that it will be smaller than 1 pixel, and is considered negligible  $\text{CaCO}_3$  content. It appears not to be visible on the XRCT image (Figure 4.16a). The contribution of original slaked lime containing little carbonate may not have impact on the thresholding in XRCT image for determination of  $\text{CaCO}_3$  distribution.

In the samples not subjected to carbonation (Figure 4.16a), the kaolin particles shown as dark grey can be seen, whilst black regions shown on the image represents voids. Figure 4.16b shows noticeable differences between carbonated samples compared with non-carbonated samples. The main observable difference is the presence of white patches found on the carbonated samples (Figure 4.16b) which are lacking in non-carbonated samples (Figure 4.16a). The white patches appear to be amorphous, and are suggested to be  $\text{CaCO}_3$ . This is discussed further in Section 4.4.7.

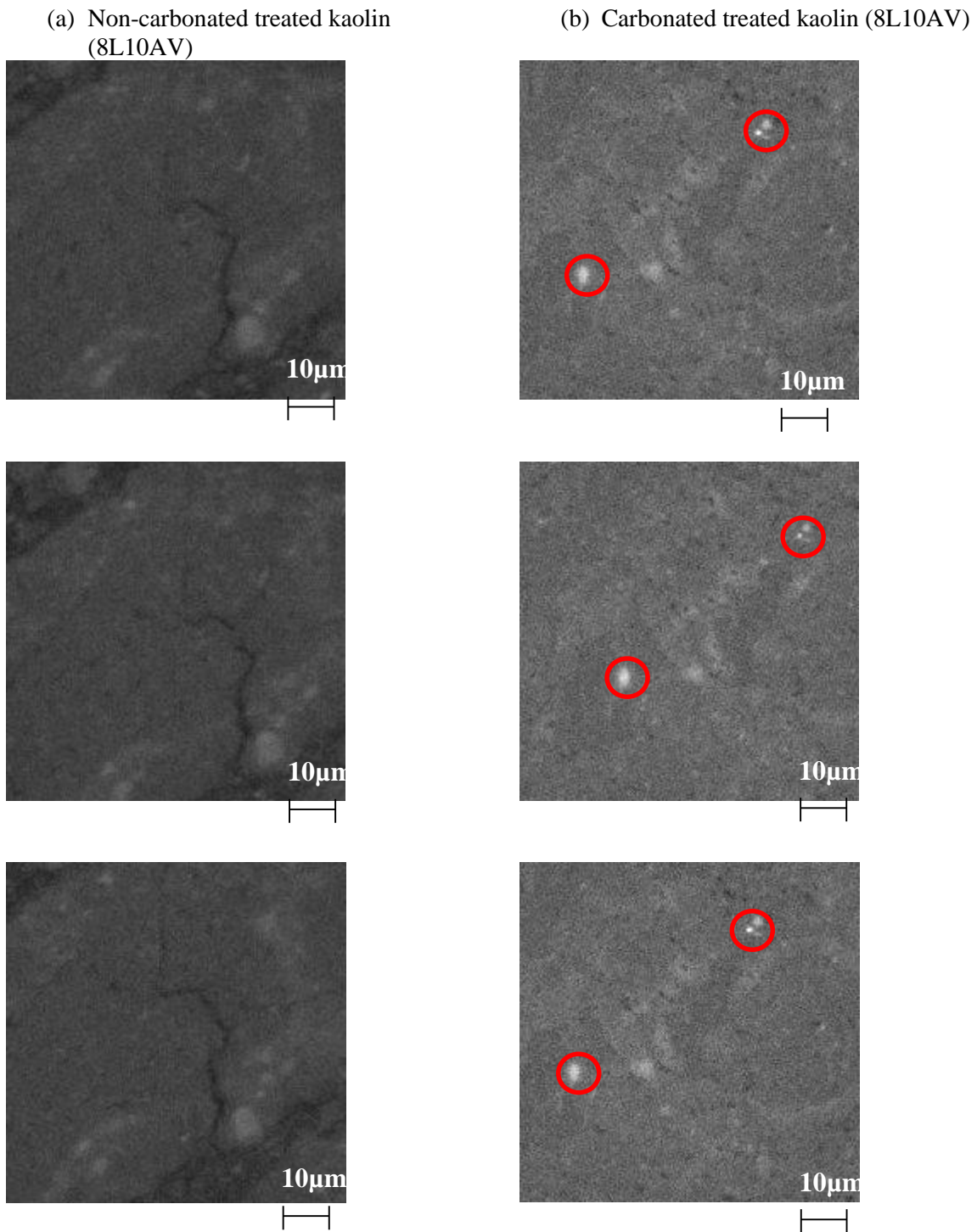


**Figure 4.16:** XRCT images of 8% calcium hydroxide 10% air voids treated kaolin. Column (a) represents non-carbonated sample, and column (b) represents carbonated specimen. Note: white patches represents calcium carbonate particles as inferred using scanning electron microscopy (Section 4.4.7). The red circles mark areas where amorphous calcium carbonate is formed.

(a) Non-carbonated treated kaolin (8L10AV)

(b) Carbonated treated kaolin (8L10AV)

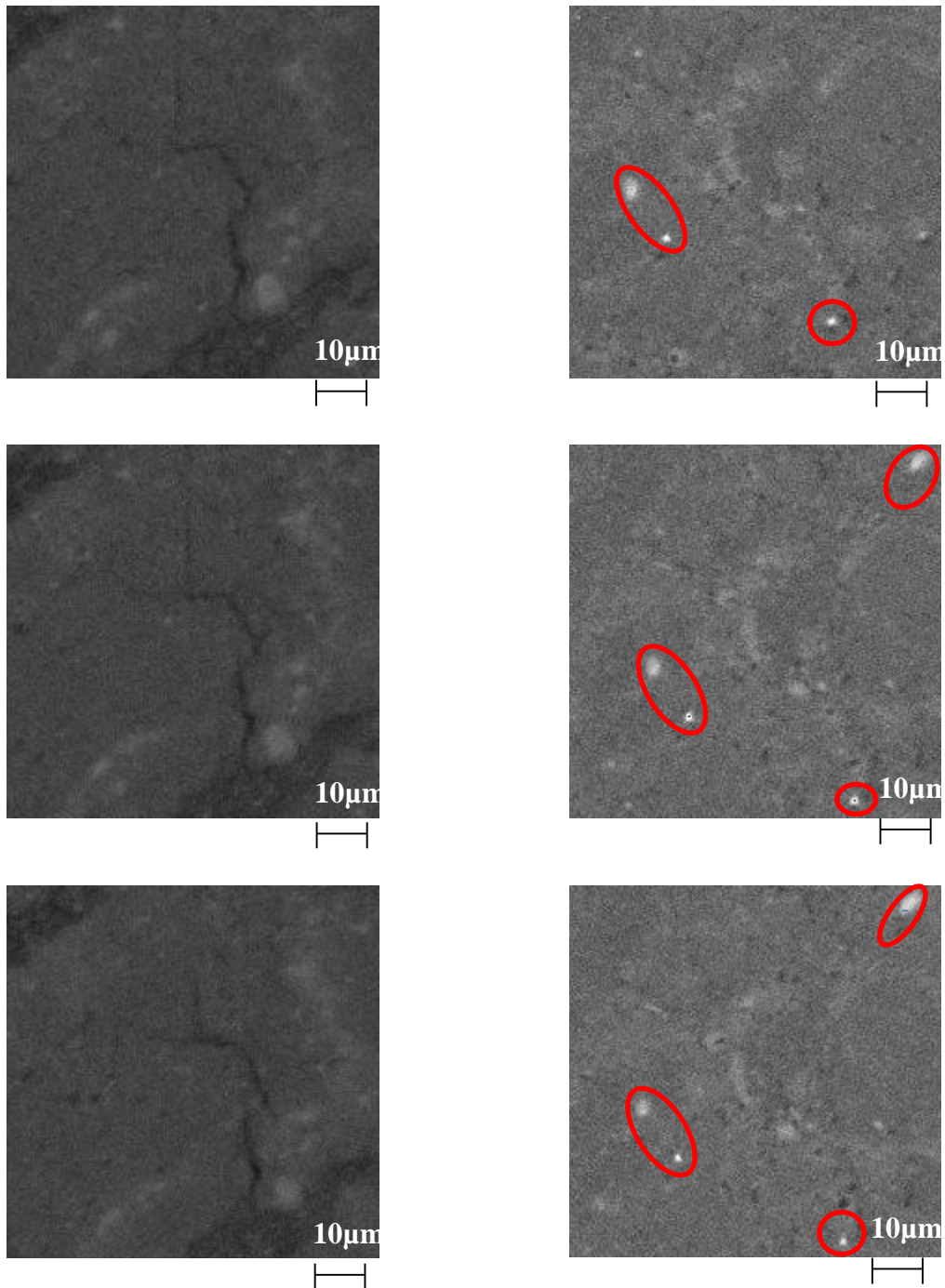


**Figure 4.16 continued:** XRCT images of 8% calcium hydroxide 10% air voids treated kaolin. Column (a) represents non-carbonated sample, and column (b) represents carbonated specimen. Note: white patches represents calcium carbonate particles as inferred using scanning electron microscopy (Section 4.4.7). The red circles mark areas where amorphous calcium carbonate is formed.

#### 4.4.3 Sample Slice Analysis Using ImageJ Software

Typical images of sample slice analysed using Image J are presented in Figures 4.17 and Figure 4.18. Full results of images showing calcite, and voids content, with corresponding threshold graphs of carbonated treated kaolin are included in Appendix C. Figure 4.17 shows sample images used for measuring  $\text{CaCO}_3$  content, whilst Figure 4.18 shows images used in measuring voids content.

It was observed that the threshold values that identified the  $\text{CaCO}_3$  were  $>31$ . As shown in Figure 4.17, when thresholding is applied, the XRCT image is divided into foreground and background. The identified white particles represent the presence of  $\text{CaCO}_3$  formed and the black regions represents the kaolin.

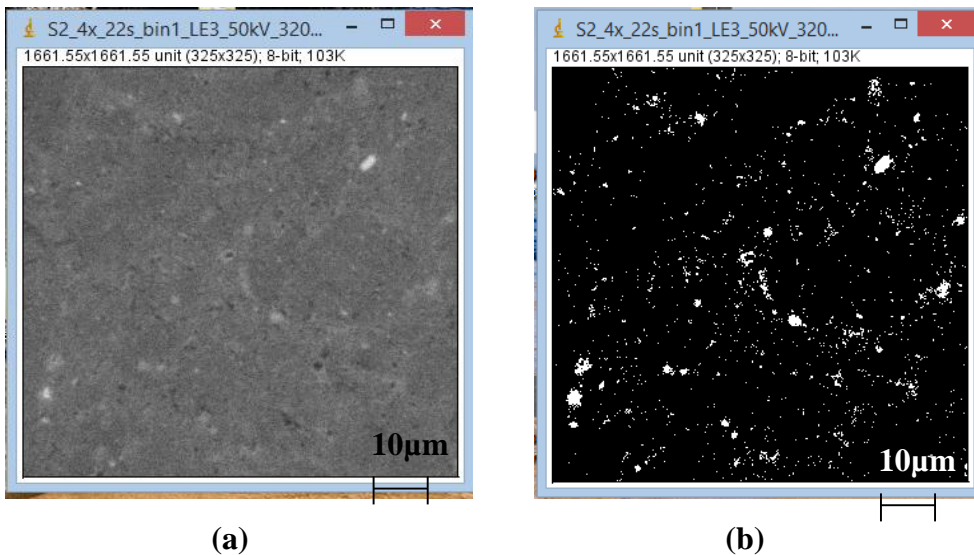


**Figure 4.17:** XRCT image of 8% calcium hydroxide 10% air voids treated kaolin (a) carbonated sample (b) image showing black background (non-  $\text{CaCO}_3$ ), and white foreground ( $\text{CaCO}_3$ ) after application of threshold intensity of 125. Note: white patches represents calcium carbonate particles as inferred using scanning electron microscopy (Section 4.4.7).

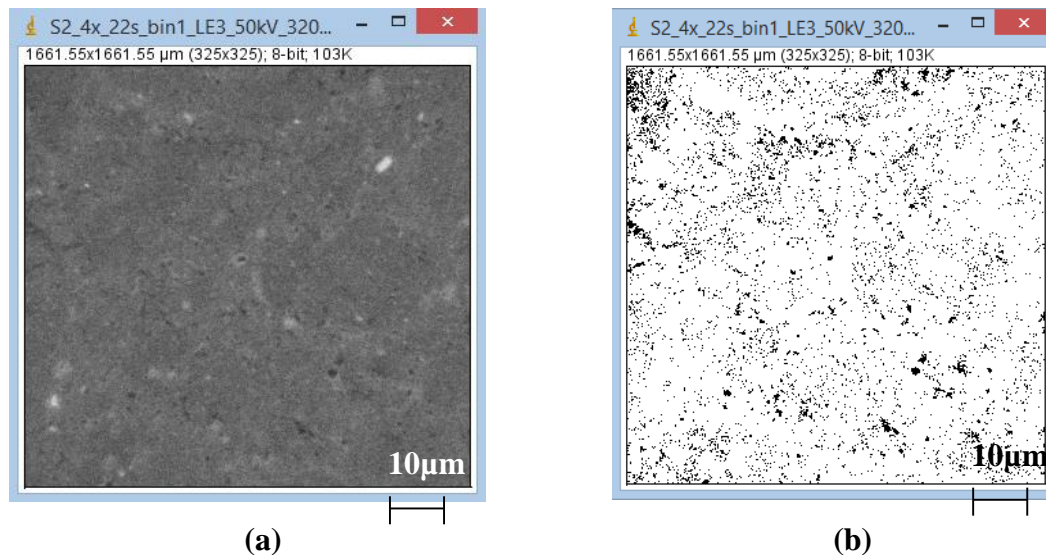


**Figure 4.18:** XRCT image of 8% calcium hydroxide 10% air voids treated kaolin (a) carbonated sample (b) image showing white background (solid material), and black foreground (voids) after application of threshold intensity of 88. Note: black patches represents voids, white patches represents solid material.

The black ‘particles’ represent the air voids, whereas the white patches represent the solid material (combination of kaolin clay, and  $\text{CaCO}_3$ ). This shows that the XRCT analysis has an advantage of also detecting and quantifying the percentage of air voids in carbonated clays. The detection of voids was achieved using ImageJ software and thresholding technique. As noted earlier, a simple threshold cannot guarantee consistent good results. As such, different thresholds were used to detect the voids as shown in Figure 4.19.

It is observed that the threshold values that identified the voids were between 15 and 88. To achieve the voids the foreground and background were separated using the thresholding technique.

Due to the fact that  $\text{CaCO}_3$  grains formed during the carbonation process are measurable in microns (De Silva *et al.*, 2006), a mechanism is required that could effectively detect this formation. One way to detect the  $\text{CaCO}_3$  formation is by using XRCT. XRCT produces high resolution images because X-rays can penetrate deeply through the soil, as such it can effectively detect  $\text{CaCO}_3$  formed. The results showing the detected  $\text{CaCO}_3$  in treated kaolin using XRCT for 90 slices per sample are presented in Figure 4.19 and Table 4.7. The results show that the  $\text{CaCO}_3$  formation is distributed down the depth of carbonated treated kaolin (Figure 4.19).

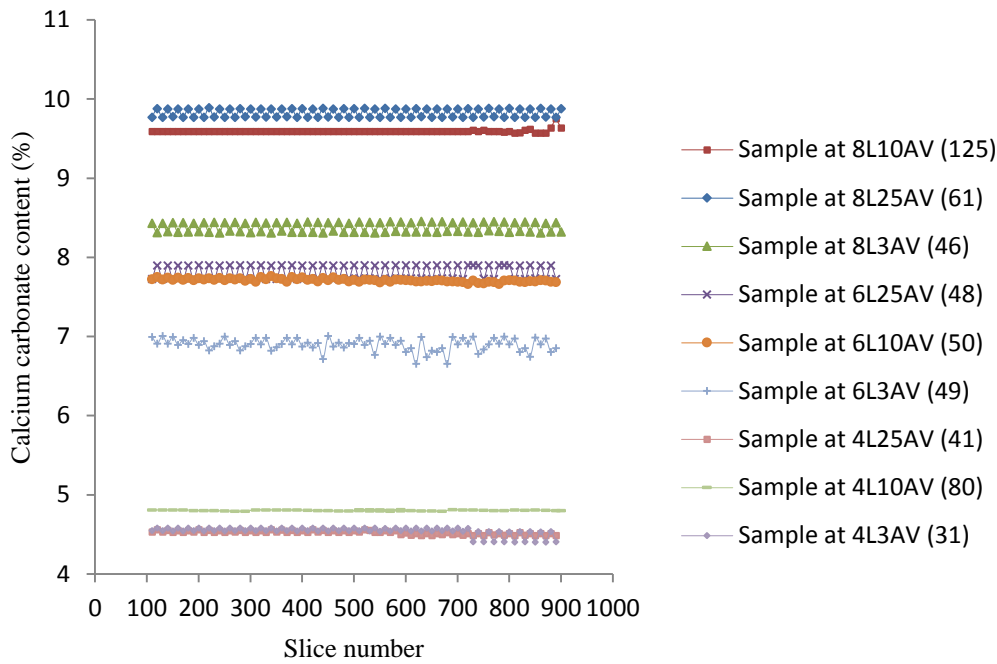


**Figure 4.19:** Calcium carbonate content relationship with sample slices of carbonated treated kaolin. Note: threshold values are given in parentheses. L represents percentage calcium hydroxide content; AV represents percentage air void content.

As mentioned in the previous section (Section 4.1), that carbonation assessment was performed on samples with lime contents from the minimum lime requirements for significant strength improvement. The minimum lime content in the current study was equal to the ICL value, which was 4 %  $\text{Ca}(\text{OH})_2$  (3% CaO equivalent).

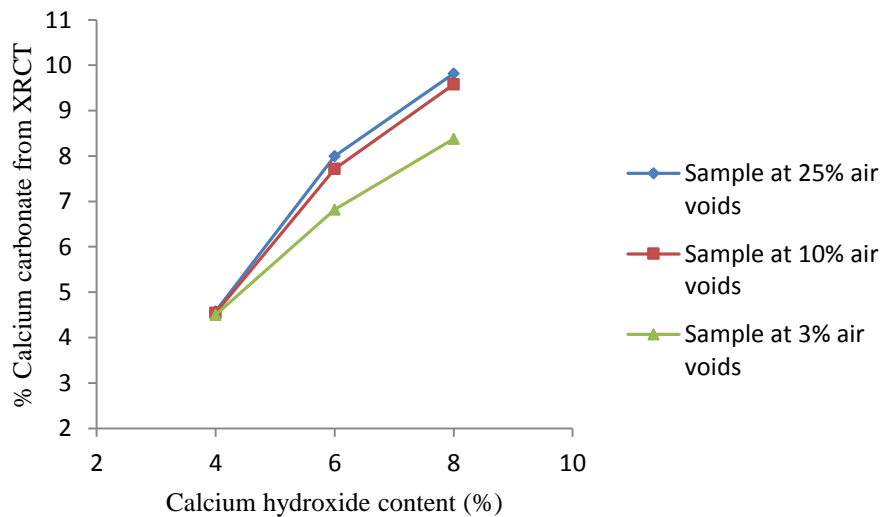


**Figure 4.20:** Detected calcium carbonate in treated kaolin clay using XRCT. Note: XRCT represents X-ray computed tomography. Average of 90 slices per sample.

The detected  $\text{CaCO}_3$  content increased with increase in lime content (Figure 4.20 and Table 4.7). For example,  $\text{CaCO}_3$  increased by more than 2 % for increase in  $\text{Ca}(\text{OH})_2$  content from 4 to 8 % for samples at 3% air void (4L 3AV to 8L 3AV). Similarly,  $\text{CaCO}_3$  content increased by more than 3% for increase in lime content from 4 % to 8 % for samples at 10 % air voids (4L 10AV to 8L 10AV). Again,  $\text{CaCO}_3$  increased by more than 3% for increase in  $\text{Ca}(\text{OH})_2$  content from 4 to 8 % for samples at 25 % air voids (4L 25AV to 8L 25AV). In all cases the XRCT detected  $\text{CaCO}_3$  is shown to increase with increases in lime contents.

**Table 4.7:** Results of calcium carbonate content determined by image analysis using XRCT

Sample Name	Thresholding intensity	Theoretical calcium carbonate content (% by mass)	Average calcium carbonate content from XRCT images (% by mass)
4L3AV	31	5.41	4.50±0.07
6L3AV	49	8.11	6.82±0.04
8L3AV	46	10.81	8.38±0.06
4L10AV	41	5.41	4.54±0.01
6L10AV	50	8.11	7.72±0.06
8L10AV	125	10.81	9.47±0.01
4L25AV	41	5.41	4.58±0.06
6L25AV	48	8.11	8.03±0.05
8L25AV	61	10.81	9.82±0.06

#### 4.4.4 Calcium Carbonate Content from XRCT versus Calcimeter Analysis

The relationship between the amount of  $\text{CaCO}_3$  obtained from XRCT and that obtained from calcimeter analysis is presented in Figure 4.21. The results comprised of carbonated treated kaolin at 3%, 10% and 25% air voids content.

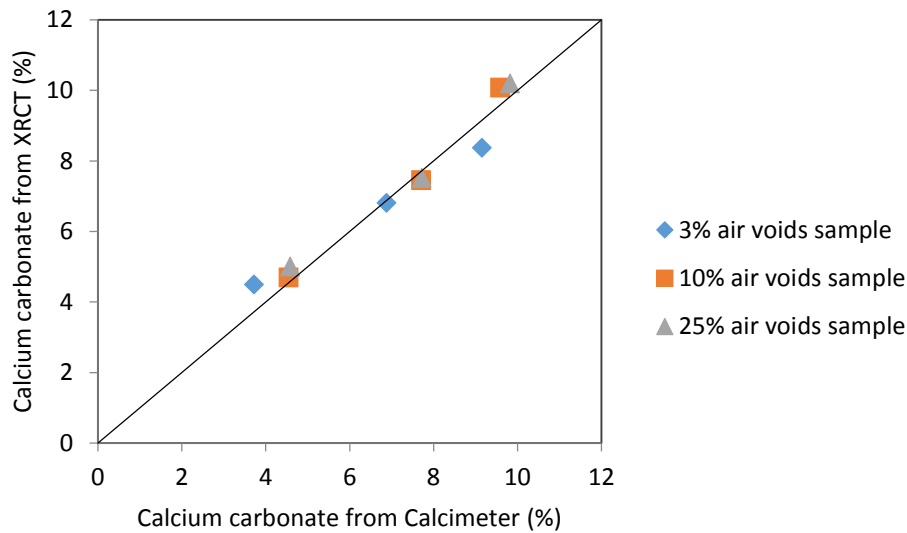


**Figure 4.21:** Relationship between calcium carbonate contents obtained from XRCT and from calcimeter analysis for samples at 3% air voids, 10% air voids and 25% air voids content. Note: XRCT represents X-ray computed tomography.

In all cases the points of  $\text{CaCO}_3$  from XRCT versus those in calcimeter fall closely to the line of equality as shown in Figures 4.21. Based on the line of equality, a comparison of the three points shows that both XRCT  $\text{CaCO}_3$  values and the calcimeter values give similar results.

In order to compare the detected accuracy of  $\text{CaCO}_3$  content obtained from the TGA, calcimeter and XRCT methods, a t-test was performed on the  $\text{CaCO}_3$  results from the three methods as shown in Table 4.8. Statistical significance of the difference in  $\text{CaCO}_3$  contents obtained from each pair of techniques were determined by a paired t-test.  $P \leq 0.05$  was considered to be significant.

The results of t-test (Table 4.8) shows that there was no significance difference between the results from calcimeter and XRCT at  $p = 0.56$ , TGA and XRCT at  $p = 0.37$ , and TGA and calcimeter at  $p = 0.10$ . Considering that if the p-value is greater than 0.05, then the results are similar (in this case results from the techniques), else they are not. Overall, the amount of  $\text{CaCO}_3$  increased proportionally with  $\text{Ca(OH)}_2$  content in the treated kaolin. It may be seen that doubling the  $\text{Ca(OH)}_2$  additions doubles the  $\text{CaCO}_3$  formed and may be predicted from Equation 4.4, where  $\text{Ca(OH)}_2$  addition is proportional to the resulting  $\text{CaCO}_3$ . Additionally, there is reasonable agreement between the three techniques for determining  $\text{CaCO}_3$  content. It is observed that calcimeter detected higher percentages of  $\text{CaCO}_3$ , followed by the XRCT method, and lastly by the TGA approach. Overall, all these approaches detected the  $\text{CaCO}_3$  formation in solid carbonate as shown in Table 4.8.

**Table 4.8:** Comparison of calcium carbonate content from TGA, calcimeter and XRCT analysis for sample at 10% air voids content.

Ca(OH) <sub>2</sub> content (%)	Theoretical CaCO <sub>3</sub> (%)	<sup>a</sup> CaCO <sub>3</sub> content from TGA (%)	<sup>b</sup> CaCO <sub>3</sub> content from calcimeter (%)	<sup>c</sup> CaCO <sub>3</sub> content from XRCT (%)	Comparison of CaCO <sub>3</sub> results		
					TGA versus XRCT	Calcimeter versus XRCT	TGA versus Calcimeter
4	5.40	4.54±0.21	4.70±0.24	4.54±0.01	-	-	-
6	8.11	6.97±0.13	7.46±0.16	7.72±0.06	-	-	-
8	10.81	9.40±0.23	10.08±0.15	9.47±0.01	-	-	-
P-value					0.37	0.56	0.10

<sup>a</sup>Analytical error from TGA based on 1 standard deviation ranged from ±0.13 to ± 0.23 % wt CaCO<sub>3</sub>. <sup>b</sup>Analytical error from calcimeter based on 1 standard deviation (average of 3 samples per combination) ranged from ±0.15 to ± 0.24 % wt CaCO<sub>3</sub>. <sup>c</sup>Analytical error from XRCT based on 1 standard deviation ranged from ±0.01 to ± 0.06 % wt CaCO<sub>3</sub>.

Note: TGA represents thermogravimetric analysis, XRCT represents X-ray computed tomography, Ca(OH)<sub>2</sub> represents calcium hydroxide, and CaCO<sub>3</sub> represents calcium carbonate. - Represents not applicable.

#### 4.4.5 Determination of Voids Content Using XRCT

The results showing the detected voids content in carbonated treated kaolin using XRCT are presented in Table 4.9. The results show a reduction in voids contents for carbonated samples when compared to the corresponding non-carbonate samples. For example there was 16 % (from 9.97±0.15 to 8.32±0.07 voids) reduction in voids content for carbonate 8L10AV sample when compared to the corresponding non-carbonate 8L10AV sample.

**Table 4.9:** Voids contents and reduction in voids of samples after carbonation

Sample Name	Target air voids content at preparation (%)	XRCT determined voids content for carbonated samples (%)	XRCT determined voids content for non-carbonate sample (%)	Reduction in voids content (%)
4L3AV	3	1.95±0.01	NT	35.00
6L3AV	3	1.60±0.01	NT	46.67
8L3AV	3	1.44±0.25	NT	52.00
4L10AV	10	8.81±0.12	NT	11.9
6L10AV	10	8.78±0.07	NT	12.2
8L10AV	10	8.32±0.07	NT	16.8
<sup>a</sup> 8L10AV	10	NA	9.97 ±0.15	NA
4L25AV	25	24.39±0.26	NT	2.44
6L25AV	25	24.09±0.08	NT	3.64
8L25AV	25	23.93±0.20	NT	4.28

<sup>a</sup>Non-carbonated sample (8L10AV). L represents percentage Ca(OH)<sub>2</sub> content, AV= Percentage air voids content. NT: not tested. NA= not applicable. XRCT represents X-ray computed tomography.

#### ***4.4.6 Relationship between Lime Contents and Reduction in Voids Content of Carbonated Treated Kaolin.***

The results showing the relationship between Ca(OH)<sub>2</sub> contents and detected voids content for carbonated samples are shown in Figure 4.22 and Table 4.9. The results show greater reduction in voids contents with increase in Ca(OH)<sub>2</sub> contents (as from ICL level) (Figure 4.22). For example there was 18 % increase in reduction in voids contents (from 35-53 % voids) for Ca(OH)<sub>2</sub> content of 4-8 % (in samples at 3 % air void). Similarly, an increase of 5 % in reduction in voids contents for Ca(OH)<sub>2</sub> contents from 4-8 % (for samples at 10 % air void) was obtained. Also an increase of 3 % in reduction in voids content for lime contents from 4-8 % (in samples at 25 % air void) was obtained.

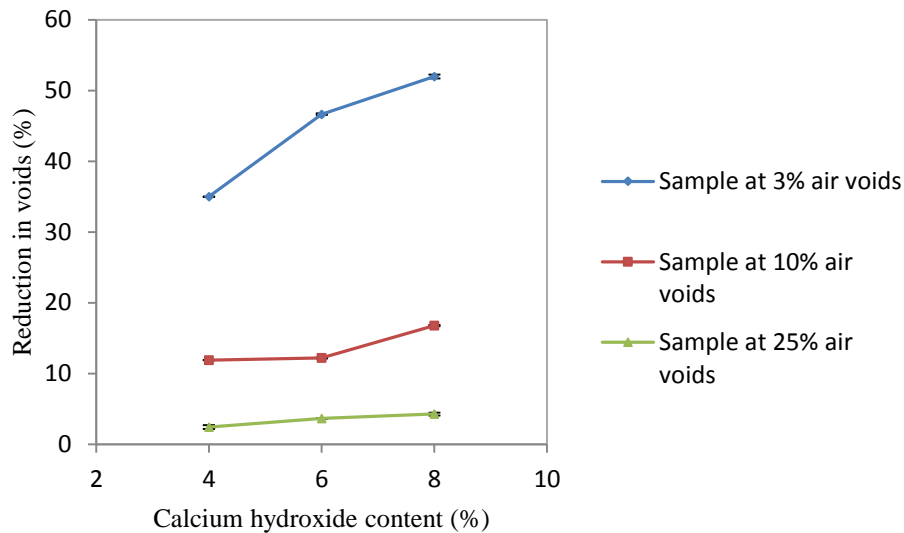


**Figure 4.22:** Reduction in voids content relationship with calcium hydroxide ( $\text{Ca}(\text{OH})_2$ ) content in carbonated treated kaolin using XRCT. Note: XRCT Represents X-ray Computed Tomography.

#### 4.4.7 Scanning Electron Microscopy Analysis

Broken clay surfaces and polished thin sections of the carbonated treated kaolin samples were analysed using an XL30 ESEM. Due to the cost and time involved only three samples (two broken clay surfaces and one thin section, both of 8L10AV sample) were analysed. This sample combination was selected because of its highest  $\text{CaCO}_3$  content based on TGA analysis (previously presented in Figure 4.10). A number of sample images are reproduced in this section. Figures 4.23-4.25 show SEM images of carbonated treated kaolin samples. Point elemental analysis performed on the red spots (Points 0-3) is shown on the images and the results presented in Figure 4.26.

It needs to be borne in mind that the use of SEM secondary electron images (SEI) combined with energy dispersion analysis (EDA) is not a fully quantitative approach. The Figures as follows (Figures 4.23-4.25) show the texture after treatment and tentatively identified grains of kaolin. As reported in Figure 4.10, thermal analysis unambiguously demonstrated the presence of  $\text{CaCO}_3$  in the samples used for SEM.

In general, it is not possible to identify  $\text{CaCO}_3$  unambiguously using this approach. The images show many amorphous white patches (Figure 4.23) and white flaky crystals (Figures 4.24-4.25). On the basis of their morphology, it is assumed that the flaky grains are kaolinite particles. Grains with a less clear morphology may be  $\text{CaCO}_3$ . These grains were about 2-3

$\mu\text{m}$  in size, similar to the dimensions observed using XRCT where grain contrast was consistent with the identification as  $\text{CaCO}_3$ . Point elemental analysis was performed on areas of the sample and this indicated the presence of a range of elements including calcium (Figure 4.26). Other elements such as Si and Al were seen, suggesting kaolinite. The SEM-EDA system cannot resolve grains as small as 2-3  $\mu\text{m}$ , and so the spectra represent an analysis of a composite mixture of kaolin and calcite, simply because of the poor spatial resolution of the technique.

The inferred  $\text{CaCO}_3$  crystals were seen to grow on the surface of the clay (Figures 4.23-4.25) and probably into void spaces, consistent with the XRCT images. The black regions shown on the images indicate void spaces (Figures 4.23-4.24). The presence of voids on the images indicates that calcium carbonate did not fill the voids completely (Figures 4.23-4.24).

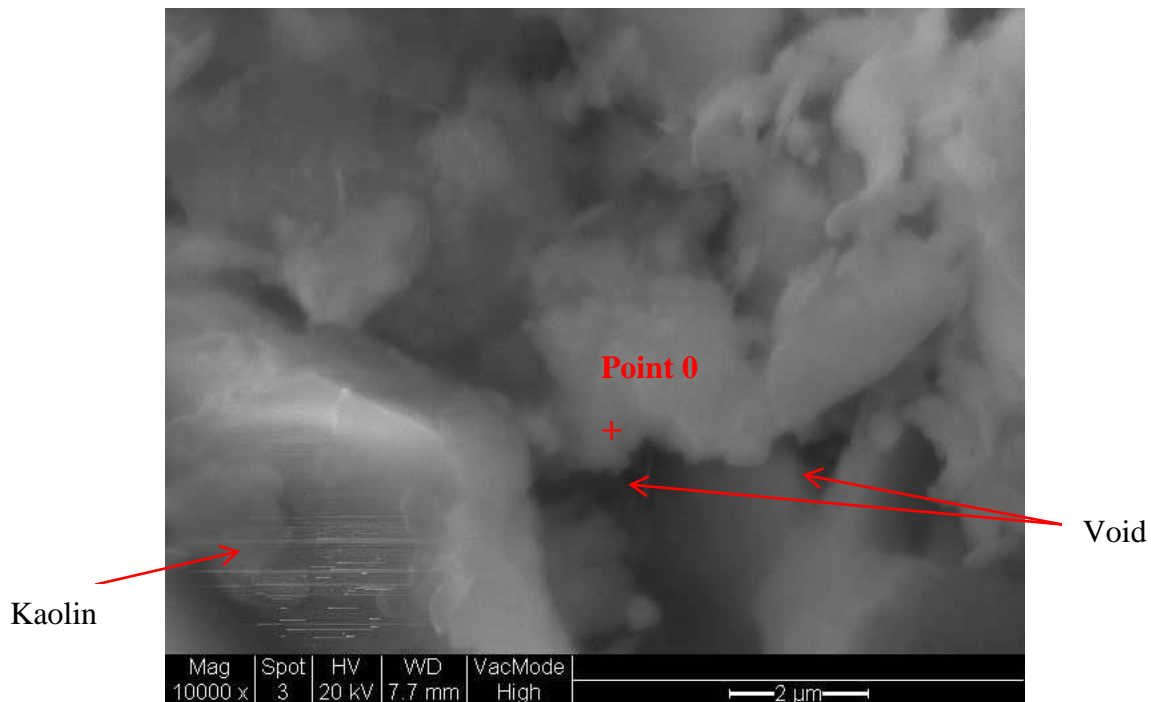


**Figure 4.23:** Broken section of 8L10AV carbonated treated kaolin (a) Spots Point 0=  $\text{CaCO}_3$

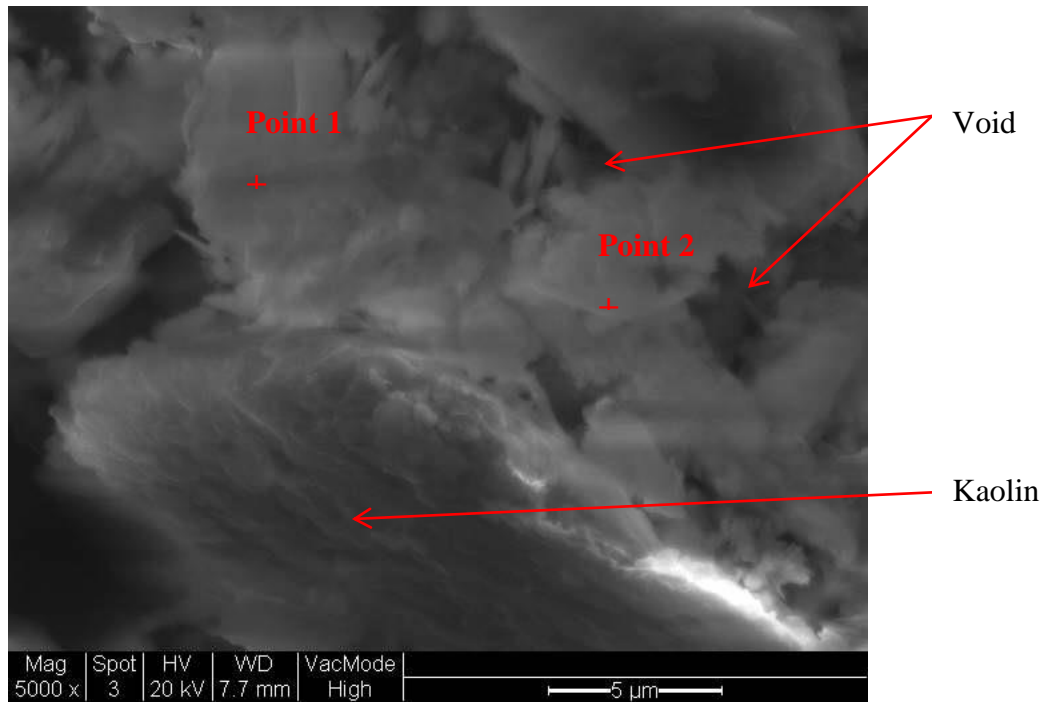


**Figure 4.24:** Broken section of 8L10AV carbonated treated kaolin, spots: Point 1=  $\text{CaCO}_3$ , Point 2=  $\text{CaCO}_3$ . L= Percentage  $\text{Ca}(\text{OH})_2$  Content, AV= Air Voids Content

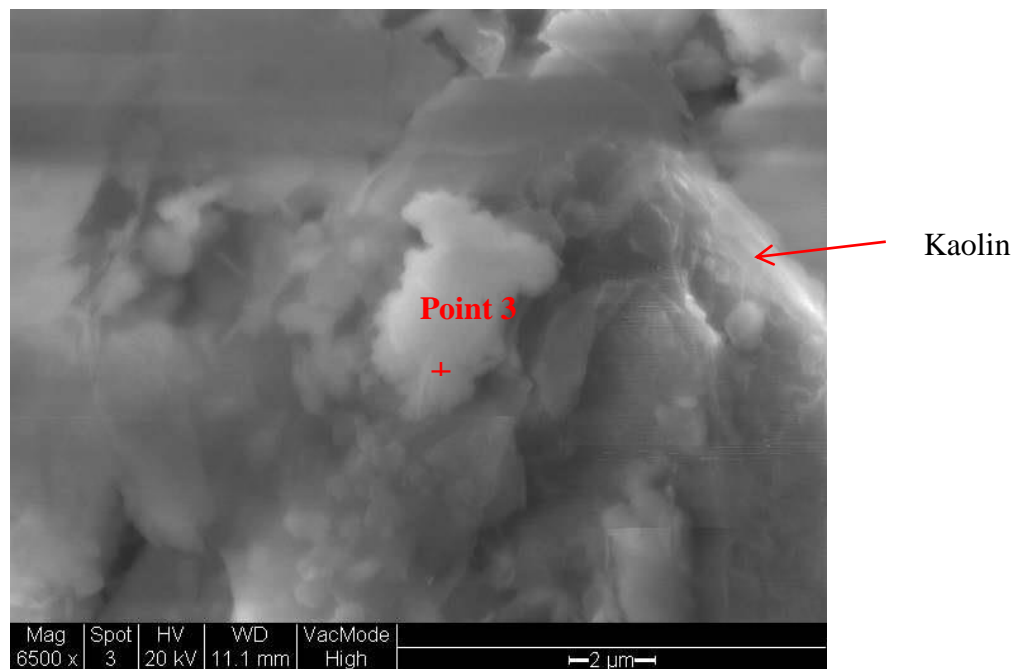


**Figure 4.25:** Polished Section of 8L10AV Carbonated treated kaolin, Spot Point 3= $\text{CaCO}_3$ , L= Percentage  $\text{Ca}(\text{OH})_2$  Content, AV= Air Voids Content

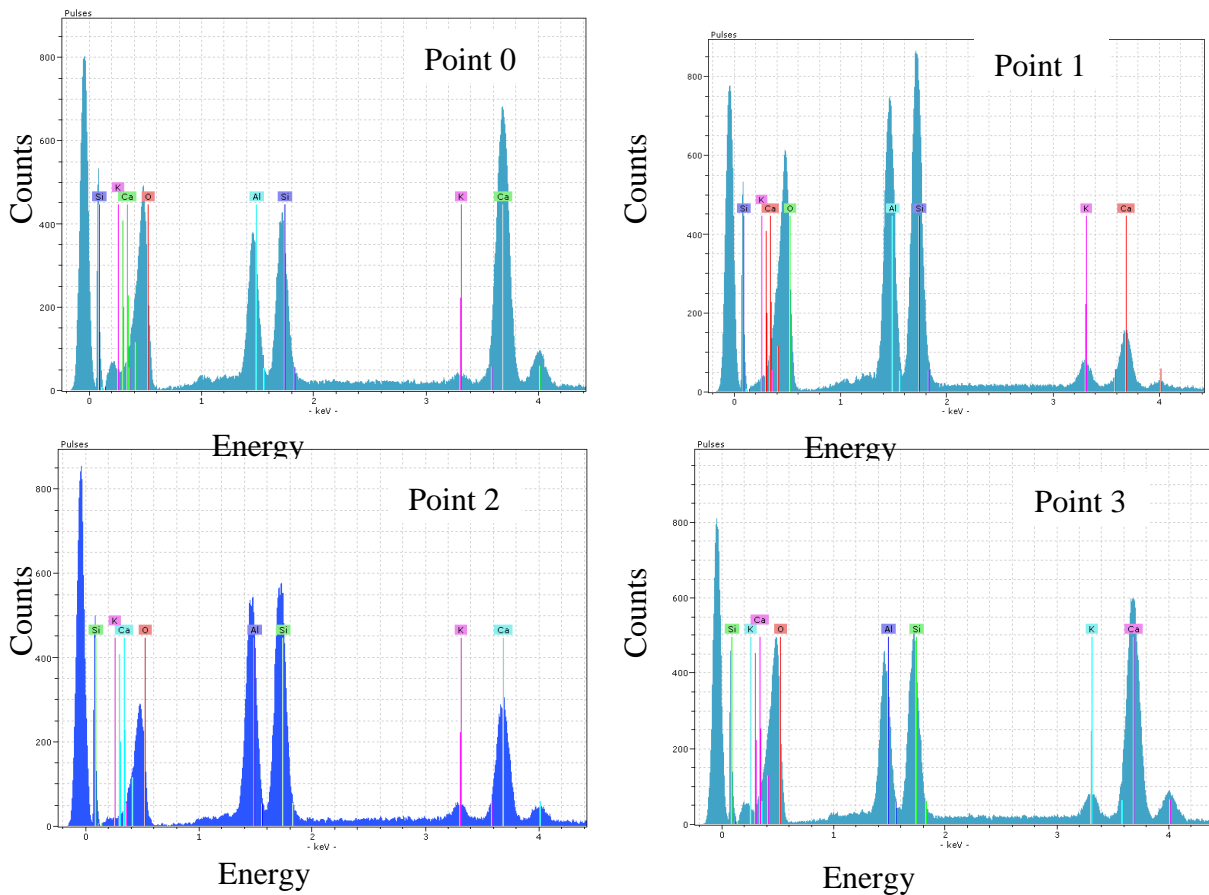


**Figure 4.26:** Elemental Analysis Points 0-3 from Figure 4.23-4.25.

## 4.5 Chapter Summary

Preliminary  $\text{Ca}(\text{OH})_2$  additions to kaolin were first made to determine the ICL for use as baseline lime ( $\text{Ca}(\text{OH})_2$  in this case) additions for treated kaolin, followed by carbonation treatment. A combination of modification and carbonation treatment techniques was applied to treated kaolin clay. The resulting effects on strength development based on UCS tests, and FT durability of the treated kaolin, are summarised below. Additionally,  $\text{CaCO}_3$  formation based on geochemical (such as calcimeter, and TGA) and mineralogical tests (such as XRCT and SEM) of the treated kaolin are summarised below.

- Based on the modified ICL test according to the definition presented by Rogers *et al.* (1997), the ICL value was derived as 4 %  $\text{Ca}(\text{OH})_2$  content (which is 3% CaO equivalent) by dry mass. The UCS data supports the argument that 3% CaO is the ICL value.
- The minimum lime content applied for combined modification and carbonation treatment of the kaolin clay in the current study was based on the ICL value.

- Based on UCS results of combined modification and carbonation treatment, an increase in lime additions up to 6 %  $\text{Ca(OH)}_2$  resulted in peak strength, however further lime additions above 6 % resulted in decrease in the strength. The lime content of 6%  $\text{Ca(OH)}_2$ , which is equivalent of 4.5%  $\text{CaO}$ , corresponds to 'ICL+1 $\frac{10}{2}$ %  $\text{CaO}$ ' value.
- The OLC of 6%  $\text{Ca(OH)}_2$  gave the highest strength for the carbonated treated kaolin.
- Based on calcimeter analysis, an average  $\text{CaCO}_3$  content was obtained from 4.70-10.08 % weight  $\text{CaCO}_3$  for 4-8 %  $\text{Ca(OH)}_2$  contents (for samples at 10 % air voids)
- An increase in air voids up to 10 % value resulted in increase in  $\text{CaCO}_3$  formation; further increases above 10 % air voids did not show remarkable change in the formation of  $\text{CaCO}_3$ .
- An increase in air voids content up to 10 % resulted in highest strength of carbonated treated kaolin, but further increase in air voids content above 10 % resulted in decrease in strength.
- Based on calcimeter and XRCT analysis, an increase in lime additions resulted in increase in  $\text{CaCO}_3$  contents.
- Based on 7 days cured treated kaolin prior to carbonation and water saturation, the carbonated treated kaolin showed higher strength than the corresponding non-carbonated treated kaolin. The UCS at OLC (6%  $\text{Ca(OH)}_2$ ) and 10% air voids) combination in carbonated treated kaolin was 280 kPa (that is at peak strength), compared with 170 kPa, the UCS of corresponding non-carbonated treated kaolin at the same combination.
- The combination at peak strength, 6%  $\text{Ca(OH)}_2$  and 10% air voids content produced a reasonable resistance to FT of 24% for the carbonated treated kaolin.
- From the analysis of XRCT images, it is shown that  $\text{CaCO}_3$  formed could be detected and quantified using imageJ software. This has a great advantage to geotechnical engineering in the sense that carbonate formation and strength improvement process could take place in cohesive soil and hence aid carbonation development and soil improvement.
- XRCT image analysis has proved to be advantageous in the detection and quantification of voids and carbonate in soils.
- Due to the presence of voids spaces on the images, it suggests that  $\text{CaCO}_3$  did not fill the voids completely in carbonated treated kaolin.

- Based on XRCT analysis, an increase in lime contents resulted in reduction in voids contents of the carbonated treated kaolin.
- Based on SEM results, calcium carbonate grains were shown to grow on surface of the clay (about 2-3  $\mu\text{m}$  in size), and do not completely occupy the pore space.
- Overall, the proposed modification and carbonation treatment techniques could be used to understand the combined effects of modification and carbonation treatment of kaolin clay.

## Chapter 5 – Performance of Carbonated Modified Soil

### 5.1 Introduction

One of the aims of this project is to develop a specification for the design of modified soil for combined carbon capture and engineering functions. To facilitate the design specification, a combination of modification and carbonation treatment techniques were applied to kaolin clay.

To assess the effect of CO<sub>2</sub> on Ca(OH)<sub>2</sub> modified clay, characterisation of treated kaolin clay was investigated. The amount of CaO equivalent to be added to the clay was based on the results of the Modified ICL Test according to the definition presented by Rogers *et al.* (1997). The ICL value is the minimum amount of CaO at which the pH curve flattens off and a marginal change in pH results from a large change in CaO content. This was used to determine the minimum amount of CaO equivalent addition by dry mass. The quantity of CaO equal to the ICL value for kaolin clay in the current study is 3% CaO equivalent by dry mass. Kaolin clay was treated with Ca(OH)<sub>2</sub> with equivalent CaO content of 3% (ICL), 4.5% (ICL+1.5%) and 6% (ICL+3%) by dry mass for subsequent assessment of carbon capture and strength development. The equivalent amount of CaO is 75% of the Ca(OH)<sub>2</sub> content (BS 1924-2, BSI 1990a).

This chapter is structured to discuss the carbonation and strength development in treated kaolin permeated with CO<sub>2</sub>. Carbonation and modification processes which determine the feasibility of combined carbon capture and engineering functions are discussed with respect to lime contents and air voids content. The optimum air voids content and lime content for the assessment of combined carbonation and strength development are also discussed. Finally, the optimum air voids content obtained was used to suggest a design specification for CaO modified soil with combined carbon capture and engineering functions.

The discussion explores carbonation and strength development followed by the implications for carbon capture. This leads to conclusions, followed by development of specifications for combined carbon capture and engineering functions.

## 5.2 Initial Consumption of Lime and its Implication

The concept of ICL is very important for soil stabilisation purposes. The minimum amount of lime required for the stabilisation of the soil is determined by this concept (Kassim *et al.*, 2005) as explained in BS 1924 (BSI, 1990a; clause 5.4). This property is achieved at a pH value of 12.40 at 25°C. In order to achieve the recommended pH value of 12.40, experiments were performed on different quantities of lime as previously presented in Figure 4.1.

Quantities of  $\text{Ca}(\text{OH})_2$  content were 2%-7% and it was observed that a 12.40 pH value was achieved at 4%  $\text{Ca}(\text{OH})_2$  (3% CaO equivalent). Hence, this explains why an ICL value of 3% CaO is chosen in the current study.

## 5.3 The Use of Lime for Modification and Stabilisation

It is well known that lime has been used effectively for soil modification and stabilisation purposes (Sherwood, 1993). Modification of soil is carried out to improve soils for construction purposes (Rogers and Glendinning, 1996). In order to modify clay for construction purposes, Atterberg Limit tests are recommended. The modification is deemed complete only when the values of PL have risen to asymptote. The lime content at which PL rises to asymptote is regarded as the lime content for the clay modification (Rogers and Glendinning, 1996). PL is known to be the most important indicator compared to LL for achieving the lime content required for clay modification (Rogers and Glendinning, 1996; Muhmed and Wanatowski, 2013). This is because LL and hence PI of the clay could produce a more variable pattern (Rogers and Glendinning, 1996). In the current study, kaolin was to be treated with sufficient lime to achieve combined modification and carbonation. Therefore one of the objectives of the current study is to perform the Atterberg limit test and determine the lime content that achieves a stable PL value for modification of the kaolin, then compare the lime content for modification with that required for combined modification and carbonation treatment of kaolin.

It is observed that the  $\text{Ca}(\text{OH})_2$  content of 2% has the most stable PL value for the improvement to workability of kaolin clay (Figure 4.2). This implies that clay soils that are composed of very high contents of kaolin could be modified for construction purposes with an added  $\text{Ca}(\text{OH})_2$  content of approximately 2%. It is noticed that the  $\text{Ca}(\text{OH})_2$  content of 2% at full PL for modification is lower than the ICL value of 4%  $\text{Ca}(\text{OH})_2$  (3% CaO equivalent) (Figure 4.1). To add sufficient  $\text{Ca}(\text{OH})_2$  for combined modification and carbonation, 4%  $\text{Ca}(\text{OH})_2$  (3% CaO equivalent) was chosen based on the ICL value.

Furthermore, our objective is to establish the relationship between ICL value with respect to compressive strength of non-carbonated treated kaolin. As explained in Section 5.2, an ICL value of 3% CaO equivalent (4% Ca(OH)<sub>2</sub>) achieved a full stabilisation at a pH value of 12.40. It is further confirmed in Figure 4.5 that 4% Ca(OH)<sub>2</sub> (3% CaO equivalent) content achieves the peak compressive strength of non-carbonated treated kaolin. This shows that there exists a correlation between the ICL value of 4% Ca(OH)<sub>2</sub> (3% CaO equivalent) that achieved the full stabilisation with the current experimental results in Figure 4.5. This ICL value is consistent with that in Vitale *et al.* (2016), who reported the value of ICL for kaolin to be 3% CaO.

This has an implication that, for non-carbonated treated kaolin, the addition of 3% CaO could achieve the highest strength for stabilisation purposes.

#### **5.4 Permeability of Treated Kaolin**

Usually, carbonation of compacted lime material is influenced by the permeability of the material (De Silva *et al.*, 2006). Permeability is important in carbonation of compacted material because it allows for the transportation of moisture and dissolved gases such as CO<sub>2</sub> into the voids of the material. In construction of engineering functions such as road pavement, very high air voids could cause moisture damage due to excessive permeability and hence reduction in the pavement durability (Gogula *et al.*, 2005). Therefore, one of the objectives of the current study is to determine the air voids that could produce permeability for the transportation of CO<sub>2</sub> to the reaction site, without too much detrimental effect on the treated kaolin soil properties.

The current study found that air voids contents from 3% to 15% could achieve permeability values of  $1.8 \times 10^{-9}$  m/s to  $7.4 \times 10^{-9}$  m/s (Section 4.1.6). These permeability results compared reasonably well with those from the values of approximately  $0.6 \times 10^{-9}$  m/s to  $7.0 \times 10^{-9}$  m/s in kaolin (Al-Tabbaa and Wood, 1987). These results suggest that treated kaolin compacted to air voids content from 3% to 15% could achieve permeability values of  $1.8 \times 10^{-9}$  m/s to  $7.4 \times 10^{-9}$  m/s for carbonation purposes. These permeability values allow carbonation reactions whilst not having too much detrimental effect on other properties such as durability. Carbonation development in treated kaolin will be discussed in Section 5.5.

## 5.5 Carbonation Development

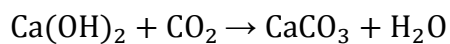
### 5.5.1 Background

The addition of  $\text{Ca}(\text{OH})_2$  to clay causes a release of calcium ions and hydroxyl ions to the water in the voids of the clay, and reacts with clay minerals and carbon dioxide by modification due to cation exchange, carbonation and pozzolanic reactions.

Pozzolanic reaction occurs when sufficient lime ( $\text{CaO}$  or  $\text{Ca}(\text{OH})_2$ ) addition releases hydroxyl ions and creates a pH that is sufficiently high to cause dissolution of silica and alumina from the clay minerals. The dissolved clay minerals react with calcium (released by  $\text{Ca}(\text{OH})_2$ ) to produce CSH and CAH gels as represented by equation 5.1 (Sherwood, 1993). The resulting gel subsequently crystallises to bind a compacted soil structure together, and results in strength and stiffness improvement (Rogers and Glendinning, 1996).



The carbonation reaction occurs in  $\text{Ca}(\text{OH})_2$  mixed compacted clay, by the reaction of dissolved atmospheric  $\text{CO}_2$  in water which is in voids and calcium ions (released by lime), resulting in the production of  $\text{CaCO}_3$  as previously represented by equation 4.4:



Usually, slow pozzolanic reaction in treated kaolin would start as from 28 days curing (Vitale *et al.*, 2017). This suggests that pozzolanic reaction may not occur in treated kaolin which is cured for a period lower than 28 days. In the current study, treated kaolin clay was cured for 7 days prior to treatment with carbonation. Additionally, there was negligible cation exchange with kaolin (4 cmol/kg) compared with bentonite, which is typically 80-100 cmol/kg (Kaufhold and Dohrmann, 2013; Reeves *et al.*, 2006), carbonation was considered the main reaction to occur. The kaolin used here had a CEC of 4 cmol/kg (previously presented in Section 4.1.2). The CEC of 4 cmol/kg instead of the theoretical value of zero (0) for kaolin, could be due to impurities (other clay minerals) in the kaolin, which is manufactured by Imerys (formally English China Clays; Psyrillos *et al.*, 1999).

TGA, calcimeter analysis and XRCT techniques were used to detect  $\text{CaCO}_3$  which is the product of carbonation. One means to precisely detect  $\text{CaCO}_3$  in soils is by the TGA technique according to the method of Manning *et al.* (2005). TGA measures weight loss as a function of

temperature, and allows for a discrete quantification of  $\text{CaCO}_3$  and other heat-sensitive soil components.

The calcimeter technique is used for quantification of bulk carbonates in a sample based on a volumetric approach (BS 7755-3.10: BSI, 1995a). XRCT is a non-destructive technique used to detect internal structure (such as volume of mineral crystals and voids volume) of solid material (Ketcham and Carlson, 2001). The quantity of  $\text{CaCO}_3$  derived from TGA, calcimeter and XRCT methods were comparable with that from theoretical estimation (Section 4.4.4).

The carbonation reaction in treated kaolin is influenced by the air voids contents under which they are compacted. The current study has found that a control of air voids content of treated kaolin produces a desired effect of carbonation reaction for a combined carbon capture and strength improvement.

In practical application air voids would be controlled in treated kaolin by compaction at the dry side of OMC, because compaction at dry side of OMC produces high air voids that are filled with air as opposed to water, which occurs on the wet side (Barnes, 2010).

A field trial would be required to determine the most efficient type of compaction plant for method 7 of Specification for Highway Works (MCHW 1, 2009; Series 600), and the number of passes suitable for achieving the desired air voids contents. Method 7 is required for the compaction of stabilised material (7E) for capping layer of class (9E) (Table 6/4, Specification for Highway Works: MCHW 1, 2009). This would require addition of the pre-determined water content to the soil, in situ lime treatment, running the compaction plant over the material, and measuring the dry density of the material at given number of passes. This would be used to determine the most economical plant that achieves the desired air voids content.

### ***5.5.2 Degree of Carbonation and Lime Additions***

The ability of treated kaolin clay to promote the carbonation reaction is fundamental to its potential for carbon capture, and so it is appropriate to consider the degree of carbonation of treated kaolin as a function of  $\text{Ca(OH)}_2$  additions.

A common means to assess the extent of carbonation is by using the degree of carbonation (DOC). This allows quantification of the experimentally determined carbonates of cation-rich material relative to the amount of carbonates that would be formed if a complete carbonation

of available cations was achieved (Matsushita *et al.*, 2000). The DOC has been applied to calcium rich concrete materials due to carbonation of CaO (Matsushita *et al.*, 2000). Since Ca(OH)<sub>2</sub> is used in treated kaolin in the current study, the treated kaolin is a calcium rich material. Additionally, the Ca(OH)<sub>2</sub> would produce CaO for carbonation, thus it is reasonable to apply DOC to the current study.

The DOC has been determined as:

$$DOC = \frac{MCO_2(d)}{MCO_2(th)} \quad (5.2)$$

where MCO<sub>2(d)</sub> is the amount of experimentally determined carbonate, and MCO<sub>2(th)</sub> is the amount of theoretically determined carbonate based on stoichiometry. The amount of theoretical carbonation for pure oxides of lime [Ca(OH)<sub>2</sub> or CaO] is chemically derived by equations 4.4 and 5.3 (Lackner *et al.*, 1995).



The DOC as a function of treated kaolin is presented in Figure 5.1, using calcimeter data. Analysing the degree of carbonation for individual combinations with respect to the Ca(OH)<sub>2</sub> content (whilst maintaining constant air voids), the achieved results are shown in Table 5.1.

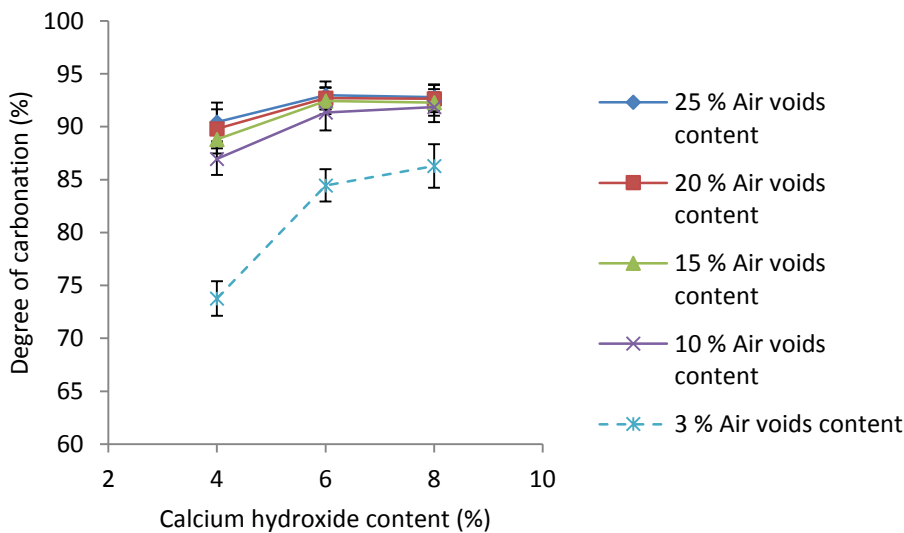


**Figure 5.1:** Variation in degree of carbonation with calcium hydroxide content in treated kaolin (error bars are based on one standard deviation).

**Table 5.1:** Degree of carbonation and percentage uncarbonated calcium hydroxide

Calcium hydroxide content (%) Air voids content (%)	Degree of carbonation			<sup>a</sup> Percentage uncarbonated calcium hydroxide		
	4%	6%	8%	4%	6%	8%
3%	74	84	86	26	16	14
10%	87	92	92	13	8	8
15%	89	92	92	11	8	8
20%	90	93	93	10	7	7
25%	90	93	93	10	7	7

<sup>a</sup>Determined by the difference between the percentage degree of theoretical carbonation and that of determined carbonation (100-degree of determined carbonation).

To achieve the highest amount of  $\text{CaCO}_3$  that would be captured as carbonate in kaolin at 3% air voids, 8%  $\text{Ca}(\text{OH})_2$  content is most suitable. For the combination at 10%, 15%, 20% and 25% air voids content, the mix at 6%  $\text{Ca}(\text{OH})_2$  content produced the highest amount of  $\text{CaCO}_3$ .

In all the cases based on the DOC (Table 5.1), the combination of 6%  $\text{Ca}(\text{OH})_2$  content and 20% air voids content was the minimum mix that produced the highest  $\text{CaCO}_3$  in the treated kaolin. The maximum DOC derived from the Eijkelkamp calcimeter analysis in the current study was 93 %. 100% degree of carbonation was not attained; this could be due to incomplete dissolution of  $\text{Ca}(\text{OH})_2$  into pore solution where carbonation occurs. The combination of 6%  $\text{Ca}(\text{OH})_2$  content and 20% air voids content in kaolin gives the maximum  $\text{CO}_2$  removed, and so is optimum for climate change mitigation.

### 5.5.3 Degree of Carbonation and Air Voids Content

The effect of increase in air voids content on carbonation of equivalent  $\text{CaO}$  treated kaolin is presented in Figure 5.2. Equivalent  $\text{CaO}$  was determined from the  $\text{Ca}(\text{OH})_2$  used in the current study for comparison with  $\text{MgO}$  used by Yi *et al.* (2013; 2015).  $\text{CaO}$  and  $\text{MgO}$  are both stabilisers used for soil improvement.  $\text{CaO}$  and  $\text{MgO}$  have similar mechanisms of carbonation reaction for strength improvement of soil. The carbonation reaction with  $\text{CaO}$  treatment of soil is represented by equation 5.3, whilst that with  $\text{MgO}$  treatment of soil is represented by equation 5.4 (Lackner *et al.*, 1995).



There is however a shortcoming in this comparator because different researchers used different clays. The current study used pure kaolin clay for CaO treatment, whilst Yi *et al.* (2013) used clayey silty sand for MgO treatment, and Yi *et al.* (2015) used lean clay soil (as classified by ASTM 2011) for MgO treatment.

To plot Figure 5.2, moisture content and density data from Yi *et al.* (2013; 2015) were used to calculate the equivalent air voids content, and DOC data were taken directly from their report. For clarity the result has been separated into two distinct stages and plotted in Figure 5.3.

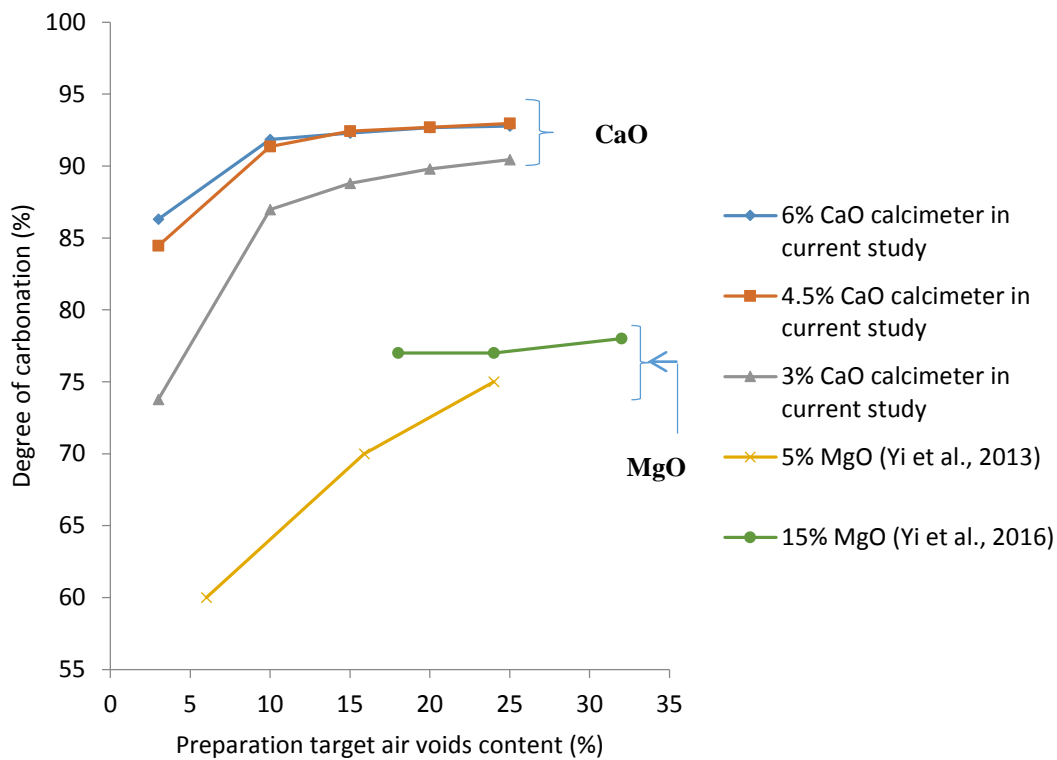


**Figure 5.2:** Degree of carbonation development as a function of calcium oxide treatment in the current study and magnesium oxide treatment after Yi *et al.* (2013; 2015)

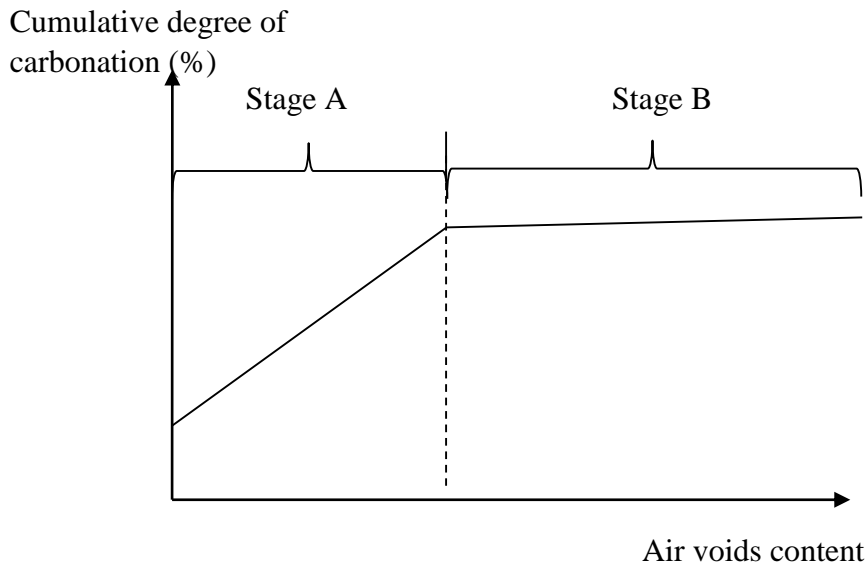


**Figure 5.3:** Two stages of the degree of carbonation at constant calcium oxide content.

In the first stage (A), the cumulative DOC of CaO has a linear relationship with the air voids content. The relationship remains until the air voids value reaches a limit (10% in this study). Above the limiting air voids value only marginal increases in DOC were observed. Throughout stage A, the air voids value of the soil was increasing and resulted in increased DOC. During the second stage (B) negligible further carbonation occurs on further increase in air voids content, because the lime has been consumed.

The linear relationship of cumulative DOC with air voids content (first stage (A) Figure 5.2) is similar to that produced by Yi *et al.* (2013), for carbonated MgO treated clayey silty sand. The similar pattern observed for both studies suggests that there is an air voids content in CaO treated kaolin for achieving desirable carbonation (as the asymptote of carbonation curve is approached), in the current study 10 % air voids. It is interesting to note that the 10% air voids value corresponds to the peak strength (UCS), and this is further discussed in Section 5.6.

It is observed that the limiting air voids for remarkable DOC is more distinct in CaO treatment than that in MgO: this could be because all the lime has been dissolved, and that MgO does not dissolve as easily. As presented in Figure 5.2, the highest degree of carbonation for 6% CaO additions in the current study was 93%, whilst that for 15 % MgO additions was 78 %. This indicates that by application of an amount of CaO at about one-third the amount of magnesium oxide for carbonation would result in 15% more carbonate bonded than that produced using the full amount of MgO.

It is known that chemical reactions are energetically favourable when they have negative heat of reaction, negative  $\Delta H$  (Kotz *et al.*, 2012). The carbonation of CaO is an exothermic reaction with negative heat of reaction value -179 kJ/mol (Equation 5.3). Similarly, that for the carbonation of MgO has negative heat of reaction value of -118kJ/mol (Equation 5.3). The negative heat of reaction value for carbonation of CaO is higher than that for carbonation of MgO. The current study suggests that CaO has greater carbon capture potential than MgO, this might be due to the higher negative heat of reaction value for carbonation of CaO than that for carbonation of MgO.

#### **5.5.4 Carbonation and Reduction in Air Voids**

Carbonation of treated kaolin resulted in a growth of  $\text{CaCO}_3$  grains on the surface of the clay particles, and led to a reduction in air voids content in the current study (Section 4.4.6).

The reduction in air voids content as a function of carbonation in treated kaolin in the current study and that in MgO treated lean clay soil produced by Yi *et al.* (2015) is presented in Figure 5.4. Reduction in air voids content is determined by the change in air voids between preparation target air voids and the post carbonation air voids expressed as a percentage of the preparation target air voids. The reduction in air voids content at preparation air void of 10%, which corresponds to the peak strength was approximately 12%, 17% and 12% for 3%, 4.5% and 6% CaO contents respectively. The reduction in air voids content decreased as the volumes of preparation air voids content increases. This is consistent with the result produced by Yi *et al.* (2015). The highest reduction in air voids in the current study is 52% for 8%  $\text{Ca(OH)}_2$  content at 3% preparation target air voids contents, whilst the highest value produced by Yi *et al.* (2015) is 15% for 15% MgO content at 18 % preparation target air voids contents. The highest value of reduction in air voids in the current study is approximately thrice the value reported by the study of Yi *et al.* (2015). This extent of reduction in air voids content could be attributed to the corresponding DOC as discussed in Section 5.5.3.

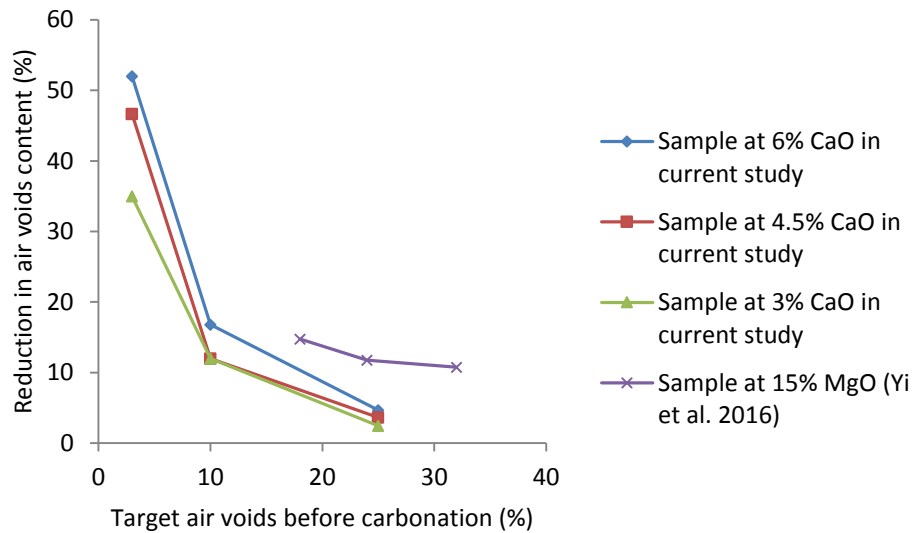


**Figure 5.4:** Reduction in air voids as a function of carbonation of calcium oxide treated kaolin clay in the current study and magnesium oxide treated lean clay soil produced by Yi *et al.* (2015).

This indicates that carbonated treated kaolin (whilst maintaining constant air voids content) would contain less air voids content than the corresponding non-carbonated treated kaolin. This has a benefit to strength improvement of treated kaolin and will be discussed in section 5.6.

## 5.6 Carbonation and Strength Improvement

### 5.6.1 Carbonated Treated Kaolin Strength Improvement Relatively to Kaolin Clay Only

Carbonation of treated kaolin resulted in strength improvement (Section 4.3.1). The strength improvement of treated kaolin due to carbonation relatively to that of kaolin clay only is presented in Figure 5.5 and Table 5.2. It is observed from Table 5.2 that 6%  $\text{Ca(OH)}_2$  (4.5% CaO equivalent) with 10% air voids combination achieved the highest strength improvement factor (2.6 factor). The strength improvement factor of carbonation is derived as the multiplier of the strength of the carbonated treated specimen compared to the corresponding non-carbonated untreated specimen, as also determined by De Silva *et al.* (2006).

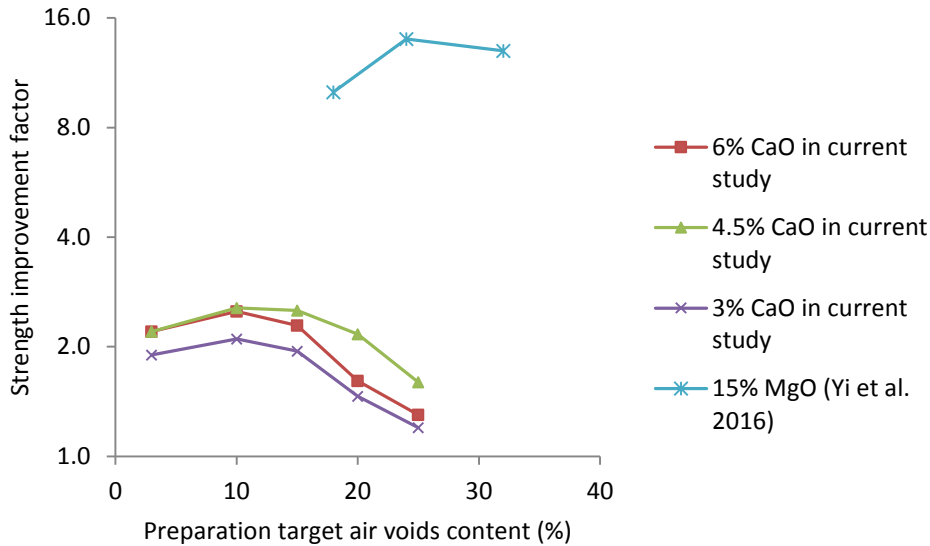


**Figure 5.5:** Strength improvements as a function of increasing air voids for carbonated specimens.

**Table 5.2:** Strength improvement with air voids content.

Air voids content (%)	<sup>a</sup> Strength improvement factor		
	Calcium hydroxide content (%)		
	4%	6%	8%
3%	1.9	2.2	2.2
10%	2.1	2.6	2.5
15%	1.9	2.5	2.3
20%	1.5	2.2	1.6
25%	1.2	1.6	1.3

<sup>a</sup>Derived as the multiplier of the strength of the carbonated treated specimen compared to the corresponding non-carbonated untreated specimen.

Similar results of increase in strength improvement factor as a function of carbonation are presented by Yi *et al.* (2015), who reported a strength improvement factor of approximately 14 for a specimen with 15% MgO content by dry mass at 24% air voids content (Figure 5.5). The strength improvement factor of carbonated treated kaolin is approximately 5 times lower than that produced by MgO treated lean clay. MgO treatment produced higher strength than that produced with CaO or Ca(OH)<sub>2</sub> treatment, because the current study used pure kaolin, whilst Yi *et al.* (2015) used a lean clay soil as classified according to ASTM (2011). The pure kaolin in the current study composed of 35% clay (grain size <0.002mm) and 65% silt (grain size 0.002mm -0.075 mm), whilst the lean clay soil in Yi *et al.* (2015) composed of 6.4% clay (grain size <0.002mm), 75.7% silt (grain size 0.002mm -0.075 mm), and 17.9% sand (grain size 0.075 mm – 2 mm). The strength improvement may reflect carbonate cement formation that binds sand grains together. So the strength results reflect the strength of quartz, which is

the mineral likely to be in the silt and sand fractions. Although the strength improvement results are not directly comparable due to very different clay used in each study, the observed improvement in strength indicates the improvement produced due to carbonation.

Whilst CaO seems to produce far lower strengths than MgO the carbon capture potential is greater in CaO carbonation (Section 5.5.3).

The peak UCS (280 kPa) in carbonated treated kaolin in the current study was achieved at 6% Ca(OH)<sub>2</sub>, and 10% air void combination. For comparison purpose, the peak UCS was expressed in terms of CBR as represented in Equation 5.5 (Danistan and Vipulanandan, 2010).

$$\text{CBR} = 0.56S_u^{1.07} \quad (5.5)$$

where  $S_u$  is the UCS (in pound-force per square inch, psi). The UCS of 280 kPa was converted to psi unit using 1 kPa= 0.145 psi (that is 280 kPa = 40.60 psi)

$$\text{Therefore the CBR} = 0.56 *(40.60)^{1.07} = 29 \%$$

Considering that the carbonated treated kaolin in the current study has a CBR of 29 %, it is observed to be greater than the CBR value of 15% which is the minimum CBR value required for stabilised capping layer (Sherwood, 1993). Based on strength requirements, the carbonated treated kaolin is suitable for use as a stabilised capping layer.

### ***5.6.2 Carbonated Treated Kaolin Strength Improvement Relatively to Treated Kaolin***

Previous researchers (Bagonza *et al.*, 1987) have found carbonation to cause strength reductions to lime stabilised materials. One of the aim of this study was to work out whether carbonated treated kaolin could achieve acceptable strength increases whilst also re-capturing some or all of the CO<sub>2</sub> produced by the manufacture of the lime.

The comparison between saturated compressive strength of carbonated treated kaolin with that of equivalent treated kaolin based on 7 days curing prior to carbonation and UCS testing is presented in Table 5.3. The saturated compressive strength of carbonated treated kaolin shows slight strength increases up to 1.6 times relatively to that of saturated treated kaolin only (Table 5.3).

Based on 7 days curing, the highest saturated compressive strength of saturated carbonated treated kaolin (280 kPa) is higher than the undrained shear strength of treated kaolin (approximately 80 kPa) in Boardman *et al.*, (2001). The reason for this could be that different researchers used different lime content. The current study used minimum of 3% CaO equivalent content, whilst Boardman *et al.* (2001) used maximum of 2.5% CaO content.

Conversely, the compressive strength of saturated carbonated treated kaolin in the current study is much reduced compared to the compressive strength of some non-saturated treated kaolin. Based on 7 days curing, the highest saturated compressive strength in carbonated treated kaolin of 280 kPa, is lower than the highest non-saturated compressive strength (approximately 830 kPa) of treated kaolin in Bell (1996) (Table 5.3). The reason for the differences may be that most researchers including Bell (1996) do not look at saturated strengths. Also, it may be that strengths later than 7 days are more critical as the lime gets used up in carbonation reactions rather than being available for pozzolanic reactions. As earlier mentioned, at 7 days no pozzolanic reactions are likely to have occurred (Boardman *et al.*, 2001).

**Table 5.3:** Compressive strength improvement due to carbonation of treated kaolin relatively to treated kaolin (average results based on three tests per mix). Part of the data is a replication of Table 4.4.

Author	Kaolin description	CaO content (%)	Sample Description	<sup>a</sup> UCS of water saturated non-carbonate treated kaolin specimen (kPa)	<sup>b</sup> UCS of HC solution saturated carbonated treated kaolin specimen (kPa)	Undrained shear strength of treated kaolin compacted at 2% wet of OMC (kPa)	<sup>c</sup> Carbonation strength improvement factor relatively to lime treated kaolin	<sup>d</sup> Non-saturated 7 days UCS of treated kaolin mixed at OMC from Literature (kPa)
Current study	Polwhite grade E kaolin.	3.0 <sup>a</sup>	4L 3AV	200±3.1	210±4.2	—	1.1	—
		3.0 <sup>a</sup>	4L 10AV	180 ±1.6	230±2.1	—	1.3	—
		4.5 <sup>a</sup>	6L 3AV	190±1.0	240±3.1	—	1.3	—
		4.5 <sup>a</sup>	6L 10AV	170±1.2	280±3.5	—	1.6	—
		6.0 <sup>a</sup>	8L 3AV	180±3.0	230± 4.0	—	1.3	—
		6.0 <sup>a</sup>	8L 10AV	170±2.1	270± 3.7	—	1.6	—
Boardman <i>et al.</i> (2001)	English china clay (kaolin)	2.5	—	—	—	80	—	—
Bell (1996)	Kaolinite	3.0 <sup>a</sup> 4.5 <sup>a</sup> 6.0 <sup>a</sup>	—	—	—	—	—	≈830 ≈830 ≈760
Muhmed and Wanatowski (2013)	Commercial kaolin	3.8 <sup>a</sup>	—	—	—	—	—	224
Saeed <i>et al.</i> (2015)	Tropical kaolin clay from Malaysia.	3.8 <sup>a</sup>	—	—	—	—	—	≈ 300

<sup>a</sup>CaO equivalent calculated from actual Ca(OH)<sub>2</sub> additions. <sup>b</sup>Prior to UCS testing, carbonated specimens were saturated with HC solution in triaxial cell set-up prior to UCS testing. <sup>c</sup>Determined by comparing the UCS of carbonated treated specimen to the equivalent non-carbonated lime treated specimen. <sup>d</sup>UCS data taken directly from the authors report. Note: UCS represents unconfined compressive strength, HC represents high carbon.

## 5.7 Effect of Soil pH on the Strength of Carbonated Soil

Results reported by Bagonza *et al.* (1987) on the effect of carbonation on strength of clay sand (calcrete) are inconsistent with those reported in the current study. Bagonza *et al.* (1987) reported that carbonation curing under normal atmospheric CO<sub>2</sub> conditions for 3, 7, 14 and 28 days of 2.25% CaO equivalent (3% Ca(OH)<sub>2</sub>) treated calcrete resulted in a loss of compressive strength. The results showed a 77 % loss of compressive strength of the specimen for 7 days carbonation curing, and 72 % loss of compressive strength of the specimen for 28 days carbonation curing, when compared to the compressive strength of corresponding non-carbonated air tight cured specimens. The soil material used in Bagonza *et al.* (1987) was clay sand (described by the author as ‘a poor quality calcrete’) which is predominantly made up of palygorskite (Netterberg, 1980). The stability of palygorskite clay minerals depends on pH, and it tends to decompose at a pH below 9.0 for a low magnesium concentration and a pH below 7.7 for high magnesium concentrations (SncBn and Nonnrsn, 1974). Since carbonation leads to a reduction of pH to 8.3, carbonated lime treated calcrete would have a pH of about 8.3. This would result in instability of palygorskite, hence the reduction in strength after carbonation.

Other studies have shown an increase in strength of carbonated stabilised soil minerals which are stable under acidic pH (pH below 7). Yi *et al.* (2013) has shown that there is an increase in strength of carbonated MgO treated clayey silty sand (90% sharp sand, 5% kaolin clay and 5% silica flour). This soil is mainly composed of quartz, feldspar and kaolinite minerals (Yi *et al.*, 2013). Kaolinite is stable between approximately pH of 4.5 and pH of 8.5, but decomposes under more acid pH (lower than 4.5) and under more basic conditions (>pH 8.5) (Grant, 1965). Quartz is a resistant mineral in the sedimentary environment (Pettijohn *et al.*, 2012). Thus the clayey silty sand in (Yi *et al.*, 2013) would be stable under a pH of 8.3, which is typical of the carbonation environment. Similar strength improvement of carbonated lean clay soil due to carbonation was reported by Yi *et al.* (2015). The mineral composition in the lean clay soil was feldspar, quartz and kaolinite. Feldspar would be stable at a pH of 5-10 at natural conditions (room temperature and pressure; Wollast (1967)). Feldspar would therefore be stable at a pH of 8.3 which is typical for the carbonation environment. As earlier mentioned quartz and kaolinite would also be stable at a pH of 8.3, and this indicates that the lean clay in Yi *et al.* (2015) would be stable under carbonation environment with a typical pH of 8.3.

The current study of carbonated treated kaolin clay showed increase in strength due to carbonation. The main mineral composition in kaolin clay is kaolinite. Kaolinite is stable at a pH of 4.5- 8.5 Grant (1965). This indicates that kaolin would be stable at a pH of 8.3 typical of the carbonation reaction.

However our target is to improve the carbon capture as well as achieve a high strength improvement. Based on Table 5.1 and Table 5.2, it is observed that a combination of 6%  $\text{Ca}(\text{OH})_2$  and 10% air voids contents well suits our objective, hence this combination is recommended.

### **5.8 Freeze-Thaw Durability**

The performance of the carbonated treated kaolin specimen produced at the OLC shows a FT resistance of up to 24% (previously presented in Figure 4.15). FT at OLC is important because it provides the durability at the lime content which corresponds to the peak strength. This allows for the durability consideration of the specimen at peak strength, and determination of its ability to resist detrimental weather conditions. As previously stated, FT resistance was determined by comparing the UCS of carbonated treated kaolin specimen subjected to FT with that of equivalent specimen not subjected to FT.

The current studies show that there is an increase in FT resistance up to 24% (from 0%-24%) in carbonated treated kaolin at OLC compared with corresponding untreated specimen after 3 FT cycles. Similar increase in FT resistance was observed in treated kaolin specimen at OLC (3% CaO) by Hotineanu *et al.* (2015). The author's results (Hotineanu *et al.*, 2015) showed an approximate 100% resistance (approximately 450 kPa for the UCS of specimen at 0FT and 5 FT cycles respectively) for 28 days cured treated kaolin prior FT testing.

It is observed that the resistance to FT (100%) of treated kaolin in the studies by Hotineanu *et al.*, (2015) is higher than that in the carbonated treated kaolin (24%) in the current study. The reason for this could be due to a 'closed system' FT approach used in the study by Hotineanu *et al.*, (2015). Whereas in the current study, specimens were not wrapped, and free water was placed under the felt pads during the thawing phase of FT cycles in accordance with D560-03 (ASTM, 1989). The 'closed system' FT approach wraps the specimen in paraffin film and ensures that there is no inflow nor outflow of water to the specimen during the FT testing (Jones, 1987; Aldaood *et al.*, 2014). The 'closed system' FT approach is suitable in soil conditions where the change in water content between winter and summer season could not be

significant (Güllü and Khudir, 2014). Additionally, the reason for difference in resistance to FT between the study by Hotineanu *et al.*, (2015) and the current study may be because there was no carbonation in Hotineanu *et al.*, (2015).

The British specification requires a minimum of 80% durability of stabilised material for its use as a sub-base or base material for road pavement. However, the durability requirement for lime-stabilised capping layer is less stringent (Sherwood, 1993). Therefore FT resistance value of 24% may be considered sufficient for capping layer.

The design manual for roads and bridges (The Highways Agency, 2007) specifies that all lime stabilisation including lime-stabilised capping should be constructed from the period of March to September, and when the shade temperature is at least 7°C. Considering that treated kaolin for carbonation involves the use of lime for clay strength improvement, the treated kaolin need to be constructed as a capping layer from the period of March to September in accordance with British Standard (Sherwood, 1993; The Highways Agency, 2007 and MWCH 1; 2009). The reason for this is to avoid construction of treated kaolin during low temperatures, which does not favour lime-clay reactions.

## **5.9 Carbonate Distribution**

Because the  $\text{CaCO}_3$  grains formed during carbonation process are microns in size (De Silva *et al.*, 2006), a mechanism is required that could effectively detect this formation. One way to detect and quantify the  $\text{CaCO}_3$  formation is by using XRCT. XRCT produces high resolution internal images of a sample because X-rays can penetrate deeply through the soil, as such it can effectively detect  $\text{CaCO}_3$  formed, and so yield information about its distribution within a sample as well as the amount formed.

The results determined using XRCT show that  $\text{CaCO}_3$  formed is distributed down the depth of treated kaolin clay. This indicates that by design, the soil improvement due to carbonate formation could be distributed deep down the lime treated cohesive soil, based on the volume of the soil required. To the best of the researchers' knowledge, the use of XRCT to measure the amount of carbonate is being performed for the first time for geotechnical engineering functions.

### 5.10 Conceptual Model of the Carbonation Process in Lime Treated Clay.

Based on results of derived carbonates, strength development,  $\text{Ca}(\text{OH})_2$  additions and air voids content, a conceptual model of  $\text{CO}_2$  in  $\text{Ca}(\text{OH})_2$  treated soil was proposed as presented in Figure 5.6. Atmospheric  $\text{CO}_2$  permeates through the treated kaolin, dissolves in water in the voids of the specimen and hydrates to form  $\text{H}_2\text{CO}_3$ , which ionises to  $\text{CO}_3^{2-}$ ,  $\text{H}^+$ ,  $\text{HCO}_3^-$ .

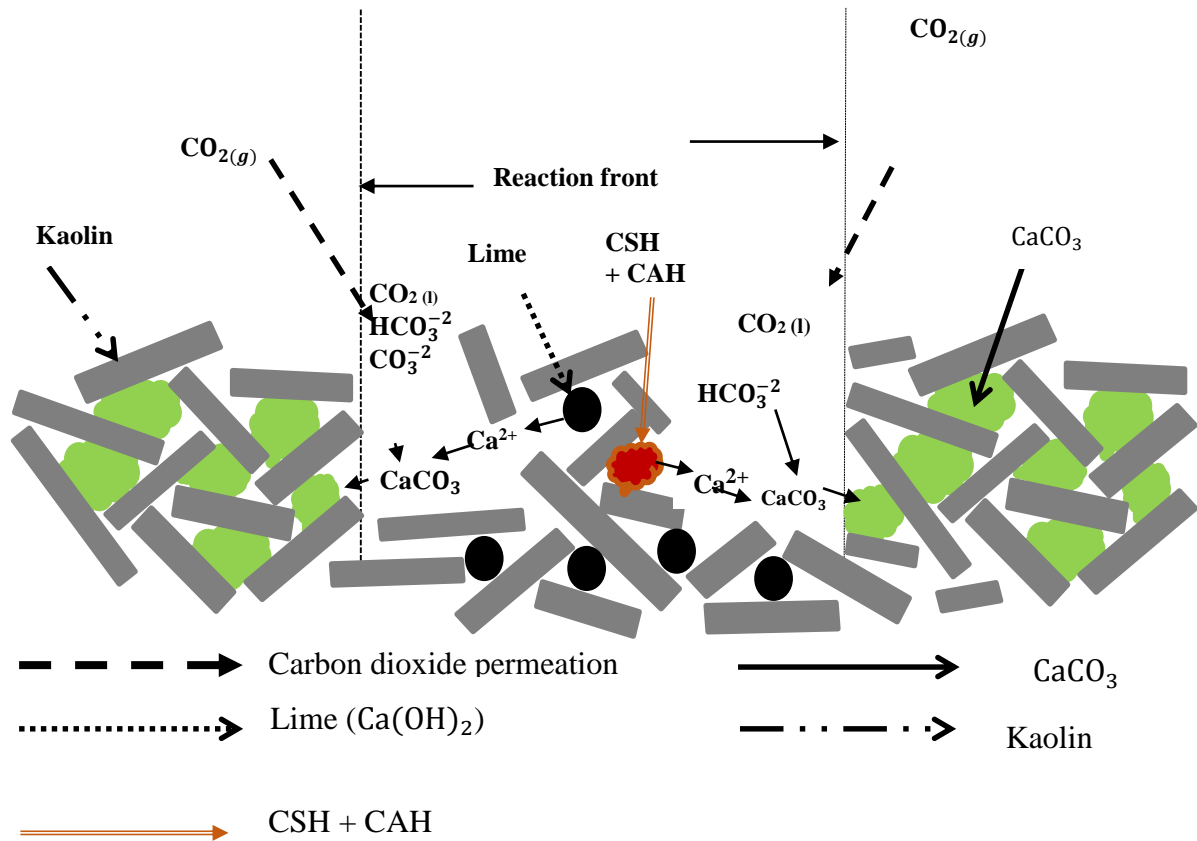
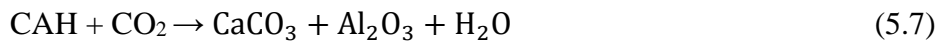


**Figure 5.6:** Conceptual model of a carbonation process considered to occur in calcium hydroxide treated kaolin clay (kaolin clay: grey particles; calcium hydroxide  $[\text{Ca}(\text{OH})_2]$ : black circle; calcium silicate hydrate (CSH) plus calcium aluminate hydrate (CAH): orange particles; calcium carbonate ( $\text{CaCO}_3$ ): green particles).

The  $\text{Ca}(\text{OH})_2$  dissolves in water in the voids and releases  $\text{Ca}^{2+}$  and  $\text{OH}^-$  ions. Also, CAH and CSH gels (the products of pozzolanic reaction) in voids releases  $\text{Ca}^{2+}$ ,  $\text{SiO}_2$ ,  $\text{Al}_2\text{O}_3$  and  $\text{OH}^-$  ions. The  $\text{Ca}^{2+}$  ions (from  $\text{Ca}(\text{OH})_2$ , CAH and CSH) and  $\text{CO}_3^{2-}$  ions (from  $\text{CO}_2$ ) chemically react to form  $\text{CaCO}_3$  nuclei, which crystallise further to produce  $\text{CaCO}_3$  on the surface of the clay particles. The carbonation of  $\text{Ca}(\text{OH})_2$  is chemically represented by Equation 4.4 (previously presented), whilst the carbonation of CSH and CAH gels are chemically represented by Equations 5.6 and 5.7 respectively.





where C represents CaO, S represents SiO<sub>2</sub>, A represents Al<sub>2</sub>O<sub>3</sub>, H represents H<sub>2</sub>O.

Considering that in the current study treated kaolin was cured for 7 days prior to carbonation, CSH and CAH gels may not occur (Vitale *et al.*, 2017). Equations 5.7 and 5.8 may not occur in the current study.

In general, air void control influences the degree of carbonation of treated kaolin, in particular by changing the permeability of the compacted material to fluid flow, which in turn influences the availability of CO<sub>2</sub> to the reactive site.

The results from XRCT analysis demonstrates that there is more CaCO<sub>3</sub> detected in larger void volumes than that observed at the lowest voids volume in treated kaolin clay (Section 4.4.3). 2-D reconstructions of XRCT scanned samples are given in Figures 5.7, showing CaCO<sub>3</sub> content at different air voids content of 3% and 10% for a 8% Ca(OH)<sub>2</sub> treated sample. There are more CaCO<sub>3</sub> deposits (shown as white patches as inferred using scanning electron microscopy) in samples at high air voids content of 10 % than in samples at low air voids content of 3%. This supports the observation made in Section 5.5.3 that control of air voids content influences the carbonation reaction.

This result also supports the conceptual model in which porous and permeable treated kaolin favours carbonation reaction.

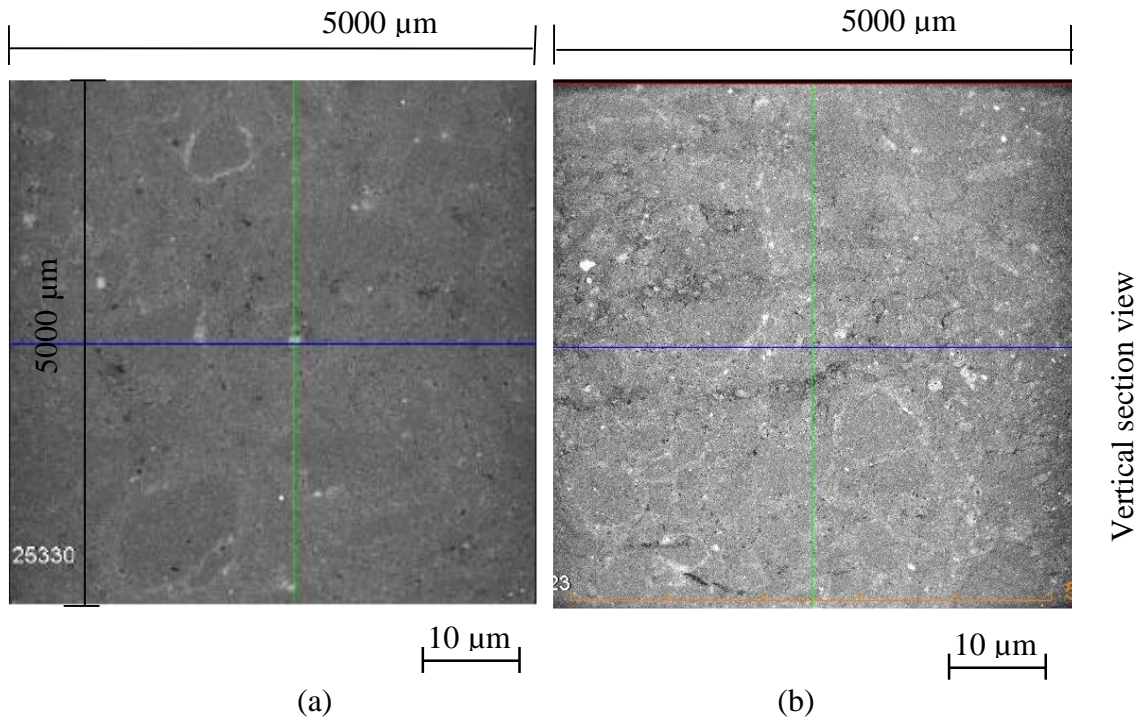


**Figure 5.7:** Typical reconstructed 2-d calcium carbonate formation as a function of air voids content detected using XRCT analysis for carbonated 8% calcium hydroxide treated kaolin (a) 3% air voids content (b) 10% air voids content. Note: white patches represents calcium carbonate grains as suggested by scanning electron microscopy (Section 4.4.7).

### 5.11 Implication for Carbon Capture

Lime is used for a range of purposes for which it is uniquely suitable. The study addresses the carbon capture function that operates alongside the primary purpose that justifies its manufacture.

There are earlier works in the area of carbon capture and storage in soil stabilisation by carbonation of materials rich in magnesium cations (Yi *et al.*, 2013, 2016). The control of air voids content in  $\text{Ca}(\text{OH})_2$  treated clay promotes carbonation of calcium and offers potential for carbon capture in clay soil. Treated kaolin in the current study suggests, from volumetric and mass balance data, that approximately 5 %-10 % of  $\text{CaCO}_3$  has been produced, fixing carbon. This has been achieved as a result of carbonation of 4%-8%  $\text{Ca}(\text{OH})_2$  content in kaolin clay (section 4.2.2).

Lime is manufactured from natural deposits of limestone, which mostly is  $\text{CaCO}_3$ . As mentioned in Chapter 2, the production of lime involves three main stages: limestone preparation, calcination, and hydration. The preparation stage involves quarrying, transportation, and crushing of limestone ( $\text{CaCO}_3$ ). At the calcination stage, high temperatures

are supplied in the kilns, which roast the limestone and trigger chemical reaction to produce CaO and CO<sub>2</sub> (previously presented in Equation 2.5). Lime is produced as quick lime (CaO) or as Ca(OH)<sub>2</sub> by the hydration of quick lime (previously presented in Equation 2.6).

CO<sub>2</sub> is generated mainly during the calcination stage (Ecofys, 2009). Based on CO<sub>2</sub> emission from calcination stage (Equation 2.5), it can be estimated that the global CO<sub>2</sub> emissions from lime production (for all purposes) of 350 Mty<sup>-1</sup> (USGS, 2016) is approximately 275 Mt CO<sub>2</sub> y<sup>-1</sup>. This represents 0.6% of the total amount of global CO<sub>2</sub> emissions. This estimate is compared with the contribution to world's CO<sub>2</sub> emissions from CaO in cement production which is 4% calcination emissions (this does not include fuel combustion emission which is 4%) (Olivier, 2016). The detailed calculation is contained in Appendix D. In view of current concerns about climate change due to increasing atmospheric CO<sub>2</sub> concentrations, the use of Ca(OH)<sub>2</sub> stabilised soil for both engineering and carbon capture functions needs to be considered. To determine whether the use of lime to improve the strength of soil, can re-captured some or all of the CO<sub>2</sub> produced in the manufacture of the lime.

The design manual for roads and bridges (The Highways Agency, 2007) recommends a capping layer at locations where weak cohesive soil (with CBR of less than 15%) is encountered as a subgrade of highway pavement. The capping layer is required between subgrade and sub-base to provide a suitably firm working platform for placement and compaction of sub-base. The capping layer acts as a structural layer in the long term and reduces the thickness of sub-base which otherwise would be required (Sherwood, 1992).

The cost for construction of granular capping layer if granular material is to be imported include the costs of excavating, processing and hauling of the material to the site. There is an added cost of removal and disposal of the in-situ soil (to make space for granular capping material). On the other hand, if in-situ stabilised cohesive material is used, the cost incurred is that of stabiliser (lime or cement), the cost of processing and the cost of any increase in supervision or testing resulting from the use of stabilised soil. Lime stabilised cohesive soil for the capping layer is used when it is a cheaper alternative to the use of granular material or if environmental benefits are considered. This reduces the demand for quarrying natural resources, which would otherwise be required (MCHW 1, 2009; The Highways Agency, 2007; Sherwood, 1992).

Lime stabilisations have been widely used in capping layers construction of highway projects in the UK. Some road projects which used lime stabilised capping layers in the UK are

presented in Table 5.4. Nine out of the projects performed satisfactorily, whilst there were problems in three (Sherwood, 1992). Experience and knowledge gained from the few cases where problems arose were attended to and advice provided in design manual for roads and bridges (The Highways Agency, 2007). Heave problems occurred at some projects which include M40 Banbury IV, Huntingdon Bypass, and the Saxmundham Bypass (Table 5.4). Heave problems in the M40 road occurred in 1989/90 and were reported by Snedker (1996), who attributed the problem to sulphate contents and too high air voids. It has been found from the observations of problems with sulphate and lime stabilisation that too high air voids and sulphate content can promote the formation of ettringite or thaumasite, leading to heave problems (Sherwood, 1993).

Considering that high air voids content is required for the carbonation of lime treated soil, lime treatment of soil for carbonation should be handled with caution when dealing with sulphate bearing soils.

The combined modification and carbonation technique can immediately be applied for soils that are dominated by kaolinite or non-swelling clay, and which do not contain high sulphate content (maximum total sulphate content of 1%). With reference to previous projects with stabilised capping layers in the UK (Table 5.4), the proposed technique of combined modification and carbonation can be applied to Estuarine clay. The reason for this is that, Estuarine clay soils developed in England and Wales are predominantly made up of kaolin and mica, which are non-expansive soil minerals (Loveland, 1984). Additionally the clays do not contain high sulphate content.

**Table 5.4:** Projects with stabilised capping layers (after Sherwood, 1992) (continues overleaf).

Project	Date	Approximate area or length	Thickness (mm)	Lime stabiliser content <sup>a</sup> (%)	Predominate soil type	Mineralogy	Conditions for heave problem due to ettringite/thaumasite formation
A45 Northants	1981	2500m <sup>2</sup>	300	$> 2\frac{1}{2}^b$	Estuarine clay	kaolinite and mica, (Loveland, 1984)	NA
Brackmills Industrial Estate Northants	1982	10000m <sup>2</sup>	350	3	Alluvial clay	kaolinite, illite smectite (Nzeukou <i>et al.</i> , 2013)	NA
M4 widening Heathrow Spur-M25	1984	21000m <sup>2</sup>	300	3	Brickearth	Quartz, K-feldspar, albite, mica (illite), kaolinite and smectite (Milodowski <i>et al.</i> , 2015)	NA
Saxmundham Bypass	1986	1km length	330	$2\frac{1}{2}$	Boulder clay	Fe oxides smectite chlorite kaolinite illite (Phillips <i>et al.</i> , 2011)	Too high air voids leading to increased moisture content, and sulphate content
Business Park Basingstoke	1987	10000 m <sup>2</sup>	350	$2\frac{1}{2}$	London clay	Illite, disordered kaolinite, smectite, minor quartz, and feldspar (Rogers <i>et al.</i> , 1997)	NA
A33 Dualling Basingstoke	1987	10000 m <sup>2</sup>	350	$2\frac{1}{2}$	London clay	Illite, disordered kaolinite, smectite, minor quartz, and feldspar (Rogers <i>et al.</i> , 1997)	NA

<sup>a</sup>Specified amounts, lime contents as available free lime. All lime projects were quicklime except where otherwise stated. <sup>b</sup>Half the area stabilised with quicklime, half stabilised with hydrated lime. <sup>c</sup>Laid in 200 mm layers. NA represents not applicable.

Project	Date	Approximate area or length	Thickness (mm)	Lime stabiliser content <sup>a</sup> (%)	Predominate soil type	Mineralogy	Conditions for heave problem due to ettringite/thaumasite formation
Leamington Spa Southern Relief Road	1987	12000 m <sup>2</sup>	350	4	Keuper Marl	Illite, dolomite and quartz; minor gypsum and feldspar (Rogers <i>et al.</i> , 1997)	NA
Stansted Access Road	1987	65000 m <sup>2</sup>	300	3	Boulder clay	Fe oxides smectite chlorite kaolinite illite (Phillips <i>et al.</i> , 2011)	NA
Huntingdon Bypass	1987	51000m <sup>2</sup>	250	2 $\frac{1}{2}$	Boulder clay	Fe oxides smectite chlorite kaolinite illite (Phillips <i>et al.</i> , 2011)	Too high air voids leading to increased moisture content from 20%-40%, and sulphate content
M40 Warwick North	1988/89	233000 m <sup>2</sup>	250	4	Keuper Marl	Illite, dolomite and quartz; minor gypsum and feldspar (Rogers <i>et al.</i> , 1997).	NA
M40 Gaydon	1989	73000 m <sup>2</sup>	400 <sup>c</sup>	3	Keuper Marl/Glacial Till	Illite, dolomite and quartz; minor gypsum and feldspar (Rogers <i>et al.</i> , 1997)	NA
M40 Banbury IV	1989	200000 m <sup>2</sup>	250	3	Lower Lias	Disordered kaolinite, illite and quartz; minor calcite and gypsum (Rogers <i>et al.</i> , 1997)	Too high air voids leading to increased moisture content, sulphate content of 0.37%

<sup>a</sup>Specified amounts, lime contents as available free lime. All lime projects were quicklime except where otherwise stated. <sup>b</sup>Half the area stabilised with quicklime, half stabilised with hydrated lime. <sup>c</sup>Laid in 200 mm layers. NA represents not applicable.

The current study suggests that a controlled air voids content of lime stabilised soil in road pavement capping may capture  $\text{CaCO}_3$  as carbon. The production of lime produces  $\text{CO}_2$ , therefore this can be off-set by design to maximise carbon capture.

It is interesting to speculate the carbon capture potential in stabilised soil for pavement capping, if they were designed for that purpose. For a single carriage way of 7m cross-sectional width (approximately standard 4 m lane width in each of two road directions) according to DMRB 6.1.2 (TD 27, 2005),  $3 \times 10^{-1}$  m depth of stabilised capping, based on the standard pavement dimensions according to DMRB 4.1.6 (The Highways Agency, 2007), and 1000 m length, the amount of adsorbed  $\text{CO}_2$  has been estimated. By the current study calculation, 53 kg-110 kg  $\text{CO}_2$  per km may be captured as  $\text{CaCO}_3$  for 4%-8%  $\text{Ca}(\text{OH})_2$  (by dry mass) additions to kaolin clay (Table 5.5).

A design of lime stabilisation can off-set  $\text{CO}_2$  produced by lime production. EuLA (2014) estimated approximately 0.751 tonne  $\text{CO}_2$  emission per 1 tonne of lime production based on calcination emissions. The global annual lime production is estimated at approximately 350 million tonnes (USGS, 2016). This would result in annual carbon emission from lime production of approximately 275 Mt per year. EuLA (2014) estimated 18 % of total lime production for the construction sector based on lime functionality. Lime is used by four main areas of construction, which includes lime used as a stabiliser for soil modification and stabilisation, as a binder for production of sand-lime bricks, fire resistance board and concrete. Lime is also used as a component of mortar and plasters, and as an anti-stripping agent in production of asphalt and tarmac for road construction (BLA, 2015). Considering 25 % of the construction lime for soil modification and stabilisation, by the current study calculation, 106 kt  $\text{CO}_2$ -113 kt  $\text{CO}_2$  may be captured for the addition of 4%-8%  $\text{Ca}(\text{OH})_2$  by dry mass to kaolin clay (Table 5.5). These figures can be extrapolated to the global carbon capture scale, under the assumption that 4.5 % of global lime is used for soil modification and stabilisation as estimated in the current study. Using a combined modification and carbonation technique proposed in the current study, a global carbon capture potential of approximately 19-20 Mt $\text{CO}_2$  may be speculated for 4%-8%  $\text{Ca}(\text{OH})_2$  by dry mass, which is equivalent to 93% of the  $\text{CO}_2$  emissions associated with lime production for stabilisation (Table 5.5). This carbon capture potential represent 0.03% of the total global carbon emissions. The current study suggests that lime treated soil may recover 93% of the  $\text{CO}_2$  emissions associated with lime production for stabilisation (representing 0.03% global

CO<sub>2</sub> emissions), whilst providing additional engineering functions of ground stability improvement.

**Table 5.5:** Carbon capture potential in treated kaolin using combined modification and carbonation technique based on the UK and Global lime production data (continues overleaf).

Description UK figures	Quantity of lime content (%)	Value	Notes
Carbon capture potential in road pavement (7.3m width, 0.3m depth and 1000m length)	4% Ca(OH) <sub>2</sub> 6% Ca(OH) <sub>2</sub> 8% Ca(OH) <sub>2</sub>	53kg CO <sub>2</sub> per km 83 kg CO <sub>2</sub> per km 110 kg CO <sub>2</sub> per km	Based on carbonation of Ca(OH) <sub>2</sub> derived from calcimeter analysis
UK annual high calcium lime production (quicklime, hydrated or slaked lime) and dolomitic lime.		Approximately 2 Mty <sup>-1</sup>	British Lime Association (Assessed March 30, 2016)- 2015 figures
Lime for construction		<sup>a</sup> 360 kty <sup>-1</sup>	Assume 18 % (EuLA, 2014)
Lime for soil modification/stabilisation		<sup>b</sup> 90 kty <sup>-1</sup>	25% of construction lime (4.5% of total lime), based on four areas of construction lime (BLA, 2015)
UK lime carbon capture potential	4% Ca(OH) <sub>2</sub> 6% Ca(OH) <sub>2</sub> 8% Ca(OH) <sub>2</sub>	106 kt CO <sub>2</sub> 112 kt CO <sub>2</sub> 113 kt CO <sub>2</sub>	Based on carbonation of lime for stabilisation
Global figures			
Global lime production		350 Mt y <sup>-1</sup>	USGS (2016)- 2015 figures
Global lime for construction		<sup>a</sup> 63 Mt y <sup>-1</sup>	18% of total lime EuLA (2014)

Note Mty<sup>-1</sup> represents million tonnes per year, kty<sup>-1</sup> represents kilo tonne per year

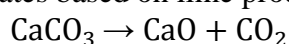
<sup>a</sup>Estimates based on 18% lime for construction function (EuLA, 2014)

<sup>b</sup>Estimates based on one-fourth out of four main uses of construction lime (BLA, 2015)

Description	Quantity of lime content (%)	Quantity	Notes
Global lime for soil modification and stabilisation		16 Mt y <sup>-1</sup>	25% of constructions lime (4.5% of total lime), based on four areas of construction lime
Emission from global lime production		<sup>c</sup> 275 Mt y <sup>-1</sup>	Based on stoichiometry in Equation 2.5
Lime production contribution to the world's CO <sub>2</sub> emissions		0.6%	Based on world's atmospheric CO <sub>2</sub> emissions from calcium oxide in cement production (Appendix D)
Global maximum carbon capture potential	4% Ca(OH) <sub>2</sub> 6% Ca(OH) <sub>2</sub> 8% Ca(OH) <sub>2</sub>	19 MtCO <sub>2</sub> 20 MtCO <sub>2</sub> 20 MtCO <sub>2</sub>	Based on carbonation of lime for stabilisation
Carbon capture potential for global emission from lime production for stabilisation.	4% Ca(OH) <sub>2</sub> 6% Ca(OH) <sub>2</sub> 8% Ca(OH) <sub>2</sub>	90% CO <sub>2</sub> 93% CO <sub>2</sub> 93% CO <sub>2</sub>	Carbon capture potential based on degree of carbonation of Ca(OH) <sub>2</sub> for stabilisation in the current study.
Carbon capture potential representing the world's CO <sub>2</sub> emissions	4% Ca(OH) <sub>2</sub> 6% Ca(OH) <sub>2</sub> 8% Ca(OH) <sub>2</sub>	0.03% CO <sub>2</sub> 0.03% CO <sub>2</sub> 0.03% CO <sub>2</sub>	Carbon capture potential relatively to 0.6% of the world's CO <sub>2</sub> emissions from lime production.

Note Mty<sup>-1</sup> represents million tonnes per year, kty<sup>-1</sup> represents kilo tonne per year

<sup>c</sup>Estimates based on lime production CO<sub>2</sub> emission from stoichiometry in Equation 2.5:



## 5.12 Design Specifications

One of the aims of this project was to develop a specification for the design of stabilised soil for combined carbon capture and engineering functions. Works on soil stabilisation to date have focused on strength improvement for engineering function, and not yet for combined engineering and carbon capturing functions. As such a design specification that combined carbon capture and engineering functions is not yet available. Therefore the design specification for these functions in capping layer construction is suggested here.

However some specifications for lime-stabilisation (The Highways Agency, 2007; MWCH 1, 2009: Series 600) are appropriate for preliminary material requirements for the combined functions, but not completely appropriate for soil stabilisation that combines carbon capture and engineering functions.

Clause 615 of the Specification for Highway Works (MCHW 1, 2009; Series 600) and Section 3.78 of Design Manual for roads and bridges (The Highways Agency, 2007), which refers to lime stabilisation for capping materials, require that compaction of lime treated soil should be performed to a maximum air voids of 5% or MDD. This recommendation did not include carbonated lime treated soil. The air voids limit specifically acknowledged that very high air voids of lime treated cohesive soil would be susceptible to swell and loss of strength on water ingress. Based on the results of the current study, a carbonated treated kaolin compacted to 10% air voids produced the best combined results for strength improvement and carbonate capture. This was likely due to the formation of  $\text{CaCO}_3$  grains on the surface of the clay, and hence the reduction in the voids spaces (Section 5.5.4).

Unfortunately, low air voids (such as obtained at MDD) would not be able to capture as large amounts of  $\text{CaCO}_3$  as high air voids (Section 5.5.3). If combined modification and carbonation is to be adopted in practice, then an addendum needs to be included in the specification for lime-stabilisation (such as the Highways Agency, 2007; MWCH 1, 2009: Series 600) for engineering purposes. The current study suggests the addendum to include a maximum of 10% air voids for the compaction of lime treated clay such as kaolin, for a combined carbon capture and strength improvement MCHW 1, (2009) and DMRB (The Highways Agency, 2007).

Considering that high air voids content is required for lime treated soil for optimum combined carbon capture and strength improvement, lime treatment of soil should be handled with

caution when dealing with sulphate bearing soils. The air voids content for the optimum carbonation reaction should be sought based on combined results of peak strength improvement and carbonate content.

Additionally, combined modification and carbonation techniques need to be applied with caution to soil containing high organic matter (above 2%) in agreement with Sherwood, (1993) and The Highways Agency (2007). This is to avoid issues associated with lime stabilisation of soil containing high organic matter, caused by its high water holding capacity (Chen and Wang, 2006).

The conclusions drawn from this laboratory study are limited to lime treatment of kaolin clay; they certainly suggest a need for addition of an addendum to the design specification of lime stabilisation for engineering purposes, if combined modification and carbonation is to be adopted in practice. The air voids content requirement for combined modification and carbonation treatment need to be included for combined carbon capture and strength improvement. Therefore, the following specifications for lime-stabilised material for combined carbon capture and ground stability improvement purposes are suggested as follows:

1. Materials for use in soil stabilisation for combined carbon capture and engineering purpose should meet specifications for lime-stabilised materials (The Highways Agency, 2007; MWCH 1, 2009: Series 600), such as any cohesive material (7E) apart from unburnt colliery spoil. Suitable soils should have a minimum PI > 10%, maximum organic content of < 2% and maximum total sulphate content of  $\leq 1\%$ . The grain sizes of the soil when sieved should have 100% by mass passing a BS 75 mm, and at least 15% by mass passing a 63  $\mu\text{m}$  sieve.
2. The lime for use in treated kaolin should either be CaO or Ca(OH)<sub>2</sub> in accordance with BS EN 459-1 (BSI, 2015). The CaO should have a grading of 100% passing a BS 10 mm, and at least 95% by mass passing a BS 5 mm test sieve. The Ca(OH)<sub>2</sub> should comply with BS EN 459-1 (BSI, 2015). Ca(OH)<sub>2</sub> is CaO with sufficient water added to hydrate it.
3. The OLC requirement for achieving peak strength in carbonated lime treated soil should be determined based on the peak strength of carbonated treated soil. In the current study, the OLC of 6% Ca(OH)<sub>2</sub> (4.5% CaO equivalent) by dry mass was achieved. The CaO content is equivalent to the ICL plus 1.5% CaO by dry mass.

4. The air voids content for combined modification and carbonation treatment should be sought based on combined strength and carbonation development, which in the current study, 10 % air voids content was achieved.
5. A control of air voids content of treated kaolin would produce desired carbonation, and hence the optimum combined carbon capture and strength improvement. Air voids control on the site would be achieved by compaction on the dry side of OMC, because compaction at dry side of OMC produces high air voids that are filled with air as opposed to water, which occurs on the wet side.
6. Considering that high air voids is required to achieve the optimum combined carbon capture and strength improvement of lime treated soil, lime treatment of sulphate bearing soils should be handled with caution.
7. The compaction of each capping layer using lime treated class 7E material should be based on most efficient compaction plant for Method 7 in Table 6/4 after a field trial, in accordance with Clause 612, of Specification for Highway Works (MCHW 1, 2009; Series 600). The layers should be compacted to a maximum thickness of 250 mm, and minimum thickness of 130 mm.
8. The construction of capping using carbonated lime treated class 7E material such as kaolin should be conducted only from the months of March- September in accordance with The Highways Agency (2007) and MWCH 1 (2009). The reason for this is to avoid the likely frost attack during construction of the carbonated treated material.

### 5.13 Chapter Summary

Treated kaolin under controlled air voids content has been shown to recover part of CO<sub>2</sub> emissions associated with lime production alongside strength improvement for engineering functions. A design specification for lime-stabilised material for combined carbon capture and engineering purposes has been suggested. The following is the summary:

- The minimum amount of lime added to kaolin for combined modification and carbonation treatment was based on the results of the Modified ICL Test according to the definition presented by Rogers *et al.* (1997). The ICL value for kaolin clay in the current study is 4% Ca(OH)<sub>2</sub> (3% CaO equivalent) by dry mass.
- The air voids content for combined modification and carbonation treatment should be sought based on combined strength and carbonation development, which in the current study, 10 % air voids content was achieved.
- Treated kaolin which is compacted to air voids content from 3% to 15% could achieve a permeability values of  $1.8 \times 10^{-9}$  m/s to  $7.4 \times 10^{-9}$  m/s for carbonation purposes.
- Carbonation of treated kaolin resulted in a growth of CaCO<sub>3</sub> grains on the surface of the clay particles and probably into void spaces. Due to the growth, carbonated treated kaolin (whilst maintaining constant air voids content) would contain less air voids content than the corresponding non-carbonated treated kaolin.
- The treated kaolin made up of 6% Ca(OH)<sub>2</sub> (4.5% CaO equivalent) with 10% air voids combination achieved the highest strength improvement factor (2.6 factor). The strength improvement factor of carbonation is derived as the multiplier of the strength of carbonated treated specimen compared to the corresponding non-carbonated untreated specimen.
- The peak UCS (280 kPa) in carbonated treated kaolin in the current study was achieved at 6% Ca(OH)<sub>2</sub>, and 10% air void combination.
- Based on 7 days cured specimen prior to carbonation and UCS testing, the compressive strength of saturated carbonated treated kaolin in the current study is much reduced compared to the compressive strength of some non-saturated treated kaolin from the literature. The highest compressive strength of 280 kPa in the current study is much reduced compared to the highest compressive strength of approximately 830 kPa in Bell (1996). The reason for the differences could be that most researchers including Bell (1996) do not look at saturated strengths, however the current study looked at saturated compressive strengths for carbonated treated kaolin, and non-carbonated treated kaolin. Also, it may be that strengths later than 7 days are more

critical as the lime gets used up in carbonation reactions rather than being available for pozzolanic reactions.

- The peak UCS of 280 kPa in the current study is equivalent of 29% CBR when the strength is expressed in terms of CBR. The CBR of carbonated treated kaolin in the current study is greater than the CBR value of 15% which is the minimum CBR value required for stabilised capping layer (Sherwood, 1993). Based on strength requirements, the carbonated treated kaolin is suitable for use as a stabilised capping layer.
- Carbonated treated kaolin in the current study has shown that there is an increase in FT resistance by 24% (from 0%-24%) in carbonated treated kaolin at OLC compared with equivalent untreated specimen after 3 FT cycles.
- The FT resistance for carbonated treated kaolin in the current study was found to be approximately 24%. This FT resistance value is much lower than that achieved in non-carbonated treated kaolin from literature. A FT resistance of 100% for non-carbonated treated kaolin was found in Hotineanu *et al.*, (2015). The reason for the difference could be that the current study used non-wrapped specimen during the FT testing, whilst Hotineanu *et al.*, (2015) used wrapped specimen during the FT testing. Also, in the current study non-wrapped specimens were placed upon soaked felt pads underlain by free water, to allow the specimen absorb water by capillary during thawing phase in accordance with D560-03 (ASTM, 1989), whilst in Hotineanu *et al.*, (2015) the specimen was prevented from inflow nor outflow of water in accordance with the ‘closed system’ FT approach used. Additionally, the reason for difference in resistance to FT between the study by Hotineanu *et al.*, (2015) and the current study may be because there was no carbonation in Hotineanu *et al.*, (2015).
- Based on less stringent durability requirements for the capping layer (Sherwood, 1993), the FT resistance of up to 24% in carbonated treated kaolin in the current study is suggested to be suitable for the carbonated treated kaolin for use as capping layer
- The results obtained using XRCT indicate the formation of  $\text{CaCO}_3$  grains distributed throughout the sample. This implies that XRCT could be used for identification of the texture of  $\text{CaCO}_3$  within the stabilised soil
- Air void control influences the DOC of treated kaolin, in particular by changing the permeability of the compacted material to fluid flow, which in turn influences the availability of  $\text{CO}_2$  to the reactive site.

- Considering that high air voids content is required for the carbonation of lime treated soil, lime treatment of soil for carbonation should be handled with caution when dealing with sulphate bearing soils.
- The combined modification and carbonation technique can immediately be applied for soils that are dominated by kaolinite or non-swelling clay, and which do not contain high sulphate content (maximum total sulphate content of 1%).

With reference to previous projects with stabilised capping layers in the UK, the proposed technique of combined modification and carbonation can be applied to Estuarine clay. The reason for this is that, Estuarine clay soils developed in England and Wales are predominantly made up of kaolin and mica, which are non-expansive soil minerals (Loveland, 1984). Additionally the clays do not contain high sulphate content.

- The current study suggests that lime treated soil may recover part of the CO<sub>2</sub> emissions associated with lime production, whilst providing additional engineering functions. A global carbon capture potential of approximately 19-20 MtCO<sub>2</sub> may be speculated for 4%-8% Ca(OH)<sub>2</sub> by dry mass, which is equivalent to 93% of the CO<sub>2</sub> emissions associated with lime production for stabilisation (representing 0.03% global CO<sub>2</sub> emissions), whilst providing additional ground stability improvement engineering functions.

## Chapter 6 – Conclusions and Recommendations

### 6.1 Conclusions

This thesis explores the links between ground modification and carbonation as a coupled process, and has defined that from experiments involving kaolin treated with lime (particularly  $\text{Ca}(\text{OH})_2$ ). This was aimed to determine if a combination of modification and carbonation of clay soils could be useful to both treat soft clay soils and reduce atmospheric  $\text{CO}_2$  and in so doing use  $\text{CO}_2$  reduction to off-set some of the  $\text{CO}_2$  generated by the production of lime for stabilisation. Previous work by Silva *et al.* (2006) noted that carbonation of lime is decreased when density of compacted lime is increased, thereby decreased air voids. In order to promote carbonation in treated soils, increased air voids were created by varying compaction. This work tried to identify the minimum air voids content required to promote carbonation whilst also generating sufficient increase in strength and stiffness for applications in capping improvement. The following are the key conclusions that arose from this research:

Lime treated kaolin clay has shown the potential to be used to capture atmospheric  $\text{CO}_2$  alongside improving the stability of weak ground. Using a combination of 6%  $\text{Ca}(\text{OH})_2$  with 10% air voids, treated kaolin has the potential to capture carbon by the precipitation of up to  $7.46 \pm 0.01\%$   $\text{CaCO}_3$  through combined modification and carbonation processes.

The compressive strength, based on 7 days cured specimens, has shown that carbonation of treated kaolin results in compressive strength development. A carbonated kaolin specimen with a combination of 6%  $\text{Ca}(\text{OH})_2$  with 10% air voids resulted in 60% increase in strength (from 170 kPa to 280 kPa) when compared to corresponding non-carbonated lime treated kaolin specimen. This strength is equivalent to CBR value of 29%. It is observed that the CBR value of carbonated treated kaolin in the current study is greater than the value of 15% which is the minimum CBR required for a stabilised capping layer (The Highways Agency, 2007; MWCH 1, 2009: Series 600). Based on strength requirements, the carbonated treated kaolin could be suitable for use as a stabilised capping layer. The strength and stiffness increases in carbonated lime treated specimens are much reduced compared to what might be predicted from the literature for non-carbonated equivalents. However, the increases are sufficient for application to capping layers.

Additionally, when durability is considered, the FT resistance increased by approximately 24% (from 0 to 24%) for carbonated treated kaolin compared with that at corresponding non-carbonated treated kaolin in the combination of 6%  $\text{Ca}(\text{OH})_2$  with 10% air voids, which underwent 7 days curing prior to testing. The FT resistance durability test employed is important to determine the ability to resist detrimental weather conditions. The FT resistance for carbonated treated kaolin was found to be approximately 24%. The British Specification requires a minimum of 80% durability of stabilised material for its use as a sub-base or base material for road pavement. However, the durability requirement for lime-stabilised capping layer is less stringent (Sherwood, 1993). The FT resistance durability in carbonated treated kaolin is low (24%) compared to that required for sub-base and base material. However, this FT resistance is suggested to be sufficient for capping layer when viewed in the context of the less stringent requirements for FT durability for capping material.

The amount of  $\text{CaCO}_3$  in the carbonated treated kaolin could be determined using XRCT, with good agreement with the chemical methods (such as calcimeter, TGA). A t-test was employed to determine the similarity between XRCT and the chemical methods and showed no significant difference between the results from calcimeter and XRCT at  $p = 0.56$ , TGA and XRCT at  $p = 0.37$ , and TGA and calcimeter at  $p = 0.10$ . This validates the XRCT method. XRCT has the additional benefit that it shows the distribution of both air voids and  $\text{CaCO}_3$  through the sample.

Permeability testing employed in the current study has shown that treated kaolin compacted to air voids content from 3% to 15% could achieve permeability values of  $1.8 \times 10^{-9}$  m/s to  $7.4 \times 10^{-9}$  m/s. This is important for the transportation of moisture and dissolved gases such as  $\text{CO}_2$  into the voids of the material for carbonation purposes.

This combined modification and carbonation technique has shown the potential to offset up to 93% of the  $\text{CO}_2$  released from lime production for stabilisation (representing 0.03% global  $\text{CO}_2$  emissions), alongside the compressive strength improvement of up to 280 kPa (equivalent to CBR value of 29%). It is suggested that carbonated treated kaolin could be used as a stabilised capping layer in road pavement. Ultimately, if combined modification and carbonation is applied to lime treated clay it has the potential to mitigate climate change alongside ground improvement of soft clay.

If combined modification and carbonation is to be adopted in practice, then an addendum needs to be included in the specification for lime-stabilisation (such as the Highways Agency,

2007; MWCH 1, 2009: Series 600) for engineering purposes. The air voids content for combined modification and carbonation treatment is recommended to be sought based on peak strength of carbonated treated specimen. The current study suggests a maximum air voids content of 10 % for carbonated treated kaolin.

The lime content requirement for peak strength for combined modification and carbonation treatment is recommended to be sought based on the peak strength in carbonated treated clay. It is shown in the current study that 6%  $\text{Ca}(\text{OH})_2$  (4.5% CaO equivalent) content by dry mass could result in the peak compressive strength in carbonated treated kaolin.

## **6.2 Recommendations for Future Work**

In this section, comments on limitations and recommendations for research future work are presented for areas covered in this thesis

### ***6.2.1 Improve Carbon Capture and Modification Process***

The current study applied manual thresholding using ImageJ software in the image analysis process for  $\text{CaCO}_3$  detection. This is time consuming and is identified as a limitation of the analytical process in the current study. It is suggested that future studies be performed in an automatic manner using the thresholding process. An automated analysis would produce a much faster detection of the  $\text{CaCO}_3$  and would be relatively simple to apply. This would represent an important improvement of the analytical process.

### ***6.2.2 Investigate and Discover More Cost Effective Stabilisers***

A considerable next step based on the findings of this work is considered to be the application of this technique (combined modification and carbonation) to lime-based waste treated clay. The presented work in this thesis showed that lime has proved to be very effective for the application of combined modification and carbonation technique in treated kaolin clays. However, there is need to investigate and discover more stabilisers that are less expensive than pure lime. The stabilisers include lime-based waste such as PFA, WSA, GGBS, SS, LFS etc. By so doing, lime-based waste could be used for combined modification and carbonation in clay to achieve carbon capture alongside ground stability improvement on a large scale but with a minimal cost.

Additionally, the current major downside of lime modification of soils is CO<sub>2</sub> emissions from lime production used for the modification. This study of combined modification and carbonation have shown to off-set 93% in this way. In order to have a net positive impact on carbon capture then one way to do this would be to replace the lime with a waste product. To achieve this, future work would need to replace lime with lime-based waste (such as PFA, GGBS, SS, LFS) in the combined modification and carbonation of clay.

### ***6.2.3 Investigate Carbon Capture and Modification in Lime Treatment using more Clays.***

Although the combined carbon capture and engineering performance of the carbonated treated kaolin at combination of 6% Ca(OH)<sub>2</sub> and 10% air voids has proven to be successful in the laboratory in treated kaolin, it would be useful to carry out further studies on combined modification and carbonation studies involving swelling clays such as bentonite.

In addition to the geotechnical laboratory tests already conducted on the carbonated treated kaolin, another recommended engineering performance test which this specimen need to be subjected to is the full Atterberg Limits test. This would allow full examination of plasticity changes in the physical particles due to carbonation of lime treated clays. Furthermore, field trials are recommended to test out compaction techniques and to study the rate and depth of carbonation under field conditions.

## References

- Aldaood, A., Bouasker, M. and Al-Mukhtar, M. (2014) Impact of freeze–thaw cycles on mechanical behaviour of lime stabilized gypseous soils. *Cold Regions Science and Technology*, 99, pp.38-45.
- Allen, M. R., Frame, D. J., Huntingford, C., Jones, C. D., Lowe, J. A., Meinshausen, M. and Meinshausen, N. (2009) Warming caused by cumulative carbon emissions towards the trillionth tonne. *Nature*, 458(7242), pp.1163-1166.
- Al-Mukhtar, M., Khattab, S. and Alcover, J. F. (2012) Microstructure and geotechnical properties of lime-treated expansive clayey soil. *Engineering Geology*, 139, pp.17-27.
- Al-Mukhtar, M., Lasledj, A. and Alcover, J. F. (2010) Behaviour and mineralogy changes in lime-treated expansive soil at 20 °C. *Applied Clay Science*, 50(2), pp.191-198.
- Al-Tabbaa, A. and Wood, D.M. (1987) Some measurements of the permeability of kaolin. *Geotechnique*, 37(4), pp.499-514.
- Arnell, N. W. and Gosling, S. N. (2016) The impacts of climate change on river flood risk at the global scale. *Climatic Change*, 134(3), pp.387-401.
- Arrhenius, S. (1896) XXXI. On the influence of carbonic acid in the air upon the temperature of the ground. *The London, Edinburgh, and Dublin Philosophical Magazine and Journal of Science*, 41(251), pp.237-276.
- ASTM (1989) D560-03: Standard test methods for freezing and thawing compacted soil cement mixtures. American Society for Testing and Materials, West Conshohocken, Pennsylvania, USA.
- ASTM (1992) E1441: Standard guide for computed tomography (CT) Imaging. American Society for Testing and Materials, Philadelphia, PA.
- ASTM (1999) D6276-99a. Standard Test Method for using pH to Estimate the Soil–lime Proportion Requirement for Soil Stabilization, American Society for Testing and Materials, West Conshohocken, Pennsylvania, USA.

ASTM (2011) D2487-11: Standard Practice for Classification of Soils for Engineering Purposes (Unified Soil Classification System), ASTM International, West Conshohocken, PA.

ASTM (2012) C618-12a: Standard Specification for Coal Fly Ash and Raw or Calcined Natural Pozzolan for Use in Concrete. Developed by Subcommittee C09.24. Annual Book of American Society for Testing and Materials (ASTM) Standards. 4.02, West Conshocken: Pa.

ASTM (2013) D4972-13. Standard Test Method for pH of Soils, American Society for Testing and Materials, West Conshohocken, Pennsylvania, USA.

Bagonza, S., Peete, J. M., Newill, D. and Freer-Hewish, R. (1987) Carbonation of stabilised soil-cement and soil-lime mixtures-developing countries: highway construction. Proceedings of Seminar held at the PTRC Transport and Planning Summer Annual Meeting, Bath University, England 7-11 September 1987. London: PTRC Education and Research Services, 29-48.

Barnes, G.E. (2010) Soil mechanics: principles and practice. Third Edition, Palgrave Macmillan, England.

Bell, F.G. (1996) Lime stabilization of clay minerals and soils. *Engineering Geology*, 42(4), pp.223-237.

BLA (British Lime Association) (2015) Mineral Products Association. [online] [www.mineralproducts.org](http://www.mineralproducts.org). (accessed 01.04.16).

Blencoe, J.G., Anovitz, L.M., Palmer, D.A. and Beard, J.S. (2003) Carbonation of calcium silicates for long-term CO<sub>2</sub> sequestration. In 2nd Annual Conference on Carbon Sequestration, Alexandria, VA, USA (Vol. 4).

Boardman, D.I., Glendinning, S. and Rogers, C.D.F. (2001) Development of stabilisation and solidification in lime-clay mixes. *Geotechnique*, 51(6), pp.533-543.

Boucher, O., Forster, P.M., Gruber, N., Ha-Duong, M., Lawrence, M.G., Lenton, T.M., Maas, A. and Vaughan, N.E. (2014) Rethinking climate engineering categorization in the context of climate change mitigation and adaptation. *Wiley Interdisciplinary Reviews: Climate Change*, 5(1), pp.23-35.

BSI (1990a) BS 1924-2: Stabilized materials for civil engineering purposes Part 2: Methods of test for cement-stabilized and lime-stabilized materials. British Standards Institution, Milton Keynes.

BSI (1990b) BS 1377: Methods of test for Soils for civil engineering purposes. British Standards Institution, Milton Keynes.

BSI (1995a) BS 7755-3.10: Soil quality. Chemical methods. Determination of carbonate content. Volumetric method. British Standard Institution, Milton Keynes.

BSI (1995b) BS 7755-3.4: Soil quality. Chemical methods. Determination of specific electrical conductivity. British Standard Institution, Milton Keynes.

BSI (1996) BS 7755-3.12: Soil quality. Chemical methods. Determination of the potential cation exchange capacity and exchangeable cations using barium chloride solution buffered at pH = 8.1. British Standard Institution, Milton Keynes.

BSI (2015) BS EN 459-1 Building lime Part 1: Definitions, specifications and conformity criteria. British Standards Institution, Milton Keynes.

Butler, C. D. (2016) Sounding the alarm: health in the anthropocene. *International Journal of Environmental Research and Public Health*, 13(7), pp.1-15.

Calcimeter (2012) Operating instructions. [online] Available at: [http://www.ecosearch.info/sites/default/files/prodotto\\_scheda\\_tecnica/calciometro.pdf](http://www.ecosearch.info/sites/default/files/prodotto_scheda_tecnica/calciometro.pdf) [Accessed 19 January, 2014].

Cement, L. (2010) Magnesium oxide manufacturing industries. Dokument Referencyjny BAT.

Chang, E.E., Chen, C.H., Chen, Y.H., Pan, S.Y. and Chiang, P.C. (2011) Performance evaluation for carbonation of steel-making slags in a slurry reactor. *Journal of Hazardous Materials*, 186(1), pp.558-564.

Chen, H. and Wang, Q. (2006) The behaviour of organic matter in the process of soft soil stabilization using cement. *Bulletin of Engineering Geology and the Environment*, 65(4), pp.445-448.

Cherian, C. and Arnepalli, D.N. (2015) A critical appraisal of the role of clay mineralogy in lime stabilization. *International Journal of Geosynthetics and Ground Engineering*, 1 (8), pp.1-20.

Cherian, C., Bandipally, S., Arnepalli, D. N, Dhulipala, V. R. and Korupolu, R.N. (2016) Reappraisal of optimum lime content determination for lime stabilization of fine-grained soils. 6th Asian Regional Conference on Geosynthetics - Geosynthetics for Infrastructure Development, New Delhi, India, 8-11 November 2016, pp. 260-275.

Cizer, Ö, Van Balen, K. and Van Gemert, D. (2010) Competition between hydration and carbonation in hydraulic lime and lime-pozzolana mortars. *Advanced Materials Research* Vols. 133-134, pp. 241-246.

Cocks, G., Clayton, R., Hu, Y., Han, G. and Chakrabarti, S. (2010) Treatment of reactive soil subgrade for pavement construction in Western Australia. In ARRB Conference, 24TH, 2010, Melbourne, Victoria, Australia.

Cui, Z.D., Wu, S.L., Zhu, S.L. and Yang, X.J. (2006) Study on corrosion properties of pipelines in simulated produced water saturated with supercritical CO<sub>2</sub>. *Applied Surface Science*, 252(6), pp.2368-2374.

Cuisinier, O., Auriol, J.C., Le Borgne, T. and Deneele, D. (2011) Microstructure and hydraulic conductivity of a compacted lime-treated soil. *Engineering geology*, 123(3), pp.187-193.

Danistan, J., and Vipulanandan, C. (2010) Correlation between California Bearing Ratio (CBR) and soil parameters. "In: CIGMAT-2010 conference and exhibition, 2010. Available from: <http://cigmat.cive.uh.edu/>.

Dash, S.K. and Hussain, M. (2011) Lime stabilization of soils: reappraisal. *Journal of Materials in Civil Engineering*, 24(6), pp.707-714.

Davidson, D.T. and Handy, R.L. (1960) Lime and lime-pozzolan stabilization. *Highway Engineering Handbook*, pp.21-100.

Dawson, R. J., Thompson, D., Johns, D., Gosling, S., Chapman, L., Darch, G., Watson, G., Powrie, W., Bell, S., Paulson, K., Hughes, P., and Wood, R. (2016) UK climate change risk

assessment evidence report: Chapter 4, infrastructure. Report prepared for the adaptation subcommittee of the committee on climate change, London.

De Silva, P., Bucea, L., Moorehead, D.R. and Sirivivatnanon, V. (2006) Carbonate binders: reaction kinetics, strength and microstructure. *Cement and Concrete Composites*, 28(7), pp.613-620.

Dorr, A. (2016) Technological change and climate scenarios. *Nature Climate Change*, 6, pp.638-639.

Eades, J. L. and Grim, R. E. (1960) Reaction of hydrated lime with pure clay minerals in soil stabilization. *Highway Research Board Bulletin*, 262, pp. 51–63.

Eades, J. L., Nichols Jr, F. P. and Grim, R. E. (1962) Formation of new minerals with lime stabilization as proven by field experiments in Virginia. *Highway Research Board Bulletin*, 335, pp. 31-39.

Ebrahimi, A., Edil, T.B. and Son, Y.H. (2012) Effectiveness of Cement Kiln Dust in Stabilizing Recycled Base Materials. *Journal of Materials in Civil Engineering*, 1059, p.1066.

Ecofys (2009) Methodology for the free allocation of emission allowances in the EU ETS post 2012 Sector report for the lime industry.

Edwards, A.J. (2005) Properties of hydraulic and non-hydraulic limes for use in construction (Doctoral dissertation, Edinburgh Napier University).

Egerton, R.F. (2006) *Physical principles of electron microscopy: an introduction to TEM, SEM, and AEM*. Springer Science & Business Media.  
[www.springer.com/br/book/9780387258003](http://www.springer.com/br/book/9780387258003)

EU (2000) ECCP (European Climate Change Programme II) from 2005.

EuLA (2014) A competitive and efficient lime industry- cornerstone for a sustainable Europe. Elaborated by Stork M, Meindertsma, W., Overgaag, M., Neelis, M. The European Lime Association, [www.eula.eu](http://www.eula.eu).

EuroSoilStab, (2002) Development of design and construction methods to stabilise soft organic soils Design Guide Soft Soil Stabilisation. CT97-0351 Project No.: BE 96-3177.

- FAO (1998) Basic statistical tools: in Guidelines for quality management in soil and plant laboratories. Food and Agriculture Organization of the United Nations, Issue 74, pp 73-84.
- Frölicher, T.L. (2016) Strong warming at high emissions. *Nature Climate Change*, 6, pp.823-824.
- Gogula, A., Gogula, A.K. and Hossain, M. (2004) A study of factors affecting the permeability of superpave mixes in Kansas. Kansas Department of Transportation.
- Goldberg, I. and Klein, A. (1953) Some effects of treating expansive clays with calcium hydroxide. In: *Symposium on Exchange Phenomena in Soils*. ASTM Special Publication, 142, pp.53–71.
- Gomez, C., Lagacherie, P. and Coulouma, G. (2008) Continuum removal versus PLSR method for clay and calcium carbonate content estimation from laboratory and airborne hyperspectral measurements. *Geoderma*, 148(2), pp.141-148.
- Gough, C., Mander, S. and Haszeldine, S. (2010) A roadmap for carbon capture and storage in the UK. *International Journal of Greenhouse Gas Control*, 4(1), pp.1-12.
- Grant, W.H. (1965) Kaolinite stability in the central piedmont of Georgia. *Clays and Clay Min*, 13, pp.131-140.
- Grim, J.E.R. and Eades, J.L. (1966) A quick test to determine lime requirements of lime stabilisation. *Highway Research Record*, 139, pp.61-72.
- Güllü, H. and Khudir, A. (2014) Effect of freeze–thaw cycles on unconfined compressive strength of fine-grained soil treated with jute fiber, steel fiber and lime. *Cold Regions Science and Technology*, 106, pp.55-65.
- Hammond, G., and Jones, C. (2011) “Inventory of carbon and energy (ICE). Version 2.0.” Sustainable Energy Research Team (SERT), Univ. of Bath, Bath, U.K.
- Hayob, J. L. (2012) Clay mineralogy of Estuarine cores collected from the tidal reaches of the rappahannock river, tributary to chesapeake bay.
- Henry, B.M., Kilmartin, B.A. and Groves, G.W. (1997) The microstructure and strength of carbonated aluminous cements. *Journal of materials science*, 32(23), pp.6249-6253.

- Higgins D.D, Thomas B, & Kinuthia J.M. (2002) "Pyrite oxidation, expansion of stabilised clay and the effect of ggbs", 4th European Symp. on the Performance of Bituminous and Hydraulic Materials in Pavements, University of Nottingham UK.
- Hilt, G.H. and Davidson, D.T. (1960) Lime fixation in clayey soils. Highway Research Board Bulletin, (262).
- Ho, L.S., Nakarai, K., Ogawa, Y., Sasaki, T. and Morioka, M. (2017) Strength development of cement-treated soils: Effects of water content, carbonation, and pozzolanic reaction under drying curing condition. *Construction and Building Materials*, 134, pp.703-712.
- Hotineanu, A., Bouasker, M., Aldaood, A. and Al-Mukhtar, M. (2015) Effect of freeze–thaw cycling on the mechanical properties of lime-stabilized expansive clays. *Cold Regions Science and Technology*, 119, pp.151-157.
- Hu, F. and Yang, X. (2016) Geochemical and geomorphological evidence for the provenance of aeolian deposits in the Badain Jaran Desert, northwestern China. *Quaternary Science Reviews*, 131, pp.179-192.
- Hughes, P. N. and Glendinning, S. (2004) Deep dry mix ground improvement of a soft peaty clay using blast furnace slag and red gypsum. *Quarterly Journal of Engineering Geology and Hydrogeology*. 37, 205-216.
- Huijgen, W.J., Comans, R.N. and Witkamp, G.J. (2007) Cost evaluation of CO<sub>2</sub> sequestration by aqueous mineral carbonation. *Energy Conversion and Management*, 48(7), pp.1923-1935.
- Huijgen, W.J., Ruijg, G.J., Comans, R.N. and Witkamp, G.J. (2006) Energy consumption and net CO<sub>2</sub> sequestration of aqueous mineral carbonation. *Industrial & Engineering Chemistry Research*, 45(26), pp.9184-9194.
- Huntzinger, D.N., Gierke, J.S., Kawatra, S.K., Eisele, T.C. and Sutter, L.L. (2009) Carbon dioxide sequestration in cement kiln dust through mineral carbonation. *Environmental Science & Technology*, 43(6), pp.1986-1992.
- ImageJ (2016) ImageJ Principles. [online] Available at: <https://imagej.net/Principles> [Accessed 12 December, 2016].

IPCC (1990) [J.T. Houghton, G.J. Jenkins and J.J. Ephraums (eds.)]. *Climate Change: The IPCC Scientific Assessment Report*, prepared for Intergovernmental Panel on Climate Change by Working Group I. Cambridge University Press

IPCC (1995) *Climate Change: Impacts, Adaptations and Mitigation of Climate Change. Scientific-Technical Analyses 1996*.

IPCC (2001) [Metz, B., Davidson, O., Swart, R., Pan, J., (eds.)] *Climate change 2001: mitigation, contribution of Working Group III to the third assessment report of the Intergovernmental Panel on Climate Change*.

IPCC (2007) [Solomon, S., Qin, D., Manning, M., Chen, Z., Marquis, M., Averyt, K.B., Tignor, M., Miller, H.L. (eds.)] (2007). *Climate Change 2007: The Physical Science Basis Contribution of Working Group I to the Fourth Assessment Report of the Intergovernmental Panel on Climate Change*.

IPCC (2013) Stocker, T.F., Qin, D., Plattner, G.K., Tignor, M., Allen, S.K., Boschung, J., Nauels, A., Xia, Y., Bex, V. and Midgley, P.M., (eds.)]. *Climate change 2013: The physical science basis. Contribution of working group I to the fifth assessment report of the intergovernmental panel on climate change*.

Jones, C. W. (1987) Long term changes in the properties of soil linings for canal seepage control. Report No. RECERC-87-1. U.S. Department of the Interior, Bureau of Reclamation, Engineering and Research Center, Denver, CO.

Jung, C. and Bobet, A. (2008) Post-construction evaluation of lime treated soils. Joint Transport Research Program Technical Reports, No. FHWA/IN/JTRP-2007/25, pp 1–231.

Kassim, K.A., Hamir, R. and Kok, K.C. (2005) Modification and stabilization of Malaysian cohesive soils with lime. *Geotechnical Engineering*, 36(2), pp. 123–132.

Kaufhold, S. and Dohrmann, R. (2013) The variable charge of dioctahedral smectites. *Journal of Colloid and Interface Science*, 390(1), pp.225-233.

Keith, D.W. (2000) *Geoengineering the climate: history and prospect 1*. *Annual Review of Energy and the Environment*, 25(1), pp.245-284.

- Ketcham, R. A. and Carlson, W.D. (2001) Acquisition, optimization and interpretation of X-ray computed tomographic imagery: applications to the geosciences. *Computers & Geosciences*, 27(4), pp.381-400.
- Khryashchev, V.V., Priorov, A.L., Apalkov, I.V. and Zvonarev, P.S. (2005) Image denoising using adaptive switching median filter. In *IEEE International Conference on Image Processing 2005* (Vol. 1, pp. I-117). IEEE.
- Konrad, J.M. (1989) Physical processes during freeze-thaw cycles in clayey silts. *Cold Regions Science and Technology*, 16(3), pp.291-303.
- Kotz, J.C., Treichel, P.M. and Townsend, J. (2012). *Chemistry and chemical reactivity*. Cengage Learning.
- Lackner, K.S., Wendt, C.H., Butt, D.P., Joyce Jr, E.L. and Sharp, D.H. (1995) Carbon dioxide disposal in carbonate minerals. *Energy*, 20(11), pp.1153-1170.
- Lal, R. (2004) Soil carbon sequestration to mitigate climate change. *Geoderma*, 123(1), pp.122.
- Le Runigo, B., Ferber, V., Cui, Y.J., Cuisinier, O. and Deneele, D. (2011) Performance of lime-treated silty soil under long-term hydraulic conditions. *Engineering geology*, 118(1), pp.20-28.
- Lim, M., Han, G.C., Ahn, J.W. and You, K.S. (2010) Environmental remediation and conversion of carbon dioxide (CO<sub>2</sub>) into useful green products by accelerated carbonation technology. *International Journal of Environmental Research and Public Health*, 7(1), pp.203228.
- Little, D. L. (2000) Evaluation of structural properties of lime stabilized soils and aggregates, mixture design and testing protocol for lime stabilized soils, (Vol. 3). National Lime Association report. (<http://www.lime.org/SOIL3.PDF>)
- Lobell, D.B. and Tebaldi, C. (2014) Getting caught with our plants down: the risks of a global crop yield slowdown from climate trends in the next two decades. *Environmental Research Letters*, 9(7), p.074003.

- Loveland, P. J. (1984) The soil clays of Great Britain: I. England and Wales. *Clay Minerals*, 19(5), pp.681-707.
- Lu, H. Y., Lin, C. K., Lin, W., Liou, T. S., Chen, W. F. and Chang, P. Y. (2011) A natural analogue for CO<sub>2</sub> mineral sequestration in miocene basalt in the Kuanhsi-Chutung area, Northwestern Taiwan. *International Journal of Greenhouse Gas Control*, 5(5), pp.1329-1338
- Magwood, C. (2016) *Essential hempcrete construction: the complete step-by-step guide sustainable building essentials series*. New Society Publishers, Canada, pp. 23-36.
- Manning, D.A.C. (1995) Industrial clays: kaolin (china clay), ball clay and bentonite. In: *Introduction to Industrial Minerals*. First edition. Chapman and Hall, London, UK, pp. 35-71).
- Manning, D.A.C. and Renforth, P. (2012) Passive sequestration of atmospheric CO<sub>2</sub> through coupled plant-mineral reactions in urban soils. *Environmental Science & Technology*, 47(1), pp.135-141.
- Manning, D.A.C., Lopez-Capel, E. and Barker, S. (2005) Seeing soil carbon: use of thermal analysis in the characterization of soil C reservoirs of differing stability. *Mineralogical Magazine*, 69(4), pp.425-435.
- Manning, D.A.C., Renforth, P., Lopez-Capel, E., Robertson, S. and Ghazireh, N. (2013) Carbonate precipitation in artificial soils produced from basaltic quarry fines and composts: An opportunity for passive carbon sequestration. *International Journal of Greenhouse Gas Control*, 17, pp.309-317.
- Marceau, M. L., Nisbet, M. A., and VanGeem, M. G. (2007) *Life Cycle Inventory of Portland Cement Concrete, SN3011*, Portland Cement Association, Skokie, Illinois, PCA, 121 pages.
- Matsushita, F., Aono, Y. and Shibata, S. (2000) Carbonation degree of autoclaved aerated concrete. *Cement and concrete research*, 30(11), pp.1741-1745.
- Matthews, H.D., Gillett, N.P., Stott, P.A. and Zickfeld, K. (2009) The proportionality of global warming to cumulative carbon emissions. *Nature*, 459 (7248), p.829.
- Maubec, N., Deneele, D. and Ouvrard, G. (2017) Influence of the clay type on the strength evolution of lime treated material. *Applied Clay Science*, 137, pp.107-114.

- McCarthy, G. J., Swanson, K. D., Keller, L. P. and Blatter, W. C. (1984) Mineralogy of Western fly ashes. *Cement and Concrete Research*, 14 (3), 471-478.
- MCHW 1 (2009) (Manual of contract documents for highway works). Volume 1, Specification for Highway Works: Amended February 2016, HMSO, London
- Meyer, M., Flood, M., Keller, J., Lennon, J., McVoy, G., Dorney, C., Leonard, K., Hyman, R. and Smith, J. (2014) Strategic Issues Facing Transportation, Volume 2: Climate Change, Extreme Weather Events, and the Highway System: Practitioner's Guide and Research Report (No. Project 20-83 (5)).
- Milodowski, A. E., Rochelle, C. A., Lacinska, A. and Wagner, D. (2011) A natural analogue study of CO<sub>2</sub>-cement interaction: carbonation of calcium silicate hydrate-bearing rocks from Northern Ireland. *Energy Procedia*, 4, pp.5235-5242.
- Milodowski, A.E., Northmore, K.J., Kemp, S.J., Entwisle, D.C., Gunn, D.A., Jackson, P.D., Boardman, D.I., Zoumpakis, A., Rogers, C.D., Dixon, N. and Jefferson, I. (2015) The mineralogy and fabric of 'Brickearths' in Kent, UK and their relationship to engineering behaviour. *Bulletin of Engineering Geology and the Environment*, 74(4), pp.1187-1211.
- Mir, B.A. and Sridharan, A. (2013) Physical and compaction behaviour of clay soil-fly ash mixtures. *Geotechnical and Geological Engineering*, 31(4), pp.1059-1072.
- Morad, S. editor., (2009) Carbonate cementation in sandstones: Distribution Patterns and Geochemical Evolution (Special Publication 26 of the IAS) (Vol. 72). John Wiley & Sons.
- Morandea, A., Thiery, M. and Dangla, P. (2014) Investigation of the carbonation mechanism of CH and CSH in terms of kinetics, microstructure changes and moisture properties. *Cement and Concrete Research*, 56, pp.153-170.
- Muhmed, A. and Wanatowski, D. (2013) Effect of lime stabilisation on the strength and microstructure of clay. *IOSR Journal of Mechanical and Civil Engineering (IOSR-JMCE)*, 6(3), pp.87-94.
- Murray, H. H. (1980) Major kaolin processing developments. *International Journal of Mineral Processing*, 7, pp.263-274.

Nakarai, K. and Yoshida, T. (2015) Effect of carbonation on strength development of cement-treated Toyoura silica sand. *Soils and Foundations*, 55(4), pp.857-865.

NLA (2006) Mixture design and testing procedures for lime stabilized soil. Technical Brief. National Lime Association, Arlington, VA. [http://www.lime.org/Oct2006VerMix Design.pdf](http://www.lime.org/Oct2006VerMix%20Design.pdf).

NOAA (2017) National Centers for Environmental Information, State of the Climate: Global Climate Report for March 2017, published online April 2017, retrieved on October 14, 2017 from <https://www.ncdc.noaa.gov/sotc/global/201703>.

Nzeukou, A.N., Fagel, N., Njoya, A., Kamgang, V.B., Medjo, R.E. and Melo, U.C. (2013) Mineralogy and physico-chemical properties of alluvial clays from Sanaga valley (Center, Cameroon): Suitability for ceramic application. *Applied Clay Science*, 83, pp.238-243.

Olivier, J.G.J., Janssens-Maenhout, G., Muntean, M. and Peters, J.A.H.W. (2016) Trends in global CO<sub>2</sub> emissions; 2016 Report, The Hague: PBL Netherlands Environmental Assessment Agency; Ispra: European Commission, Joint Research Centre.

Ortega-López, V., Manso, J.M., Cuesta, I.I. and González, J.J. (2014) The long-term accelerated expansion of various ladle-furnace basic slags and their soil-stabilization applications. *Construction and Building Materials*, 68, pp.455-464.

Partanen, A.I., Leduc, M. and Matthews, D. (2017) Seasonal climate change patterns due to cumulative CO<sub>2</sub> emissions. *Environmental Research Letters*, 12(075002), pp.1-9.

Peethamparan, S., Olek, J. and Lovell, J. (2008) Influence of chemical and physical characteristics of cement kiln dusts (CKDs) on their hydration behavior and potential suitability for soil stabilization. *Cement and concrete research*, 38(6), pp.803-815.

Pendleton, L., Comte, A., Langdon, C., Ekstrom, J.A., Cooley, S.R., Suatoni, L., Beck, M.W., Brander, L.M., Burke, L., Cinner, J.E. and Doherty, C. (2016) Coral Reefs and People in a High-CO<sub>2</sub> World: Where Can Science Make a Difference to People? *PloS one*, 11(11), p.e0164699.

Pettijohn, F.J., Potter, P.E. and Siever, R. (2012) Sand and sandstone. Springer Science & Business Media.

- Phillips, D.H., Sinnathamby, G., Russell, M.I., Anderson, C. and Paky, A. (2011) Mineralogy of selected geological deposits from the United Kingdom and the Republic of Ireland as possible capping material for low-level radioactive waste disposal facilities. *Applied Clay Science*, 53(3), pp.395-401.
- Poh, H.Y., Ghataora, G.S. and Ghazireh, N. (2006) Soil stabilization using basic oxygen steel slag fines. *Journal of Materials in Civil Engineering*, 18(2), pp.229-240.
- Psyrillos, A., Howe, J.H., Manning, D.A.C. and Burley, S.D. (1999) Geological controls on kaolin particle shape and consequences for mineral processing. *Clay Minerals*, 34(1), pp.193-193.
- Rahmat, M.N. and Ismail, N. (2011) Sustainable stabilisation of the Lower Oxford Clay by non-traditional binder. *Applied Clay Science*, 52(3), pp.199-208.
- Rasband, W.S. (2002) NIH Image J. <http://imagej.nih.gov/ij/index.html>, verified 2 August, 2011.
- Raven, J., Caldeira, K., Elderfield, H., Hoegh-Guldberg, O., Liss, P., Riebesell, U., Shepherd, J., Turley, C. and Watson, A. (2005) Ocean acidification due to increasing atmospheric carbon dioxide. The Royal Society, London.
- Reeves, G.M., Sims, I. and Cripps, J.C. eds. (2006) Clay materials used in construction. Geological Society, London, *Engineering Geology Special Publications*, 21, 73-138.
- Renforth, P. (2011) Mineral carbonation in soils: Engineering the soil carbon sink. PhD Thesis, School of Civil Engineering and Geosciences, Newcastle University, UK.
- Renforth, P. and Manning, D.A.C. (2011) Laboratory carbonation of artificial silicate gels enhanced by citrate: Implications for engineered pedogenic carbonate formation. *International Journal of Greenhouse Gas Control*, 5(6), pp.1578-1586.
- Renforth, P., Manning, D.A.C. and Lopez-Capel, E. (2009) Carbonate precipitation in artificial soils as a sink for atmospheric carbon dioxide. *Applied Geochemistry*, 24(9), pp.1757-1764.

Rogers, C. D. F. and Glendinning, S. (1996) Modification of clay soils using lime, in: Dixon, N., Glendinning, S. and Rogers, C. D. F. (Eds.), *Lime Stabilisation*. Thomas Telford. London, pp.99-114.

Rogers, C.D.F., Glendinning, S. and Roff, T.E.J. (1997) Lime modification of clay soils for construction expediency. *Proceedings of the Institution of Civil Engineers-Geotechnical Engineering*, 125(4), pp.242-249.

Saeed, K.A.H., Kassim, K.A., Yunus, N.Z.M. and Nur, H. (2015) Physico-chemical characterization of lime stabilized tropical kaolin clay. *Jurnal Teknologi*, 72(3), pp.83-90.

Sanders, C.H. and Phillipson, M.C. (2003) UK adaptation strategy and technical measures: the impacts of climate change on buildings. *Building Research & Information*, 31(3-4), pp.210-221.

Sargent, P., Hughes, P.N. and Rouainia, M. (2016) A new low carbon cementitious binder for stabilising weak ground conditions through deep soil mixing. *Soils and Foundations*, 56(6), pp.1021-1034.

Seifritz, W. (1990) CO<sub>2</sub> disposal by means of silicates. *Nature*, 345, p.486.

Setién, J., Hernández, D. and González, J.J. (2009) Characterization of ladle furnace basic slag for use as a construction material. *Construction and Building Materials*, 23(5), pp.1788-1794.

Shand, M.A. (2006) *The chemistry and technology of magnesia*. John Wiley & Sons.

Shepherd, J.G. (2009) *Geoengineering the climate: science, governance and uncertainty*. Royal Society, London.

Sherwood, P. T. (1993) *Soil stabilisation with cement and lime – state of the art review*. Transport Research Laboratory, Department of Transport. HMSO publications, ISBN 0-11-551171-7.

Shihata, S.A. and Baghdadi, Z.A. (2001) Simplified method to assess freeze-thaw durability of soil cement. *Journal of materials in civil engineering*, 13(4), pp.243-247.

Shillaber, C.M., Mitchell, J.K., Dove, J.E. and Ostrum, Z.A. (2016) Framework to Account for Uncertainty in Energy and Carbon Assessment of Ground Improvement Works. *Journal of Geotechnical and Geoenvironmental Engineering*, 143(5), p.04016122.

Siddique, R. (2007) *Waste materials and by-products in concrete*. Springer Science & Business Media.

Smith, J. (2015) *Examining soil based construction materials through X-Ray computed tomography* (Doctoral dissertation, Durham University).

Snodgrass, A., and Nonnenbrun, K. (1974) Pedogenic palygorskite occurrences in Australia. *American Mineralogist*, 59, pp.508-517.

Snedker EA (1996) M40 - Lime stabilisation experiences, In *Proc. of a seminar on Lime Stabilisation* (Rogers CDF, Glendinning S. and Dixon N. (eds.)), Loughborough University, UK, pp. 142-153.

The Highways Agency (2007) *Design Manual for Roads and Bridges, Vol 4.1, Part 6. HA74/07 Treatment of fill and capping materials using either lime or cement or both*. HMSO, London.

US Environmental Protection Agency (2016) *Inventory of U.S. Greenhouse Gas Emissions and Sinks: 1990–2014* <https://www.epa.gov/ghgemissions/us-greenhouse-gas-inventory-report-1990-2014>.

USGS (2016) U.S. Geological Survey, *Mineral Commodity Summaries*, January 2016.

Van Gerven, T., Van Keer, E., Arickx, S., Jaspers, M., Wauters, G. and Vandecasteele, C. (2005) Carbonation of MSWI-bottom ash to decrease heavy metal leaching, in view of recycling. *Waste Management*, 25(3), pp.291-300.

Verbrugge, J.C., De Bel, R., Gomes Correia, A., Duvigneaud, P.H. and Herrier, G. (2011) Strength and micro observations on a lime treated silty soil. In *Proceedings of the 2011 GeoHunan International Conference, in Road Materials and New Innovations in Pavement Engineering (GSP 223)*.

Vitale, E., Deneele, D., Paris, M. and Russo, G. (2017) Multi-scale analysis and time evolution of pozzolanic activity of lime treated clays. *Applied Clay Science*, 141, pp.36-45.

- Vitale, E., Deneele, D., Russo, G. and Ouvrard, G. (2016) Short-term effects on physical properties of lime treated kaolin. *Applied Clay Science*, 132, pp.223-231.
- Washbourne, C.L. (2014) Engineering soils to act as carbon sinks. PhD Thesis, School of Civil Engineering and Geosciences, Newcastle University, UK.
- Washbourne, C.L., Lopez-Capel, E., Renforth, P., Ascough, P.L. and Manning, D.A.C. (2015) Rapid removal of atmospheric CO<sub>2</sub> by urban soils. *Environmental Science & Technology*, 49(9), pp.5434-5440.
- Washbourne, C.L., Renforth, P. and Manning, D.A.C. (2012) Investigating carbonate formation in urban soils as a method for capture and storage of atmospheric carbon. *Science of the Total Environment*, 431, pp.166-175.
- Wild S., Kinuthia J.M., Jones G.I. and Higgins D.D. (1998) "Effects of partial substitution of lime with ground granulated blastfurnace slag (ggbs) on the strength properties of lime stabilised sulphate bearing clay soils". *Engineering Geology*, 51, pp37-53.
- Wollast, R. (1967) Kinetics of the alteration of K-feldspar in buffered solutions at low temperature. *Geochimica et Cosmochimica Acta*, 31(4), pp.635-648.
- Yi, Y., Liska, M., Unluer, C. and Al-Tabbaa, A. (2013) Carbonating magnesia for soil stabilization. *Canadian Geotechnical Journal*, 50(8), pp.899-905.
- Yi, Y., Lu, K., Liu, S. and Al-Tabbaa, A. (2015) Property changes of reactive magnesia–stabilized soil subjected to forced carbonation. *Canadian Geotechnical Journal*, 53(2), pp.314-325.
- Yildirim, I. Z. and Prezzi, M. (2011) Chemical, mineralogical, and morphological properties of steel slag. *Advances in Civil Engineering*, 2011. [Article ID 463638: pp.1-13]. <http://dx.doi.org/10.1155/2011/463638>.
- Yoon, T.K., Seo, K.W., Park, G.S., Son, Y.M. and Son, Y. (2016) Surface soil carbon storage in urban green spaces in three major South Korean cities. *Forests*, 7(6), p.115.
- Yunus, N. Z. M., Wanatowski, D., Hassan, N.A. and Marto, A. (2016) Shear strength and compressibility behaviour of lime-treated organic clay. *KSCE Journal of Civil Engineering*, 20(5), pp.1721-1727.

Zangeneh, H., Jamshidi, S. and Soltanieh, M. (2013) Coupled optimization of enhanced gas recovery and carbon dioxide sequestration in natural gas reservoirs: case study in a real gas field in the south of Iran. *International Journal of Greenhouse Gas Control*, 17, pp.515-522.

Zhang, X., Fan, J. L. and Wei, Y. M. (2013) Technology roadmap study on carbon capture, utilization and storage in China. *Energy Policy*, 59, pp.536-550.

Zhou, J. H. Yan, and J. M. Mo (2006) Old-growth forests can accumulate carbon in soils, *Science*, 314(5804), 1417.

## Appendix A-Material Properties

**Table A1:** Chemical properties and particle size distribution of kaolin (Polwhite E) provided by supplier, Imerys Performance Minerals (2008).

### Polwhite™ E

Polwhite E is a high quality medium particle size kaolin produced from deposits in the South West of England.

#### SPECIFICATION

Brightness	(ISO R457)	78.5 ± 1.5
+ 300 mesh	(mass % max.)	0.05
+ 10 µm	(mass % max.)	35
- 2 µm	(mass % min.)	25
Moisture	(mass % max.)	1.5

#### TYPICAL VALUES

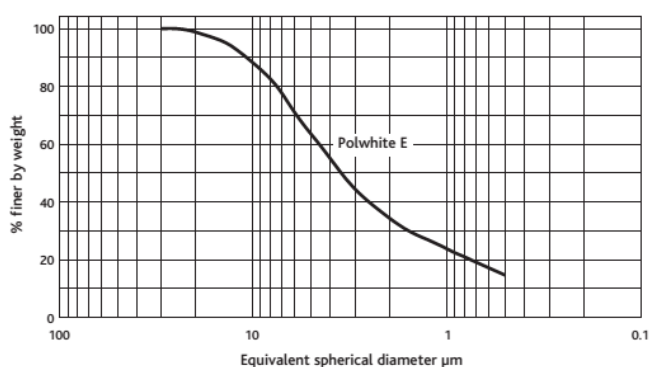
Yellowness		7
Specific gravity		2.6
pH		5.0
Surface area	(BET; m <sup>2</sup> /g)	8
Oil absorption	(g/100g)	33
Water soluble salt content	(mass %)	0.15
Aerated powder density	(kg/m <sup>3</sup> )	360
Tapped powder density	(kg/m <sup>3</sup> )	810

#### Chemical analysis by X-ray fluorescence

SiO <sub>2</sub>	(mass %)	50
Al <sub>2</sub> O <sub>3</sub>	(mass %)	35

CAS No. 1332-58-7

#### TYPICAL PARTICLE SIZE DISTRIBUTION



**IMERYS PERFORMANCE & FILTRATION MINERALS**  
 Par Moor Centre,  
 Par Moor Road, Par  
 Cornwall, PL24 2SQ - UK  
 Tel: +44 1726 818000  
 Fax: +44 1726 811200



ISO 9001  
 FM 14752

Kaolin does not appear in EINECS as an individual entry but is classified as "naturally Occurring Substance" with the EINECS No. 310-127-6.

*The data quoted are determined by the use of IMERYS Minerals Ltd Standard Test Methods, copies of which will be supplied on request. Every precaution is taken to ensure the products conform to our published data, but since the products are based on naturally occurring raw materials, we reserve the right to change these data should it become necessary. Sales are in accordance with our 'Conditions of Sale', copies of which will be supplied on request.*



**DAT020K**  
 March 2008 - Sixth Edition.  
 This data sheet supersedes the data sheet dated March 2004.

**Table A2:** Physical and chemical properties of lime as used in the current study.

## 'LIMBUX' (High Calcium Hydrated Lime)

### PRODUCT SPECIFICATION AND DATA SHEET

'LIMBUX' (*High Calcium Hydrated Lime*) is a high purity, CL90-S hydrated lime complying with BS EN 459-1:2010 and BS EN 12518:2008 Class 1 Type A. It has a wide range of applications in a variety of processes and industries, including construction materials, chemical manufacture, water & waste treatment and agriculture

*Hydrated Lime* is manufactured from high-purity quicklime at Tunstead, near Buxton, Derbyshire under a quality system registered to BS EN ISO 9001:2008. The process involves calcining very pure processed limestone at high temperatures in modern, efficient kilns after which the lime is crushed, screened, hydrated and processed to the required quality and grading profile. As the product is obtained from a naturally occurring raw material there may be some variation in parameters and the following specifications are given at 95% confidence levels.

<u>Chemical Properties</u>	<u>Typical Analysis (% mass)</u>	<u>Specification (% mass)</u>
Ca(OH) <sub>2</sub>	96.9	95.0 min
CaCO <sub>3</sub>	1.4	2.0 max
Mg(OH) <sub>2</sub>	0.5	1.4 max
CaSO <sub>4</sub>	0.03	0.1 max
Free Moisture	0.25	0.75 max
Neutralising Value (as CaO)	75.1	74.0 min

#### Physical Properties

% passing 500 µm	100	100 min
% passing 75 µm	99.0	95 min
SSA (air permeability method)	1800 m <sup>2</sup> /kg	
Bulk Density	450-520 kgs/m <sup>3</sup>	

#### Other Chemical Properties

<u>(% Mass)</u>	<u>(% Mass)</u>	
SiO <sub>2</sub>	0.7	1.0 max
Al <sub>2</sub> O <sub>3</sub>	0.1	0.2 max
Fe <sub>2</sub> O <sub>3</sub>	0.06	0.1 max
Mn	175 ppm	250 ppm max
F	65 ppm	110 ppm max
Pb	1.3 ppm	3 ppm max
As	0.3 ppm	1 ppm max

(Analysis carried out in accordance with BS EN 459-2: 2010 & BS 6463-102: 2001 & 103: 1999 and BL&C in-house methods)

#### Packaging

*Bulk* - Delivery up to 29 tonne lots by air pressure discharge tanker.

*Bags* - In 25kg paper sacks, packed 40 per shrink wrapped pallet (returnable)

*Bags* - In 1000 kg non - returnable woven polypropylene IBCs (Big Bags)

#### Storage

*Bags* - Avoid contact with water. Kept in original packaging in a dry, cool, draught free atmosphere shelf life is up to six months.

*Bulk* - Recommended minimum silo capacity 60m<sup>3</sup>. Further advice/information available on request

#### Safety

Refer to our Safety Data Sheet  
AA 0103 LBX

Issue 14 – Jan 2013

Lafarge Tarmac Cement & Lime, Tunstead House, Buxton, Derbyshire SK17 8TG  
Tel. 01298 768555 Fax 01298 72195

**Table A3:** Chemical properties of sodium carbonate as used in the current study.

Sodium Carbonate Anhydrous, ACS Grade.



White solid

Sodium carbonate



**R:** 36  
**S:** 22-26  
**H:** H319



**P:** P280 P305+P351+P338  
Warning

**Formula:** Na<sub>2</sub>CO<sub>3</sub>  
**MW:** 105.99 g/mol  
**Boiling Pt:** 1600 °C (1013 hPa)  
**Melting Pt:** 854 °C  
**Density:** 2.53 g/cm<sup>3</sup> (20 °C)

**MDL Number:** MFCD00003494  
**CAS Number:** 497-19-8  
**Index:** 011-005-00-2  
**EINECS:** 207-838-8  
**REACH:** 01-2119485498-19

**Specification Test Results**

Assay (dried basis)	99.5% (Na <sub>2</sub> CO <sub>3</sub> ) min
Insoluble matter	0.01% max
Loss on heating at 285°C	1.0% max
Chloride (Cl)	0.001% max
Phosphate (PO <sub>4</sub> )	0.001% max
Silica (SiO <sub>2</sub> )	0.00005
Sulfur compounds (as SO <sub>4</sub> )	0.003% max
Heavy metals (as Pb)	5 ppm max
Iron (Fe)	5 ppm max
Calcium (Ca)	0.03% max
Magnesium	0.005% max
Potassium (K)	0.005% max

## Appendix B-Soil Characterisation Test Results

**Table B1:** Atterberg Limits of calcium hydroxide mixed kaolin.

Calcium hydroxide addition (%)	Liquid Limit (%)	Plastic Limit (%)	Plasticity Index (%)
0	59	31	28
1	64	33	31
2	63	34	29
3	64	34	30
4	64	34	30
6	63	33	30
8	63	35	28

**Table B2:** Mechanical and chemical properties of kaolin (Polwhite E) as used in the current study

Property	Typical Analysis (% mass)
<b>1. Chemical composition</b>	<sup>a</sup> As used in this studies
SiO <sub>2</sub> (mass %)	50
Al <sub>2</sub> O <sub>3</sub> (mass %)	35
Alkali (K <sub>2</sub> O, Na <sub>2</sub> O)	-
Fe <sub>2</sub> O <sub>3</sub>	-
CaO	-
Loss on ignition	-
<b>2. Physical properties :Particle size distribution</b>	
0.06 – 0.002 mm (%)	65
Less than 0.002 mm (<2 μm) (%)	35
Surface area (BET; m <sup>2</sup> /g)	8
pH	5.5
Specific gravity	2.6
Liquid limit (%)	59
Plastic limit	31
Plasticity index (%)	28
Optimum moisture content (%)	27
Maximum dry density (Mg/m <sup>3</sup> )	1.44
Unconfined compressive strength (kPa) <sup>b</sup>	200

<sup>a</sup> Chemical analysis by X-ray fluorescence as provided the supplier, Imerys Performance Minerals (2008).

<sup>b</sup> At optimum moisture content.

## Appendix C- Carbonate and Air Voids Content

### C1: Procedure Used for XRCT Data Processing

XRCT Image Processing:

1. Delete first and last 100 image slices to prevent shadowing
2. Import image sequence
3. Set scale: analyse → set scale
4. Covert image to 8-bit: Image → type → 8-bit (required for thresholding)
5. Crop image to prevent shadowing:  
Edit → selection → specify (650 x 650 pixels, constrain square, centred)  
Image → crop
6. Filter image: process → filter → median (2 pixels radius)
7. Set threshold value: Image → adjust → threshold (default, black and white)
8. Analyse calcite and air void area content:  
Analyse → set measurements (area, mean grey value, min and max grey value)  
Edit → selection → create selection  
Analyse → measure

**Figure C1:** Procedure used for XRCT data processing (using ImageJ software) (Adapted from Beckett *et al.*, 2013).

**C2: XRCT Images Showing Carbonate and Air Voids Content, with corresponding Threshold Graphs.**

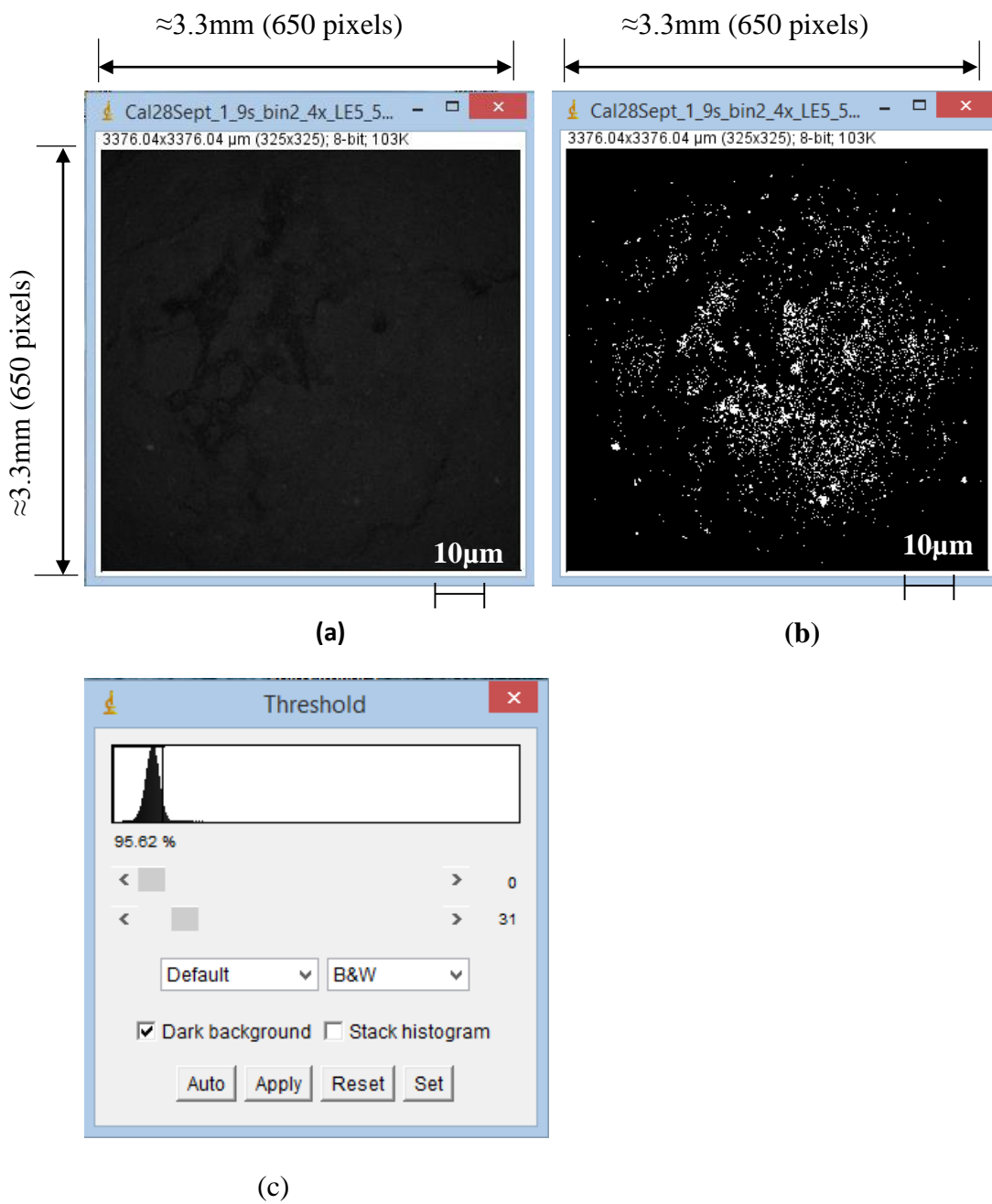
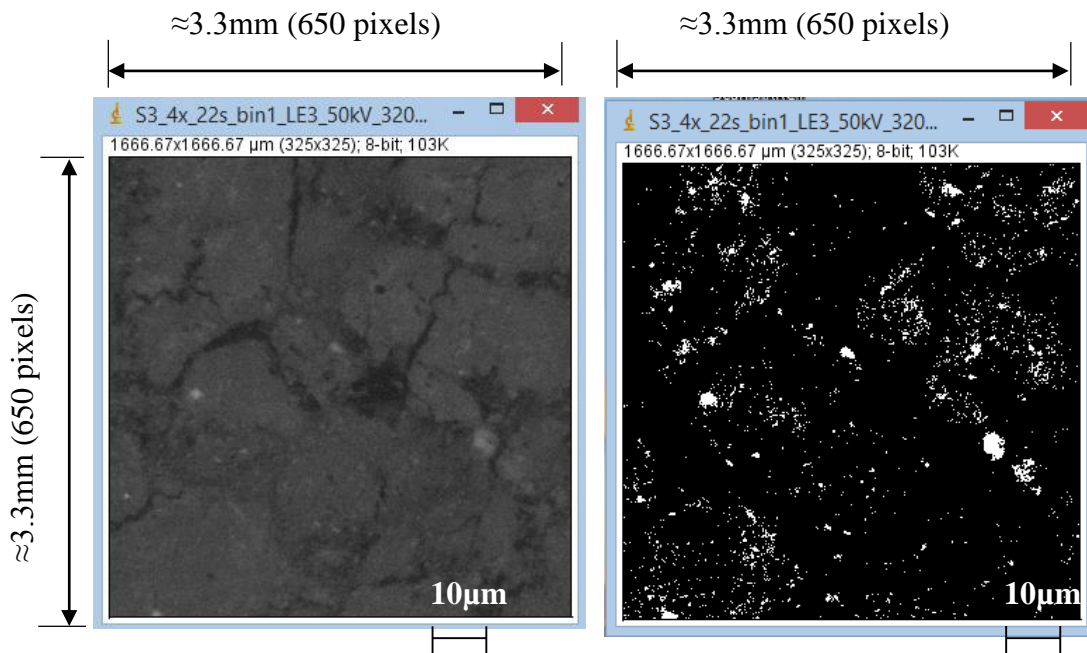
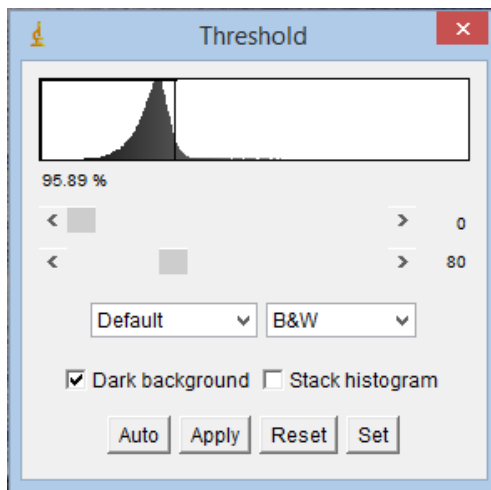


**Figure C2.1:** XRCT Image of 4% calcium hydroxide 3% air voids treated kaolin (a) carbonated sample (b) threshold image showing black background (non-calcium carbonate), and white Foreground (calcium carbonate) (c) threshold intensity of 31 on histogram.



(a)

(b)



(c)

**Figure C2.2:** XRCT image of 4% calcium hydroxide 10% air voids treated kaolin (a) carbonated sample (b) threshold image showing black background (non-calcium carbonate), and white foreground (calcium carbonate) (c) threshold intensity of 80 on histogram

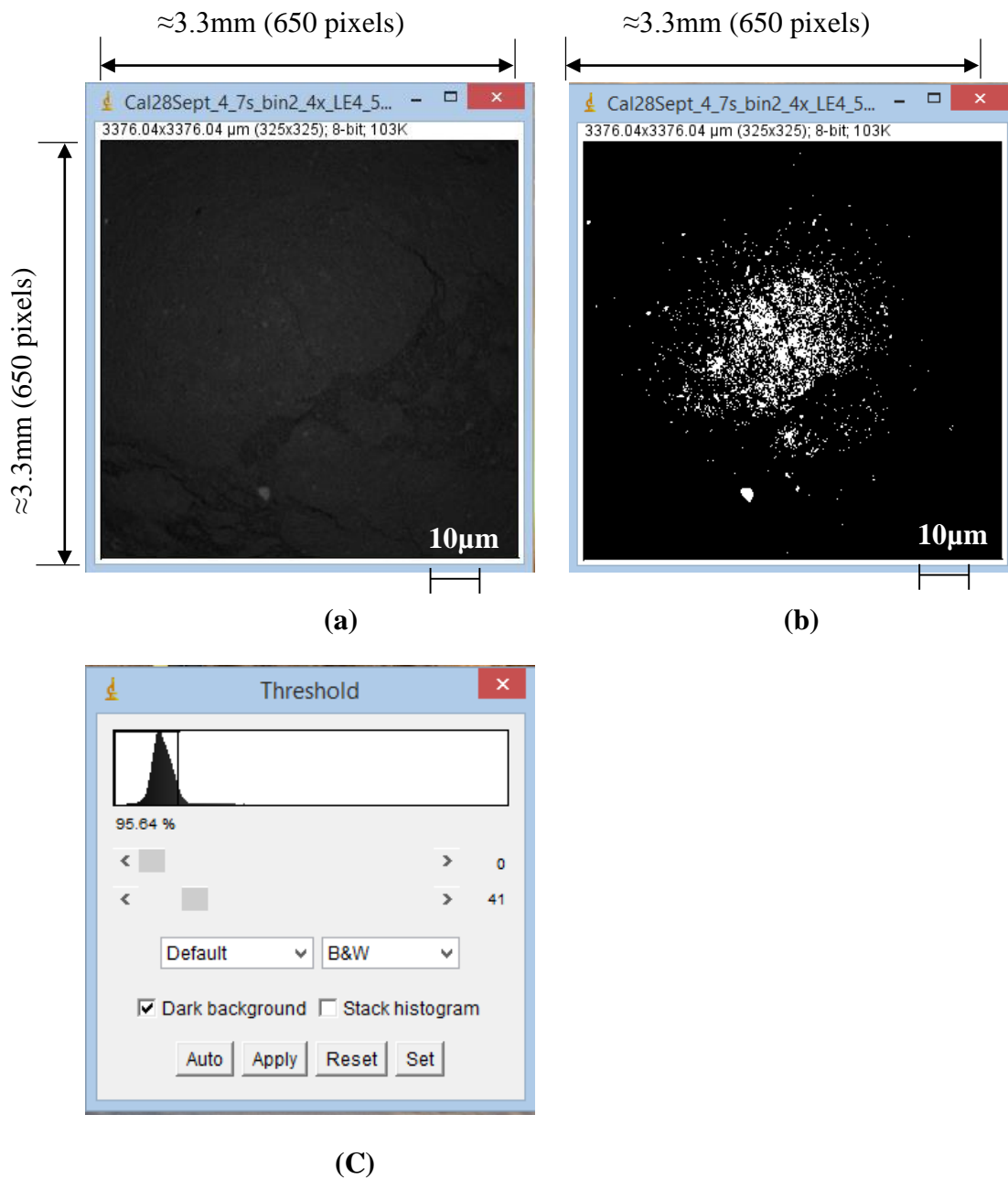


**Figure C2.3:** XRCT image of 4% calcium hydroxide 25% air voids treated kaolin (a) carbonated sample (b) threshold image showing black background (non-calcium carbonate), and white foreground (calcium carbonate) (c) threshold intensity of 41 on histogram.

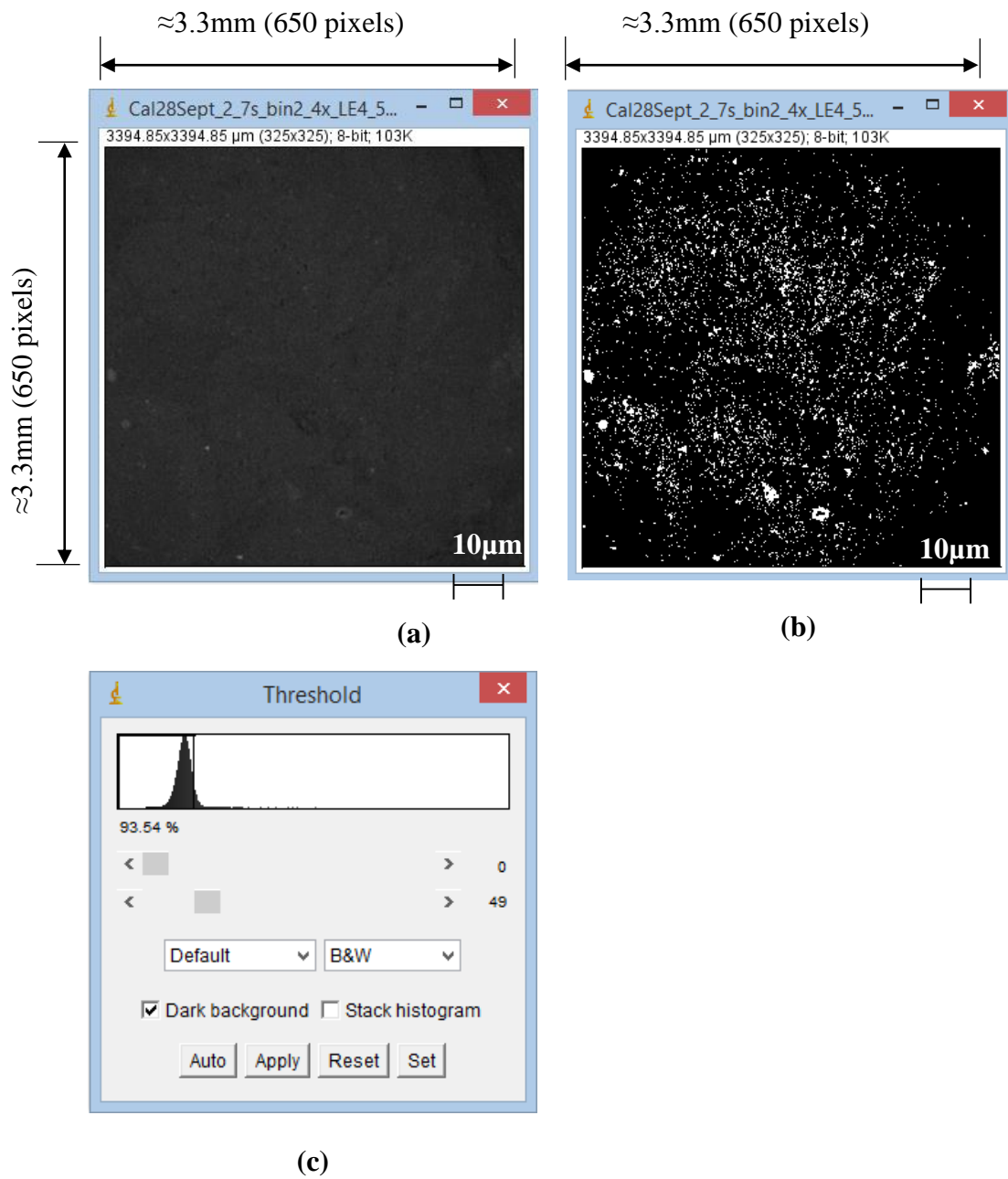


**Figure C2.4:** XRCT image of 6% calcium hydroxide 3% air voids treated kaolin (a) carbonated sample (b) threshold image showing black background (non-calcium carbonate), and white foreground (calcium carbonate) (c) threshold intensity of 49 on histogram.

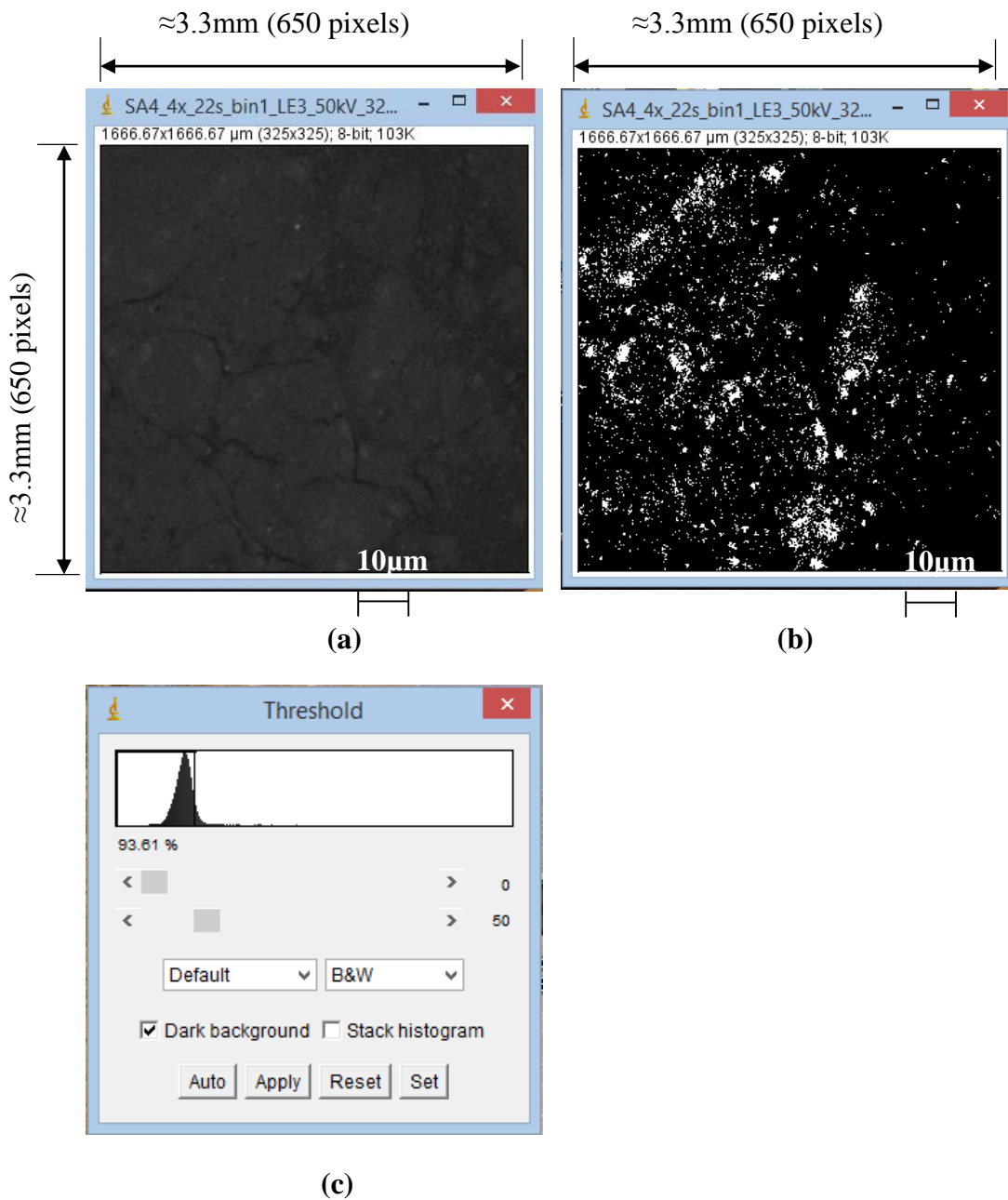


**Figure C2.5:** XRCT image of 6% calcium hydroxide 10% air voids treated kaolin (a) carbonated sample (b) threshold image showing black background (non-calcium carbonate), and white foreground (calcium carbonate) (c) threshold intensity of 50 on histogram.

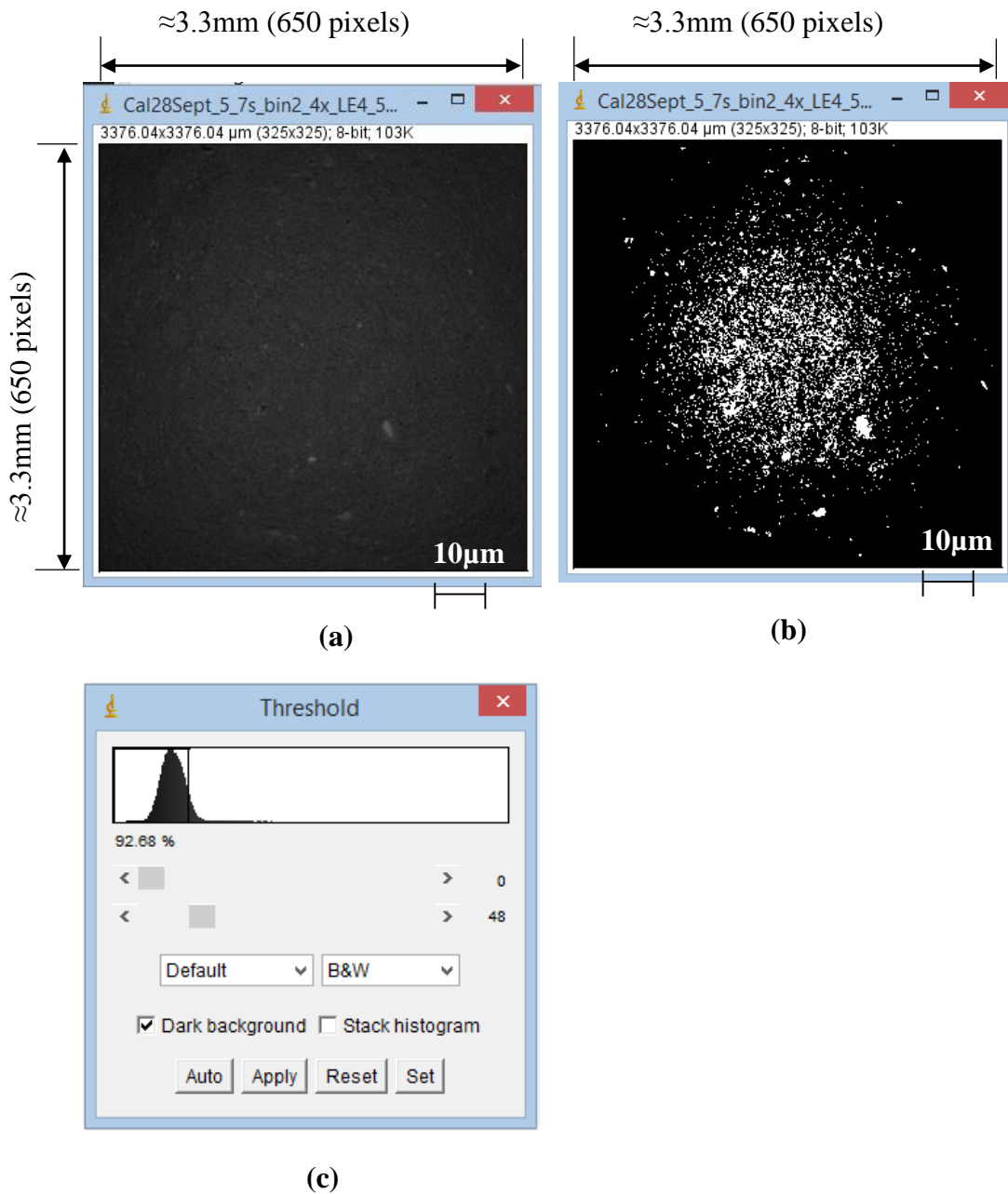


**Figure C2.6:** XRCT image of 6% calcium hydroxide 25% air voids treated kaolin (a) carbonated sample (b) threshold image showing black background (non-calcium carbonate), and white foreground (calcium carbonate) (c) threshold intensity of 48 on histogram

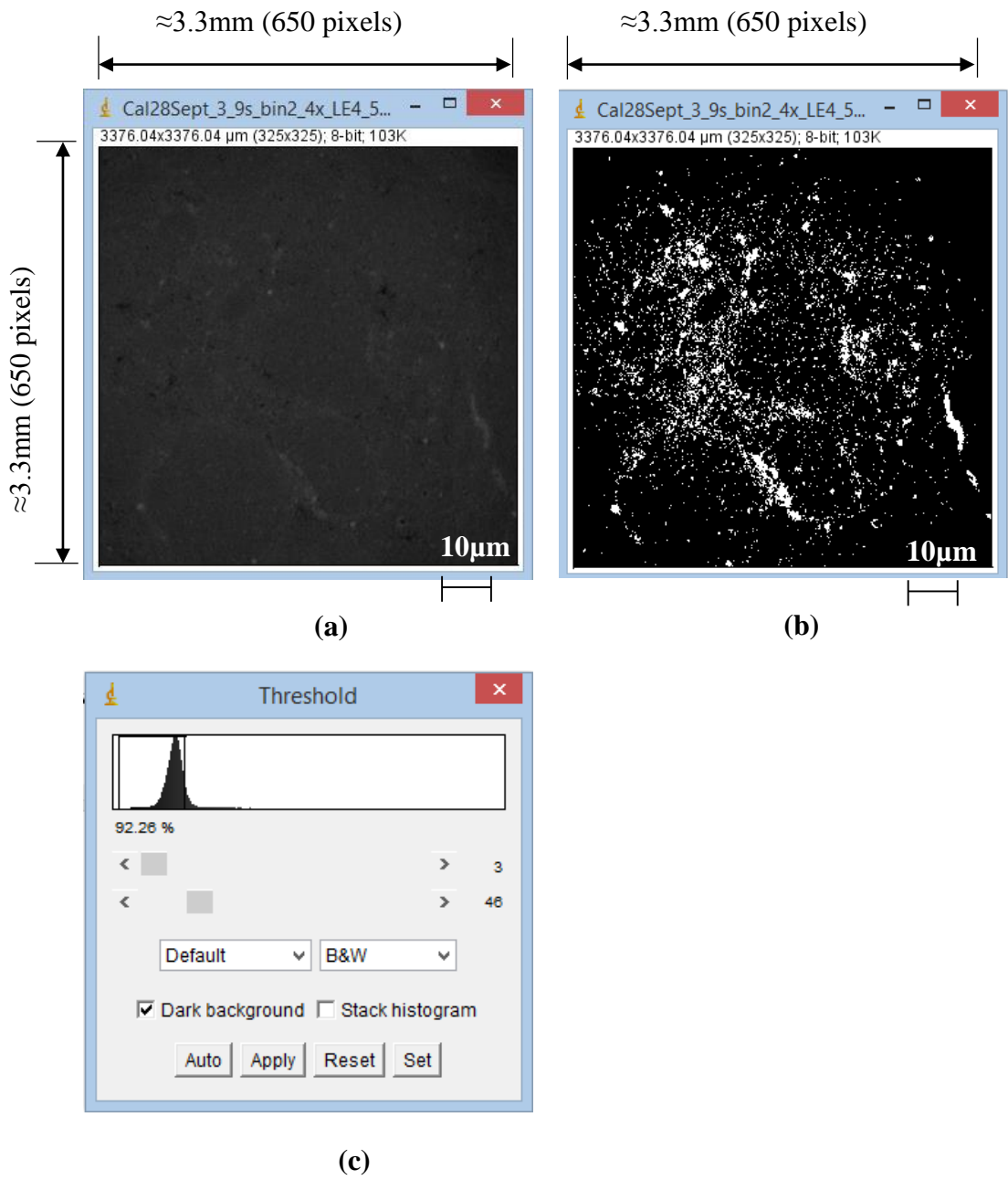


**Figure C2.7:** XRCT image of 8% calcium hydroxide 3% air voids treated kaolin (a) carbonated sample (b) threshold image showing black background (non-calcium carbonate), and white foreground (calcium carbonate) (c) threshold intensity of 46 on histogram

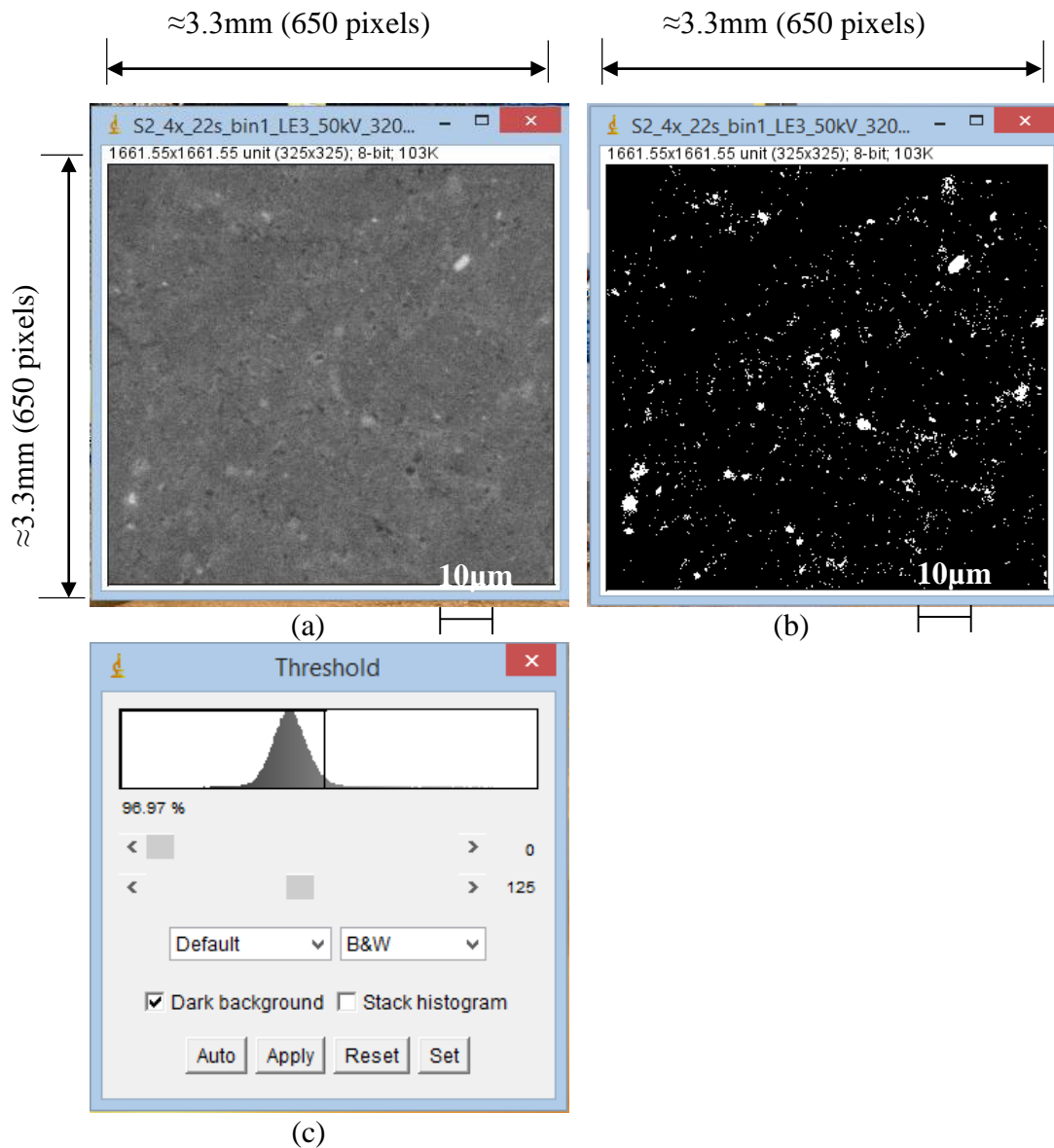


**Figure C2.8:** XRCT image of 8% calcium hydroxide 10% air voids treated kaolin (a) carbonated sample (b) threshold image showing black background (non-calcium carbonate), and white foreground (calcium carbonate) (c) threshold intensity of 125 on histogram.

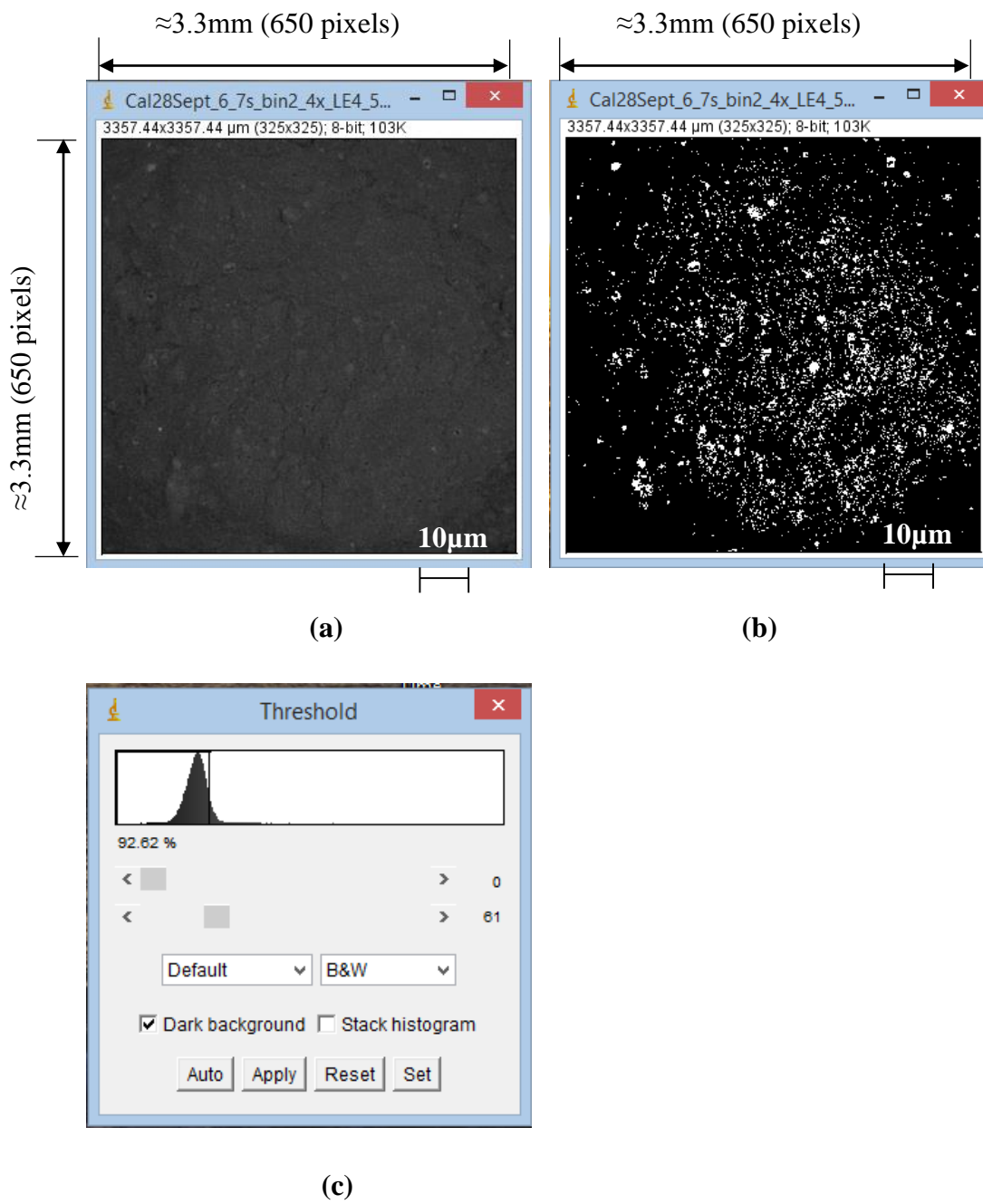


**Figure C2.9:** XRCT image of 8% calcium hydroxide 25% air voids treated kaolin (a) carbonated sample (b) threshold image showing black background (non-calcium carbonate), and white foreground (calcium carbonate) (c) threshold intensity of 61 on histogram.

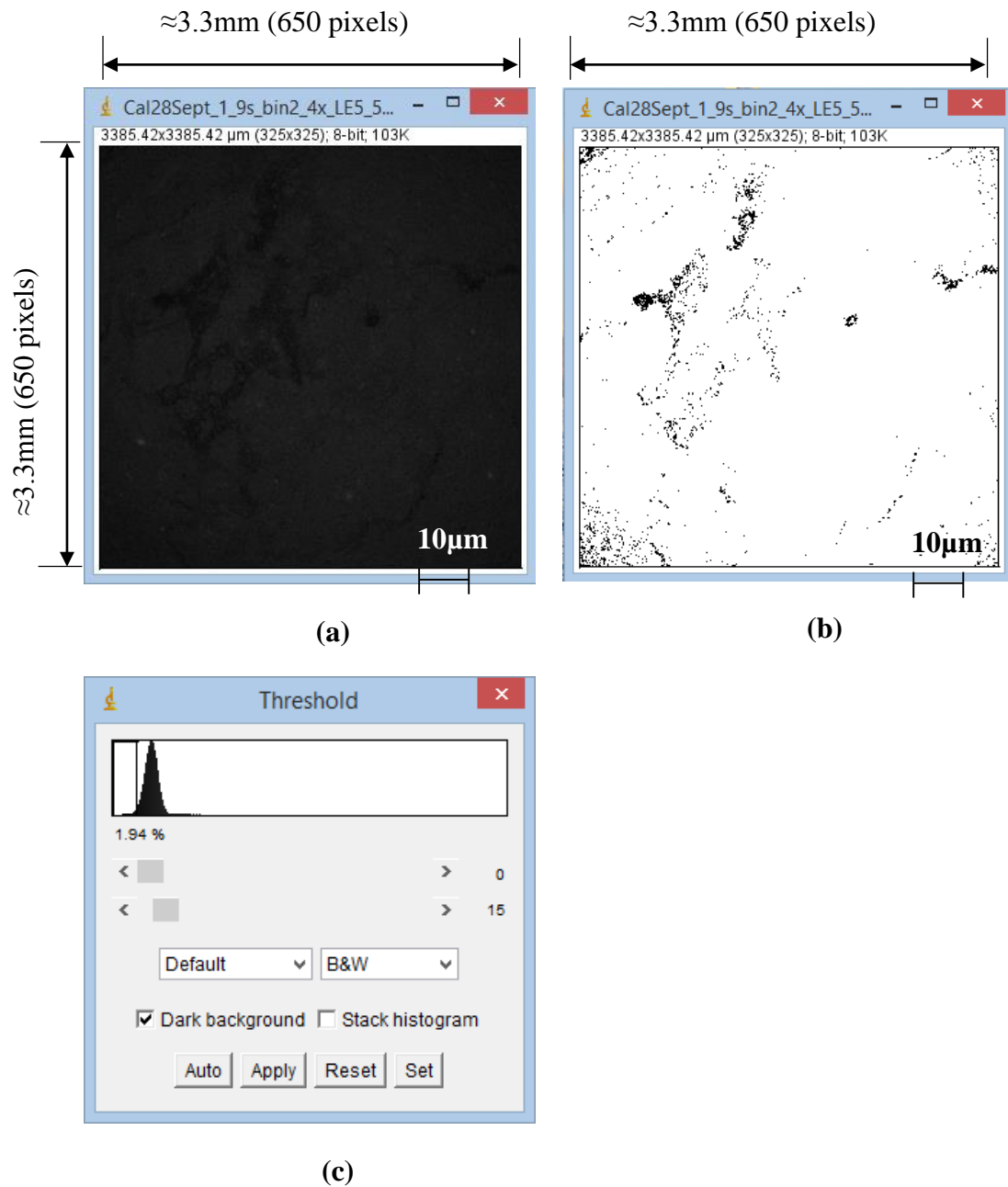


**Figure C2.10:** XRCT image of 4% calcium hydroxide 3% air voids treated kaolin (a) carbonated sample (b) threshold image showing white background (solid material), and black foreground (voids) (c) threshold intensity of 15 on histogram. Note: Black patches represents voids, white patches represents solid material.

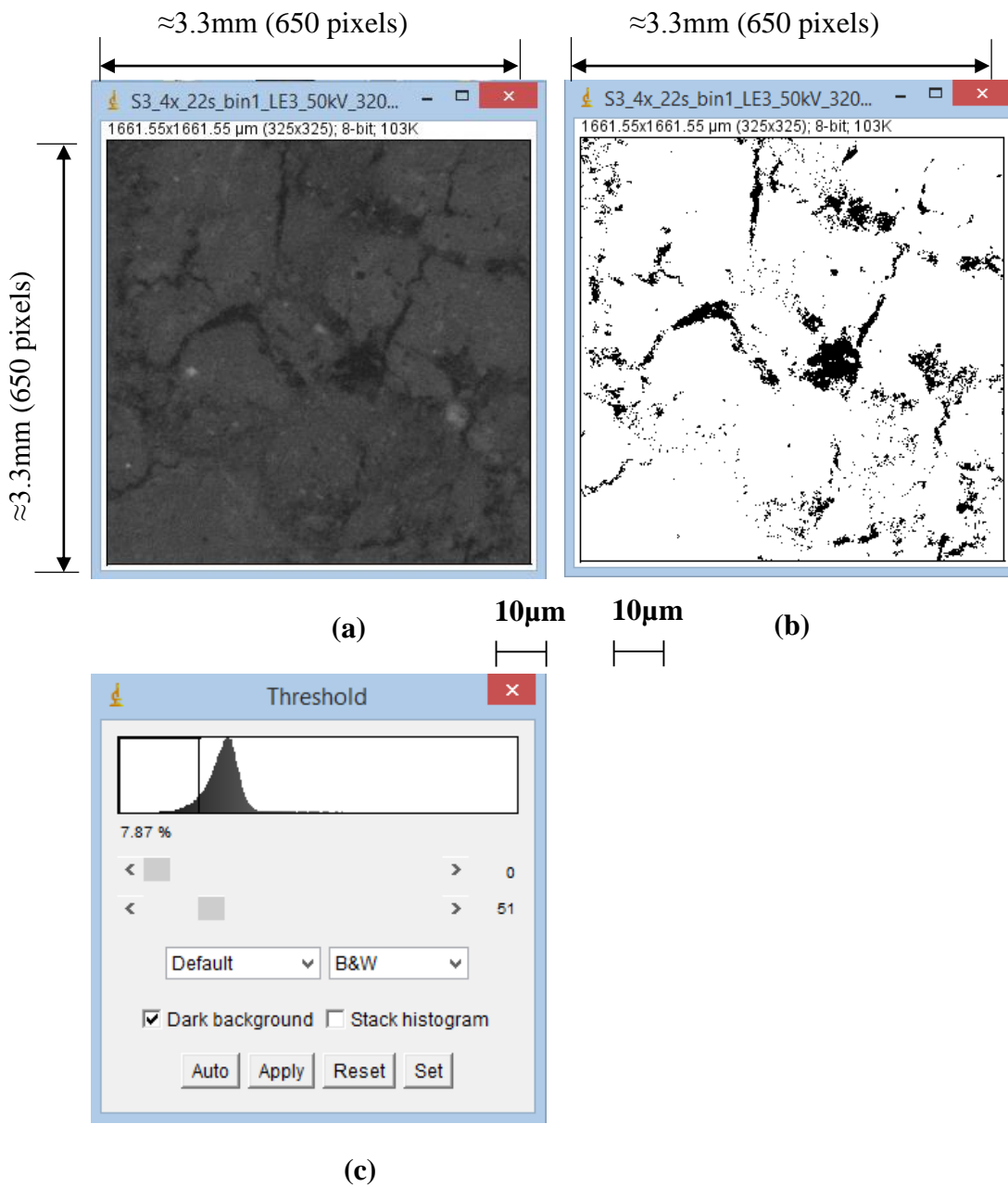


**Figure C2.11:** XRCT image of 4% calcium hydroxide 10% air voids treated kaolin (a) carbonated sample (b) threshold image showing white background (solid material), and black foreground (voids) (c) threshold intensity of 51 on histogram. Note: Black patches represents voids, white patches represents solid material.

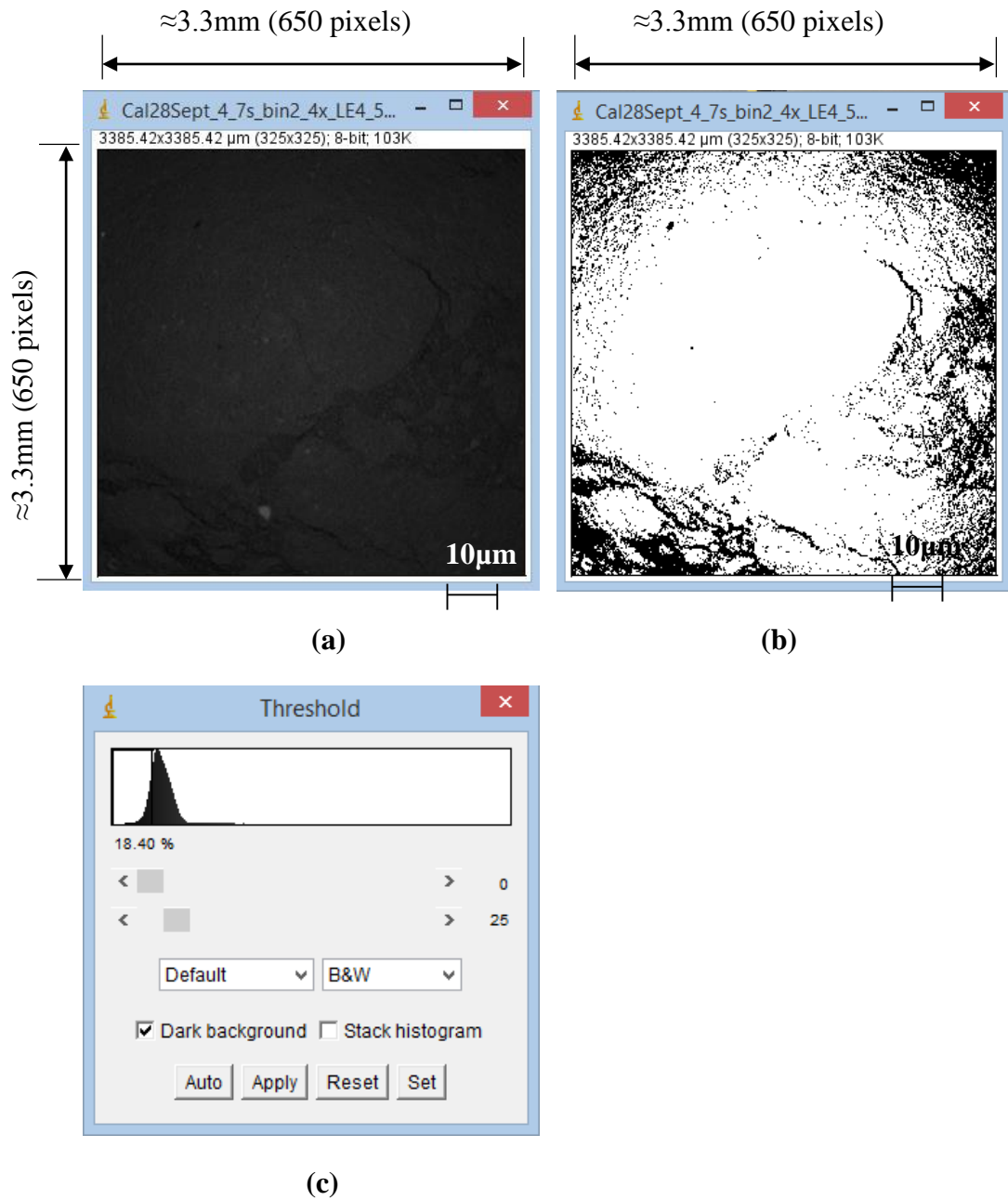


**Figure C2.12:** XRCT image of 4% calcium hydroxide 25% air voids treated kaolin (a) carbonated sample (b) threshold image showing white background (solid material), and black foreground (voids) (c) threshold intensity of 25 on histogram. Note: Black patches represents voids, white patches represents solid material.

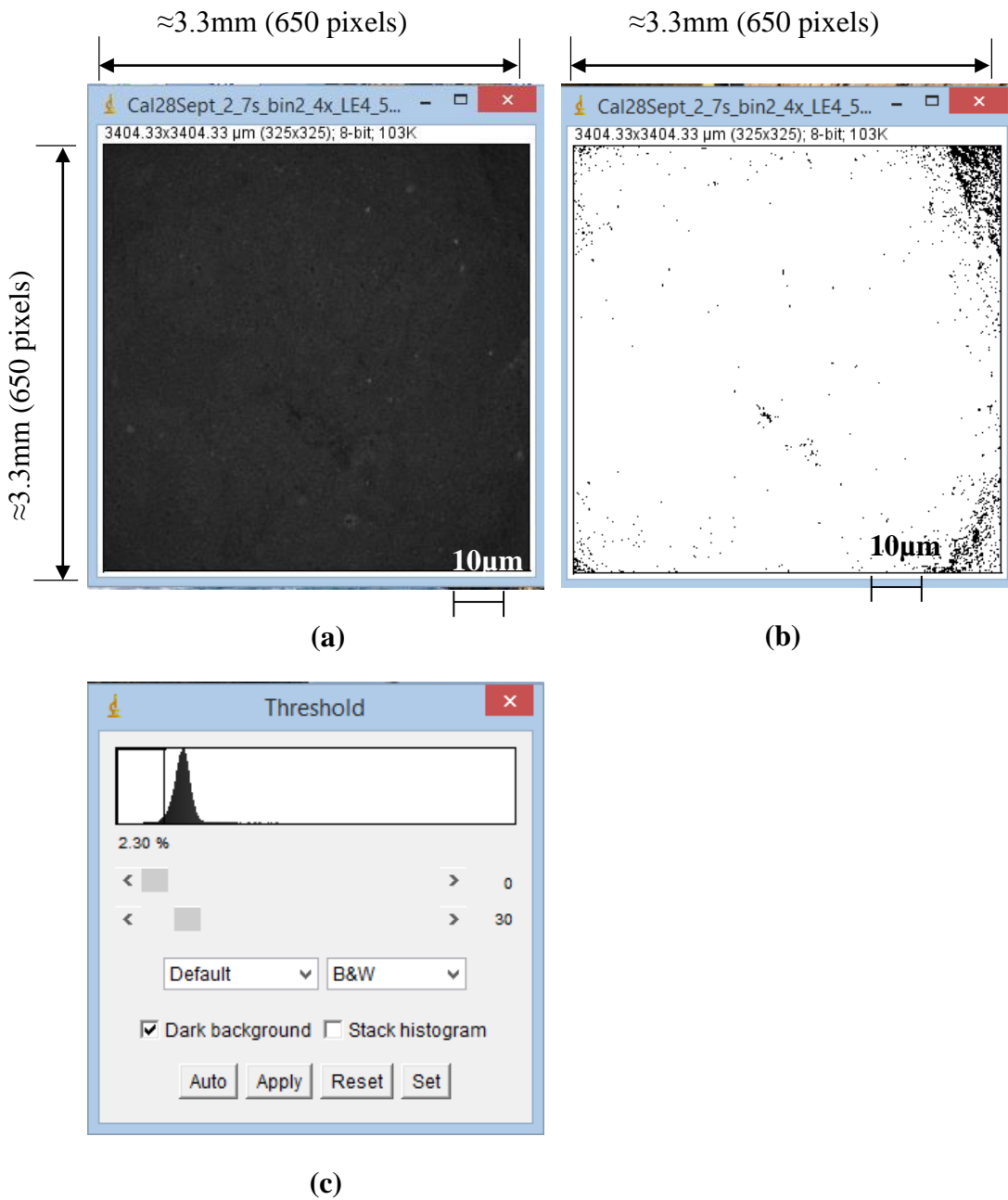


**Figure C.2.13:** XRCT image of 6% calcium hydroxide 3% air voids treated kaolin (a) carbonated sample (b) threshold image showing white background (solid material), and black foreground (voids) (c) threshold intensity of 30 on histogram. Note: Black patches represents voids, white patches represents solid material.

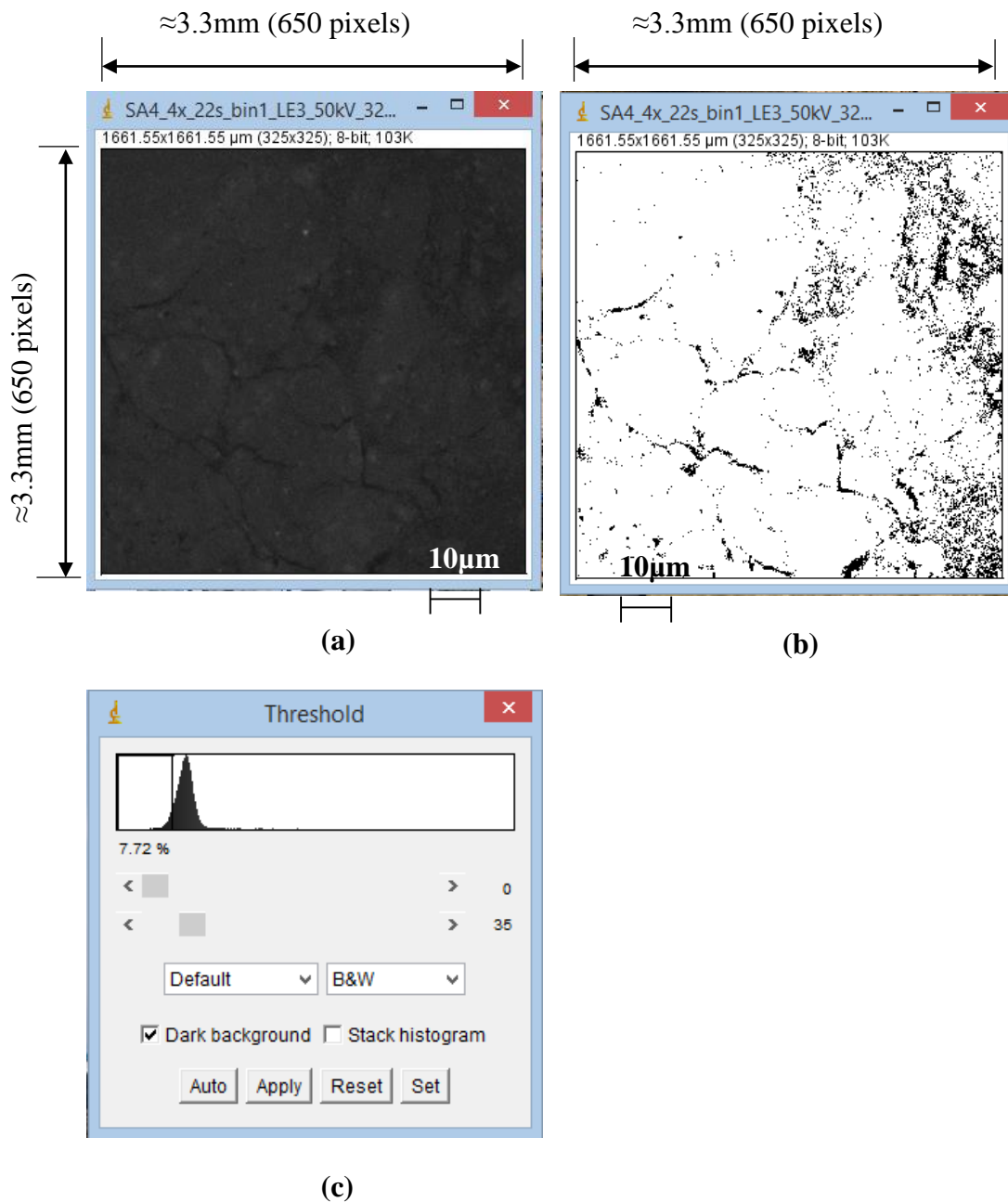


**Figure C2.14:** XRCT image of 6% calcium hydroxide 10% air voids treated kaolin (a) carbonated sample (b) threshold image showing white background (solid material), and black foreground (voids) (c) threshold intensity of 35 on histogram. Note: Black patches represents voids, white patches represents solid material.

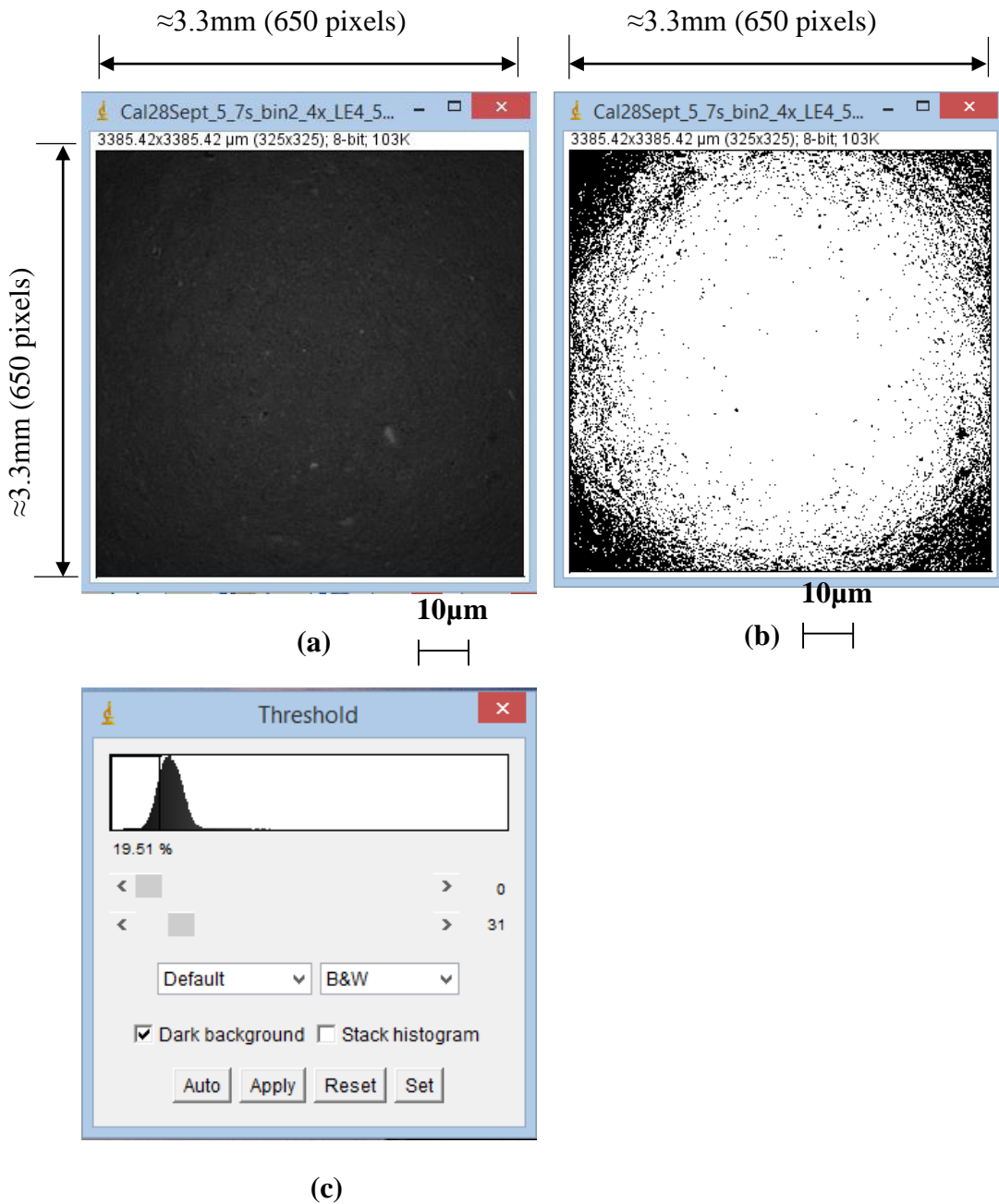


**Figure C2.15:** XRCT image of 6% calcium hydroxide 25% air voids treated kaolin (a) carbonated sample (b) threshold image showing white background (solid material), and black foreground (voids) (c) threshold intensity of 31 on histogram. Note: Black patches represents voids, white patches represents solid material.

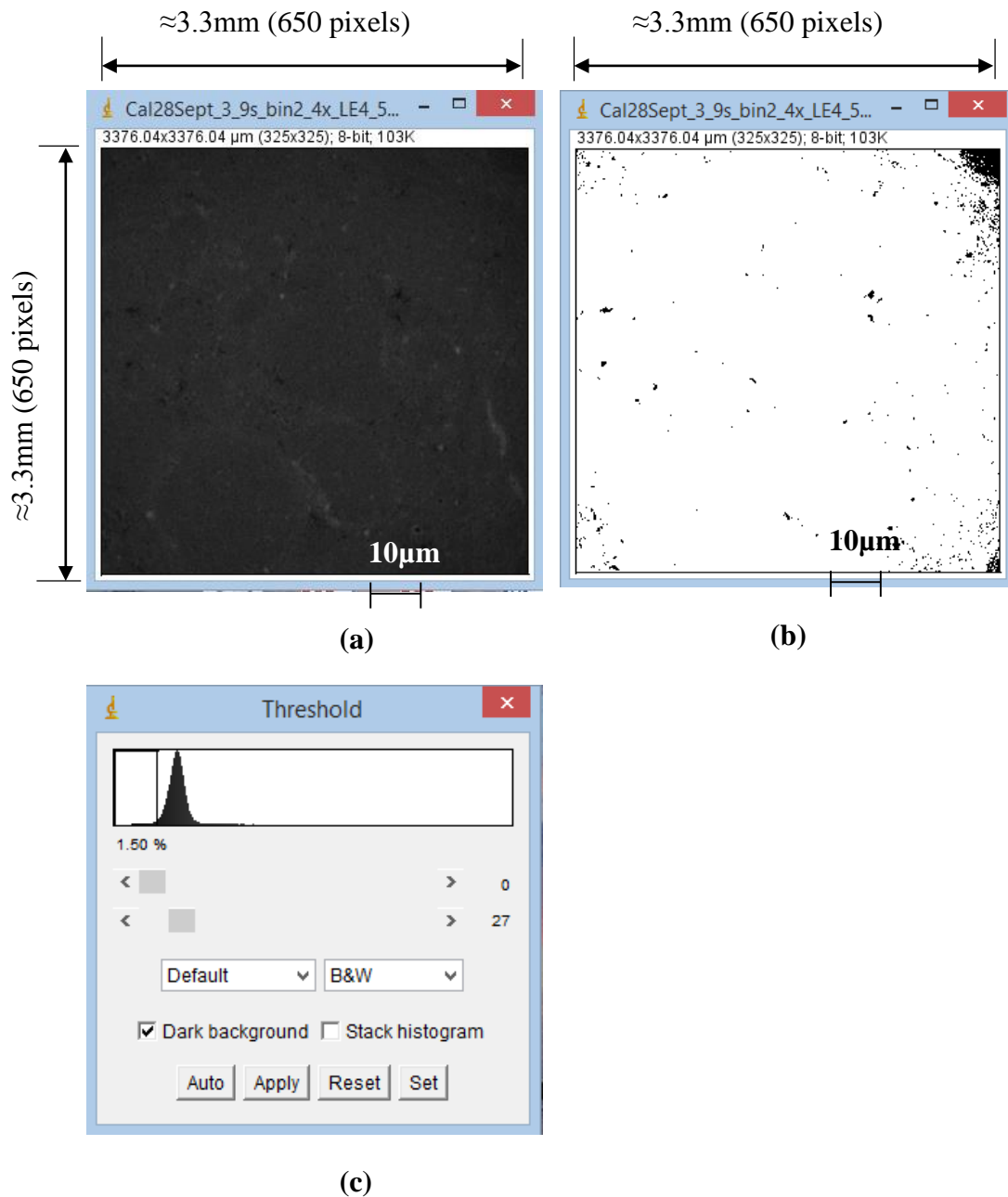


**Figure C2.16:** XRCT image of 8% calcium hydroxide 3% air voids treated kaolin (a) carbonated sample (b) threshold image showing white background (solid material), and black foreground (voids) (c) threshold intensity of 27 on histogram. Note: Black patches represents voids, white patches represents solid material.

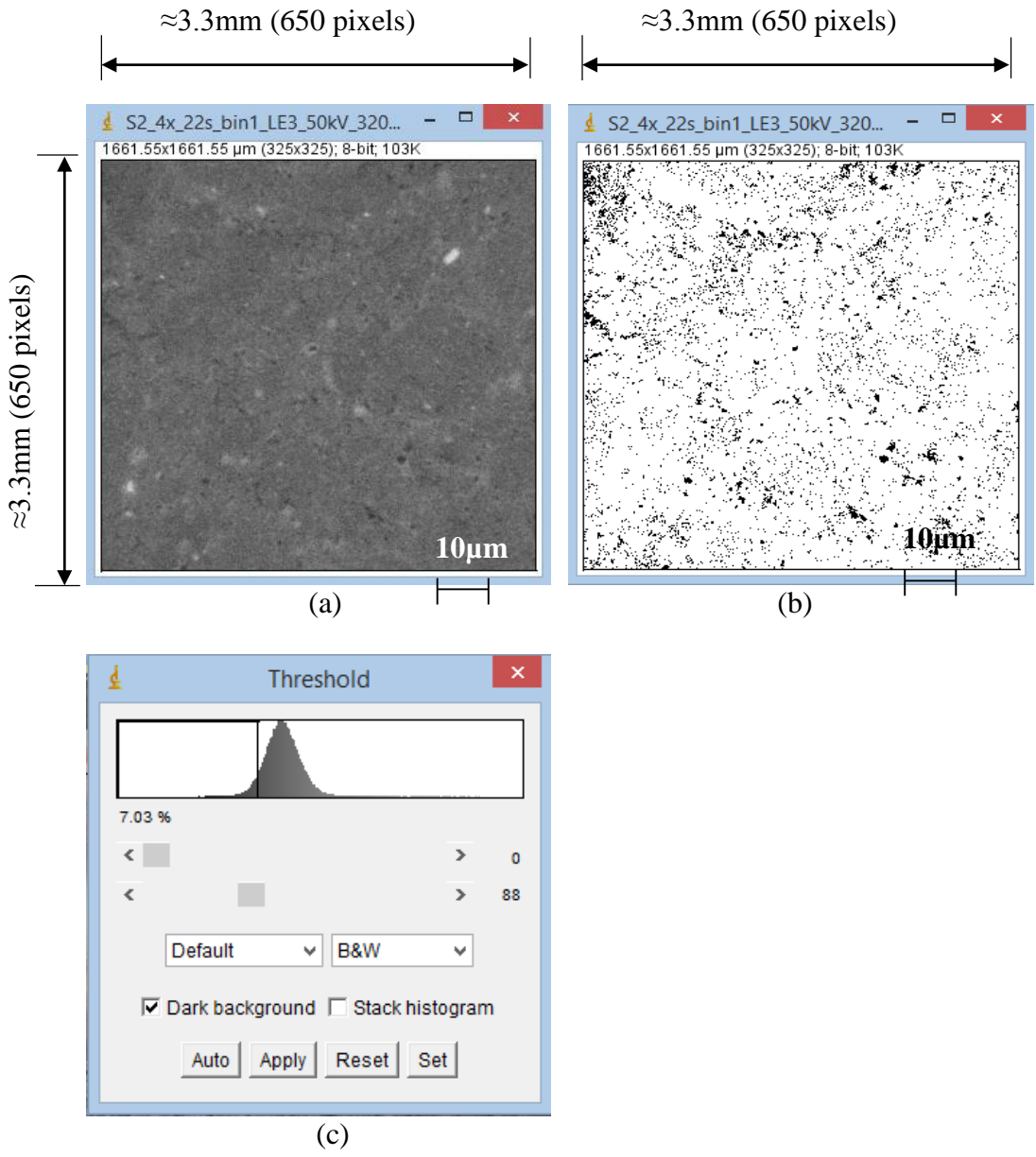


**Figure C2.17:** XRCT image of 8% calcium hydroxide 10% air voids treated kaolin (a) carbonated sample (b) threshold image showing white background (solid material), and black foreground (voids) (c) threshold intensity of 88 on histogram. Note: Black patches represents voids, white patches represents solid material.

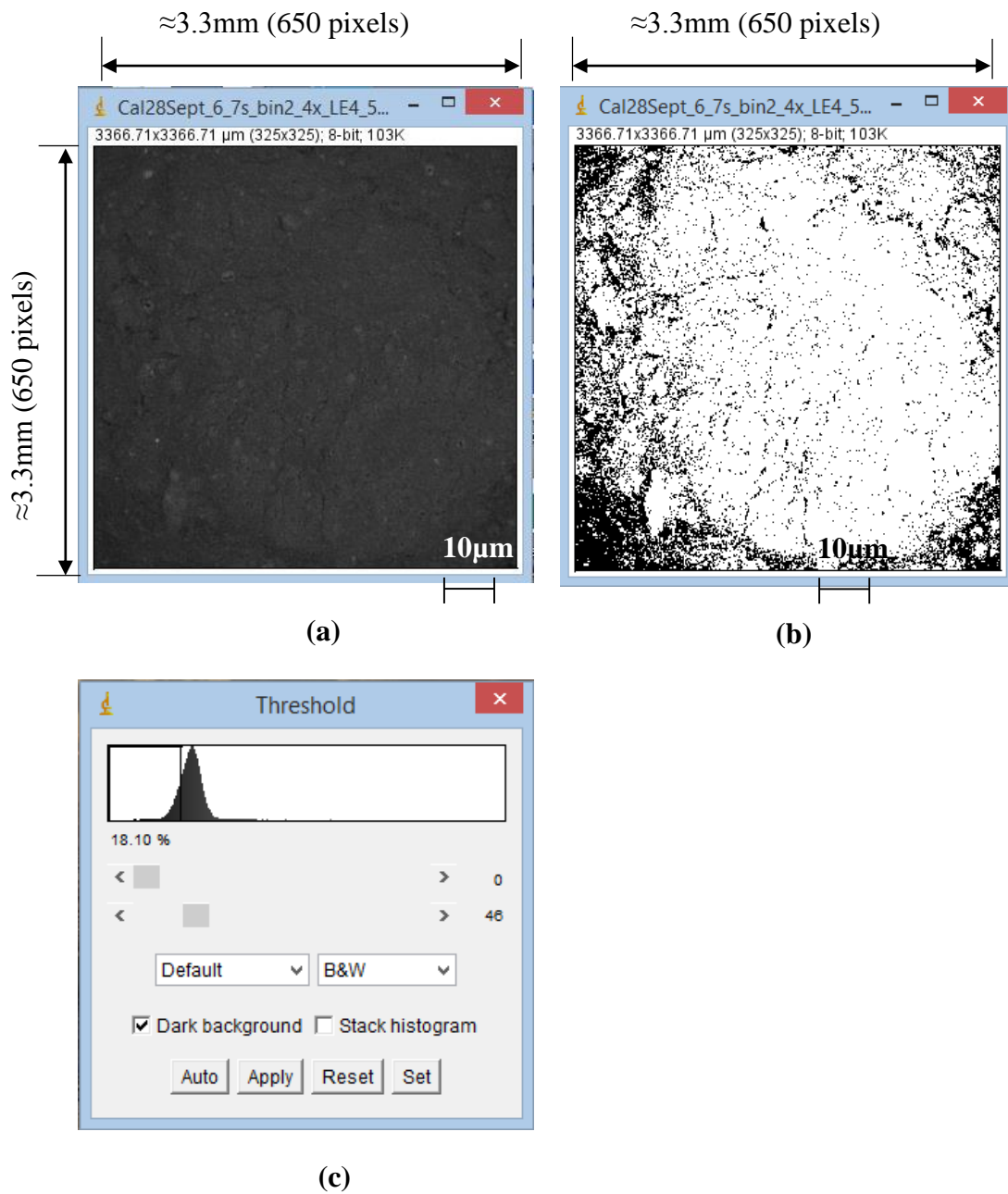


**Figure C2.18:** XRCT image of 8% calcium hydroxide 25% air voids treated kaolin (a) carbonated sample (b) threshold image showing white background (solid material), and black foreground (voids) (c) threshold intensity of 88 on histogram. Note: Black patches represents voids, white patches represents solid material.



## References

Gibbs M.J, Soyka, P., Conneely, D. (2001). CO<sub>2</sub> emissions from cement production. Good practice guidance and uncertainty management, National Greenhouse Gas Inventories. Intergovernmental Panel on Climate Change (IPCC).

Olivier, J.G.J., Janssens-Maenhout, G., Muntean, M. and Peters, J.A.H.W. (2016). Trends in global CO<sub>2</sub> emissions; 2016 Report, The Hague: PBL Netherlands Environmental Assessment Agency; Ispra: European Commission, Joint Research Centre.

USGS (2016). U.S. Geological Survey, Mineral Commodity Summaries, January 2016.